2018-03-01

# Contribution of Bulky <&alpha>,<&beta>-Dehydroamino Acids to the Proteolytic Stability andEnhanced Folding of <&beta>-Hairpins and Progress Towards the Total Synthesis of Yaku<'>amide A

Ankur Jalan
*Brigham Young University*

# Contribution of Bulky $\alpha,\beta$-Dehydroamino Acids to the Proteolytic Stability and Enhanced Folding of $\beta$-Hairpins and Progress Towards the Total Synthesis of Yaku'amide A

Ankur Jalan

A dissertation submitted to the faculty of
Brigham Young University
in partial fulfillment of the requirements for the degree of

Doctor of Philosophy

Steven L. Castle, Chair
Merritt B. Andrus
Joshua L. Price
David J. Michaelis
Matthew R. Linford

Department of Chemistry and Biochemistry

Brigham Young University

## ABSTRACT

Contribution of Bulky *α,β*-Dehydroamino Acids to the Proteolytic Stability and Enhanced Folding of *β*-Hairpins and Progress Towards the Total Synthesis of Yaku'amide A

Ankur Jalan
Department of Chemistry and Biochemistry, BYU
Doctor of Philosophy

This dissertation primarily covers the impact of bulky *α,β*-dehydroamino acids on the proteolytic stability and enhanced folding of *β*-hairpins. It partly describes the progress towards the total synthesis of yaku'amide A, a potent anticancer peptide with an $IC_{50}$ value of 14 ng/mL against leukemia cells. Proteins and peptides are a very attractive source of potential medicinal agents as they can target various protein–protein interactions that are implicated in several diseases and disorders. The global sales of peptide drugs in 2013 were estimated to be about $28 billion and are constantly rising at an appreciable rate. However, peptide drugs have a short plasma half-life because of their susceptibility to proteolysis. Multiple approaches have been discovered to overcome this shortcoming, but there is still an urgent need for better peptidomimetics to increase the stream of peptides entering the pharmaceutical market. Here, it has been demonstrated that the incorporation of a bulky *α,β*-dehydroamino acid in the turn regions of *β*-hairpins can substantially increase their proteolytic stability and folding. Insertion of a dehydrovaline (ΔVal) residue at the *i+1* position imparted ca. 7-fold increase in proteolytic resistance and ca. 15% increase in folding when compared to the parent peptide. Since the insertion of a bulky *α,β*-dehydroamino acid into the turn regions of *β*-hairpins can promote proteolytic stability without perturbing the secondary structures, it is believed that this novel approach is very promising in stabilizing bioactive turn-containing peptides for therapeutic use.

Yaku'amide A is a medium-sized peptide that contains several bulky dehydroamino acids, *β*-hydroxyamino acids and unique N- and C-termini. It has an unprecedented anticancer profile, and potent bioactivity, hence it was imperative to accomplish its total synthesis to elicit its unique mode of action and biological target. More efficient methods were developed to synthesize bulky dehydroamino acids and *β*-hydroxyamino acids. A regioselective base-free aminohydroxylation was developed for the synthesis of *β*-hydroxyamino acids. The major focus was the three-step synthesis of the N-terminal acyl group from a known compound by a one-pot indium-catalyzed cross-Claisen condensation/reduction and the synthesis of (2*S*,3*R*)-*β*-hydroxyisoleucine, and racemic *β*-hydroxyisoleucine, which are the precursors of *E*- and *Z*-dehydroisoleucine.



Keywords: bulky *α,β*-dehydroamino acids, *β*-hairpins, proteolytic stability, increased folding, aminohydroxylation, *β*-hydroxyamino acids, N-terminal acyl group

## ACKNOWLEDGEMENTS

At the very outset, I extend my gratitude to the Department of Chemistry and Biochemistry at Brigham Young University for providing me with an opportunity to pursue doctoral study, constant support and encouragement throughout the graduate program. I also want to thank them for granting access to the wonderful research facility and a very conducive research atmosphere. My gratitude is also due to the Simmons Center for Cancer Research Fellowship and the Woolley family for Telford & Frank Woolley Memorial Research Award.

I would like to express my sincere gratitude to my mentor Professor Steven L. Castle for his constant motivation, guidance, research insights, patience and kindness. It was my privilege to work under his mentorship on diverse research projects and learn immensely from his scientific acumen. I attribute the development of my research and writing skills to him. He has been an ideal source of inspiration and I tried my best to emulate his perseverance, punctuality and professionalism. I am also grateful to him for supporting my career goals and his valuable guidance regarding the same. I always looked forward to the yearly group picnic with him and his amazing family.

I am grateful to each of my graduate committee members: Professor Merritt B. Andrus, Professor Paul B. Savage, Assistant Professors Joshua L. Price, Dr. David J. Michaelis and Professor Matthew R. Linford. I am extremely indebted to Dr. Price for his valuable insights on the synthesis and analysis of peptides, materials and access to the HPLC instrument. He has been very supportive and helpful throughout. I was always encouraged by Dr. Andrus and Dr. David J. Michaelis and they were always forthcoming for fruitful discussions on several challenging synthetic problems. I would like to thank Dr. Andrus and Dr. Price for their recommendation letters

for fellowship and post-doctoral applications. Dr. Linford, Dr. Savage, Dr. Daniel H. Ess and Dr. Matt A. Peterson have been great sources of inspiration.

I will like to profusely thank my colleagues especially Dr. Zhiwei Ma, Dr. Yu Cai, Dr. Brad M. Loertscher and Seyed Hadi Nazari for their willingness to help and guide me both professionally and personally. They provided a wonderful work environment and motivated me always to excel. I published my first scientific paper with Dr. Yu Cai and I thank him for his diligent work on iminyl radical cyclization and yaku'amide A. I would like to thank the best undergraduate students I worked with and trained. David W. Kastner and Kei G. I. Webber were instrumental in the successful and timely completion of the project "Contribution of bulky $\alpha,\beta$-dehydroamino acids to the proteolytic stability and enhanced folding of $\beta$-hairpins." I also would like to offer my gratitude to very helpful colleagues Concordia Lo, Sia Im, Seth R. Bohman, Aaron R. Kubosumi, Shi Luo, and Blake Christensen.

I would like to thank Mason S. Smith for his guidance on peptide synthesis, purification and analysis. I am also grateful to Sara Mata and Dr. Shenglou Deng for several discussions on synthetic roadblocks I came across during my Ph.D. program. Thanks to Associate Professor Scott R. Burt and Mr. Bruce J. Jackson for providing well maintained NMR and MS facilities. Dr. Burt had been very generous and allotted sufficient time for conducting 1D and 2D $^{1}$H NMR experiments on $\beta$-hairpin peptides. I am also grateful to Janet Fonoimoana and Susan Mortensen for their constant support during the graduate program.

Last but not least, I would like to especially thank my parents Shiv Kr. Jalan and Maina Devi Jalan, and my siblings Abhishek Jalan, Abhilasha Aggarwal and Amit Jalan for their unwavering love and support. I am extremely grateful to my fiancée Gunjan Sharma for her unconditional support and taking care of me when I needed it the most. She was very kind to cook

and bring delicious meals for me to the lab while I was engrossed in work. I am grateful to my uncle Suresh Jalan for motivating and helping me to pursue doctoral studies in the United States. I would also like to thank the friends I made at BYU: Dr. Mukul Sonker, Dr. Bhupinder Singh, Dr. Pankaj Aggarwal, Dr. Anupriya Fartiyal, Dr. Anubhav Diwan, Dr. Abhijit Ghosh and Ying Zhang.

## TABLE OF CONTENTS

## LIST OF FIGURES

## LIST OF SCHEMES

## LIST OF TABLES

# 1 DEHYDROAMINO ACIDS

## 1.1 Introduction

α,β-Dehydroamino acids (ΔAAs) are non-proteinogenic amino acids with a $C_\alpha$=$C_\beta$ double bond and are often found in several natural products synthesized by microbes, marine organisms and plants (**Figure 1.1**).[1]

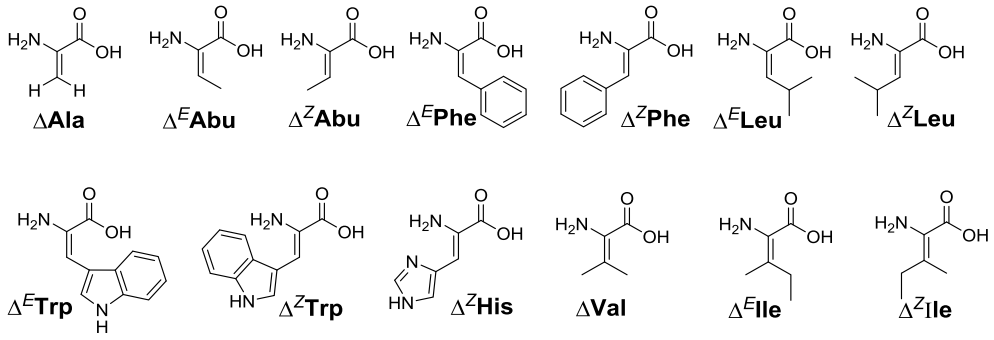


**Figure 1.1.** Dehydroamino acids seen in natural products.

Dehydroalanine (ΔAla) and *Z*-dehydrobutyrine ($\Delta^Z$Abu) are both seen in lantibiotics such as nisin and subtilin. Nisin, a well-known food preservative, occurs naturally in dairy products and is innocuous to humans, but highly toxic to bacteria.[2] Several other ΔAAs (tri- and tetra-substituted) which are encountered in natural products (**Figure 1.2.** and **Figure 1.3**) are: *E*-dehydrobutyrine ($\Delta^E$Abu), *Z*-dehydrophenylalanine ($\Delta^Z$Phe), *Z*-dehydroleucine ($\Delta^Z$Leu), *Z*–dehydrohistidine ($\Delta^Z$His), *Z*-dehydrotryptophan ($\Delta^Z$Trp), *E*- and *Z*- dehydroisoleucine ($\Delta^Z$Ile and $\Delta^E$Ile), and dehydrovaline (ΔVal). *E*- or *Z*- dehydrobutyrine ($\Delta^Z$Abu or $\Delta^E$Abu) are seen in microcystins (**1–4)** and Pahayokolides A and B (**5** and **6**, contain both $\Delta^Z$Abu and $\Delta^E$Abu).[3]

Albonoursin (**7**), a 2,5-diketopiperazine containing *Z*-dehydroleucine ((ΔZLeu), and *Z*-dehydrophenylalanine (ΔZPhe) residues, shows antibacterial, antiviral, and anticancer activity.[4]

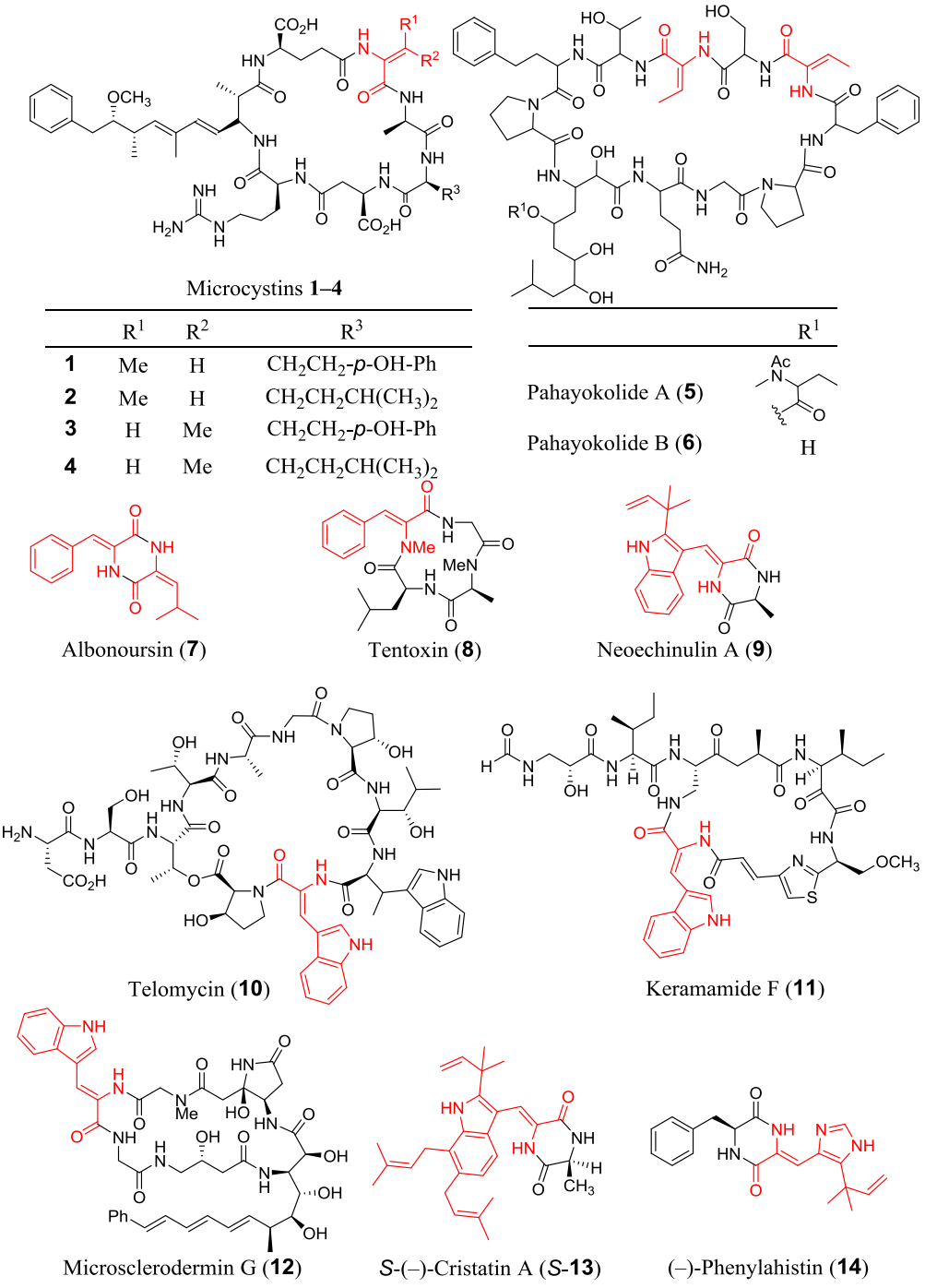


| | $R^1$ | $R^2$ | $R^3$ |
|---|---|---|---|
| **1** | Me | H | $CH_2CH_2$-*p*-OH-Ph |
| **2** | Me | H | $CH_2CH_2CH(CH_3)_2$ |
| **3** | H | Me | $CH_2CH_2$-*p*-OH-Ph |
| **4** | H | Me | $CH_2CH_2CH(CH_3)_2$ |

**Figure 1.2.** Natural products with di- and trisubstituted dehydroamino acids.

$\Delta^Z$Phe is also found in other natural products like the phytotoxic cyclic tetrapeptide tentoxin (**8**) that is known to cause chlorosis in certain plants.[5] *Z*-dehydrotryptophan ($\Delta^Z$Trp) occurs in several cyclic peptides such as neochinulins (**9**) (growth inhibitor), telomycin (1**0**) (antibiotic), keramamide F (**11**) (cytotoxic), microsclerodermin G (**12**) (antitumor and antifungal), and cristatin A (**13**) (antitumor), with a variety of biological activities.[6] *Z*–dehydrohistidine ($\Delta^Z$His) is another trisubstituted aromatic dehydroamino acid that is found in natural products. (–)-Phenylahistin ((S)-enantiomer) (**14**), a tubulin polymerization inhibitor, is reported to contain a $\Delta^Z$His residue.[7]

Apart from the trisubstituted dehydroamino acids, several natural compounds contain tetrasubstituted dehydroamino acids such as the symmetric dehydroamino acid ΔVal, and asymmetric dehydroamino acids *E*- & *Z*- dehydroisoleucine ($\Delta^Z$Ile and $\Delta^E$Ile) as shown in **Figure 1.3**. Lasiodine A (**15**), an acyclic depsipeptide isolated from the African buckthorn plant *Lasiodiscus marmoratus*, contains a ΔVal residue and is reported to prevent photophosphorylation in the chloroplasts of spinach.[8] There are multiple examples of natural products that contain both dehydrovaline and dehydroisoleucine. Myxovalargin A (**16**), an inhibitor of bacterial protein synthesis, is characterized by the presence of both ΔVal and $\Delta^E$Ile in its structure.[9] The acyclic tetradecapeptides yaku'amides A (**17a**) and B (**17b**) are found to contain both geometrical isomers of ΔIle (one $\Delta^E$Ile and two $\Delta^Z$Ile) and one ΔVal residue. Both of these linear peptides exhibit very potent activity against P388 murine leukemia cells, with excellent $IC_{50}$ values of 14 ng/mL and 4 ng/mL respectively.[10] Antrimycins (**18a–18h**), FR225659 (**19a**), and its four related peptides (**19b–19e)** are characterized by the presence of either ΔVal or $\Delta^E$Ile.[11] Phomopsins A (**20a**) and B (**20b**), 13-membered lactams, each contain one $\Delta^E$Ile residue among their six nonproteinogenic amino acids. Phomopsin A (**20a**) is reported to inhibit mitosis by binding to β-tubulin.[12]

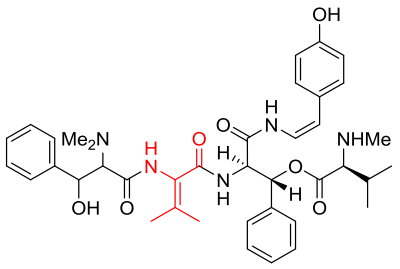

Lasiodine A (**15**)

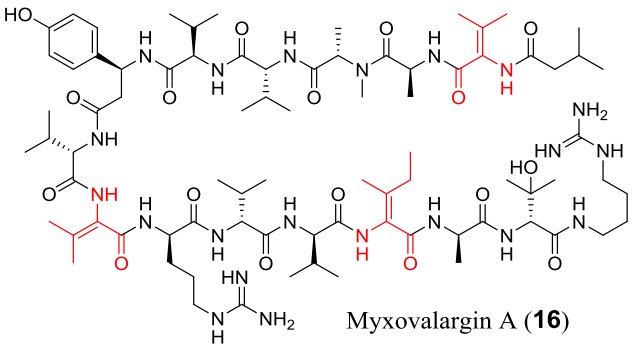

Myxovalargin A (**16**)

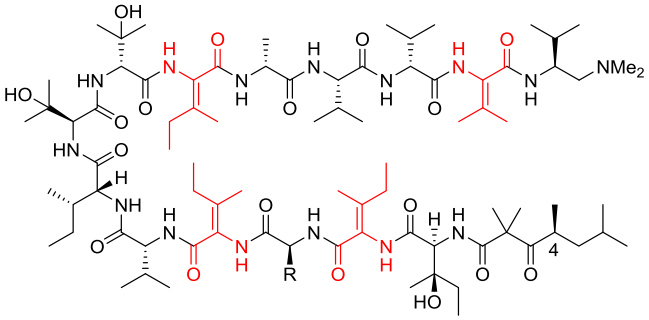

Yaku'amide A (**17a**), R = H
Yaku'amide B (**17b**), R = $CH_3$

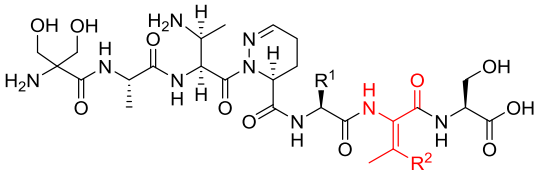

| Antrimycin | $R^1$ | $R^2$ |
|---|---|---|
| A (**18a**) | Me | Et |
| B (**18b**) | Et | Et |
| C (**18c**) | *n*-Pr | Et |
| D (**18d**) | *i*-Bu | Et |
| Av (**18e**) | Me | Me |
| Bv (**18f**) | Et | Me |
| Cv (**18g**) | *n*-Pr | Me |
| Dv (**18h**) | *i*-Bu | Me |

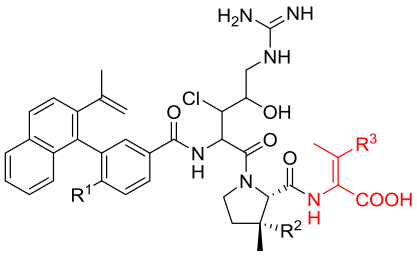

| | $R^1$ | $R^2$ | $R^3$ |
|---|---|---|---|
| **19a** | OH | OH | Me |
| **19b** | OH | OH | Et |
| **19c** | OH | H | Me |
| **19d** | OMe | OH | Et |
| **19e** | OMe | OH | Me |

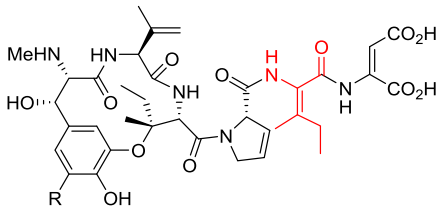

Phomopsin A (**20a**), R=Cl
Phomopsin B (**20b**), R=H

**Figure 1.3.** Natural products with tetrasubstituted dehydroamino acids.

*α,β*-Dehydroamino acids are non-coded amino acids and their salient feature is a carbon–carbon double bond between the *α* and *β* carbons. This double bond has a profound effect on the conformational properties of the dehydroamino acid residue as there is an achiral $sp^2$ hybridized α-carbon instead of the usual chiral $sp^3$ hybridized α-carbon. This in turn can immensely affect the

overall conformation of a peptide containing a dehydroamino acid residue. *α,β*-Dehydroamino acids can be used as inducers of certain folded conformations in peptides and hence, they can potentially be used to design peptides to target protein-protein interactions.[13]

## 1.2 Methods for *α, β*-dehydroamino acids (ΔAAs) synthesis

Along with their unique and challenging chemical structures, these natural products containing *α,β*-dehydroamino acids (**Figure 1.2 and 1.3**) are of great importance because of their wide-ranging biological activities. Hence, multiple methods have been devised to synthesize these nonproteinogenic amino acids. Some of these methods are covered here.

Since 1893, Erlenmeyer's condensation has been a well-known procedure for the synthesis of amino acids and dehydroamino acids from *N*-protected glycine derivatives. For example, an azlactone (**22**) is formed via Perkin-type condensation of N-acetylglycine (**21**) and benzaldehyde in the presence of acetic anhydride and anhydrous sodium acetate (**Scheme 1.1**). This azlactone can be further elaborated to synthesize desired dehydropeptides.[14]

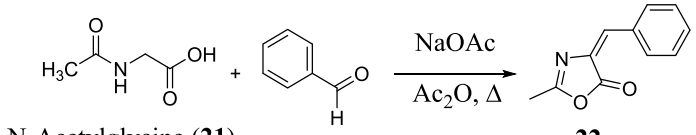


N-Acetylglycine (**21**) **22**

**Scheme 1.1.** Erlenmeyer's condensation.

In 1926, Bergmann and co-workers synthesized several azlactones of dehydroamino acids. *N*-chloroacetyl amino acids in the presence of acetic anhydride afforded dehydroamino acid azlactones via cyclization and elimination. Similarly, they obtained the azlactone (**26**) upon heating of *N*-chloroacetyl-*β*-hydroxyphenylalanine (**25**) with acetic anhydride, which provided glycyl–dehydrophenylalanine dipeptide (**28**) after treatment with water and ammonia (**Scheme 1.2**).

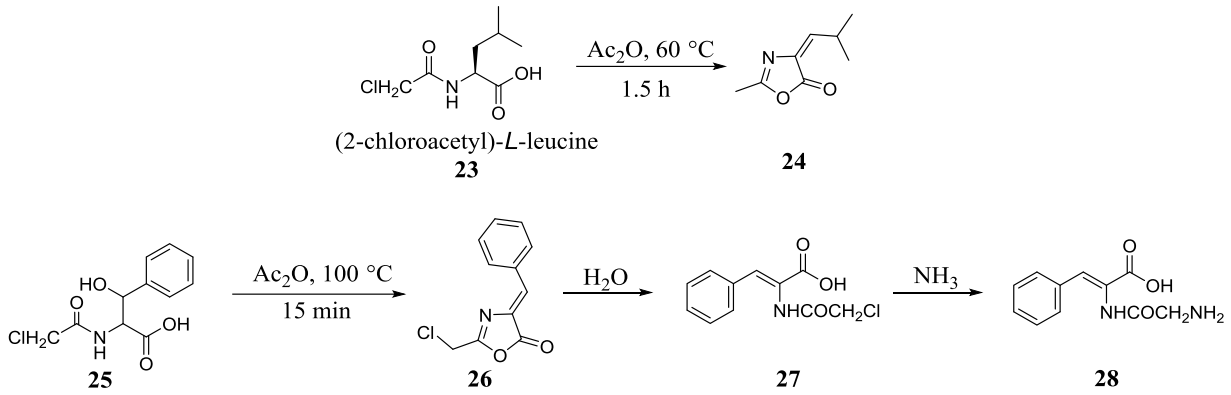


**Scheme 1.2.** Synthesis of azlactones and a dipeptide via azlactone-opening.

In 1943, Bergmann et al. utilized their strategy along with the Erlenmeyer's condensation to synthesize many small peptides containing one to four *Z*-dehydrophenylalanines.[15] A protocol similar to Bergmann's method was adopted by Ohta and co-workers in 1967 to synthesize the *Z*-dehydroisoleucine residue of albonoursin (**7**). Heating of *N*-dichloroacetyl-L-leucine (**29**) with acetic anhydride provided the azlactone **30** containing dehydroisoleucine, which was further manipulated to give albonoursin (**7**) (**Scheme 1.3**).[16]

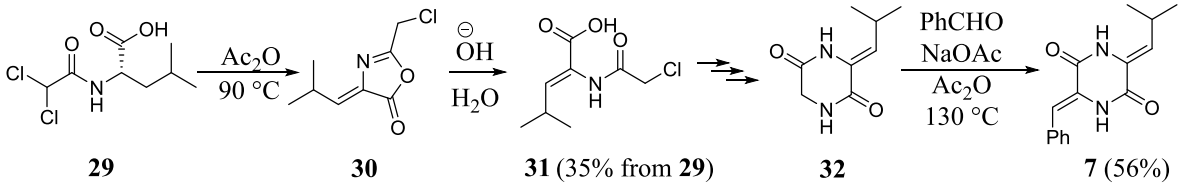


**Scheme 1.3.** Synthesis of (*Z*)-ΔIle residue of albonoursin (**7**).

Several researchers have prepared dipeptides containing a dehydroamino acid by the condensation of α-keto acids with carboxamides in the presence of catalytic *p*-toluenesulfonic acid (*p*-TsOH) in refluxing benzene (**Scheme 1.4**).[17]

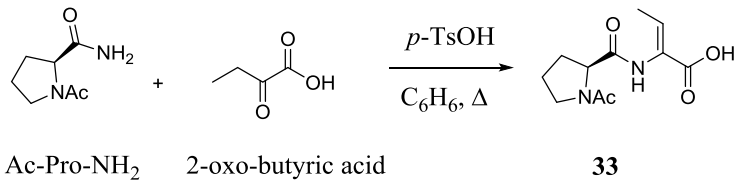


**Scheme 1.4.** Condensation of an α-keto acid with a carboxamides.

Stammer et al. reported the synthesis of dipeptide azlactones of $\Delta^{Z}$Phe by oxidation of the azlactone obtained from the dipeptide Z-Pro-Phe-OH. Activation of the dipeptide Z-Pro-Phe-OH (**34**) with dicyclohexylcarbodiimide (DCC) gave azlactone **35**, which upon oxidation with 2,3-dichloro-5,6-dicyano-*p*-benzoquinone (DDQ) at room temperature furnished the unsaturated azlactone **36** in 48 % yield (**Scheme 1.5**).[18]

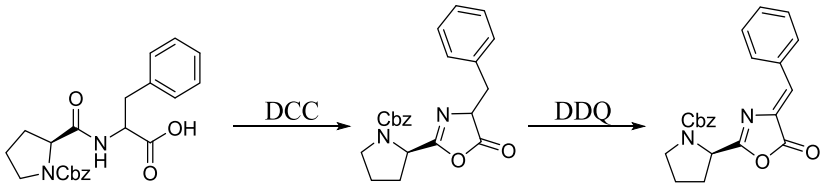


**34** **35** **36**

**Scheme 1.5.** Synthesis of (*Z*)-ΔPhe containing dipeptide azlactone **36** by DDQ oxidation.

Several elimination protocols have been developed for the synthesis of α, β-dehydroamino acids (ΔAAs) from readily available *β*-hydroxyamino acids. Various reagents have been employed to facilitate *β*-elimination from *β*-hydroxy *α*-amino acids, like diethyl chlorophosphate, oxalyl chloride, tosyl chloride, mesyl chloride, Martin's sulfurane, triphenyl phosphine/diethyl azodicarboxylate (DEAD), disuccinimidyl carbonate (DSC), N,N′-carbonyldiimidazole, diisopropylcarbodiimide/copper(I) chloride (DiPCD) and (diethylamino)sulfur trifluoride/pyridine (DAST).[19] It is noteworthy that most of these methods are stereoselective for the thermodynamically more stable *Z*-isomer.

Shanzer and co-workers realized the limitations of the previously reported methods as these protocols mostly afforded the more thermodynamically stable *Z*-isomer or a mixture of both the geometrical isomers of asymmetrical *α,β*-dehydroamino acids.[20] In 1983, they reported a one-step stereospecific method for the synthesis of *Z*- & *E*- ΔAbu and ΔLeu by the dehydration of *threo*- and *erythro*- protected *β*-hydroxyamino acids (threonine and *β*-hydroxy-leucine) respectively with

(diethylamino)sulfur trifluoride in the presence of pyridine via an E2 elimination reaction (**Scheme 1.6**).

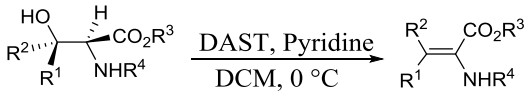


**37** **38**

| | $R^1$ | $R^2$ | $R^3$ | $R^4$ |
|---|---|---|---|---|
| **a** | H | H | Bz | Cbz |
| **b** | Me | H | Bz | Cbz |
| **c** | H | Me | Bz | Cbz |
| **d** | *i*-Pr | H | Bz | Cbz |
| **e** | H | *i*-Pr | Bz | Cbz |
| **f** | Me | H | Et | Boc |
| **g** | H | Me | Et | Boc |

**Scheme 1.6.** One-step stereospecific dehydration for the synthesis of *Z*- & *E*- ΔAbu and ΔLeu.

Later on in the year 2003, Sai and his colleagues reported the stereoselective synthesis of *E*- & *Z*- ΔAbu and ΔPhe from *threo*- and *erythro*- threonine and *β*-hydroxyphenylalanine respectively via 1-ethyl-3-(3-dimethylaminopropyl)carbodiimide and copper (II) chloride (EDC/$CuCl_2$) mediated dehydration.[21] Unlike the previous work, this method is remarkable as the cheaper *threo*-diastereomer selectively afforded the *E*-isomer.

In order to expand the limited synthetic methodologies available currently for the stereoselective synthesis of trisubstituted *E*- *α,β*-dehydroamino acids, Ohfune et al. developed new protocols based upon the very reliable and efficient Horner–Wadsworth–Emmons method of constructing ΔAAs.[22] They designed a new Schmidt's reagent (**39**) and utilized it to construct a complex $\Delta^E$AA, an important intermediate in their 12-step diastereoselective total synthesis of (–)-kaitocephalin.[23] Encouraged by this, they explored optimal conditions for the synthesis of several *E*-dehydroamino acids and their derivatives (**Scheme 1.7**). Aromatic aldehydes such as 2-

pyridinecarbaldehyde, benzaldehyde, *m*-nitro & *p*-methoxy benzaldehyde furnished the *E*-isomers in a highly stereoselective manner and in good yields. DBU/$MgBr_2$•$OEt_2$ was required instead of NaH/NaI to obtain the aliphatic $\Delta^E$AA with good *E*-selectivity.

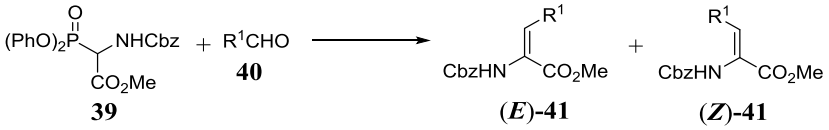


**39** (*E*)-**41** (*Z*)-**41**

| | $R^1$ | Conditions | (*E*):(*Z*) |
|---|---|---|---|
| **40a** | 2-Pyridinyl | NaH, NaI | 90:10 |
| **40b** | Phenyl | NaH, NaI | 97:3 |
| **40c** | *m*-$NO_2$-phenyl | NaH, NaI | 97:3 |
| **40d** | *p*-OMe-phenyl | NaH, NaI | 96:4 |
| **40e** | Isopropyl | DBU, $MgBr_2$•$OEt_2$ | 90:10 |
| **40f** | Methyl | DBU, $MgBr_2$•$OEt_2$ | 78:22 |

**Scheme 1.7.** Synthesis of (*E*)-ΔAAs by Horner–Wadsworth–Emmons condensation.

## 1.3 Synthesis of tetrasubstituted bulky *α,β*-dehydroamino acids

Since bulky tetrasubstituted, dehydroamino acids are commonly seen in biologically active natural peptides, many attempts have been made to invent simple and efficient methods to synthesize these unnatural amino acid residues.

While working on *β*-lactam thiazoline systems for their biogenetic type synthesis of penicillin and cephalosporin antibiotics, Kishi and co-workers synthesized ΔVal-containing dipeptide from penicillamine methyl ester (methyl (*R*)-2-amino-3-mercapto-3-methylbutanoate) via elimination of the thiol moiety.[24] In 1999, Wandless et al. developed an efficient and stereospecific method to synthesize tri- and tetrasubstituted *α,β*-dehydroamino acids by the *anti*

dehydration of *N*-acyl-*β*-hydroxyamino esters **42** with thionyl chloride and 1,8-diazabicyclo[5.4.0]-undec-7-ene (DBU) via diastereomeric cyclic sulfamidite intermediates **43**. This two-step antiperiplanar elimination protocol is suitable for dehydration of both the secondary and tertiary alcohols, and provides both (*Z*) and (*E*)-ΔAAs in moderate to good yields (**Scheme 1.8**). They devised this method to construct an (*E*)-ΔIle-containing tripeptide intermediate for the total synthesis of the antimitotic agent phomopsin A (**20a, Figure 1.3**).[25]

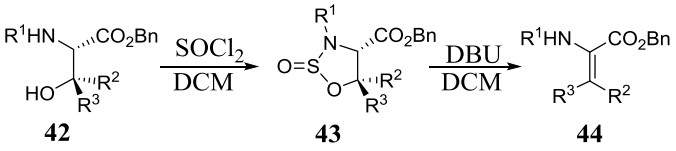


**42** **43** **44**

| | $R^1$ | $R^2$ | $R^3$ |
|---|---|---|---|
| **42a** | Ac | Me | Et |
| **42b** | 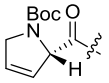 | Me | Et |
| **42c** | Ac | Et | Me |
| **42d** | 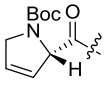 | Et | Me |

**Scheme 1.8.** Synthesis of (*Z*) and (*E*)-ΔAAs by the *anti* dehydration of *N*-acyl-*β*-hydroxyamino esters **42.**

Inspired by the *syn*-dehydration protocol developed by Sai et al., Joullié and co-workers developed a method for the stereoselective synthesis of (*E*)-ΔIle found in the phomopsins A and B (**20a** and **20b**, **Figure 1.3**) The *syn* dehydration of dipeptide **45** with EDC/$Cu(OTf)_2$ at 60 ºC in THF afforded (*E*)-ΔIle containing dipeptide **46** after 1.5 h in good yield (73 %) (**Scheme 1.9**).[19b]

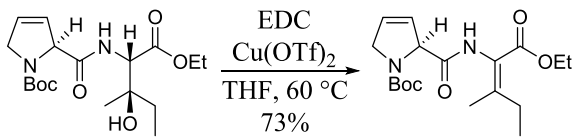


**45** **46**

**Scheme 1.9.** *Syn* dehydration mediated by EDC/$Cu(OTf)_2$.

Another important and stereoselective method for the synthesis of ΔAAs is vinyl amidation.[26] During the total synthesis of the anticancer peptide yaku'amide A (**17a**), Kuranaga and Inoue synthesized three ΔAAs, (*Z*)-& (*E*)-ΔIle and ΔVal, through copper-catalyzed cross-coupling of amides with stereodefined vinyl iodides in good yields.[27] (*Z*)-ΔIle-containing dipeptide precursors **49** and **52** were synthesized from amides **47** and **51** with vinyl iodide **52**, whereas (*E*)-ΔIle-containing dipeptide precursor **56** was obtained by coupling amide **54** with vinyl iodide **55**. Peptide **60** containing ΔVal was synthesized from vinyl iodide **59** and amide **58**, but required a much higher catalytic loading and provided a moderate yield (**Scheme 1.10**).

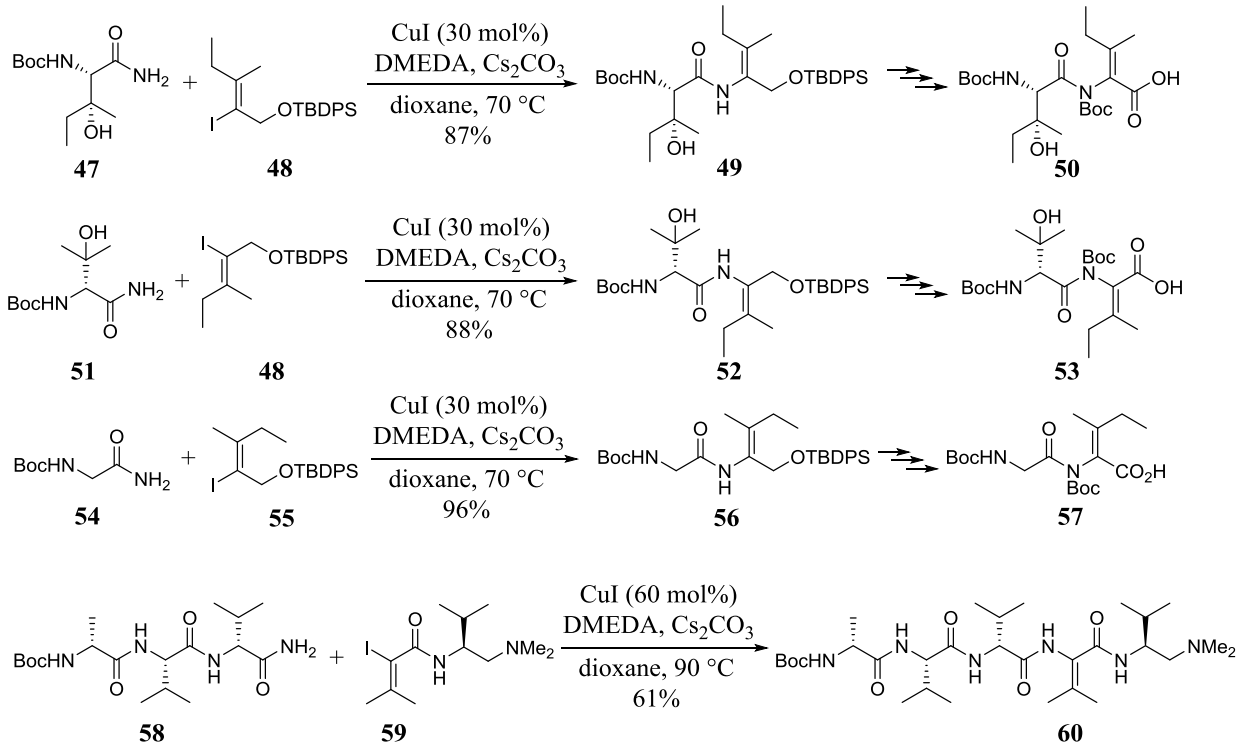


**Scheme 1.10.** Cross-coupling to access tetrasubstituted ΔAAs of yaku'amide A.

All these approaches are useful and have advanced the chemistry of dehydroamino acids tremendously. However, there were still a few shortcomings. Castle and co-workers addressed some of these gaps in 2014. They synthesized the critical (*Z*)- and (*E*)-ΔIle-containing peptide

fragments of yaku'amide A with excellent diastereoselectivity via Martin sulfurane mediated direct stereoselective *anti* dehydration of tertiary alcohols **61** and **64** respectively (**Scheme 1.11**). [28] Martin sulfurane has been previously used by Shioiri et al. to synthesize the thermodynamically favorable (*Z*)-ΔAbu isomer and ΔVal, but this new method discovered by Ma and Castle is a rare example of Martin sulfurane mediated concerted asynchronous E2 dehydration of *β-tert*-hydroxy amino acids.[29]

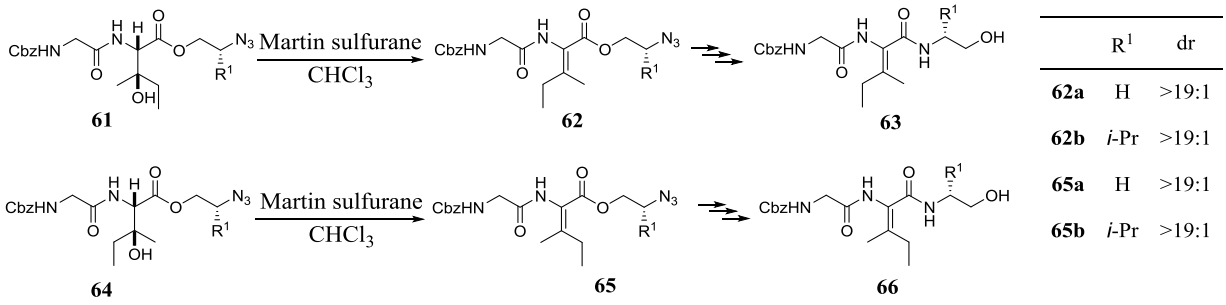


| | $R^1$ | dr |
|---|---|---|
| **62a** | H | >19:1 |
| **62b** | *i*-Pr | >19:1 |
| **65a** | H | >19:1 |
| **65b** | *i*-Pr | >19:1 |

**Scheme 1.11.** Martin sulfurane mediated *anti* dehydration of *β-tert*-hydroxy amino acids.

## 1.4 Solid-phase synthesis of peptides containing dehydroamino acids and new approaches for the synthesis of dehydroamino acids by elimination in solution

Solution-phase synthesis of peptides containing *α,β*-dehydroamino acids has progressed well since the 1920's when Bergmann et al. synthesized certain small peptides (dipeptides or tripeptides) containing *Z*-dehydrophenylalanine ($\Delta^Z$Phe) via azlactone intermediates. Several methodologies have been developed to synthesize dehydroamino acids, such as elimination, condensation, and cross-coupling. Nevertheless, the solution-phase synthesis has some inherent drawbacks, like the necessity of purification at every step, low overall yield and its time-consuming nature. Since the advent of solid-phase peptide synthesis in the mid 1960's and consequent rapid development of the orthogonal protecting groups for the amino acid side chain functional groups, solid-phase peptide synthesis has become the most important tool for the synthesis of medium to large peptides

as it can overcome some of the major drawbacks of solution-phase peptide synthesis. Solid-phase peptide synthesis also allows the preparation of a vast number of structurally diverse peptides for combinatorial libraries. Hence, researchers tried to adopt this powerful method for the synthesis of peptides containing *α,β*-dehydroamino acids. There are multiple examples of on-resin eliminations, couplings of dipeptides containing a ΔAA to peptides on resin, and chemoselective eliminations in solution after solid-phase peptide synthesis.

In 1981, Stammer and Chauhan reported the solid-phase synthesis of a few $\Delta^Z$Phe-containing analogues of the potent vasodilator peptide bradykinin (BK, Arg$^1$-Pro$^2$-Pro$^3$-Gly$^4$-Phe$^5$-Ser$^6$-Pro$^7$-Phe$^8$-Arg$^9$). They incorporated $\Delta^Z$Phe in place of the phenylalanyl residues at positions 5 and/or 8 to synthesize three analogues: [$\Delta^Z$Phe$^5$]BK, [$\Delta^Z$Phe$^8$]BK and [$\Delta^Z$Phe$^{5,8}$]BK. They introduced the $\Delta^Z$Phe into the growing resin-bound peptide by using activated dipeptides with $\Delta^Z$Phe at the terminal end of the dipeptides (**Scheme 1.12**). The dipeptide acids were synthesized by the DDQ oxidation of saturated azlactones of Boc-Pro-Phe-OH and Boc-Gly-Phe-OH to corresponding unsaturated azlactones, followed by subsequent alkaline hydrolysis to dipeptide acids. [$\Delta^Z$Phe$^5$]BK was synthesized by incorporating the dipeptide acid Boc-Gly-$\Delta^Z$Phe-OH in the resin bound peptide with the aid of dicyclohexylcarbodiimide (DCC) at rt over 20 h in methylene chloride. Boc-Pro-$\Delta^Z$Phe-OH dipeptide could not be coupled to the peptide successfully by the same procedure. Hence, Boc-Pro-$\Delta^Z$Phe-OH was activated with isobutyl chloroformate in THF at –15 °C in the presence of *N*-methyl-morpholine. Six equivalents of this activated dipeptide were required for the coupling to $H_2N$-(tosyl)Arg-resin (Merrifield resin), and the coupling was complete in ca. 36 hours at rt. This modified procedure was followed to incorporate $\Delta^Z$Phe$^8$ in the [$\Delta^Z$Phe$^8$]BK and [$\Delta^Z$Phe$^{5,8}$]BK analogues. The [$\Delta^Z$Phe$^5$]BK (Arg$^1$-Pro$^2$-Pro$^3$-Gly$^4$-$\Delta^Z$Phe$^5$-Ser$^6$-

Pro$^7$-Phe$^8$-Arg$^9$) analogue thus synthesized was found to be more potent than bradykinin at lowering the blood pressure of rats after intravenous injection.[30]

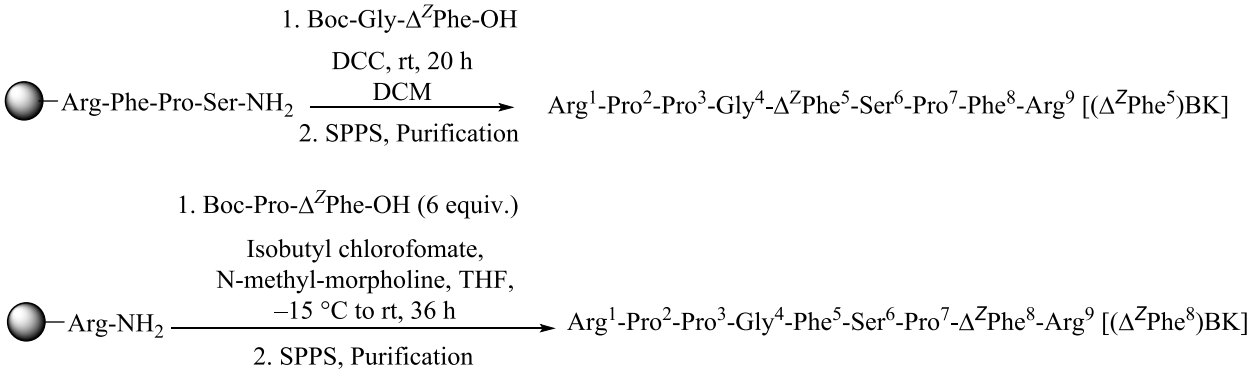


**Scheme 1.12.** Synthesis of $\Delta^Z$Phe-containing analogues of bradykinin (BK).

In 1992, Goodman and Polinsky demonstrated the first on-resin dehydration of serine to obtain ΔAla with *N,N′*-disuccinimidyl carbonate (DSC) for the synthesis of novel cyclic opioid peptide [D-Ala$_L^2$, L-Ala$_L^5$]EA (**67, Scheme 1.13**). This enkephalinamide analogue was synthesized on MBHA resin by Boc/benzyl chemistry. The serine residue at position 2 on peptide **69** was then subjected to dehydration with a solution of *N,N′*-disuccinimidyl carbonate (DSC) in acetonitrile and 5% DIEA in DCM. The *S*-protecting group fluorenyl methyl (Fm) was cleaved by treatment with 20% piperidine/DMF and then subjected to 5% piperidine/DMF-DCM (40 mL, 1:1) overnight for the Michael addition to provide cyclic peptide **72**. The peptide **72** was then cleaved from the resin with anhydrous HF in the presence of anisole at 0 °C to furnish crude cyclic peptide [D-Ala$_L^2$, L-Ala$_L^5$]EA **67**.[31]

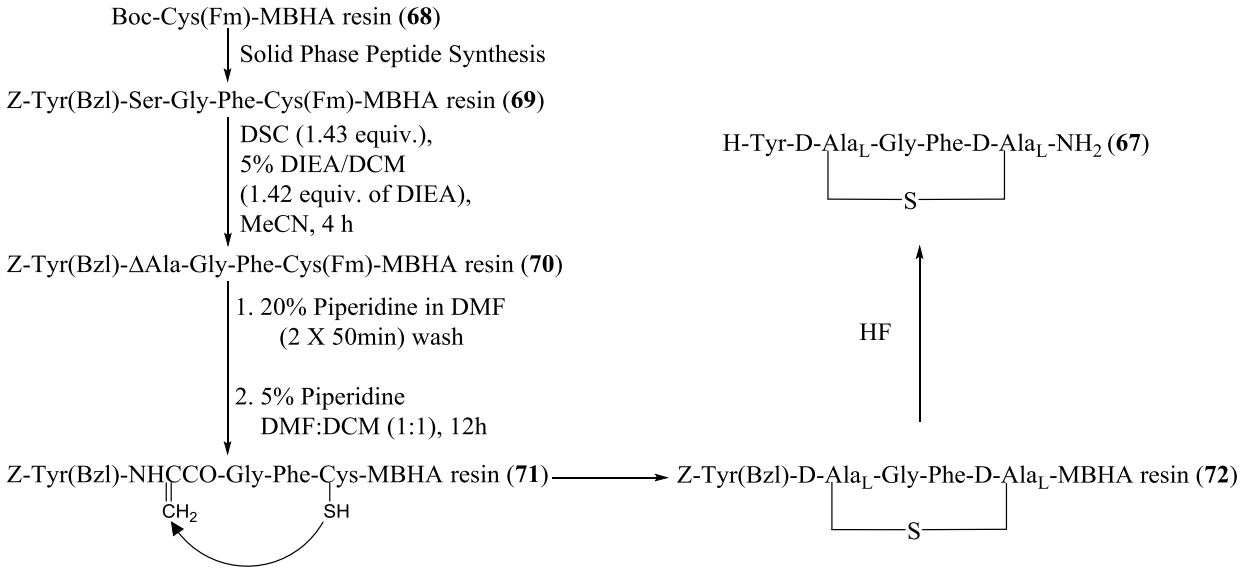


**Scheme 1.13.** On-resin dehydration of serine to ΔAla.

Bradley and co-workers reported the syntheses of a tripeptide and pentapeptide containing one and two dehydroalanine (ΔAla) residues respectively. They used asparagine as a precursor to the ΔAla residue. Peptides **73** and **74** were synthesized on the Merrifield resin by standard techniques (**Scheme 1.14**). The resin-bound peptides were then subjected to Hofmann degradation with bis(trifluoroacetoxy)iodobenzene (TIB) (1.5 equiv. for each asparagine) in the DMF/THF/$H_2O$ (1:1:1) solvent system for 10 min, followed by exposure to 1.5 equiv. of pyridine base for 2 h at rt. The washed resin was then treated with methyl iodide and potassium bicarbonate (10 equiv. for each asparagine) in methanol for 12 h to affect Hofmann elimination. Though the overall yields were quite ordinary for such short peptides (23% for the tripeptide **75** and 9% for the pentapeptide **76**), this method can be useful to synthesize branched peptides with the manipulation of the ΔAla residue.[32]

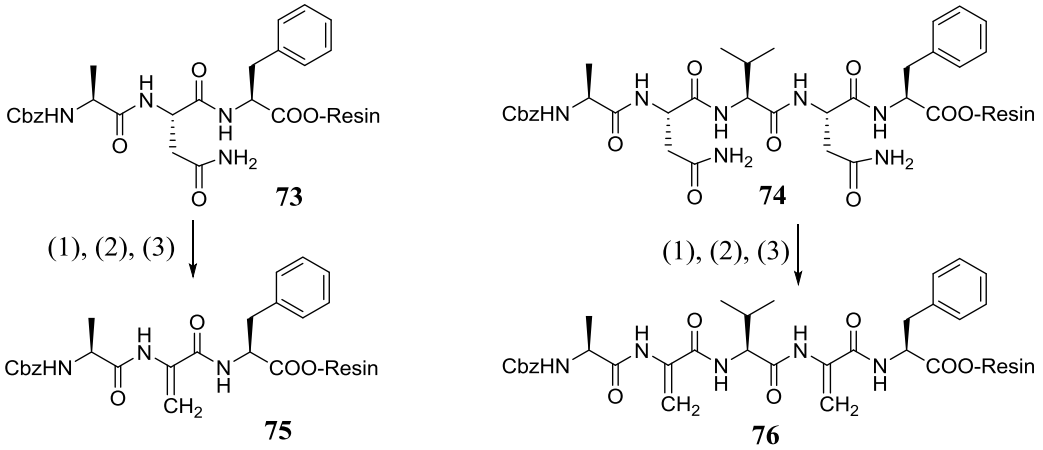


1. 1.5 equiv $PhI(O_2CCF_3)$, DMF:THF:$H_2O$ (1:1:1), after 10 min add 1.5 equiv. pyridine, 2h, rt
2. MeI (10 equiv.), $KHCO_3$ (10 equiv.), MeOH, 12 h, rt
3. 10% $NEt_3$ in MeOH, 12h, rt

**Scheme 1.14.** On-resin Hofmann degradation and elimination of asparagine to ΔAla.

Another method for the incorporation of dehydroalanine into peptides was reported by Horikawa et al. in 1998, wherein they utilized cysteine as a ΔAla precursor. They synthesized a few dipeptides on Merrifield resin by tethering the cysteine side chain to the resin. The polymer-bound cysteine could be elongated from either its N- or C- terminus.[33] *m*-Chloroperbenzoic acid (m-CPBA) mediated oxidation of sulfides **78** to sulfones **79** followed by elimination with DBU at 25 °C provided the desired peptides **80** in moderate to good yields (**Scheme 1.15**).[34]

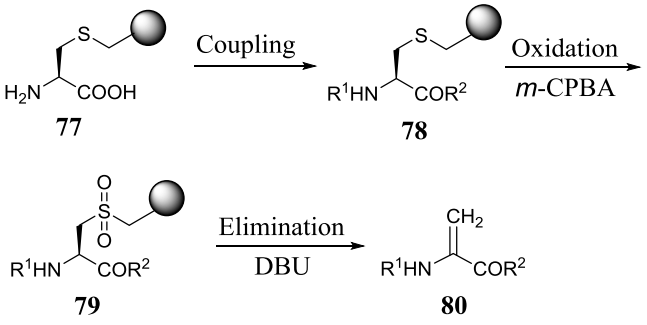


| | $R^1$ | $R^2$ |
|---|---|---|
| **a** | 1-Naphthyl-CO | $OCH_2Ph$ |
| **b** | Cbz-Phe | $OCH_2Ph$ |
| **c** | Boc | $NHCH_2Ph$ |
| **d** | Boc | Phe-OEt |

**Scheme 1.15.** Elimination of cysteine derived sulfones to ΔAla.

Similarly, Bradley and co-workers reported the synthesis of ΔAla via the elimination of an *S*-methylcysteine-derived sulfoxide with DBU or by thermolysis in solution. They utilized this strategy for the synthesis of the A-ring of subtilin (**81**) by coupling two peptide fragments: one containing two dehydroalanine residues generated from *S*-methylcysteine (**84**), and the other a dipeptide with a *S*-tritylcysteine (**85**, **Scheme 1.16**). Global deprotection and cyclization yielded cyclic peptide **81**. However, this methodology is not suitable if the peptide contains additional *S*-protected cysteine residues.[35]

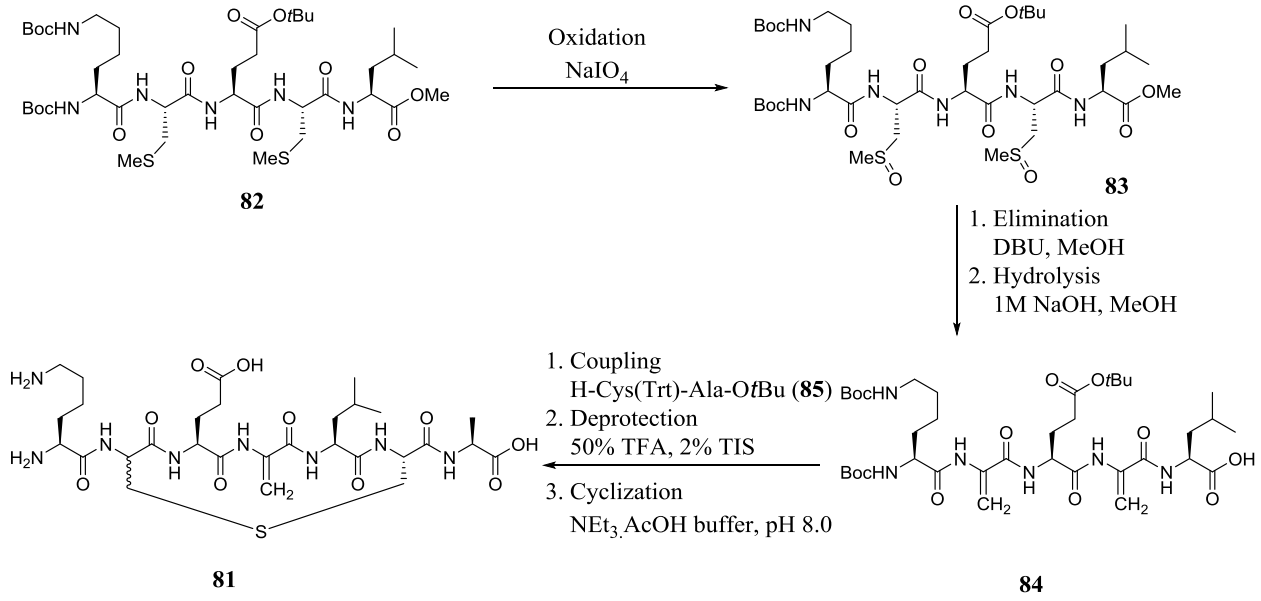


**Scheme 1.16.** Synthesis of ΔAla from *S*-methylcysteine.

Tam and co-workers reported a similar elimination protocol to generate linear and cyclic peptides, wherein *S*-cyanocysteine or *S*-methylcysteine sulfoxide furnished the ΔAla residue upon *β*-elimination.[36]

In order to overcome the limitation mentioned above, van der Donk and co-workers demonstrated that peptides containing ΔAla can be accessed in the presence of oxidation-sensitive residues like *S*-protected cysteine, methionine, and unprotected tryptophan by using

phenylselenocysteine (Sec(Ph)) as the precursor for ΔAla. Peptides were synthesized by standard Fmoc-*t*-Bu chemistry, deprotected (cysteine was left protected), and cleaved from the resin. The purified peptides **87** were subjected to oxidative elimination with $NaIO_4$ /$H_2O_2$ at 25 °C for 0.5–2 h in order to transform (Sec(Ph)) into ΔAla with good yields (**Scheme 1.17**).[37]

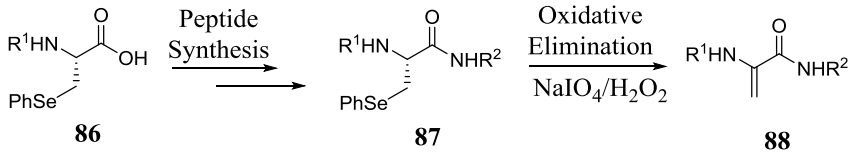


**86** **87** **88**

| Purified Substrates | Dehydropeptides **(88)** | Oxidant |
|---|---|---|
| Fmoc-GLPSec(Ph)VIA (**87a**) | Fmoc-GLPΔAlaVIA (**88a**) | $NaIO_4$ |
| Fmoc-ISVSec(Ph)RSTS (**87b**) | Fmoc-ISVΔAlaRSTS (**88b**) | $NaIO_4$ |
| Ac-GLPSec(Ph)VIA (**87c**) | Ac-GLPΔAlaVIA (**88c**) | $H_2O_2$ |
| Ac-ISVSec(Ph)RSTS (**87d**) | Ac-ISVΔAlaRSTS (**88d**) | $NaIO_4$ |
| Ac-GGC(S*t*Bu)PSec(Ph)VIA(**87e**) | Ac-GGC(S*t*Bu)PΔAlaVIA(**88e**) | $NaIO_4$ |
| LSec(Ph)PGC(Trt)VG (**87f**) | LΔAlaPGC(Trt)VG (**88f**) | $NaIO_4$ |
| $[LSec(Ph)ANCKI]_2$ (**87g**) | $[L\Delta AlaANCKI]_2$ (**88g**) | $NaIO_4$ |
| RIASec(Ph)IALC(S*t*Bu)K (**87h**) | RIAΔAlaIALC(S*t*Bu)K (**88h**) | $NaIO_4$ |

**Scheme 1.17.** Sec(Ph) as the precursor for ΔAla.

Even though this methodology has not been developed yet for oxidative elimination on the solid-support, these mild oxidation conditions are compatible with other amino acid functional groups like amines, guanidines, amides, alcohols and acids.

In 2001, Nakamura et al. reported the synthesis of AM-toxin II (**89**), a cyclic depsipeptide containing ΔAla. They developed a novel selenyl anchoring residue (a selenated alanine, **90**) which on oxidative cleavage with *tert*-butyl hydroperoxide (TBHP) solution reveals the ΔAla residue. Cyclization and oxidative elimination were performed on the resin to give AM-toxin II (**89**) from peptide **91** (**Scheme 1.18**).[38]

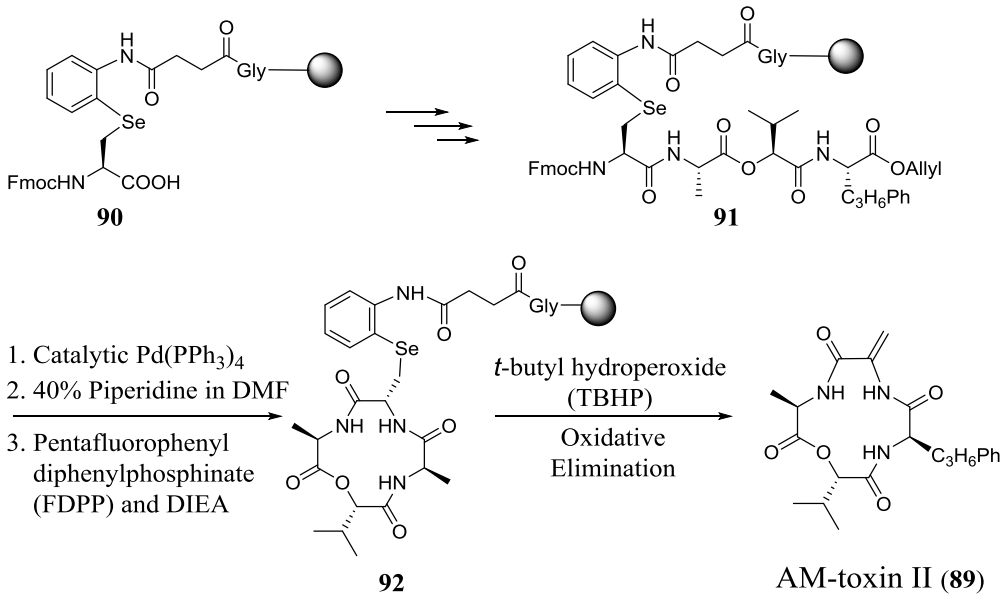


**Scheme 1.18.** Oxidative elimination of a selenated alanine to ΔAla.

In the same year, Albericio and co-workers reported the first EDC/CuCl-mediated dehydration of the resin-bound peptides Ac-Tyr(*t*Bu)-Gly-Thr-Phe-Leu-amide-linker-resin and Ac-Val-Phe-Thr-Val-amide-linker-resin to make thermodynamically stable *Z*-ΔAbu from threonine residues. They tried various reagents and conditions for on-resin elimination: DSC/DIEA, DSC/DABCO, DAST/DIEA, $Tos_2O$/DABCO, TosCl/DABCO, $PPh_3$/DEAD and EDC/CuCl. Other conditions did not lead to clean dehydration, whereas elimination with EDC (100 equiv.)/CuCl (30 equiv.) provided clean conversion of the Thr residue to *Z*-ΔAbu under $N_2$ over 2 weeks in DMF/DCM (1:1) at room temperature. Similarly, they successfully synthesized small peptides containing ΔAla and (*Z*)-ΔPhe from L-Ser and D, L- phenylserine respectively.[39]

This single step elimination protocol was subsequently used by them in the total synthesis of kahalalide F (**93**), an antitumor cyclic depsipeptide (**Scheme 1.19**). Kahalalide F (**93**) contains 13 amino acids and exhibits a *Z*-ΔAbu residue. The linear peptide **94** was synthesized on 2-chlorotrityl chloride-resin (Cl-Trt-Cl-resin), and the *Z*-ΔAbu precursor L-Thr was introduced unprotected. Elimination on solid-phase was performed by treating the resin-bound peptide **94**

with EDC (100 equiv.) and CuCl (60 equiv.) at rt for 6 days in DMF: DCM (5:1). The dehydration of unprotected L-Thr exclusively yielded the *Z*-ΔAbu.

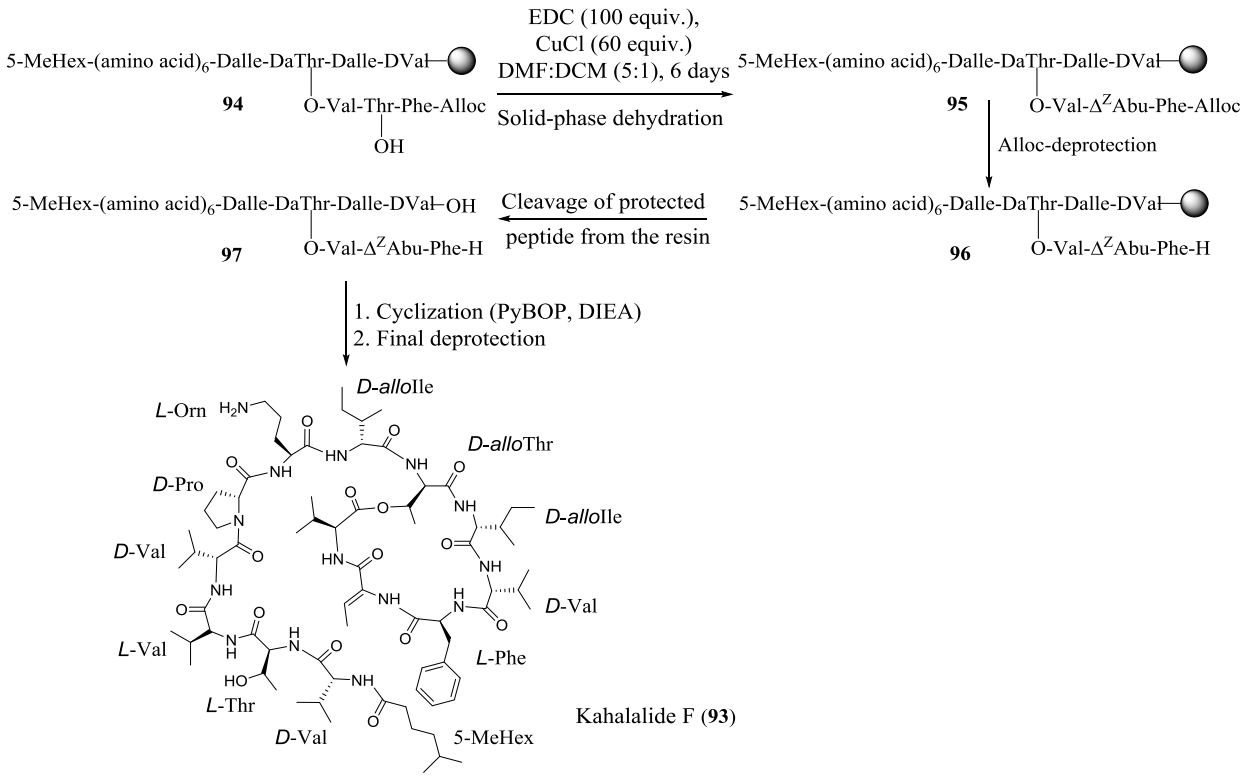


**Scheme 1.19.** On-resin dehydration of threonine to *Z*-ΔAbu in the total synthesis of Kahalalide F Cyclization and final deprotection were performed in solution on peptide **97** to yield kahalalide F (**93**) after Alloc deprotection and cleavage of the protected peptide from the resin (**96**) under very mild acid conditions.[40]

In 2003, Jiménez and Albericio further reported the utility of the same approach in the solid-phase synthesis of the *Z*-ΔPhe-containing phytotoxic cyclic peptide tentoxin (**8**). Herein, the dehydration of DL-phenylserine was performed on resin-bound peptide **98** with EDC (40 equiv.) and CuCl (20 equiv.) for 3 days in DMF (**Scheme 1.20**).[41]

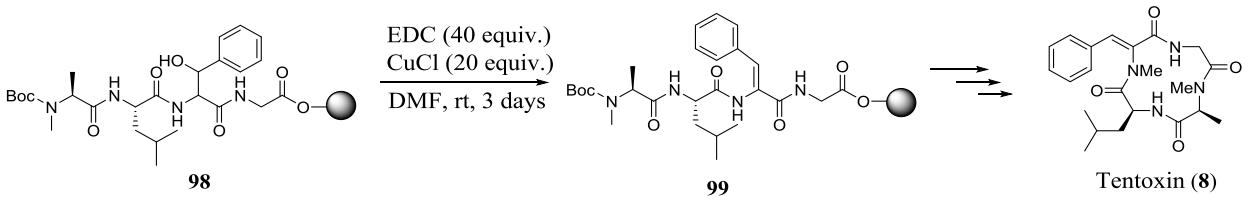


**Scheme 1.20.** Dehydration of DL-phenylserine to *Z*-ΔPhe.

Magos and co-workers reported the total synthesis of (–)-phenylahistin (**14**) and (–)-aurantiamine (**100**) on solid-phase (**Scheme 1.21**). These 2,5-diketopiperazines contain an isoprenylated *Z*-dehydrohistidine, which was constructed by the Horner–Wadsworth–Emmons protocol. Schmidt's phosphonate **102** was tethered to the modified Merrifield resin **101** and coupled to a *L*-amino acid (Phe or Val), followed by olefination with the aldehyde **106**. After Boc-deprotection, the base-promoted amidation yielded the desired natural targets **14** and **100** with their concomitant cleavage from the resin. This simple strategy was then used to create a library of dehydro-2,5-diketopiperazines (**108**–**113**) by varying the *L*-amino acid and the aromatic aldehyde. The mild olefination conditions mainly favored the *Z*-isomer of the dehydroamino acids formed except for with the *L*-proline containing compounds. Though the yields of these compounds are poor, Magos and co-workers were able to synthesize various trisubstituted aromatic dehydroamino acids by this method.[42]

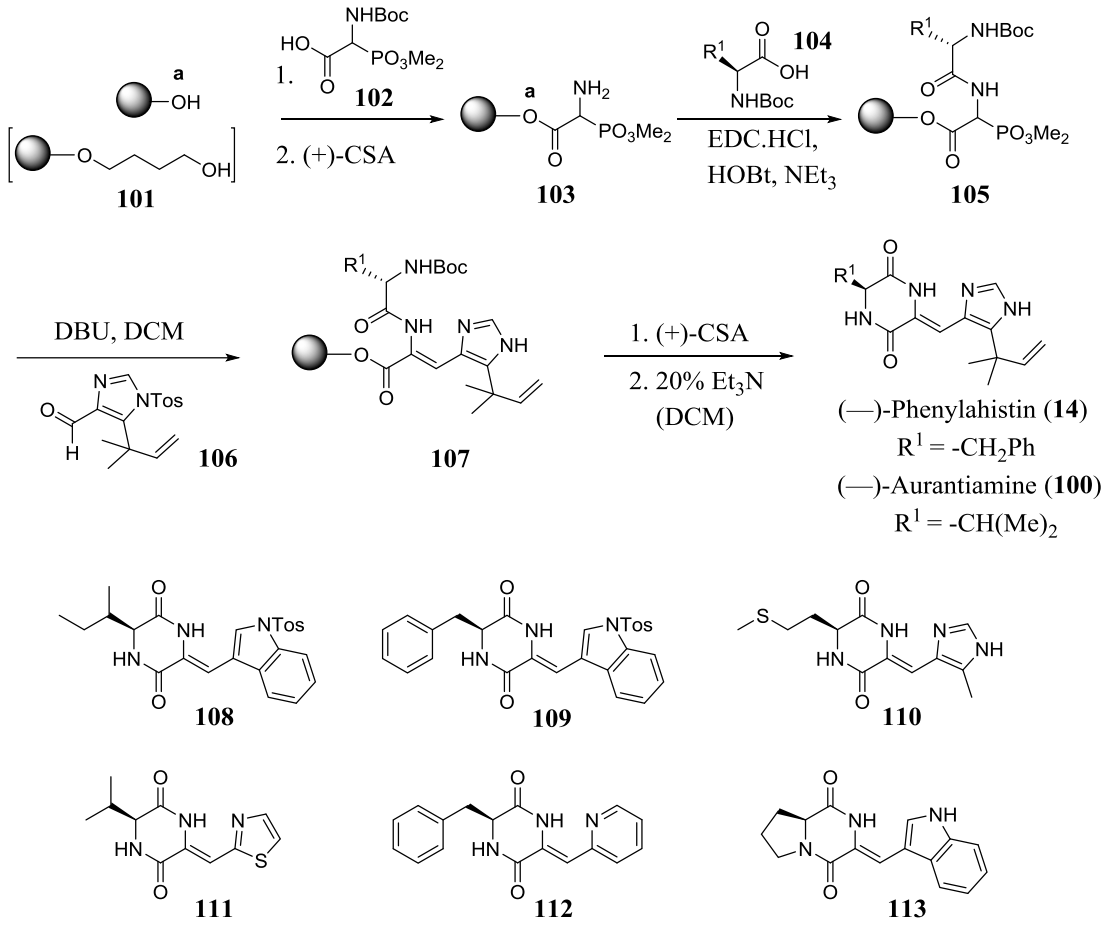


**Scheme 1.21.** On-resin synthesis of *Z*-ΔAA by Horner-Wadsworth-Emmons condensation.

Since the free amine (enamine) of a dehydroamino acid is weakly nucleophilic for the coupling reaction, the most widely applicable method for the introduction of dehydroamino acids in peptides is by coupling a small peptide (di- or tripeptide) containing a ΔAA to another peptide fragment. In 2011, Chauhan and co-workers synthesized several *Z*-ΔPhe containing cationic antimicrobial peptides (AMPs) on solid-phase via azlactone dipeptide coupling strategy. They synthesized several *Z*-ΔPhe containing azlactones by treating dipeptides of Fmoc-N$^{\alpha}$ amino acid (Lys(Boc)/Trp(Boc) /Ala) and DL-*threo*- β-phenylserine with anhydrous sodium acetate and acetic anhydride. These azlactones were then coupled to the growing resin-bound peptides overnight in DMF to incorporate the thermodynamically stable *Z*-ΔPhe isomer into the resin-bound peptides.[43]

Similarly, Castle and co-workers accomplished the solid-phase synthesis of four octapeptides (**114a–114d**) containing symmetrical bulky tetrasubstituted dehydroamino acids, namely dehydrovaline (ΔVal) and dehydroethylnorvaline (ΔEnv). They synthesized analogues of the C-terminal fragment of the anti-HIV agent enfuvirtide via the ring opening of azlactone dipeptides **115** by the resin-bound peptides **116** with catalytic DMAP at 60 °C in NMP over 24 h as shown (**Scheme 1.22**). Since Fmoc-protected dipeptide azlactones were unstable under the above conditions, they employed Alloc, an orthogonal protecting group compatible with the Fmoc/*t*-Bu solid-phase peptide chemistry that could be easily cleaved under neutral conditions without affecting the acid-sensitive side chain protecting groups. This is the first reported solid-phase synthesis of peptides containing tetrasubstituted dehydroamino acids and opens new avenues for the rapid synthesis of libraries of symmetrical tetrasubstituted dehydroamino-acid-containing peptides.[44]

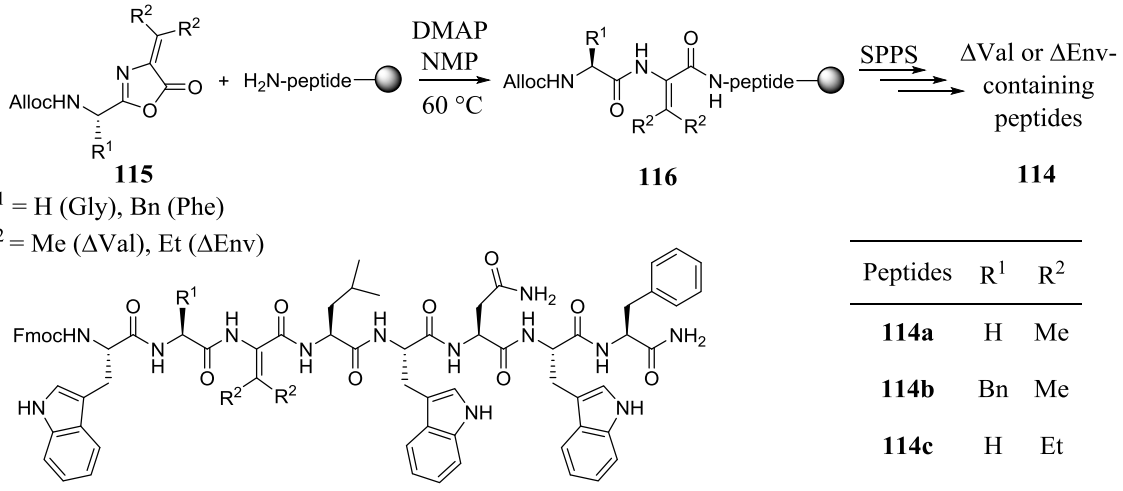


| Peptides | $R^1$ | $R^2$ |
|---|---|---|
| **114a** | H | Me |
| **114b** | Bn | Me |
| **114c** | H | Et |
| **114d** | Bn | Et |

**Scheme 1.22.** Solid-phase synthesis of octapeptides containing ΔVal and ΔEnv.

Yamashita and Inoue reported the solid-phase total synthesis of an *E*-ΔAbu-containing linear dodecapeptide bogorol A (**118**) in 2015 (**Scheme 1.23**). Bogorol A is active against methicillin resistant *Staphylococcus aureus* (MRSA, MIC = 2.5 μg/mL) and vancomycin resistant

*Enterococcus* spp. (VRE, MIC = 9 μg/mL). *E*-ΔAbu is the first amino acid from the *N*-terminus region and hence, the remaining eleven amino acids were very easily assembled on the *L*-valinol bound to the 2-chlorotrityl resin **119** in order to provide undecapeptide **120**. Vinyl azide **121** was then coupled to **120**, and this was followed by traceless Staudinger ligation with phosphine **123**. Acid-promoted global cleavage of the protecting groups and the peptide from the resin yielded bogorol A (**118**) in 30% overall yield.[45] This mild traceless Staudinger ligation protocol may be amenable to the solid-phase synthesis of peptides containing dehydroamino acids at any position in the peptides.[46]

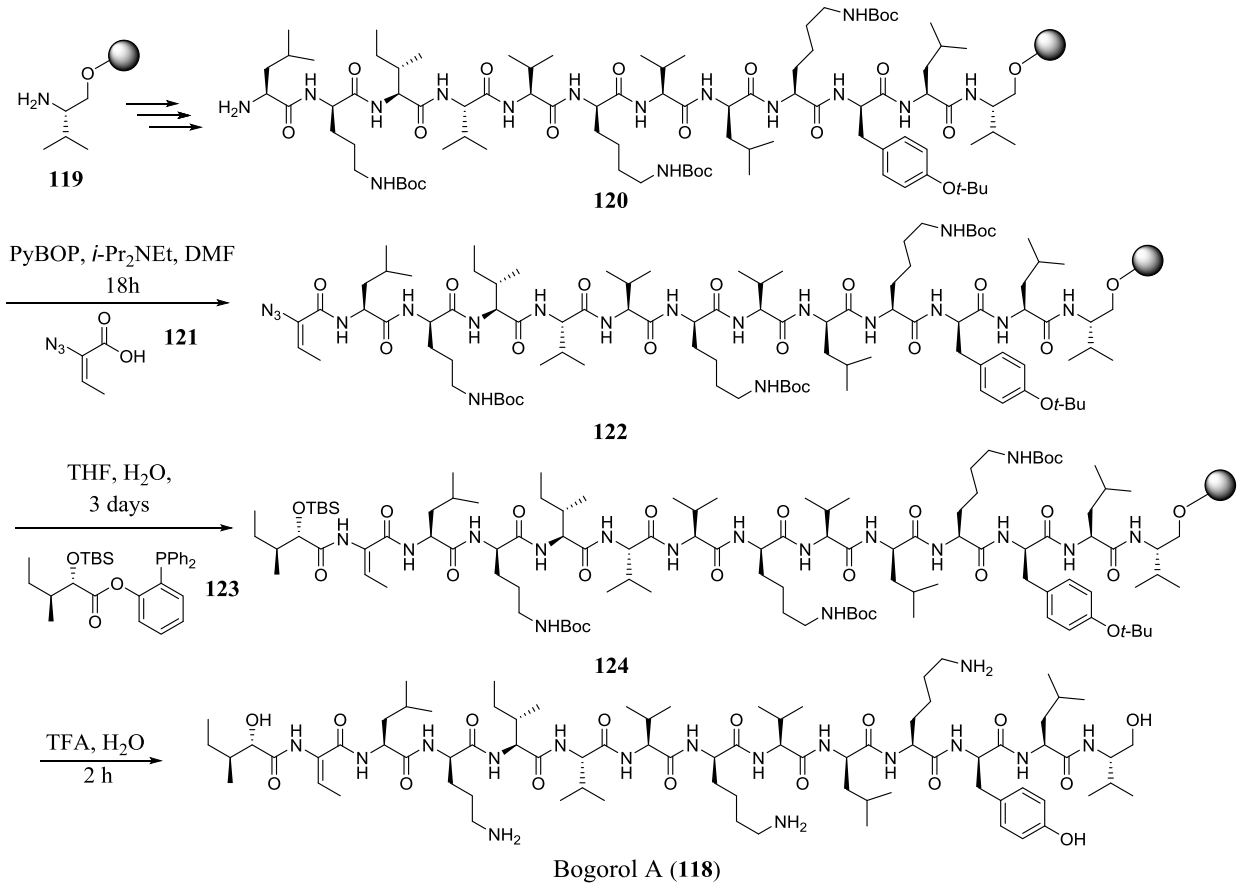


**Scheme 1.23.** On-resin synthesis of *E*-ΔAbu by mild traceless Staudinger ligation.

## 1.5 Conclusion

Natural products containing dehydroamino acids are of great importance because of their biological activities and unique chemical structures. Multiple methods have been discovered for the synthesis of dehydroamino acids and for their incorporation into peptides. In this chapter, we covered both the solution-phase and solid-phase methods available for the formation of ΔAAs. It is important to mention that the synthesis of asymmetrical ΔAAs is quite challenging when the desired geometrical isomer is not the thermodynamically favored isomer. Currently, there is only one solid-phase protocol available for the incorporation of bulky tetrasubstituted symmetrical dehydroamino acids. Rapid solid-phase synthesis of peptides containing ΔAAs can increase the types of peptidomimetics available to explore the secondary structures of peptides, and can potentially confer diverse therapeutic benefits.

## 1.6 References


1. a) Nandel, F. S; Sahrawat, T. R. *Biopolymers*, **2009**, *92*, 44; b) Jiang, J.; Ma, Z.; Castle, S. L. *Tetrahedron* **2015**, 71, 5431.

2. Breukink, E.; Wiedemann, I.; van Kraaij, C.; Kuipers, O. P.; Sahl, H. G.; de Kruijff, B. *Science* **1999**, *286*, 2361.

3. a) Sano, T.; Bewattie, K. A.; Codd, G. A.; Kaya K. *J. Nat. Prod.* **1998**, *61*, 851; b) Sano, T.; Kaya, K. *Tetrahedron* **1998**, *54*, 463; c) An, T.; Kumar, T. K. S.; Wang, M.; Liu, L.; Gantar, J. O. L. M.; Marks, V.; Gawley, R. E.; Rein, K. S. *J. Nat. Prod.* **2007**, *70*, 730.

4. a) Khokhlov, A. S., Lokshin G. B. *Tetrahedron Lett.* **1963**, 1881; b) Wang, P.; Xi, L.; Liu, P.; Wang, Y.; Wang, W.; Huang, Y.; Zhu, W. *Mar. Drugs* **2013**, *11*, 1035; c) Fukushima, K.; Yazawa, K.; Arai, T. *J. Antibiot.* **1973**, *26*, 175.

5. Cavelier, F.; Verducci, J.; André, F.; Haraux, F.; Sigalat, C.; Traris, M.; Vey, A. *Pestic. Sci*. **1998**, *52*, 81.

6. a) Maruyama, K.; Ohuchi, T.; Yoshida, K.; Shibata, Y.; Sugawara, F.; Arai, T. *J. Biochem*. **2004**, *136*, 81; b) Sheehan, J. C.; Mania, D.; Nakamura, S.; Stock, J. A.; Maeda, K. *J. Am. Chem. Soc.*

**1968**, *90*, 462; c) Davidson, B. S. *Chem. Rev.* **1993**, *93*, 1771; d) Chandrasekhar, S.; Sultana, S. S. *Tetrahedron* **2000**, *56*, 3679; e) Rahman, K. M.; Hossain, M. D.; Sohrab, M. H.; Drake, A. F.; Bui, T. T.; Husby, J.; Gunaratnam, M.; Neidle, S.; Hasan, C. M.; Thurston, D. E. *Chem. Commun.* **2012**, *48*, 8760.

7. a) Kanoh, K.; Kohno, S.; Asari, T.; Harada, T.; Katada, J.; Muramatsu, M.; Kawashima, H.; Sekiya, H.; Uno, I. *Bioorg. Med. Chem. Lett.* **1997**, *7*, 2847; b) Kanoh, K.; Kohno, S.; Katada, J.; Hayashi, Y.; Muramatsu, M.; Uno, I. *Biosci. Biotechnol. Biochem*. **1999**, *63*, 1130; c) Kanoh, K.; Kohno, S.; Katada, J.; Takahashi, J.; Uno, I. *J. Antibiot.* **1999**, *52*, 134; d) Nazari, S. H.; Bourdeau, J. E.; Talley, M. R.; Valdivia-Berroeta, G. A.; Smith, S. J.; Michaelis, D. J. *ACS Catal.* **2017**, *8*, 86.

8. Ravizzini, R. A.; Andreo, C. S.; Vallejos, R. H. *Plant Cell Physiol.* **1977**, *18*, 701.

9. Irschik, H.; Reichenbach, H. *J. Antibiot.* **1985**, *38*, 1237.

10. Ueoka, R.; Ise, Y.; Ohtsuka, S.; Okada, S.; Yamori, T.; Matsunaga, S. *J. Am. Chem. Soc.* **2010**, *132*, 17692.

11. Morimoto, K.; Shimada, N.; Naganawa, H.; Takita, T.; Umezawa, H. *J. Antibiot.* **1982**, *35*, 378.

12. a) Edgar, L. E.; Culvenor, C. C. J. *Biochem. Pharmacol.* **1987**, *36*, 2133; b) Ludueña, R. F.; Roach, M. C.; Prasad, V.; Lacey, E. *Biochem. Pharmacol.* **1990**, *39*, 1603; c) Mitra, A.; Sept, D. *Biochemistry* **2004**, *43*, 13955.

13. Hajduk, P. J.; Greer, J. *Nat. Rev. Drug Discovery* **2007**, *6*, 211.

14. Kaur, H.; Heapy, A. M.; Brimble, M. A. *Org. Biomol. Chem.*, **2011**, *9*, 5897.

15. Doherty, D. G.; Tietzman, J. E.; Bergmann, M. *J. Biol. Chem.***1943**, *147*, 617.

16. Shin, C.; Chigira, Y.; Masaki, M.; Ohta, M. *Tetrahedron Lett.* **1967**, *8*, 4601.

17. a) Shin, C.; Yonezawa, Y.; Unoki, K.; Yoshimura, J. *Tetrahedron Lett.* **1979**, *20*, 1049; b) Broda, M. A.; Ciszak, M. A.; Kozioł, A. E.; Pietrzyński, G.; Rzeszotarska B. *J. Pept. Sci.* **2006**, *12*, 538.

18. Konno, S.; Stammer, C. H. *Int. J. Pept. Protein Res.* **1978**, *12*, 222.

19. a) Goodall, K.; Parsons, A. F. *Tetrahedron Lett.* **1995**, *36*, 3259; b) Shangguan, N.; Joullie, M. M. *Tetrahedron Lett.* **2009**, *50*, 6755.

20. Somekh, L.; Shanzer, A. *J. Org. Chem.* **1983**, *48*, 907.

21. Sai, H.; Ogiku, T.; Ohmizu, H. *Synthesis* **2003**, *2*, 201.

22. Yasuno, Y.; Hamada, T.; Yamada, T.; Shinada, T.; Ohfune, Y. *Eur. J. Org. Chem.* **2013**, 1884.

23. Hamada, M.; Shinada, T.; Ohfune, Y. *Org. Lett.* **2009**, *11*, 4664.
24 a) Nakatsuka, S.; Tanino, H.; Kishi, Y. *J. Am. Chem. Soc.* **1975**, *97*, 5008; b) Nakatsuka, S.; Tanino, H.; Kishi, Y. *J. Am. Chem. Soc.* **1975**, *97*, 5010.

25. Stohlmeyer, M. M.; Tanaka, H.; Wandless, T. J. *J. Am. Chem. Soc.* **1999**, *121*, 6100.

26. Jiang, L.; Job, G. E.; Klapars, A.; Buchwald, S. L. *Org. Lett.* **2003**, *5*, 3667.

27. Kuranaga, T.; Sesoko, Y.; Sakata, K.; Maeda, N.; Hayata, A.; Inoue, M. *J. Am. Chem. Soc.* **2013**, *135*, 5467.

28. Ma, Z.; Jiang, J.; Luo, S.; Cai, Y.; Cardon, J. M.; Kay, B. M.; Ess, D. H.; Castle, S. L. *Org. Lett.* **2014**, *16*, 4044.

29. Yokokawa, F.; Shioiri, T. *Tetrahedron Lett.* **2002**, *43*, 8679.

30. Fisher, G. H.; Berryer, P.; Ryan, J. W.; Chauhan, V.; Stammer, C. H. *Arch. Biochem. Biophys.* **1981**, *211*, 269.

31. Polinsky, A.; Cooney, M. G.; Toy-Palmer, A.; Osapay, G.; Goodman, M. *J. Med. Chem.***1992**, *35*, 4185.

32. Blettner, C.; Bradley, M. *Tetrahedron Lett*. **1994**, *35*, 467.

33. Delaet, N. G. J.; Tsuchida, T. *Letters in Peptide Science* **1995**, *2*, 325.

34. Yamada, M.; Miyajima, T.; Horikawa, H. *Tetrahedron Lett.* **1998**, *39*, 289.

35. a) Burrage, S.; Raynham, T.; Williams, G.; Essex, J. W.; Allen, C.; Cardno, M.; Swali, V.; Bradley, M. *Chem*. *Eur. J*. **2000**, *6*, 1455; b) Burrage, S. A.; Raynham, T.; Bradley, M. *Tetrahedron Lett.* **1998**, *39*, 2831.

36. Tam, J. P.; Miao, Z. *Org. Lett.* **2000**, *2*, 3711.

37. Okeley, N. O.; Zhu, Y.; van der Donk, W. A. *Org. Lett.* **2000**, *2*, 3603.

38. Horikawa, E.; Kodaka, M.; Nakahara, Y.; Okuno, H.; Nakamura, K. *Tetrahedron Lett.* **2001**, *42*, 8337.

39. Royo, M.; Jiménez, J. C.; López-Macià, A.; Giralt, E.; Albericio, F. *Eur. J. Org. Chem.* **2001**, 45.

40. López-Macià, A.; Jiménez, J. C.; Royo, M.; Giralt, E.; Albericio, F. *J. Am. Chem. Soc.* **2001**, *123*, 11398.

41. Jiménez, J. C.; Chavarría, B.; López-Macià, A.; Royo, M.; Giralt, E.; Albericio, F. *Org. Lett.* **2003**, *5*, 2115.

42. Couladouros, E. A; Magos, A.D. *Mol. Diversity* **2005**, *9*, 111.

43. Pathak, S.; Chauhan, V. S. *Antimicrob. Agents Chemother.* **2011**, *55*, 2178.

44. Jiang, J.; Luo, S.; Castle, S. L. *Tetrahedron Lett.* **2015**, *56*, 3311.

45. Yamashita, T.; Kuranaga, T.; Inoue, M. *Org. Lett.* **2015**, *17*, 2170.

46. Yamashita, T.; Matoba, H.; Kuranaga, T.; Inoue, M. *Tetrahedron* **2014**, *70*, 7746.

# 2 RATIONAL DESIGN AND SYNTHESIS OF $\beta$-HAIRPIN PEPTIDES

## 2.1 Introduction

Proteins are among the most important complex biomolecules synthesized by living cells, and are essential for most of the work done by the cells. Proteins are responsible for the structure, function, transportation, biocatalysis, immunity, regulation and maintenance of tissues and organs. Proteins are the key components of spider silk, elk antlers and bacterial flagella. Spider silk is much stronger than steel, whereas bacterial flagella are microscopic motors. Hence, thermodynamically stable primary and secondary structures are very vital for the folding of proteins into highly functionalized and well-ordered tertiary and quaternary structures.

The *de novo* design of peptides and proteins is of considerable interest to the scientific community. Rational design and development of peptides as potent agonists or antagonists of protein-protein interactions may lead to medicinal agents with improved pharmacological and physico-chemical properties. Apart from utility in the field of medicine, the practical designing of peptides and proteins can vastly improve the understanding of their folding preferences. Short-range interactions are comprised of the unique conformational propensity of each amino acid and interactions of its side chain with the backbone and the side chains of adjacent residues. These interactions are essential for the determination of preferred conformations. Peptides can adopt a large number of possible conformations in order to attain the preferred short-range effects. Hence,

it is significant to devise new strategies to rigidify the peptide backbone to limit the number of desired peptide conformations.[1]

## 2.2 Conformational studies of peptides containing α,β-dehydroamino acids (ΔAAs)

As dehydroamino acids can impart proteolytic stability to a peptide, they are a very attractive tool for the synthesis of stable secondary structures. In the last few decades, α,β-dehydroamino acids (ΔAAs) have been used to constrain peptide conformations because of their rigidifying conjugated $C_\alpha$=$C_\beta$ π system and steric bulkiness. ΔAla tends to form extended conformations, whereas tri- and tetrasubstituted ΔAA residues have been shown to form stable secondary structures because of their relatively bulkier β substituents.[2] Considerable research has been done in the last few decades to investigate the role of ΔAAs in the stability of *α*-helices, $3_{10}$-helices and *β*-turns.

### 2.2.1 Conformational studies of peptides containing trisubstituted ΔAAs

Several trisubstituted dehydroamino acid containing peptides were studied in the 1980's and 1990's for their conformational preferences. X-ray crystal structures of 19 peptides with either ΔPhe or ΔLeu were studied by Singh et al. in 1990. They revealed that these dehydroamino acid residues can be suitable inducers for type II *β*-turns and that consecutive ΔPhe residues can induce a helix.[3] In their extensive review of 49 peptide units containing ΔAA residues, Singh and co-workers detailed that small peptide units like **124–127** can adopt type II *β*-turns when a ΔAA is placed at either the (*i*+1) or (*i*+2) position (**Table 1.**).[4] The ideal *φ* and *ψ* values in a type II *β*-turn are: –60° and 120° (*i+1* residue) and 80° and 0° (*i+2* residue).

**Table 2.1.** ΔAAs at *i+1/ i+2* positions of *β*-turns.

| **Peptides (ΔAA position)** | **φ** | **ψ** |
|---|---|---|
| Ac-ΔPhe-$NHCH_3$ (**124**)( ΔPhe at *i+1*) | –58.3 | 148 |
| Ac-ΔPhe-Ala-OH.$H_2O$ (**125**) (ΔPhe at *i+1*) | –68 | 147 |
| Boc-Gly-ΔPhe-$NHCH_3$ (**126**) (ΔPhe at *i+2*) | 71.5 | 7.2 |
| Boc-Pro-ΔLeu-$NHCH_3$ (**127**) (ΔLeu at *i+2*) | 74 | 8 |

They also observed the formation of $3_{10}$-helices by ΔAA-containing peptides longer than four residues. Peptides containing a single (*Z*)-ΔPhe residue do not adopt an optimum $3_{10}$-helical conformation, but peptides containing more than one (*Z*)-ΔPhe can adopt a well-formed $3_{10}$-helix with intramolecular hydrogen bonds that are suitably oriented except at the termini.[5]

Singh et al. observed that two consecutive (*Z*)-ΔPhe segments at the (*i+2*) and (*i+3*) positions in small peptides promote a stable $3_{10}$-helical conformation. If two repeating units of consecutive (*Z*)-ΔPhe residues are separated by a saturated amino acid residue as in Boc-Val-*Z*-ΔPhe-*Z*-ΔPhe-Val-*Z*-ΔPhe-*Z*-ΔPhe-Val-$OCH_3$ (**128**), the $3_{10}$-helical structure formed is highly stable and does not fray at the two termini which is otherwise usually observed (**Table 2.**).[6] Residues in a $3_{10}$-helix typically adopt $\varphi$ and $\psi$ values of –49° and –29°.

**Table 2.2.** Torsional angles of ΔPhe in the $3_{10}$-helix **128**.

| Peptide | $\varphi$ | $\psi$ |
|---|---|---|
| Boc-Val[1]-ΔPhe[2]-ΔPhe[3]-Val[4]-ΔPhe[5]-ΔPhe[6]-Val[7]-$OCH_3$ | –54.6 ($i$+2)[2]<br>–52.2 ($i$+3)[3]<br>–61.5 ($i$+2)[5]<br>–49.7 ($i$+3)[6] | –18.7 ($i$+2)[2]<br>–17.5 ($i$+3)[3]<br>–7.9 ($i$+2)[5]<br>–30.9 ($i$+3)[6] |

Note: Superscripts denote the residue positions

Chauhan and co-workers prepared several peptides containing two or three ΔPhe residues, which adopted a right-handed $3_{10}$-helical structure. They demonstrated that two consecutive ΔPhe residues (Boc-Leu-*Z*-ΔPhe-*Z*-ΔPhe-Ala-Phe-NHMe) or two ΔPhe residues separated by 1–3 saturated amino acids (Boc-Gly-*Z*-ΔPhe-Leu-*Z*-ΔPhe-Ala-NHMe, Boc-Val-*Z*-ΔPhe-Leu-Ala-*Z*-ΔPhe-Ala-OMe and Boc-Val-*Z*-ΔPhe-Phe-Ala-Phe-*Z*-ΔPhe-Val-*Z*-ΔPhe-Gly-$OCH_3$) can induce formation of right handed $3_{10}$-helices. The nonapeptide Boc-Val-ΔPhe-Phe-Ala-Phe-ΔPhe-Val-ΔPhe-Gly-OMe (**129**) contains seven overlapping type III $\beta$-turns because of seven ($i$+3)→($i$) intramolecular hydrogen bonds and adopts a right-handed $3_{10}$-helix.[7]

Mathur and Chauhan studied antimicrobial peptides that adopt helical conformations. So, they postulated that the introduction of *Z*-ΔPhe may stabilize the helical structures further and synthesized cecropin-mellitin hybrid peptides. They synthesized three analogues of cecropin-mellitin hybrid peptide CAMEL0 (Lys-Trp-Lys-Leu-Phe-Lys-Lys-Ile-Gly-Ala-Val-Leu-Lys-Val-Leu) and found that CAMELΔPhe2 (Lys-Trp-Lys-Leu-ΔPhe-Lys-Lys-Ile-Gly-Ala-Val-ΔPhe-Lys-Val-Leu) has much better antimicrobial activity than the parent peptide CAMEL0. CAMELΔPhe2 adopts a $3_{10}$-helix and a β-turn.[8] Chauhan et al. synthesized a lysine-based branched dimer ΔFd, growing from both α and ε amino groups of $lys_{10}$. This cationic dimer ΔFd (Ac-G-ΔPhe-R-K-ΔPhe-H-K-ΔPhe-W-A-K (amide $NH_2$)-A-W-ΔPhe-K-H-ΔPhe-K-R-ΔPhe-G-

Ac) (**130**) exhibited potent antimicrobial activity against *E. coli* (MIC of 2.5 μM) and *S. aureus* (MIC of 5.0 μM) and is noncytotoxic (**Figure 2.1**).[9]

In 2011, Chauhan and co-workers reported the synthesis of amphipathic helical peptide VS2 (**131**) which is very active against Gram-negative bacteria (MIC of 5.0 μM) and causes very low hemolysis. This noncytotoxic undecapeptide has good cell permeability, and can depolarize the bacterial membrane. Such proteolytically stable, short antimicrobial peptides can usher in a new era in the discovery and development of novel antimicrobials (**Figure 2.1**).[10]

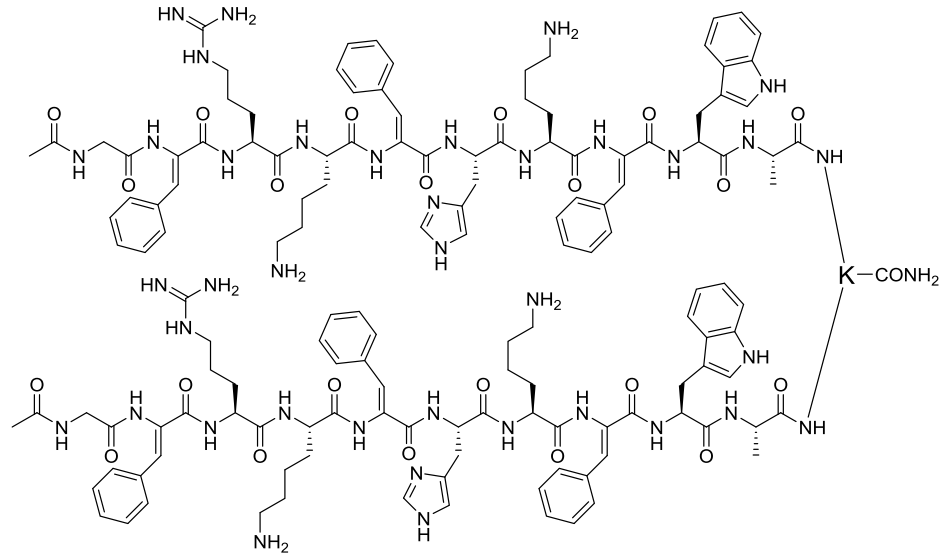

ΔFd (**130**)

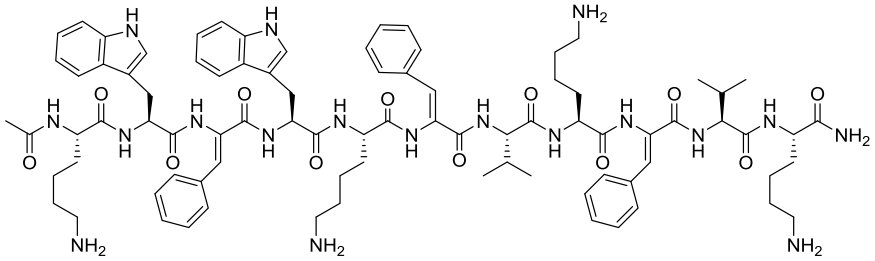

VS2 (**131**)

**Figure 2.1.** Dimer ΔFd (**130**) and VS2 (**131**).

It has been reported that *β*-sheet breakers can prevent the aggregation or formation of *β*-amyloid fibrils. Short peptides containing Pro and Aib residues can inhibit the amyloid

fibrillization.[11] Chauhan and co-workers synthesized two analogues of the 16–20 fragment (Ac-K-L-V-F-F-$NH_2$) of the A$\beta$ sequence, which is implicated in the transformation of A$\beta$ monomers to amyloid fibrils. The electron microscopic studies of these two analogues **132** (Ac-K-L-ΔPhe-V-F-$NH_2$) and **133** (Ac-K-L-V-ΔPhe-F-$NH_2$) revealed their potent antifibrillizing activity.[12] Similarly, Giordano et al. reported the synthesis of pentapeptides **134-135** containing two consecutive ΔPhe residues, which can prevent the formation of amyloid fibrils (**Figure 2.2**).[13] Mishra and Chauhan also reported the synthesis of two short peptides **136** and **137**, which could prevent the fibrillization of human islet amyloid polypeptide (hIAPP). hIAPP fibrillization leads to the formation of oligomers that are toxic to the pancreatic β-cells and can cause Type 2 diabetes. X-ray crystallography of peptide **136** showed that it adopts a type I $\beta$-turn in crystal form.[14]

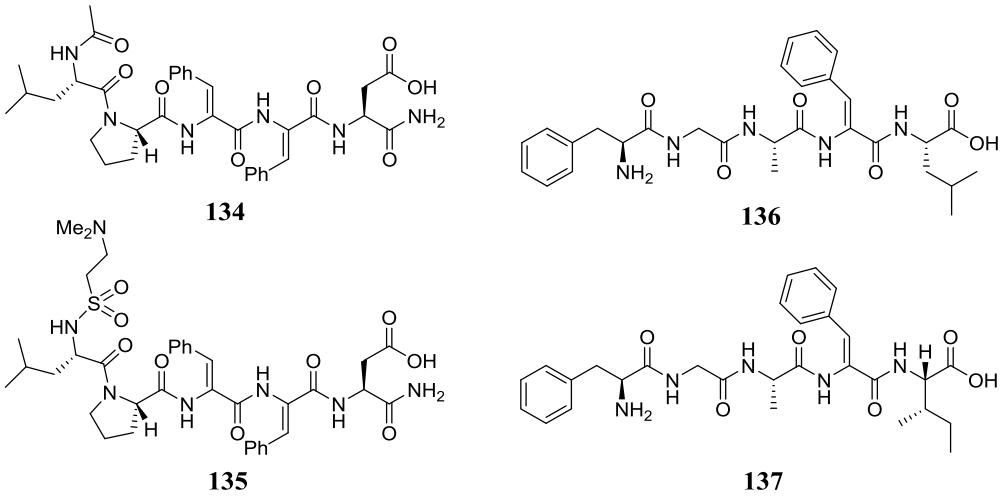


**Figure 2.2.** $\beta$-sheet breakers.

### 2.2.2 Conformational studies of peptides containing tetrasubstituted ΔAAs

Since bulky tetrasubstituted $\alpha,\beta$-dehydroamino acids are hard to construct, their roles in the conformational preferences of peptides are underexplored. Nonetheless, a few studies were performed and revealed the turn-inducing potential of some tetrasubstituted ΔAAs. Rzeszotarska et al. showed that ΔVal at the (*i+2*) position of dipeptide **138** can induce a type III $\beta$-turn, whereas

Singh and coworkers reported that ΔVal in dipeptide **139** can adopt suitable $\varphi$ (–44.2°) and $\psi$ (135.9°) angles for incorporation at the (*i*+*1*) position of a type II $\beta$-turn (**Figure 2.3**).[15]

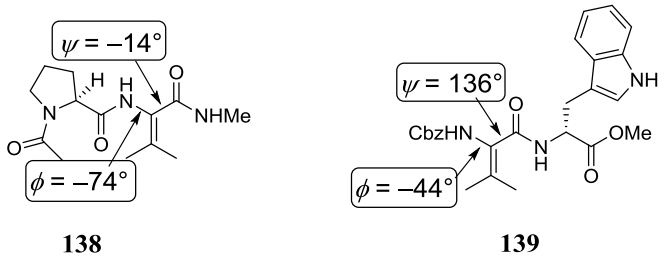


**138** **139**

**Figure 2.3.** Promotion of $\beta$-turns by ΔVal.

Further, in 2003 Vijayaraghavan and Singh reported the inclusion of ΔVal and ΔIle at the (*i*+*1*) position of a type II $\beta$-turn in two tripeptides Cbz-ΔVal-Ala-Leu-OMe (**140)** and Cbz-*Z*-ΔIle-Ala-Leu-OMe (**141)**.[16] The X-ray crystallographic studies of these peptides reveal that both the peptide structures were stabilized by intramolecular (*i*+*3*)→(*i*) hydrogen bonds between the NH (amide) of Leu and the O of the carbobenzoxy (Cbz) group. Corroborating the studies of Singh and co-workers, Rzeszotarska et al. reported the preference of ΔVal to adopt very ideal (*i*+*1*) torsional angles ($\varphi$ = –60° and $\psi$ = 125°) in Ac-ΔVal-$NMe_2$ (**142**) to form a type II/VIa $\beta$-turn (**Figure 2.4**).[17]

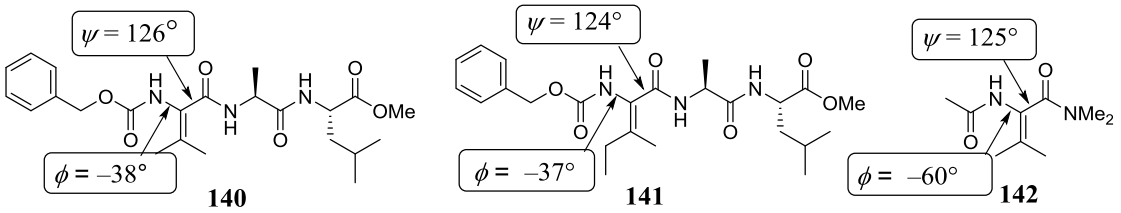


**140** **141** **142**

**Figure 2.4.** Induction of type II $\beta$-turn.

Apart from the conformational preference for $\beta$-turns, Singh et al. also showed that a ΔVal at (*i*+*1*) and ΔPhe at (*i*+*3*) positions can induce a $3_{10}$-helical conformation in similar fashion to the

incoroporation of two or more ΔPhe residues. A ΔVal residue at the (*i+1*) position favors a type II-*β*-turn and a ΔPhe surrounded by branched *β*-carbon amino acids prefers unfolded conformations, but their unique combination in Cbz-ΔVal-Val-ΔPhe-Ile-OMe adopts a $3_{10}$-helical conformation.[18]

### 2.3 *β*-Hairpins

Most of the protein secondary structures observed in nature can be categorized as α-helices, *β*-turns and antiparallel *β*-sheets. Folding of proteins to the correct single structures is very vital for cellular functions, and misfolding is very often associated with diseases or disorders. α-Helices and *β*-turns are widely studied, and our understanding of the noncovalent forces that can induce or stabilize such secondary structures has improved. However, *β*-sheets have been less explored owing to the lack of a good model system for their studies. Hence, investigating the factors that govern *β*-sheet formation can help in the rational *de novo* design of new peptides or proteins with medicinal activities and better understanding of the pathological conditions caused by protein aggregation or misfolding.

A *β*-hairpin, constituting two short antiparallel *β*-strands with a connecting loop, is a minimum representation of a *β*-sheet. Along with the turn sequence, the strand sequence has also been shown to be significant in the formation of a stable *β*-hairpin. Since the discovery of the first *β*-hairpin by Blanco et al. in 1993, several guidelines have emerged for the formation of stable *β*-hairpins.[19] The turn sequence (residues at *i+1 and i+2*) is one of the most important factors in the formation of the *β*-turn, but the *β*-sheet propensities of the strand residues and interstrand sidechain–sidechain interactions are also significant for the genesis of a stable *β*-hairpin.[20] Studies by Sibanda et al. have shown that type I and type II are usually associated with *β*-turns, but a *β*-hairpin (two-residue loop) formation typically requires type I' and type II' *β*-turns in order to be

compatible with the right-handed twist of the $\beta$-sheets.[21] Ramírez-Alvarado and coworkers designed a dodecapeptide (BH8, $NH_2$-RGITVNGKTYGR-$NH_2$) with asparagine-glycine in the loop. NMR data revealed that BH8 exhibited 37% folded population at 274 K in water and formed a type I' $\beta$-turn.[22]

L-Pro at the ($i+1$) position in a loop is known to strongly favor type I/II $\beta$-turns and hence, should not be amenable to the formation of a $\beta$-hairpin with a two-residue loop. In early 1996, Haque and Gellman reported that D-Pro-D-Ala/D-Pro-Gly in tetrapeptides (Ac-L-Val-D-Pro-Gly-L-Leu-$NMe_2$ and Ac-L-Val-D-Pro-D-Ala-L-Leu-$NMe_2$) and analogous depsipeptides induced $\beta$-hairpin formation.[23] Shortly thereafter, Balaram et al. reported the formation of a type II' $\beta$-turn in octapeptide **143** containing a D-Pro-Gly loop (Boc-Leu-Val-Val-D-Pro-Gly-Leu-Val-Val-OMe). X-ray crystallography of this octapeptide revealed four intramolecular hydrogen bonds between the two strands and favorable torsional angles for a type II' $\beta$-turn: $\varphi_{i+1} = +53°$ and $\psi_{i+1} = -132°$ for D-Pro and $\varphi_{i+2} = -96°$ and $\psi_{i+2} = +9°$ for Gly (the ideal values are $\varphi_{i+1} = +60°$, $\psi_{i+1} = -120°$ and $\varphi_{i+2} = -80°$, $\psi_{i+2} = 0°$).[24] Supporting their earlier study, Gellman et al. established that D-Pro-Gly can induce stable $\beta$-hairpin formation by incorporating this turn sequence in the N-terminal segment of ubiquitin, MQIFVKTLTGKTITLEV (**144**). They slightly modified the strand sequence of **144** and also introduced D-Pro-Gly instead of the LTG turn (three-residue loop) to obtain the 16-mer MQIFVKSpGKTITLKV-$NH_2$ (**145**), which adopted a $\beta$-hairpin conformation in aqueous solution.[25] Further, Stanger and Gellman synthesized two 12-mers of RYVEVXGOKILQ-$NH_2$ to demonstrate that a D-Pro-Gly (X= D-Pro, peptide **146**) sequence is superior to L-Asn-Gly (X= L-Asn, peptide **147**) in the nucleation of a $\beta$-hairpin.[26]

Though the role of the turn sequence in the formation of a $\beta$-hairpin with a two-residue loop is very vital as explained above, there are several other factors that also contribute to the

stability of a *β*-hairpin, namely interstrand (cross-strand) hydrogen bonding, interstrand sidechain–sidechain interactions (hydrophobic or electrostatic), and *β*-sheet propensity of the strand residues. Various researchers have shown the role of each of these factors in the stability of a *β*-hairpin. Gellman et al. studied the role of hydrophobic interactions between W2, Y4, F9 and V11 in R-W-Q-Y-V-p-G-K-F-T-V-Q-$NH_2$ and established their stabilizing impact on the well-folded *β*-hairpin.[27] Waters et al. showed the significance of van der Waals and/or electrostatic interactions over hydrophobic interactions in the stabilizing effect of aromatic interactions (sidechain–sidechain).[28] This was later supported by Balaram and coworkers.[29] Apart from this, Waters' laboratory also demonstrated the stabilizing impact of diagonal and lateral cation–π interactions (electrostatic forces) between aromatic and basic residues in several *β*-hairpins.[30] Certain amino acids have higher propensity to form *β*-sheets and are shown to favor *β*-hairpin formation when included in the strands.[31] Hence, a careful consideration is required to design a stable *β*-hairpin peptide in order to balance all the stabilizing factors.

## 2.4 Hypothesis and synthetic strategy for the solid-phase synthesis of *β*-hairpins containing bulky *α,β*-dehydroamino acids

As discussed earlier in Section 2.2, ΔAAs can be used to induce secondary structures like $3_{10}$-helices and *β*-turns. Bulky tetrasubstituted α,β-dehydroamino acid residues like ΔVal and ΔIle have been reported to form *β*-turns. Since ΔAAs are achiral, they can induce type I' or type II' *β*-turns which are often seen in stable *β*-hairpins. Hence, it is a very rational proposition that these dehydro residues can be incorporated in the loop of a *β*-hairpin. We hypothesized that bulky *α,β*-dehydroamino acids like dehydrovaline (ΔVal) and dehydroethylnorvaline (ΔEnv) can significantly restrict the rotation of the peptide backbone because of very high levels of inherent $A_{1,3}$-strain (allylic strain). This restricted rotation can lead to increased rigidity, more stable folded

states, and greater stability to proteolysis. The increased $A_{1,3}$-strain of bulky ΔAAs should stabilize a peptide more significantly than the moderate $A_{1,3}$-strain of the smaller trisubstituted ΔAAs (**Figure 2.5**).

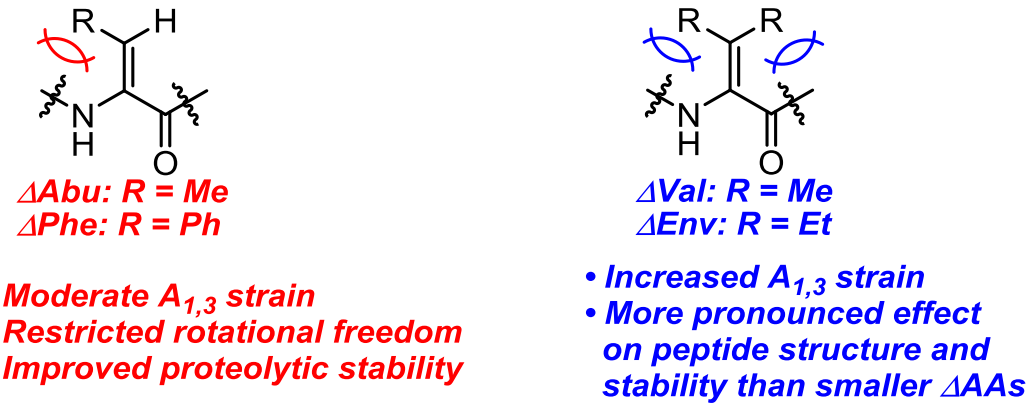


**Figure 2.5.** Comparison of tri- and tetrasubstituted ΔAAs.

These bulky ΔAAs should also be less susceptible to Michael addition, which is usually observed with di- and trisubstituted ΔAAs. Therefore, we proposed that a secondary structure like a *β*-hairpin could be significantly stabilized to proteolysis by the substitution of either (*i*+*1*) or (*i*+*2*) loop residue with a bulky tetrasubstituted ΔAA.

### 2.4.1 Synthetic strategy for the solid-phase peptide synthesis (SPPS) of *β*-hairpins containing ΔAAs (ΔVal or ΔEnv)

Encouraged by their work on the tetradecapeptide yaku'amide A, Castle and co-workers became interested in exploring the effects of bulky *α*,*β*-dehydroamino acids on peptide structure and stability. In 2014, they reported the synthesis of four octapeptides containing bulky ΔAAs via solid-phase peptide synthesis (**Scheme 2.1**).[32] We employed the same synthetic strategy to prepare several *β*-hairpins (**152**). The Fmoc-group was reported to be unstable under the coupling conditions, hence Alloc-protected dipeptide azlactones were synthesized for coupling to the resin-bound peptides.

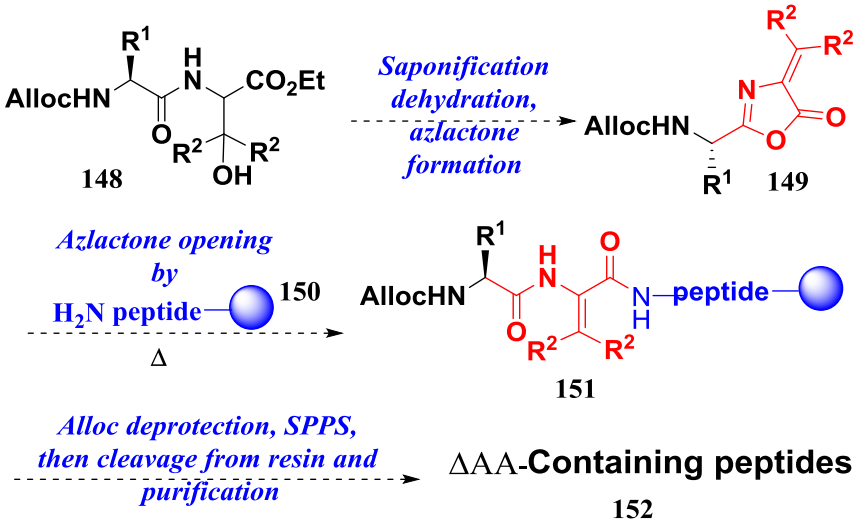


**Scheme 2.1.** Solid-phase peptide synthetic strategy.

Waters and coworkers reported the synthesis of a very stable and well-folded *β*-hairpin **153a** (**Figure 2.6**).[30c, 33] We selected this as a model *β*-hairpin for testing our hypothesis by replacing the (*i*+*1*) or (*i*+*2*) residue with a bulky tetrasubstituted ΔAA. The scheme outlining the design of analogues is given below. This is a fairly short peptide and amenable to 2D NMR studies for the elucidation of its structure.

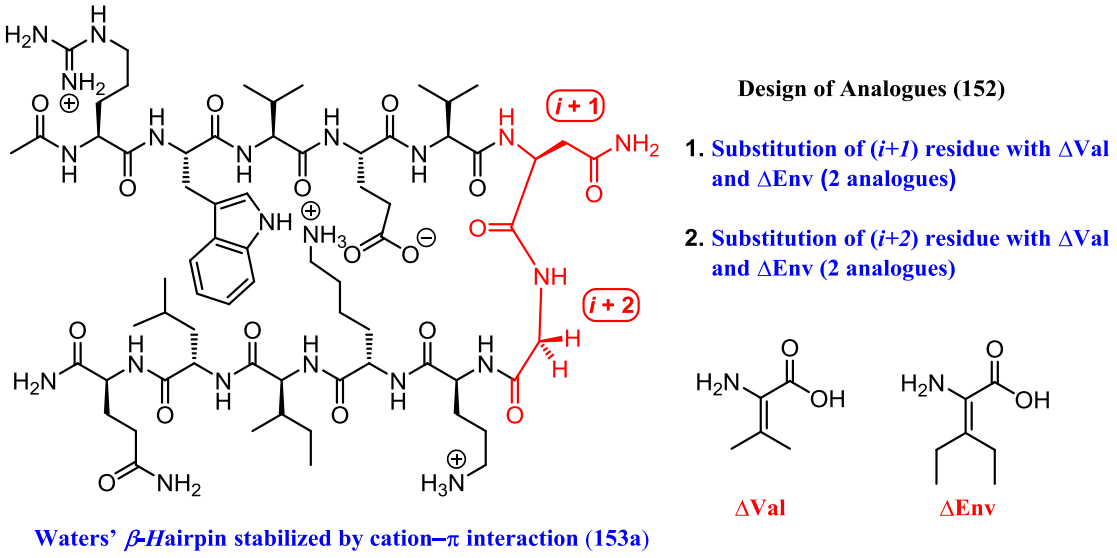


**Figure 2.6.** Waters' *β*-hairpin (**153a**) and design of analogues (**152**).

## 2.5 Solid-phase peptide synthesis (SPPS) of *β*-hairpins containing ΔAAs (ΔVal or ΔEnv) in the NG loop

As outlined in **Scheme 2.1**, we embarked upon the synthesis of the dipeptide azlactones (**149**) required for the preparation of ΔAAs (ΔVal/ΔEnv) containing *β*-hairpins. Castle et al. had reported the synthesis of *β*-hydroxyamino acids via base-free aminohydroxylation.[34] We used the same successful methodology for the synthesis of racemic mixtures of *β*-hydroxyvaline (**154a**) and *β*-hydroxyethylnorvaline (**154b**) derivatives (**Scheme 2.2**).

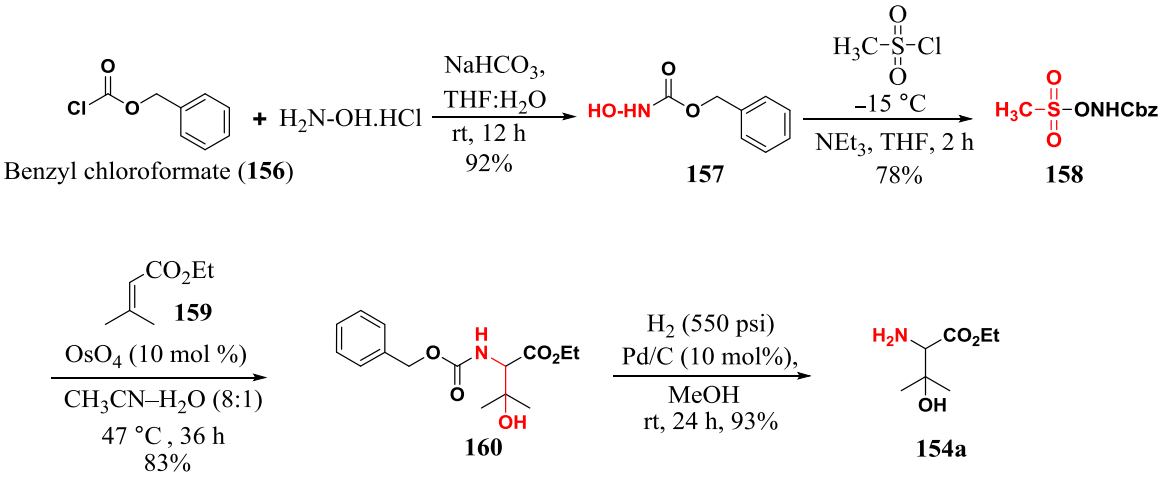


**Scheme 2.2.** Synthesis of *β*-hydroxyvaline derivative (**154a**) via aminohydroxylation.

The yields for the synthesis of bulkier *β*-hydroxyethylnorvaline were slightly less than *β*-hydroxyvaline (**Scheme 2.3**). Alloc-protected amino acids **155** were synthesized as described in the literature.[35]

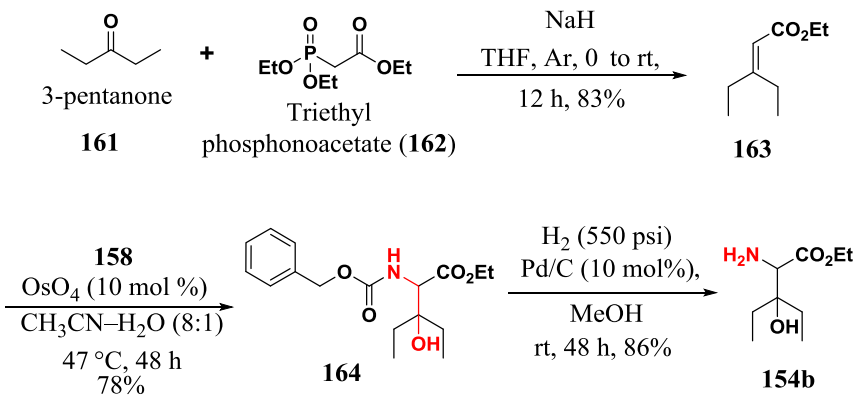


**Scheme 2.3.** Synthesis of *β*-hydroxyethylnorvaline derivative **154b** via aminohydroxylation.

Alloc-protected amino acids were coupled with *β*-hydroxyvaline (**154a)** and *β*-hydroxyethylnorvaline (**154b**) derivatives to give dipeptides **148** in good yields. Saponification of the purified dipeptides with LiOH•$H_2O$ yielded dipeptide acids **165**. As expected, activation of these acids with acetic anhydride and anhydrous sodium acetate in anhydrous THF yielded the desired dipeptide azlactones **149** in good yields. Acetic anhydride was used as a solvent for this cyclization and elimination previously, but the challenges of completely removing the high-boiling acetic anhydride dissuaded us from continuing with it. Hence, we successfully modified the previously established protocols by employing 5.0 equivalents of acetic anhydride to facilitate this cyclization and dehydration to give azlactones **149** (**Scheme 2.4**). These azlactones were susceptible to partial decomposition during the flash chromatography purification on silica gel ($SiO_2$). Hence, the yields of pure dipeptide azlactones **149** were slightly lower. In general, the quality of crude dipeptide azlactones was sufficient for direct use in couplings to the resin-bound peptides **150**.

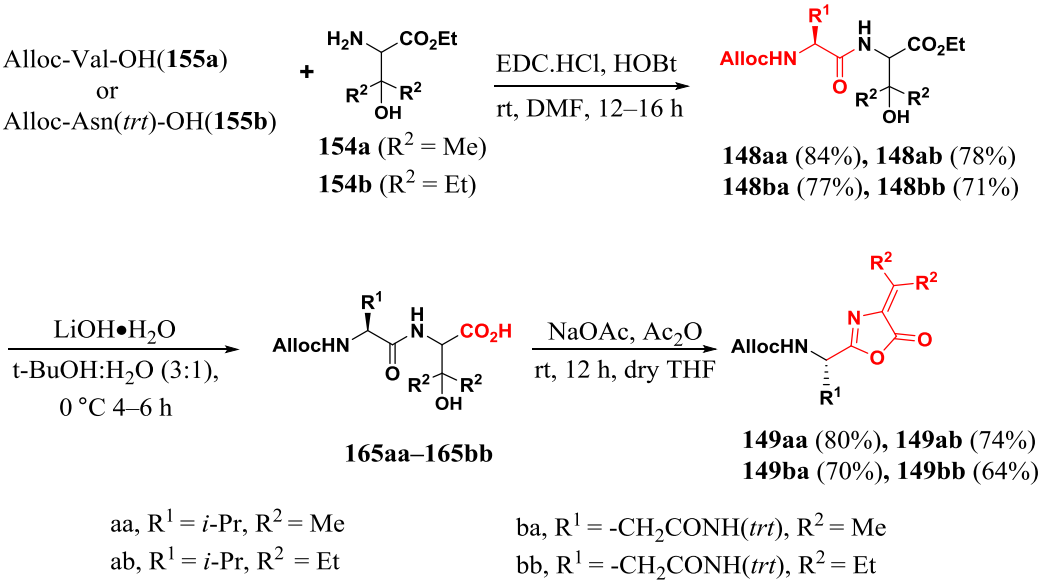


**Scheme 2.4.** Synthesis of dipeptide azlactones **149**.

Peptides **150** were synthesized by standard Fmoc/*t*-Bu protocols on Rink amide resin, and a small amount was analyzed by mass spectrometry before coupling with the azlactones. We initially tried the procedure reported by Jiang and co-workers. Azlactone **149aa** was subjected to coupling with dried resin-bound peptide **150a** under Ar by heating the suspension at 60 °C for 24 h in dry NMP. Analysis by mass spectroscopy did not show any coupling of the azlactone to the peptide. Hence, 0.1 equivalent of DMAP was added to the reaction, but there was no improvement. Optimum conditions for azlactone **149aa** ring opening were then explored and are listed in the table below (**Table 2.3**).

**Table 2.3.** Screening of ring-opening conditions for the dipeptide azlactone **149aa**.

| Solvent | Base | Equivalence of base | Temperature | Extent of coupling after 24 h |
|---|---|---|---|---|
| NMP | DMAP | 0.5 | 60–100 °C | Poor |
| DMF | DMAP | 0.5 | 60–100 °C | Poor |
| NMP/DMF (1:1) | DMAP | 0.5 to 2.0 | 60–100 °C | Poor |
| NMP | $NEt_3$ | 1.0 to 5.0 | 35–80 °C | Poor to moderate |
| NMP | $NEt_3$ | 10.0 | 80 °C | Good |

During the optimization, we realized that the integrity of the resin deteriorated over time at elevated temperatures with high rate of stirring. Hence, the reactions were then stirred at low speeds to prevent the loss of resin integrity. Similar ring-opening conditions were used for all other dipeptide azlactones. Bulkier azlactones **149ab, 149ba and 149bb** required longer periods for coupling. After the ring opening, we capped the unreacted free amines of the resin-bound peptide **150** with $Ac_2O$ to prevent the formation of undesired peptides, which could cause difficulty in the final purification (**Scheme 2.5**). Alloc-deprotection of peptide **151** with $Pd(PPh_3)_4$ and $PhSiH_3$ proceeded smoothly, and peptides were then elaborated in a straightforward fashion. Nevertheless, the coupling of the final amino acid Arg required a longer time. All the peptides were then N-acetylated and cleaved from the resin with simultaneous global deprotection of the sidechain protecting groups. The peptides **152** were lyophilized and subsequently purified by HPLC.[36]

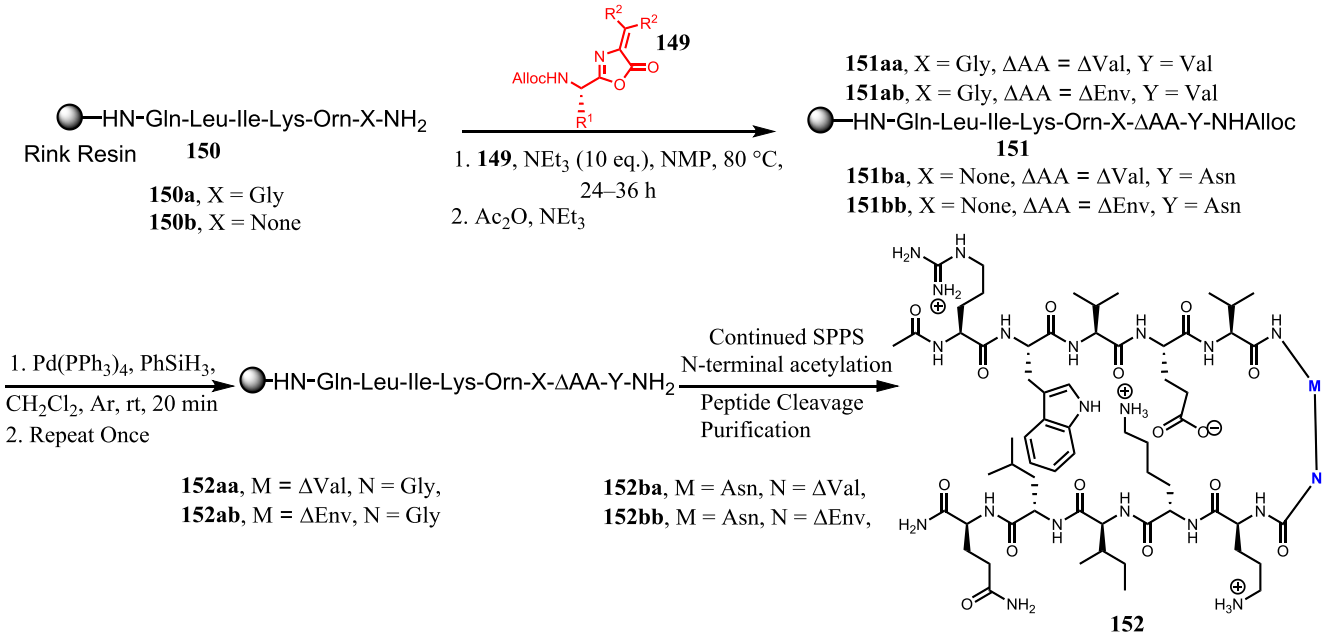


**Scheme 2.5.** Solid-phase synthesis of *β*-hairpins (**152aa–152bb**).

## 2.6 Solid-phase peptide synthesis (SPPS) of *β*-hairpins containing D-Pro at (*i+1*) and ΔAAs (ΔVal or ΔEnv) at (*i+2*) positions

Preliminary NMR studies and proteolysis experiments of peptide **152aa** were very encouraging. The peptide exhibited significant folding and stability to proteolysis. Motivated by these results, we set out to test if we could combine the stabilizing structural and proteolytic effects of ΔAAs with other stabilizing elements without hampering the *β*-hairpin structure. The D-Pro-Gly loop is known to promote *β*-hairpin formation, and a D-residue also imparts stability to enzymatic degradation. Hence, we slightly modified Waters' *β*-hairpin and synthesized two (*i+2*) ΔAA (ΔVal or ΔEnv) analogues **152ca** and **152cb** (**Scheme 2.7**) of Ac-R-W-V-E-V-p-G-O-K-I-L-Q-$NH_2$ (**153b**). Dipeptide azlactones **149ca** and **149cb** were synthesized in good yields by the reproducible protocol described earlier in Section 2.5. The scheme outlining their synthesis is shown below (**Scheme 2.6**).

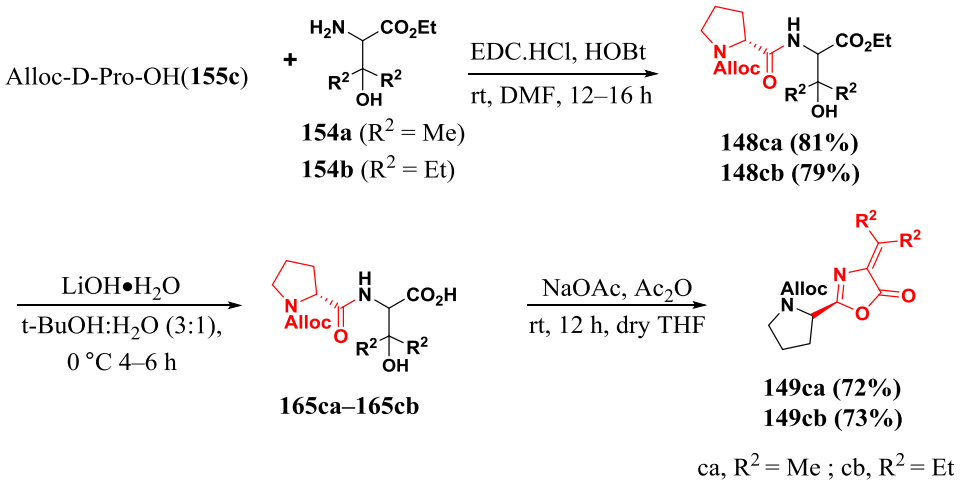


**Scheme 2.6.** Synthesis of dipeptide azlactones containing D-Proline (**149ca** and **149cb**).

Azlactone coupling to the resin-bound peptide was also straightforward and surprisingly proceeded with very good conversion. Alloc-deprotection, peptide elaboration, cleavage and purification of the peptides were uneventful and afforded peptides (**152ca** and **152cb**) in moderately good yields (**Scheme 2.7**).

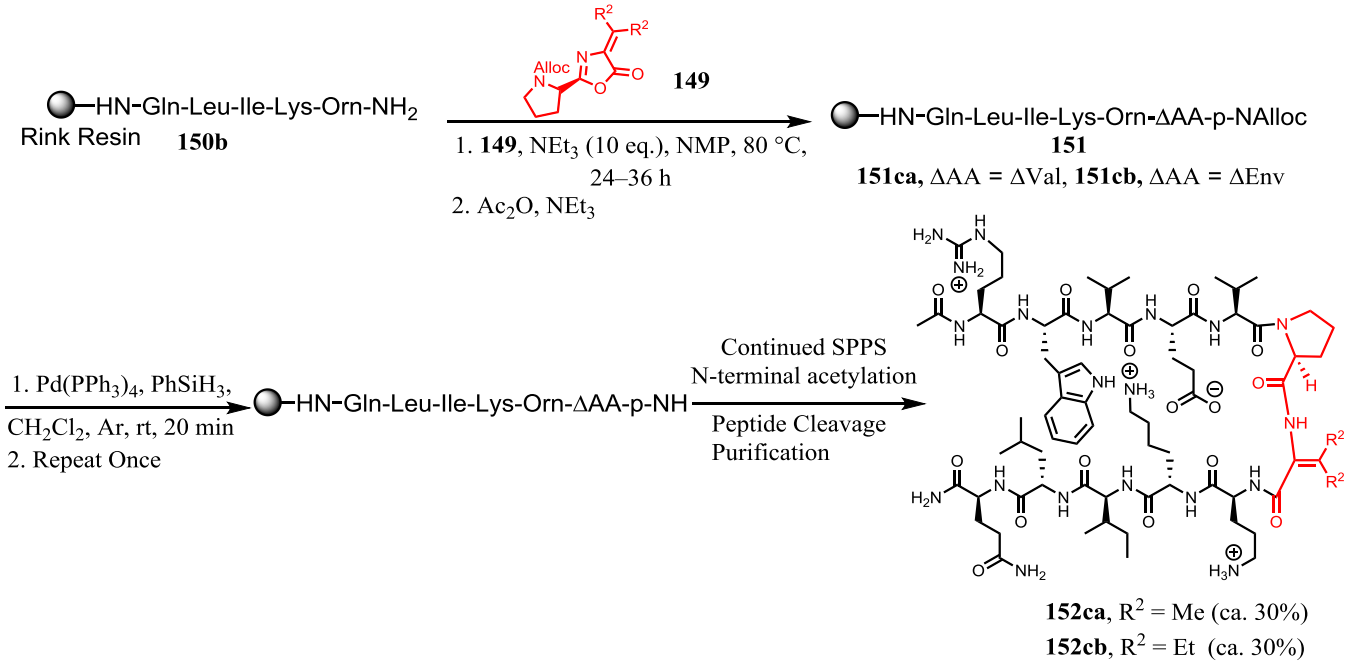


**Scheme 2.7.** Solid-phase synthesis of *β*-hairpins containing D-Pro at (*i+1*) and ΔAAs (ΔVal or ΔEnv) at (*i+2*) positions.

## 2.7 Solid-phase peptide synthesis (SPPS) of cyclic controls and random coils for *β*-hairpins 153a and 152aa

In order to elucidate and precisely compute the population of folded *β*-hairpins containing a bulky ΔAA, a cyclic control and two random coils containing a bulky ΔAA were synthesized. There are remarkable shifts in the $H_\alpha$ proton chemical shifts in a secondary structure.[29] Hence, cyclic control (100% folded) and random coils (0% folded controls) are required to accurately calculate the percent folded population. We synthesized the cyclic control **167a** and random coils (Ac-R-W-V-E-V-N-G-$NH_2$, **168a** and Ac-N-G-O-K-I-L-Q-$NH_2$, **168b**) for the model *β*-hairpin Ac-R-W-V-E-V-N-G-O-K-I-L-Q-$NH_2$ (**153a)** by the standard fmoc/*t*-Bu method. The disulfide bridge in the cyclic control **167a** was established by air oxidation of the purified peptide **166a** in 10 mM phosphate buffer solution (pH 7.5) containing 5% DMSO to affect cyclization (**Scheme 2.8**).[30c]

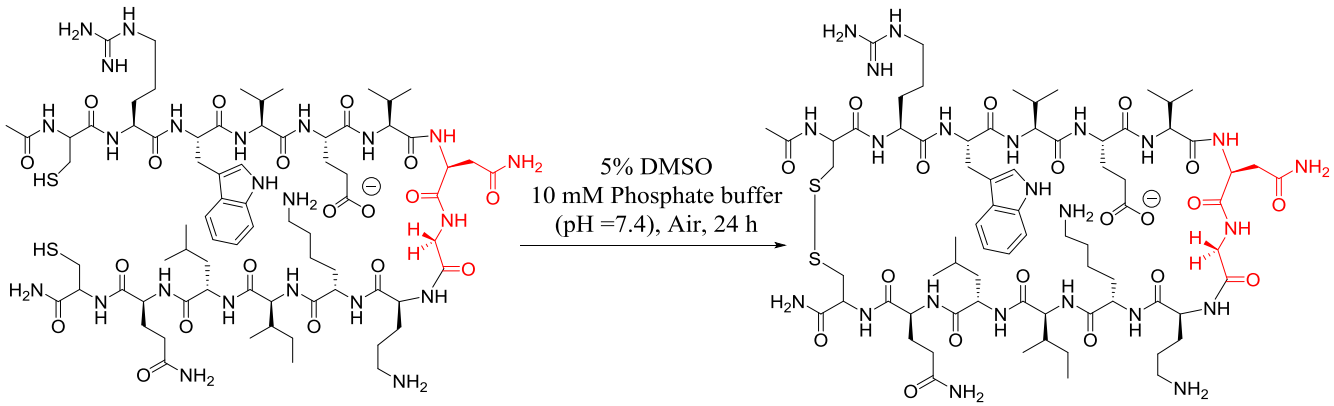


**166a** **167a**

**Scheme 2.8.** Synthesis of cyclic control (**167a**).

Similarly, we synthesized the cyclic control **167b** and random coils **168c and 168d** to calculate the percent folding of **152aa**. The dipeptide azlactone ring-opening protocol was successfully utilized to construct the control peptides. Random coils Ac-R-W-V-E-V-ΔVal-G-

$NH_2$ (**168c**) and Ac-ΔVal-G-O-K-I-L-Q-$NH_2$ (**168d**) were synthesized from dipeptide azlactone **149aa** and the azlactone Ac-ΔVal respectively.[37] Cyclic controls contain a Cys residue each at the two termini of the *β*-hairpin, which are then oxidized to form a disulfide bond to afford a cyclic peptide. Dipeptide azlactone **149aa** was utilized to synthesize the cyclic control. The purified peptide **166b** was oxidized as described above to give **167b** (**Scheme 2.9**).

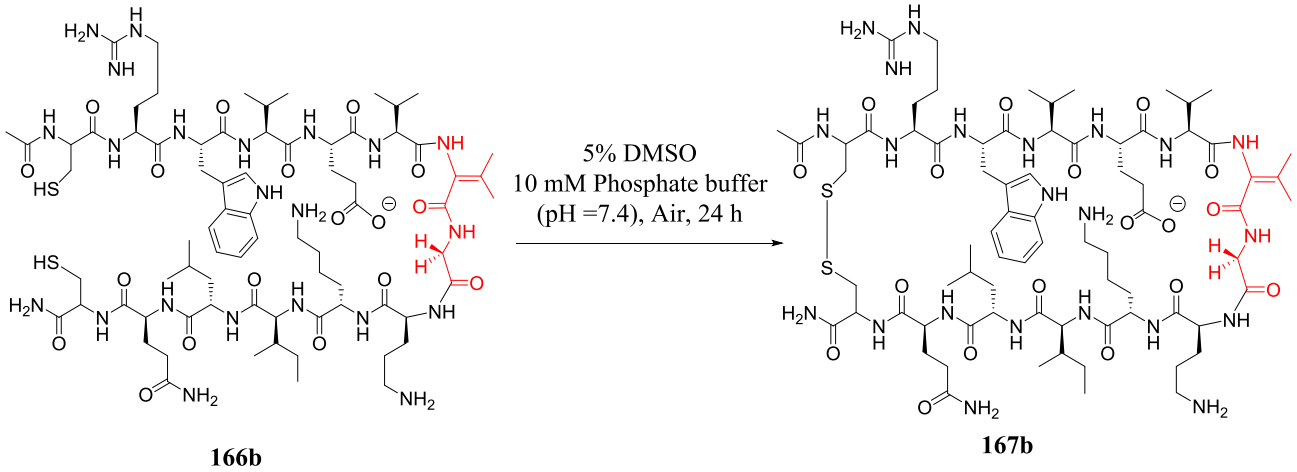


**166b** **167b**

**Scheme 2.9.** Synthesis of cyclic control containing ΔVal at (*i*+*1*) position (**167b**).

## 2.8 Summary

Insights into the factors that govern protein folding are of tremendous interest and can be extremely useful in designing new rules for the *de novo* synthesis of stable peptides or proteins. There are various noncovalent forces that control the folding of peptides or proteins into secondary structures, which consequently decide their tertiary and quaternary structures. Better understanding of these factors may help in the rational design and synthesis of peptides or proteins, which can be used to target certain protein–protein interactions. A specifc conformation is usually needed for a peptide or protein to elicit its biological activity. These novel peptides and proteins can be tuned to have desired pharmacological activities, proteolytic stability and pharmacokinetic

properties. In the last 2–3 decades, *β*-hairpins have emerged as good monomeric, non-aggregating and water-soluble model systems for the underexplored *β*-sheets. Dehydroamino acid residues have been shown to promote secondary structures like $3_{10}$-helices and *β*-turns, hence we designed and synthesized several well-folded *β*-hairpins **152aa–152cb** by substituting the (*i+1*) or (*i+2*) residues with ΔVal/ΔEnv in two model *β*-hairpins **153a** and **153b**.

## 2.9 References


1. Singh, T. P.; Kaur, P. *Prog. Biophys. Mol. Biol* .**1996**, *66*, 141.

2. Thormann, M.; Hofmann, H., J. *J. Mol. Struct. (Theochem)* **1998**, *431*, 79.

3. Jiang, J.; Ma, Z.; Castle, S. L. *Tetrahedron* **2015**, 71, 5431.

4. a) Aubry, A.; Allier, F.; Boussard, G.; Marraud, M. *Biopolymers* **1985**, *24*, 639; b) Busetti, V.; Ajò, D.; Casarin, M. *Acta. Crystallogr.* **1984**, *C40*, 1245; c) Singh, T. P.; Narula, P.; Chauhan, V. S.; Kaur, P. *Biopolymers* **1989**, *28*, 1287; d) Singh, T. P.; Narula, P.; Chauhan, V. S.; Sharma, A. K.; Hinrichs, W. *Int. J. Pept. Protein Res.* **1989**, *33*, 167.

5. a) Busetti, V.; Crisma, M.; Toniolo, C.; Salvadari, S.; Balboni, G. *Int. J. Biol. Marcomol.* **1991**, *14*, 23; b) Rajashankar, K. R.; Ramakumar, S.; Chauhan, V. S. *J. Am. Chem. Soc.* **1992**, *114*, 9225.

6. Mitra, S. N.; Dey, S.; Karthikeyan, S.; Singh, T. P. *Biopolymers* **1996**, *39*, 646.

7. Gupta, M.; Chauhan, V., S. *Biopolymers*, **2011**, *95*, 161.

8. Mathur, P.; Jagannathan, N., R.; Chauhan, V., S.; *J. Pept.* Sci. **2007**, *13*, 253.

9. Dewan, P., C.; Anantharaman, A.; Chauhan, V., S.; Sahal, D. *Biochemistry* **2009**, *48*, 5642.

10. Pathak, S.; Chauhan, V., S. *Antimicrob. Agents Chemother.* **2011**, *55*, 2178

11. a) Soto, C.; Sigurdsson, E., M., Morelli, L.; Kumar, R., A.; Castano, E., M.; Frangione, B. *Nat. Med.* **1998**, 4, 822; b) Soto, C. *Mol Med. Today* **1999**, 5, 343.

12 . Gupta, M.; Rudresh, A.; Mishra, A.; Ramakumar, S.; Faizan, A.; Chauhan, V., S. *ChemBioChem* **2008**, *9*, 1375.

13. Giordano, C.; Punzi, P.; Chiaraluce, R.; Consalvi, V. *ChemPlusChem* **2014**, *79*, 1036.

14. Mishra, A.; Misra, A.; Vaishnavi, T. S.; Thota, C.; Gupta, M.; Ramakumar, S.; Chauhan, V. S. *Chem. Commun.* **2013**, *49*, 2688.

15. a) Ciszak, E.; Pietrzyński, G.; Rzeszotarska, B. *Intl. J. Pept. Protein Res.* **1992**, *39*, 218; b) Ghandi, M.; Nazari, S. H.; Bozcheloei, A. H.; Sadeghzadeh, M.; Kia, R. *Tetrahedron Lett.*. **2011**, *52*, 6613; c) Vijayaraghavan, R.; Kumar, P.; Dey, S.; Singh, T., P. *Acta Crystallogr. Sect.C.* **2001**, *57*, 1220.

16. Vijayaraghavan, R.; Kumar, P.; Dey, S.; Singh, T., P. *J. Pept. Res.* **2003**, *62*, 63.

17. Siodlak, D.; Rzeszotarska, B.; Broda, M., A.; Kozioł, A., E.; Kołodziejczyk, E. *Acta Biochim. Pol.* **2004**, *51*, 145.
18. Makker, J.; Dey, S.; Mukherjee, S.; Vijayaraghavan, R.; Kumar, P.; Singh, T., P. *J. Mol. Struct.* **2003**, *654*, 119.

19. Blanco, F. J.; Jiménez, M. A.; Herranz, J.; Rico, M.; Santoro, J.; Nieto, J. L. *J. Am. Chem. Soc.* **1993**, *115*, 5887.

20. Hughes, R. M.; Waters, M. L. *Curr. Opin. Struct. Biol.* **2006**, *16*, 514.

21. a) Sibanda, B. L.; Thornton, J., M. *Nature*, **1985**, *316*, 170; b) Sibanda, B. L.; Blundell, T. L.; Thornton, J. M. *J. Mol. Biol.* **1989**, *206*, 759.

22. Ramírez-Alvarado, M.; Blanco, F. J.; Serrano, L. *Nat. Struct. Biol.* **1996**, *3*, 604.

23. Haque, T. S.; Little, J. C.; Gellman, S. H. *J. Am. Chem. Soc.* **1996**, *118*, 6975.

24. Karle, I. L.; Awasthi, S. K.; Balaram, P. *Proc. Natl. Acad. Sci. U.S.A.* **1996**, *93*, 8189.

25. Haque, T. S.; Gellman, S. H. *J. Am. Chem. Soc.* **1997**, *119*, 2303.

26. Stanger, H. E.; Gellman, S. H. *J. Am. Chem. Soc.* **1998**, *120*, 4236.

27. Espinosa, J. F.; Gellman, S. H. *Angew. Chem.* **2000**, *112*, 2420.

28. Tatko, C. D.; Waters, M. L. *J. Am. Chem. Soc.* **2002**, *124*, 9372.

29. Mahalakshmi, R.; Raghothama, S.; Balaram, P. *J. Am. Chem. Soc.* **2006**, *128*, 1126.

30. a) Tatko, C. D.; Waters, M. L. *Protein Sci.* **2003**, *12*, 2443, b) Tatko, C. D.; Waters, M. L. *Protein Sci.* **2004**, *13*, 2515; c) Tatko, C. D.; Waters, M. L. *J. Am. Chem. Soc.* **2004**, *126*, 2028; d) Hughes, R. M.; Waters, M. L. *J. Am. Chem. Soc.* **2005**, *127*, 6518; e) Hughes, R. M.; Waters, M. L. *J. Am. Chem. Soc.* **2006**, *128*, 13586.

31. Ramírez-Alvarado, M.; Kortemme, T.; Blanco, F. J.; Serrano, L. *Bioorg. Med. Chem.* **1999**, *7*, 93.

32. Jiang, J.; Luo, S.; Castle, S. L. *Tetrahedron Lett.* **2015**, *56*, 3311.

33. Cline, L. L.; Waters, M. L. *Biopolymers* **2009**, *92*, 502.

34. Ma, Z.; Naylor, B. C.; Loertscher, B. M.; Hafen, D. D.; Li, J. M.; Castle, S. L. *J. Org. Chem.* **2012**, *77*, 1208.

35. Dexter, H. L.; Willims, H. E. L.; Lewis, W. Moody, C. J. *Angew. Chem. Int. Ed.* **2017**, *56*, 3069.

36. Jalan, A.; Kastner, D. W.; Webber, K. G. I.; Smith, M. S.; Price, J. L.; Castle, S. L. *Org. Lett.* **2017**, *19*, 5190.

37. El-Baba, S., Nuzillard, J.M., Poulin, J.C., Kagan, H.B. *Tetrahedron* **1986**, *42*, 3851.

# 3 CONTRIBUTION OF BULKY *α,β*-DEHYDROAMINO ACIDS TO THE PROTEOLYTIC STABILITY AND ENHANCED FOLDING OF *β*-HAIRPINS

## 3.1 Introduction

Peptides and proteins play an important role in modern medicine because of their diverse therapeutic applications. Peptide-based drugs like antimicrobial peptides (e.g., vancomycin,[1a] bleomycin,[1b] lantibiotics,[1c] etc.), anticancer agents (goserelin,[1d] bortezomib,[1e] etc.), immunomodulators (cyclosporine[1f]), anti-HIV agents (enfuvirtide[1g]), and antidiabetic agents (exenatide[1h]), are widely used.[1] The global market for therapeutic peptides (insulin and its derivatives included) was estimated to be ca. $50 billion in 2015 and is growing annually by more than 10%. Since 2000, 28 new peptide-based drugs (non-insulin derivatives) have entered the market with good success.[2] However, the major drawbacks of therapeutic peptides are their susceptibility to rapid proteolysis (i.e. degradation by enzymes) and poor bioavailability. Though various promising approaches have been devised to overcome these problems (e.g., peptoids,[3] *β*-peptides,[4] D-peptides,[5] α,α-disubstituted amino acids,[6] stapling,[7] hydrogen bond surrogates,[8] PEGylation[9]), there is still a great need for better alternatives to stabilize therapeutic peptides.

## 3.2 Potential of therapeutic peptides and associated challenges

Protein–protein interactions (PPIs) have emerged as highly attractive targets for medicinal chemists because they are implicated in several human diseases and disorders, including various types of metabolic disorders and cancers.[10] Though more than 12 small-molecule PPI modulators

are in clinical trials currently, their size is not often ideal to interact with the PPI interface.[11] PPI interface or contact area is generally large and is relatively featureless with no preformed binding pockets for small molecules.[12] The salient feature of a PPI interaction surface is a collection of a few very small binding sites called "hot spots," which are scattered over the interaction surface. These hot spots are critical for the competitive binding of the PPI inhibitors.[13] Hence, an inhibitor has to be sufficiently large to interact with multiple hot spots to modulate the PPI.[14] Several biologics that target extracellular proteins are available on the market, but their size is huge and they cannot penetrate the cells to affect intracellular PPIs. Peptides are uniquely positioned between small molecules and biologics because of their moderate size and high affinity for protein targets. Their specific three-dimensional conformations make them highly selective, potent and less toxic.[15] Importantly, they can be used to target both extracellular and intracellular PPIs.

As mentioned earlier, peptides are prone to rapid proteolysis and quick hepatic and renal clearance. Hence, unmodified peptides are generally poor drug candidates. Well-folded peptides are more efficient as they are less susceptible to degradation than their unfolded counterparts, and are more likely to be taken up by the cells in a conformationally rigid form. Given their high therapeutic potential, several strategies have emerged in the last two decades to synthesize stabilized peptides with well-defined three-dimensional structures.

$\alpha$-Helical peptides are reported to be involved in many PPIs, and several methods were thus developed to synthesize stabilized $\alpha$-helices for modulating the PPIs. Some of the most common techniques are stapled peptides (all-hydrocarbon cross-linking of sidechains), hydrogen bond surrogates (HBS) and $\beta$-peptides (**Figure 3.1**).[16] In 2000, Verdine and co-workers synthesized several short $\alpha$-helices by cross-linking two side-chains through the olefin-metathesis reaction. This ruthenium catalyzed ring closing metathesis (RCM) was performed on solid support

to form an 11-carbon cross-link between the *i* and *i*+*7* residues. This peptide exhibited a 44% increase in folding and a 41-fold improvement in the half-life against trypsin digestion when compared to the unmodified peptide.[17] A well-folded peptide has fewer amide bonds exposed to the solution and is consequently less susceptible to rapid enzymatic degradation. This strategy has become very attractive for synthesizing several $\alpha$-helical PPI inhibitors. Walensky et al. synthesized a stapled $\alpha$-helical BH3 (Bcl-2 homology 3) peptide to target the BID (BH3-interacting domain death agonist) protein *in vivo* to kill cancer cells by promoting apoptosis.[18] Bernal and Walensky demonstrated that the p53 tumor suppressor pathway could be reactivated by a stapled helical peptide by modulating the p53-MDM2 protein interaction.[19] Similarly, in 2013, Aileron Therapeutics reported reactivation of the p53 tumor suppression pathway by dual inhibition of MDM2/MDMX with the stapled helical peptide ATSP-7041.[20] Several other cancer-inducing PPIs were targeted by stapled peptides such as MCL1-NOXA (small-cell lung cancer) and the EZH2-EED complex (leukemia).[21] Debnath et al. synthesized the anti-HIV-1 $\alpha$-helical stapled peptide (NYAD-1) that can penetrate cells and target the HIV-1 capsid.[22]

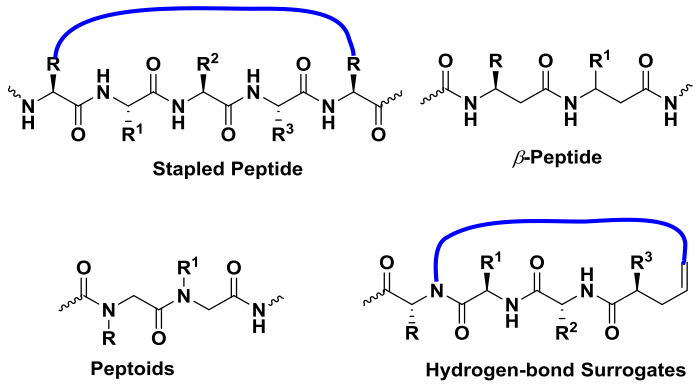


**Figure 3.1**. Some common methods of stabilizing peptides.

Arora and co-workers developed an alternative to stapled peptides. They stabilized $\alpha$-helices by replacing the intramolecular $i \rightarrow i+4$ hydrogen bond at the N-terminus of a short peptide with a covalent hydrocarbon linkage via ring-closing metathesis. Since the peptide sidechains are not altered in this hydrogen-bond surrogate (HBS) method, it retains its entire functional surface for interaction with the protein target.[23] They reported the inhibition of gp41-mediated HIV-1 fusion into the cells by the conformationally constrained $\alpha$-helical peptide HBS $\alpha$ 9 ($EC_{50}$ = 43 μM).[24]

$\beta$-peptides and peptoids are the other popular methods where oligomers are synthesized from $\beta$-amino acids and N-substituted glycine units respectively. Seebach et al. showed that amphiphilic $3_{14}$-helical $\beta$-peptides can inhibit lipid and cholesterol absorption by small intestinal brush-border membrane vesicles. These left-handed $\beta$-peptides can mimic the right-handed $3.6_{13}$-helical $\alpha$-octadecameric motif commonly seen in human apolipoproteins (involved in fat transport and uptake) and thereby inhibit the function of apolipoproteins.[25] Gellman et al synthesized $\beta$-peptides and mixtures of $\alpha$- and $\beta$-peptides to target the MDM2-p53 interaction.

Despite the recent advances in peptide modelling and stabilization, the number of peptide drugs reaching the market is very modest (28 since 2000).[2] Hence, it is imperative to find new methods of stabilizing peptides and modulating their pharmacokinetic properties to access their high therapeutic potential.

### 3.3 Proteolytic stability of peptides containing $\alpha,\beta$-dehydroamino acids

In the late 1970's, Stammer et al. explored the role of trisubstituted dehydroamino acids in the stability of enkephalin analogues. They synthesized a pentapeptide Z-Gly-Gly-Phe-$\Delta^{Z}$Phe-Ala-OH, and showed that it was very stable to the enzymes chymotrypsin and thermolysin even after 30 hours, whereas the saturated peptide Z-Gly-Gly-Phe-Phe-Ala-OH rapidly hydrolyzed.[26]

Motivated by this result, they synthesized the enkephalin analogue Tyr-D-Ala-Gly-$\Delta^Z$Phe-Met-$NH_2$ ($ED_{50}$ = 3.3 x $10^9$ M) which was five times more active in paralyzing stimulated pig-ileum than the parent peptide Tyr-D-Ala-Gly-Phe-Met-$NH_2$ ($ED_{50}$ = 1.7 x $10^8$ M), and was essentially unhydrolyzed after 30 hours of treatment with chymotrypsin.[27] Similarly, the $\Delta^Z$Leu$^5$ analogue (Tyr-D-Ala-Gly-Phe-$\Delta^Z$Leu-OH) of Tyr-D-Ala-Gly-Phe-Leu-OH was active towards the δ opioid receptor and more stable to enzymatic decomposition than its saturated parent pentapeptide.

In early 1980's, Stammer and co-workers synthesized three analogues of the vasodilator peptide bradykinin (Arg$^1$-Pro$^2$-Pro$^3$-Gly$^4$-Phe$^5$-Ser$^6$-Pro$^7$-Phe$^8$-Arg$^9$). One of the unsaturated analogues [$\Delta^Z$Phe$^5$]BK (Arg$^1$-Pro$^2$-Pro$^3$-Gly$^4$-$\Delta^Z$Phe$^5$-Ser$^6$-Pro$^7$-Phe$^8$-Arg$^9$) was found to be more potent than bradykinin at lowering the blood pressure of rats after intravenous injection and was also resistant to enzymatic degradation.[28]

As *α,β*-dehydroamino-acid-containing peptides have shown considerable proteolytic stability combined with static or enhanced biological activity, they have a huge potential to yield therapeutic peptides which could reach the market.

### 3.4 Proteolytic stability of *β*-hairpins containing a bulky *α,β*-dehydroamino acid in the turn

As described in Chapter 2, we synthesized six bulky *α,β*-dehydroamino-acid-containing analogues of the Waters' *β*-hairpin by substituting either the *i+1* or *i+2* residue of the *β*-turn region with ΔVal/ΔEnv (**Figure 3.2**). It has been reported by Waters and co-workers that well-folded *β*-hairpin peptides are more resistant to enzymatic degradation when compared to less-folded *β*-hairpins.[29] Pronase E is a mixture of about 10 different proteases that is obtained from the K-1 strain of *Streptomyces griseus* and cleaves nearly all peptide bonds. It contains five serine-type proteases, two $Zn^{2+}$ endopeptidases, two $Zn^{2+}$ leucine aminopeptidases, and one $Zn^{2+}$

carboxypeptidase. Hence, it has no preference for a cleavage site and is the most aggressive mixture of proteases commercially available.[30]

We decided to use the Pronase E mixture to test the proteolytic stability of our peptides. This highly active mixture should be able to cleave peptides non-specifically, providing a very rigorous proteolytic test for the enzymatic stability of our *β*-hairpins. We utilized the proteolysis protocols developed previously by Seebach et al.[31]

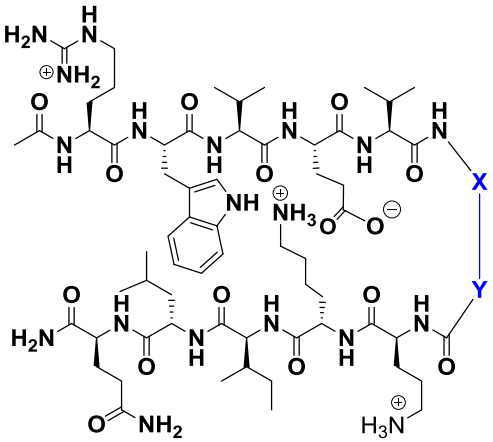


**153a** (X = Asn, Y = Gly) **153b** (X = D-Pro, Y = Gly)
**152aa** (X = ΔVal, Y = Gly) **152ab** (X = ΔEnv, Y = Gly)
**152ba** (X = Asn, Y = ΔVal) **152bb** (X = Asn, Y = ΔEnv)
**152ca** (X = D-Pro, Y = ΔVal) **152cb** (X = D-Pro, Y = ΔEnv)

**Figure 3.2.** Model *β*-hairpins and their ΔAA-containing analogues.

Pronase E from *Streptomyces griseus* (EC 3.4.24.31) was purchased from EMD Millipore. This mixture of enzymes was dissolved in 1X PBS buffer (10 mM sodium phosphate, 137 mM NaCl, 2.7 mM KCl buffer, pH 7.4) at a concentration of 0.128 mg/mL. Then, solutions of each peptide (**153a, 152aa, 152ab, 152ba, and 152bb**) in 1X PBS buffer (0.10 mM, 1.5 mL) at 37 °C were treated with an aliquot (5 µL) of the Pronase E solution. Aliquots (50 µL) were removed after 0, 30, 60, 90, 150, 210, 270, and 360 min. The aliquots were quenched with 25% v/v glacial acetic acid (10 µL), diluted to 75 µL with 1X PBS buffer, and analyzed by HPLC (Phenomenex Jupiter

C18, 5 μm particle size, 300 Å pore size, 4.6 × 250 mm, 40 μL injection volume, 10%–60% $CH_3CN$ in $H_2O$ gradient over 50 min, then 95% $CH_3CN$ in $H_2O$ for 10 min, flow rate: 1 mL/min).

Substitution of the Asn at *i+1* of **153a** with either ΔVal or ΔEnv markedly improved the proteolytic stabilities of the *β*-hairpins **152aa** and **152ab** respectively (**Figure 3.3**). They were ca. 6–7 times more resistant to proteolysis than the parent peptide **153a** containing all natural L-residues. ΔVal-containing analogue **152aa** was found to be slightly more stable than the ΔEnv analogue **152ab**.

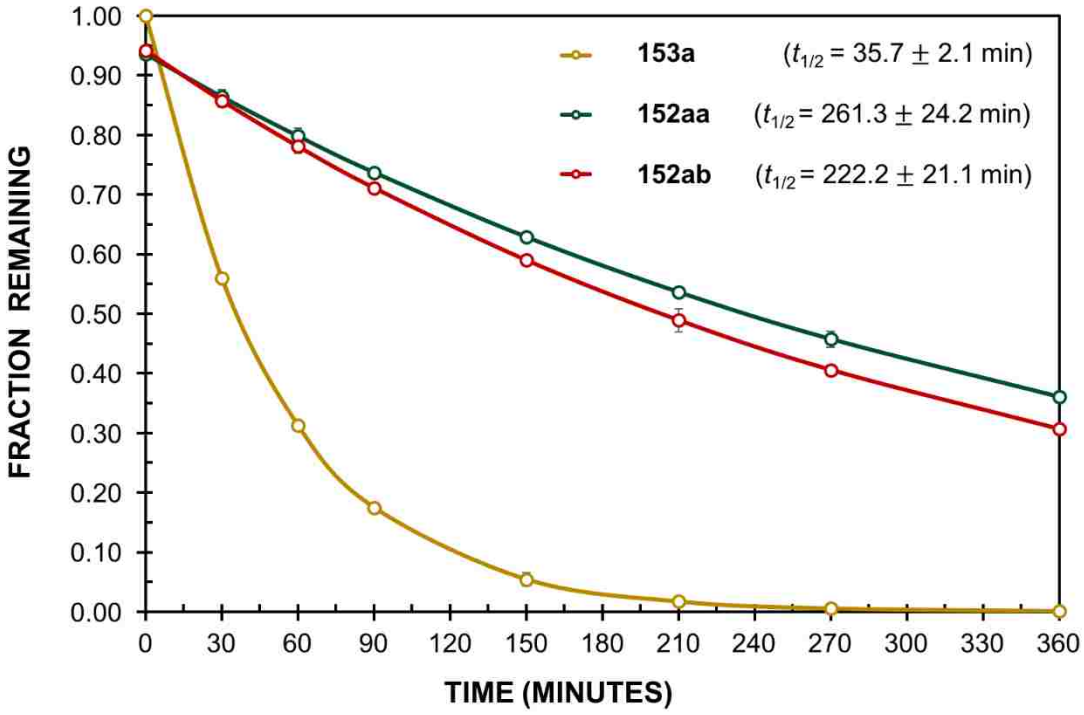


**Figure 3.3.** Proteolysis plot of Waters' *β*-hairpin **153a** and its *i+1* analogues **152aa** and **152ab**.

Substitution of the *i+2* (Gly) with the ΔAAs resulted in a more modest stabilizing effect on *β*-hairpins **152ba** and **152bb** (**Figure. 3.4**). Nevertheless, these analogues were ca. 3 times more stable when compared to the parent peptide **153a** and corroborated our hypothesis that the incorporation of a ΔAA in the turn region could impart enzymatic stability to *β*-hairpins without

destabilizing the secondary structure. The beneficial impact of both the bulky ΔAAs (ΔVal or ΔEnv) at the *i+2* position was essentially identical within experimental error.

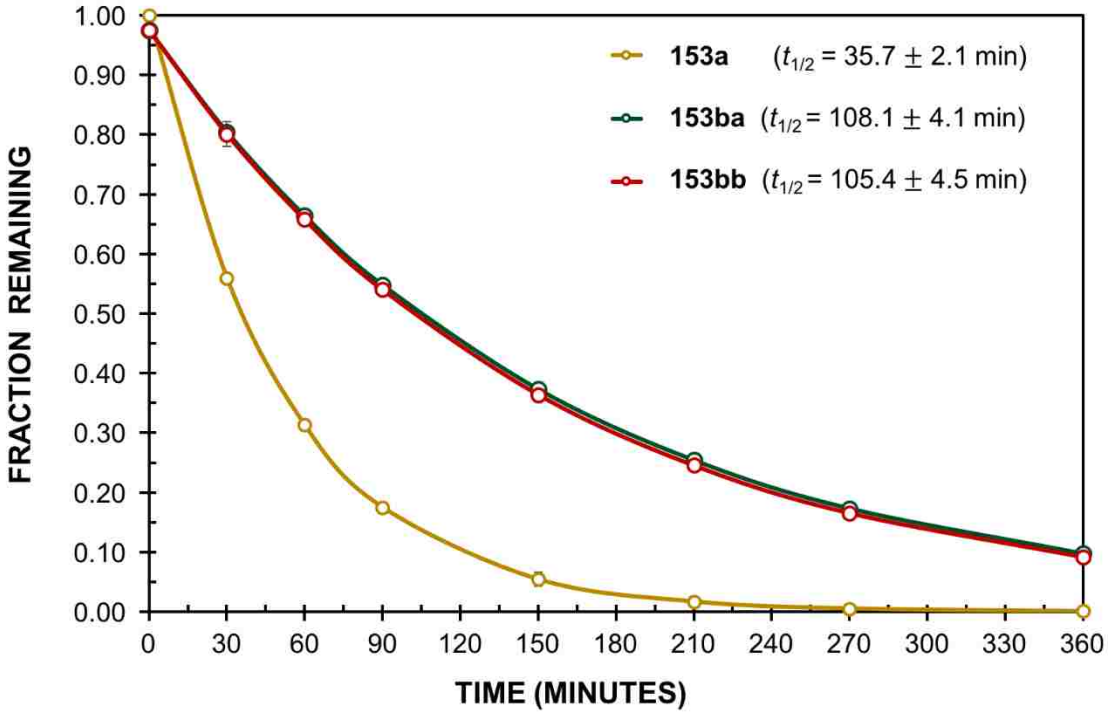


**Figure 3.4.** Proteolysis plot of Waters' *β*-hairpin **153a** and its *i+1* analogues **153ba** and **153bb**.

Similarly, the D-Pro and ΔAA-containing *β*-hairpins (**152ca** and **152cb**) were subjected to proteolysis with Pronase E. These peptides necessitated a higher concentration of the enzyme mixture, as the D-Pro residue also contributes to the stability of these peptides. Hence, we used higher concentrations of the Pronase E to digest the peptides on a reasonable time-scale. This mixture of enzymes was dissolved in 1X PBS buffer (10 mM sodium phosphate, 137 mM NaCl, 2.7 mM KCl buffer, pH 7.4) at a concentration of 0.362 mg/mL. Then, solutions of each peptide (**153b, 152ca, and 152cb**) in 1X PBS buffer (0.40 mM, 1.5 mL) at 37 °C were treated with an aliquot (10 μL) of the Pronase E solution. Aliquots (50 μL) were removed after 0, 30, 60, 90, 150, 210, 270, and 360 min. The aliquots were quenched with glacial acetic acid (10 μL), diluted to 75 μL with 1X PBS buffer, and analyzed by HPLC (Phenomenex Jupiter C18, 5 μm particle size, 300

Å pore size, 4.6 × 250 mm, 40 µL injection volume, 10%–60% $CH_3CN$ in $H_2O$ gradient over 50 min, then 95% $CH_3CN$ in $H_2O$ for 10 min, flow rate: 1 mL/min).

Here, the pairing of ΔVal or ΔEnv at the *i+2* position with D-Pro at *i+1* improved the proteolytic resistance of the already enzymatically stable *β*-hairpin **153b (Figure 3.5.)**. However, the stabilizing effect of ΔVal was larger than ΔEnv and considerably evident in this case. Peptide **153ca** was ca. 2.5 times more stable to proteolysis than **153b**, whereas **153cb** was ca. 1.5 times more stable than the original peptide. Our results demonstrate that the incorporation of a bulky ΔAA in a peptide containing a D-amino acid can synergistically increase the resistance of the peptide to enzymatic degradation. Hence, such a combination can be useful in the design of novel peptides with enhanced proteolytic stability and minimal destabilization of secondary structures.

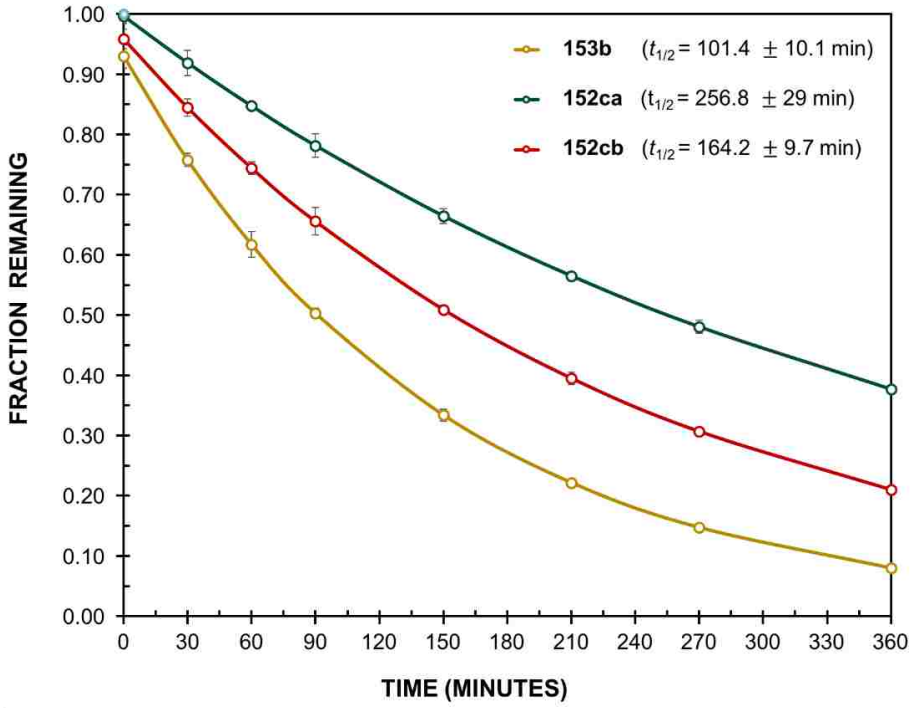


**Figure 3.5.** Proteolysis plot of Waters' *β*-hairpin **153b** and its *i+1* analogues **152ca** and **152cb**.

Analytical HPLC traces of $\beta$-hairpins **153** and their most proteolytically stable ΔAA–containing analogues are shown below (**Figures 3.6–3.9**).

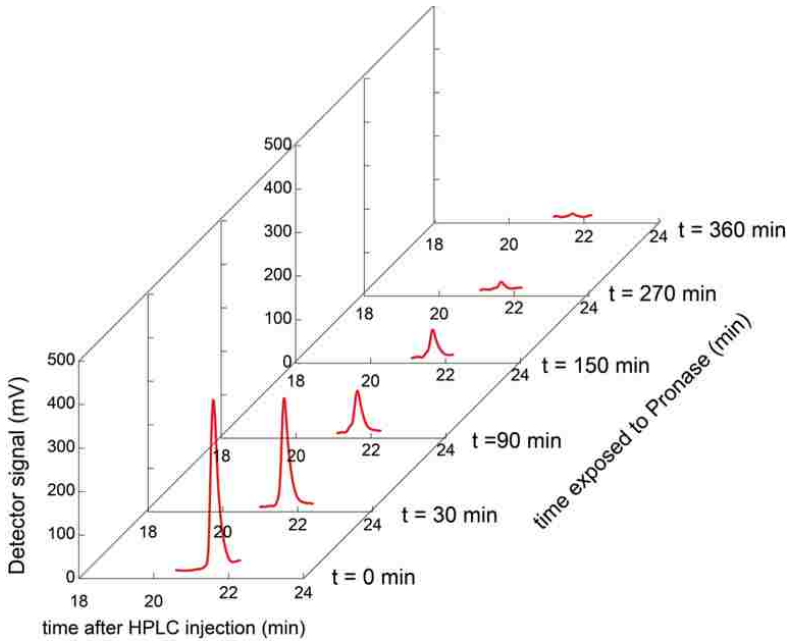


**Figure 3.6**. Analytical HPLC traces (monitored at 220 nm) for peptide **153a** (0.10 mM) after incubation in Pronase E for up to 360 min.

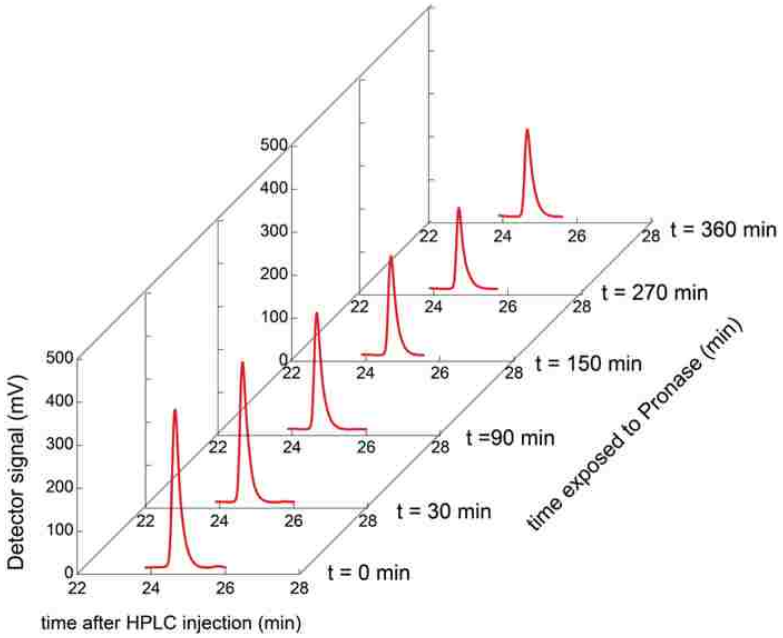


**Figure 3.7.** Analytical HPLC traces (monitored at 220 nm) for peptide **152aa** (0.10 mM) after incubation in Pronase E for up to 360 min.

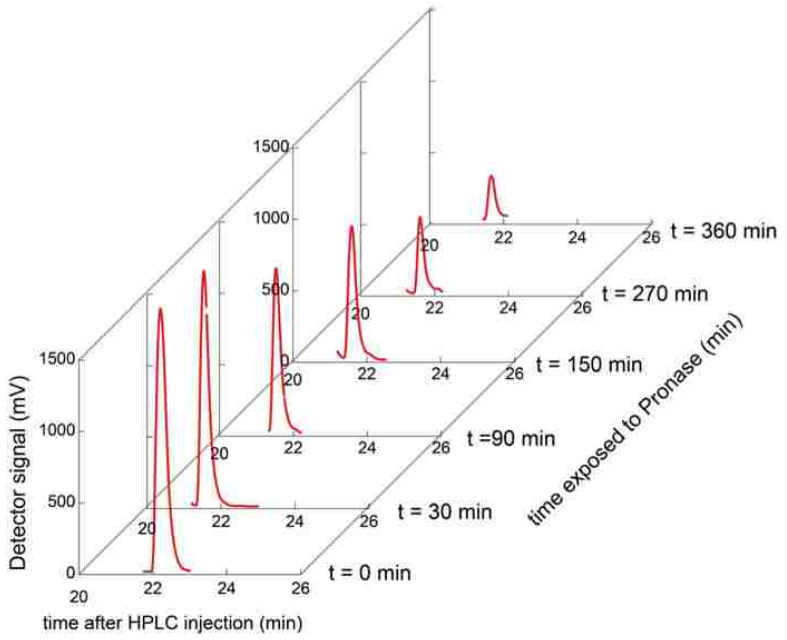


**Figure 3.8.** Analytical HPLC traces (monitored at 220 nm) for peptide **153b** (0.40 mM) after incubation in Pronase E for up to 360 min.

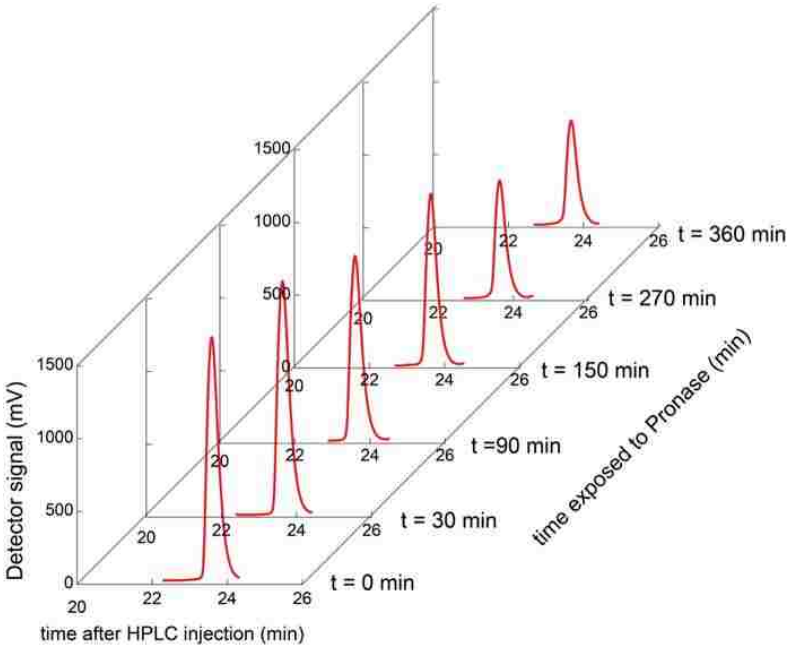


**Figure 3.9.** Analytical HPLC traces (monitored at 220 nm) for peptide **152ca** (0.40 mM) after incubation in Pronase E for up to 360 min.

## 3.5 One-dimensional and two-dimensional NMR spectroscopy to study the conformations of *α,β*-dehydroamino acid containing *β*-hairpins

Advancements in NMR methodology in the past few decades have made it possible to determine the three-dimensional structures of small proteins or peptides in solution. With the increase in magnetic field strength and subsequent higher resolution of 1D and 2D spectra, NMR sensitivity improved significantly to study peptides or proteins at millimolar concentrations. A detailed NMR study can reveal important conformational features of peptides and proteins. Peptide secondary structures induce unique chemical shifts for certain amino acids. It has been shown that a strong relationship exists between $C_\alpha H$ 1H NMR chemical shifts and protein secondary structures for all the naturally occurring 20 amino acids.[32]

The chemical shift perturbations to $C_\alpha$ protons in *α*-helices, turns and *β*-sheets have been widely studied, and provide valuable insights into the folding patterns of peptides. When compared to the random coil (0% folded) $C_\alpha$ proton chemical shift values, there is an upfield shift in $C_\alpha$ protons in *α*-helices and turns, whereas $C_\alpha$ protons are shifted downfield in *β*-sheets.[33] There are alternating hydrogen-bonded residues in the strands of *β*-hairpins, which leads to *i*, *i+2* periodicity. Sharman et al. observed that $C_\alpha$ protons of the residues in *β*-hairpin strands are exposed to two different chemical environments and hence, they classified these protons into $H_{in}$ ($C_\alpha H$ facing the opposite strand) and $H_{out}$ ($C_\alpha H$ away from the opposite strand or outward into the solvent).[34] Moreover, $H_{in}$ protons are part of residues that are not involved in hydrogen bonding, whereas $H_{out}$ protons belong to residues that are engaged in hydrogen bonding. They observed that there are larger chemical shift deviations from the random coil values for $H_{in}$ than for $H_{out}$. This observation can be attributed to the electrostatic and anisotropic effect of the carbonyl group on the residues of the opposite strand. They postulated that $C_\alpha H$ chemical shift deviations in well-folded *β*-hairpins

were higher because of the proximity of the two strands and smaller H-bonding distances between them. Further structural elucidation can be done by NOESY and ROESY studies to investigate the spatial interactions between the two strands. Hence, 1D and 2D NMR studies are very informative and crucial in the determination of $\beta$-hairpin folding.

We performed 1D and 2D NMR studies on all the $\alpha,\beta$-dehydroamino-acid-containing $\beta$-hairpins we synthesized. Peptide solutions were prepared in 20 mM sodium phosphate buffer, pH 7, and peptide concentrations were determined spectroscopically based on tryptophan absorbance at 280 nm in 6 M guanidine hydrochloride (Trp $\varepsilon_{280} = 5690\ M^{-1}cm^{-1}$). NMR samples of monomeric **152aa–152cb** were prepared (1–3.5 mM peptide) in $D_2O$ (10% v/v $D_2O/H_2O$) buffered to pD 3.9 with 5000 μM NaOAc-$d_3$/$CD_3COOD$ buffer. Sodium 2,2-dimethyl-2-silapentane-5-sulfonate (DSS) was used as an internal chemical shift reference and was set to 0 ppm. Water suppression was achieved by an excitation sculpting (ES) sequence. 2D zTOCSY and ROESY-AD experiments were performed on all the samples and enabled us to assign all the amide and $C_\alpha H$ protons unambiguously.

As discussed earlier in this section, we also observed downfield chemical shifts relative to the random coil values for all $C_\alpha H$ protons in the two strands. It is noteworthy to mention that the $C_\alpha H$ protons of the residues not involved in H-bonding shifted further downfield which is in agreement with the literature reports. The $C_\alpha H$ protons of the two turn residues are shifted upfield and the C terminus also shows upfield shifts because of fraying at the ends of the strands. The trends for $C_\alpha H$ chemical shifts of all the $\beta$-hairpins we synthesized are shown below (**Figures 3.10–3.17**). Since we synthesized random coils **168** for peptides **153a** and **152aa**, their chemical shifts are compared to their random coil shift values, whereas we used the random coil references reported in the literature for the rest of the peptides (**Figure 3.10**).[35]

Ac-R-W-V-E-V-N-G-$NH_2$ (**168a**): **N-terminal portion of 153a**

Ac-N-G-O-K-I-L-Q-$NH_2$ (**168b**): **C-terminal portion of 153a**

Ac-R-W-V-E-V-ΔVal-G-$NH_2$ (**168c**): **N-terminal portion of 152aa**

Ac-ΔVal-G-O-K-I-L-Q-$NH_2$ (**168d**): **C-terminal portion of 152aa**

**Figure 3.10.** Random coils (**168**).

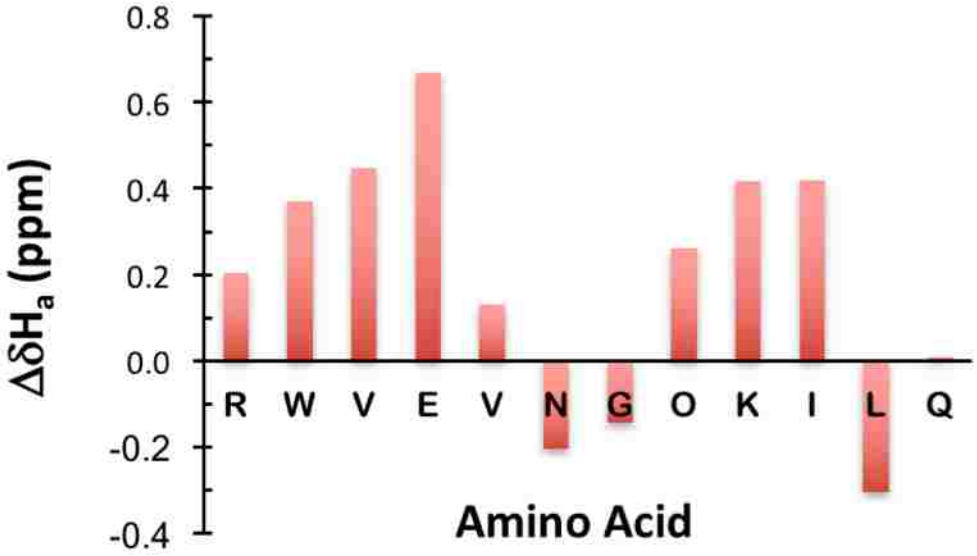


**Figure 3.11.** Hα chemical shift differences between the residues in **153a** and the corresponding random coil 7-mers **168a** and **168b**.

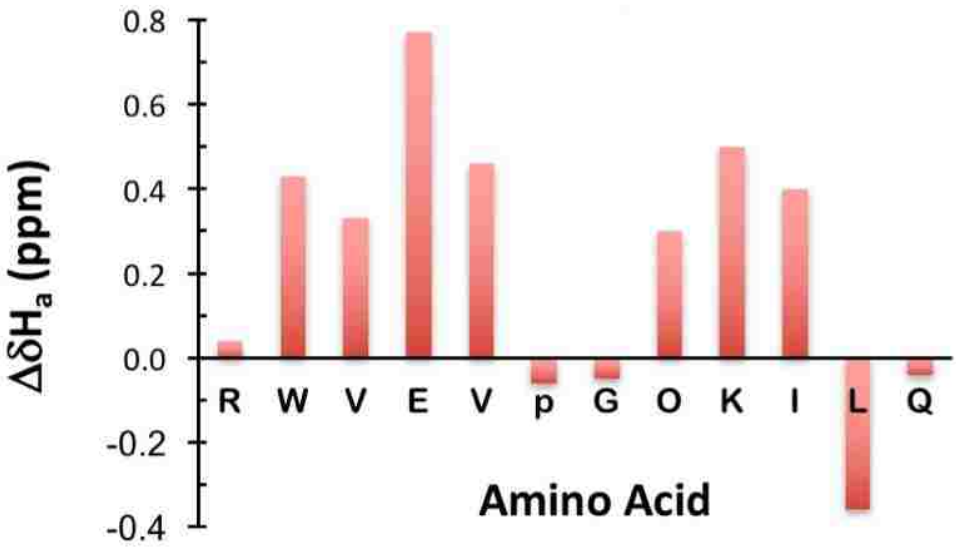


**Figure 3.12.** Hα chemical shift differences between the residues in **153b** and the random coil values obtained from Wüthrich, K. NMR of Proteins and Nucleic Acids, Wiley: New York (1986).

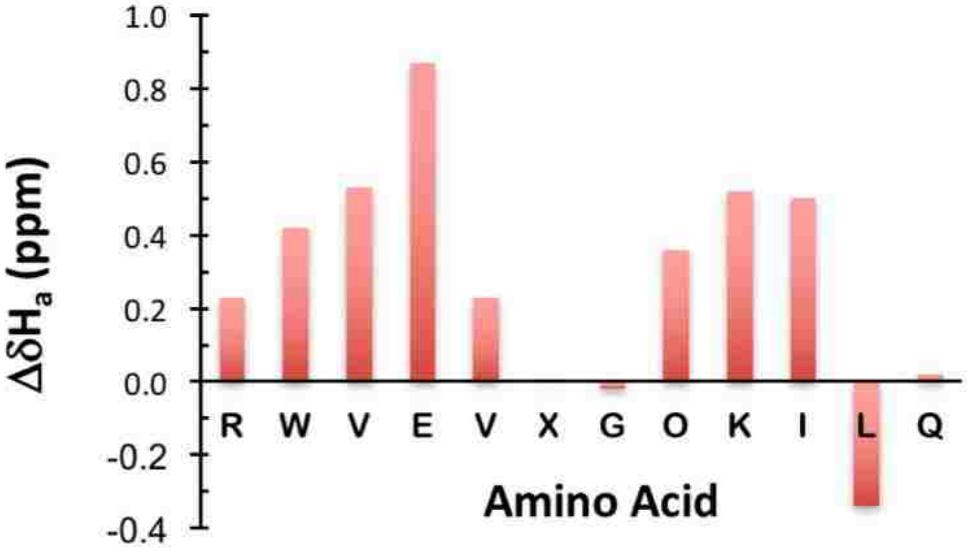


**Figure 3.13**. Hα chemical shift differences between the residues in **152aa** and the corresponding random coil 7-mers **168c** and **168d**.

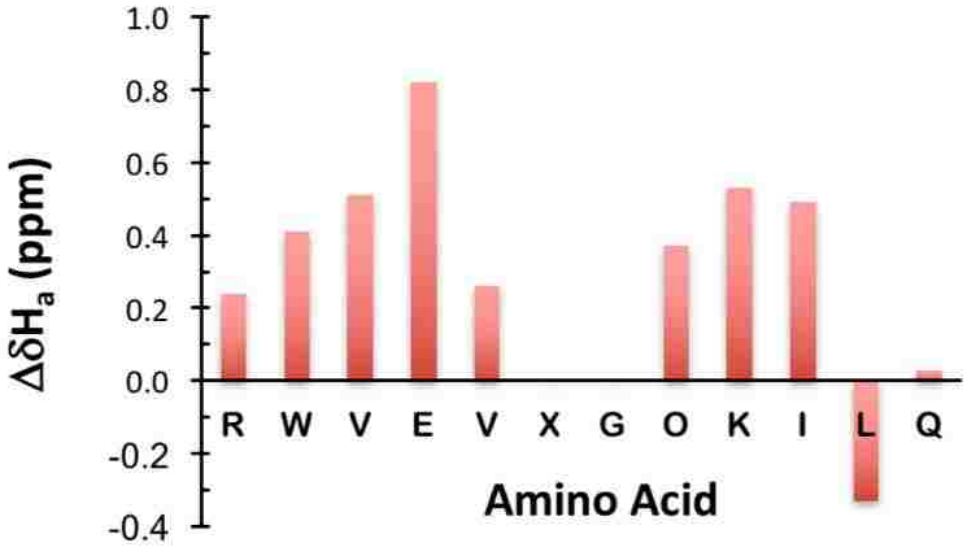


**Figure 3.14.** Hα chemical shift differences between the residues in **152ab** and the random coil values obtained from Wüthrich, K. NMR of Proteins and Nucleic Acids, Wiley: New York (1986).

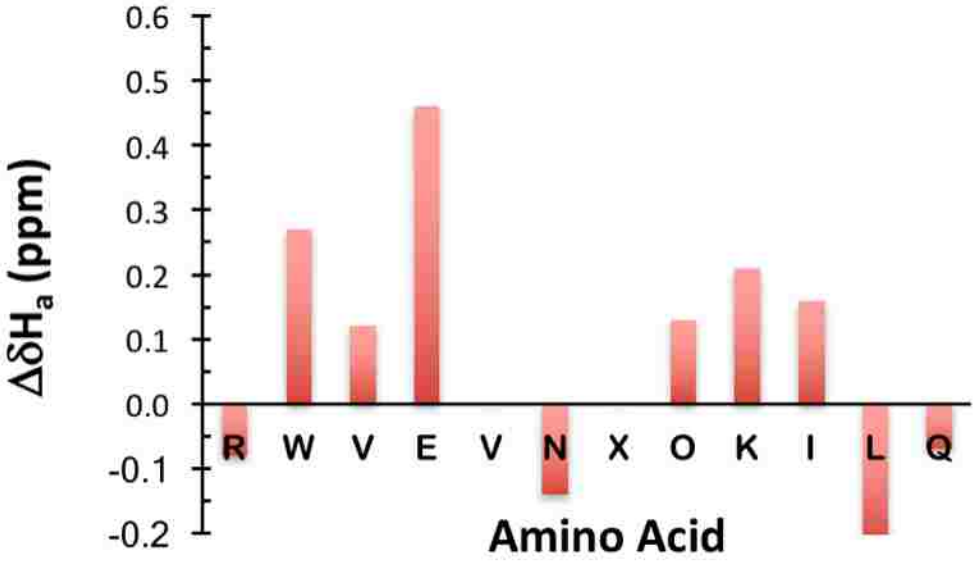


**Figure 3.15.** Hα chemical shift differences between the residues in **152ba** and the random coil values obtained from Wüthrich, K. NMR of Proteins and Nucleic Acids, Wiley: New York (1986).

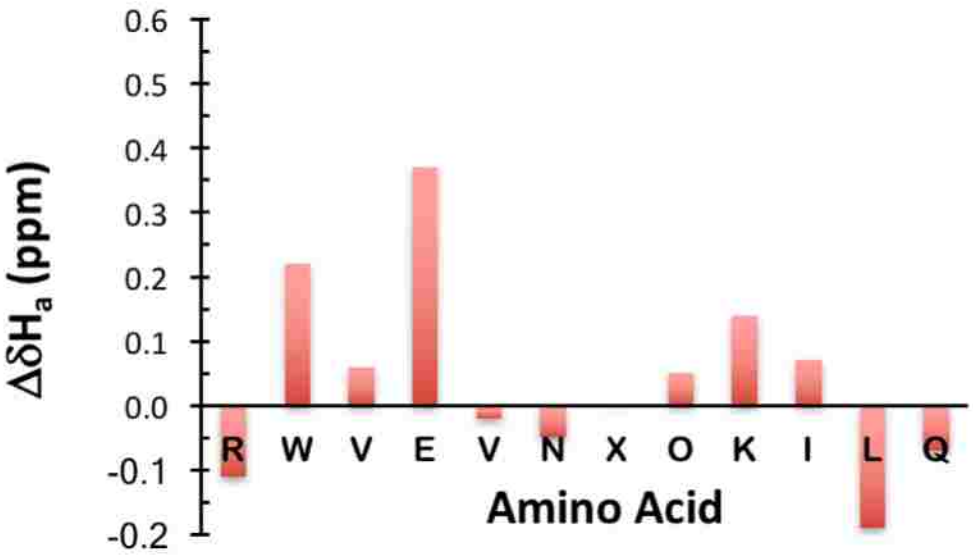


**Figure 3.16.** Hα chemical shift differences between the residues in **152bb** and the random coil values obtained from Wüthrich, K. NMR of Proteins and Nucleic Acids, Wiley: New York (1986).

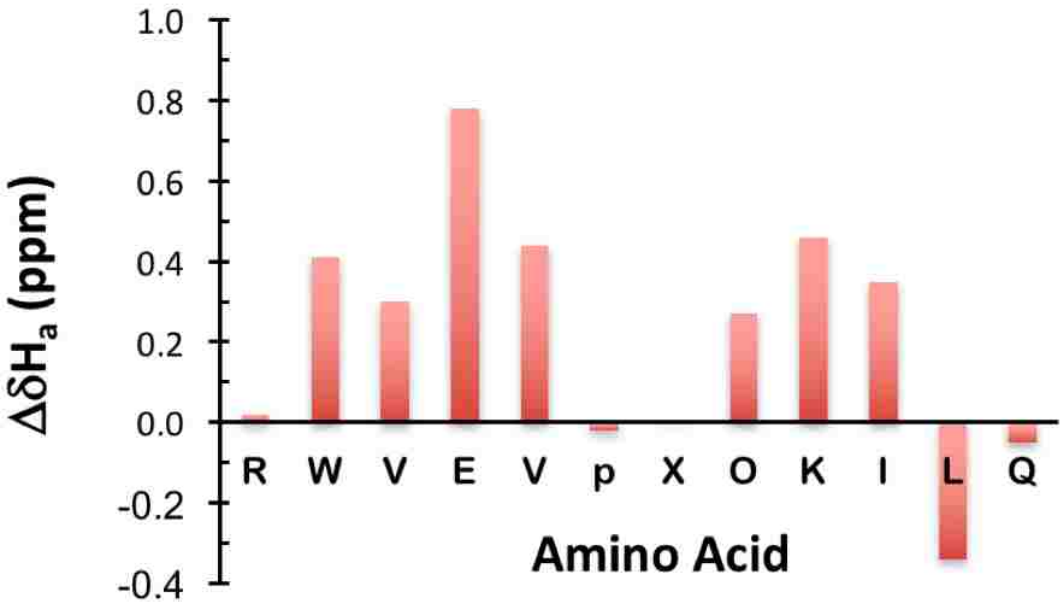


**Figure 3.17.** Hα chemical shift differences between the residues in **153ca** and the random coil values obtained from Wüthrich, K. NMR of Proteins and Nucleic Acids, Wiley: New York (1986).

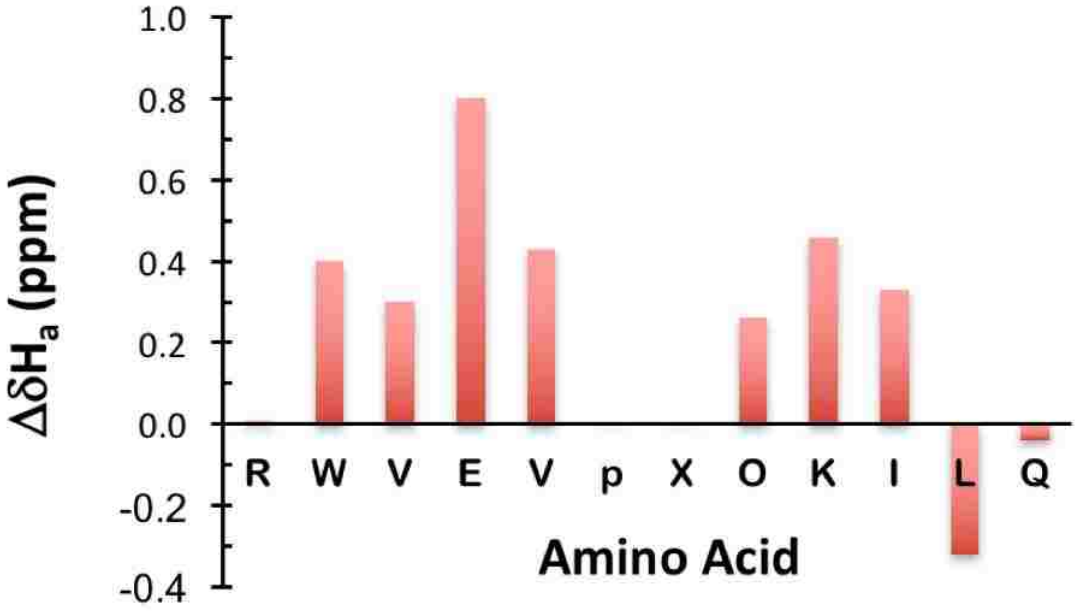


**Figure 3.18.** Hα chemical shift differences between the residues in **153cb** and the random coil values obtained from Wüthrich, K. NMR of Proteins and Nucleic Acids, Wiley: New York (1986).

It is evident from **Figures 3.11–3.18** that the Hα chemical shifts are shifted significantly downfield (i.e. ≥ 0.2 ppm) when compared to the random coil values and that *α*,*β*-dehydroamino-acid-containing peptides are in fact forming a significant population of *β*-hairpin structures in solution.

Multiple cross-strand NOEs were observed in all the peptides, which further corroborates that the two opposite strands are in close proximity. These NOE peaks are characteristic features of *β*-hairpins or *β*-sheets. Except for **152ab** and **152bb**, all the peptides exhibited one set of well-defined spin systems suggesting the existence of a highly populated single low-energy conformation. This can also be attributed to rapid equilibration between multiple conformations. Extra spin systems were detected in homogeneous solutions of peptides **152ab** and **152bb**, which

can be explained by the occurrence of two or more conformations that interconvert slowly on the NMR time scale (**Figure 3.19**).

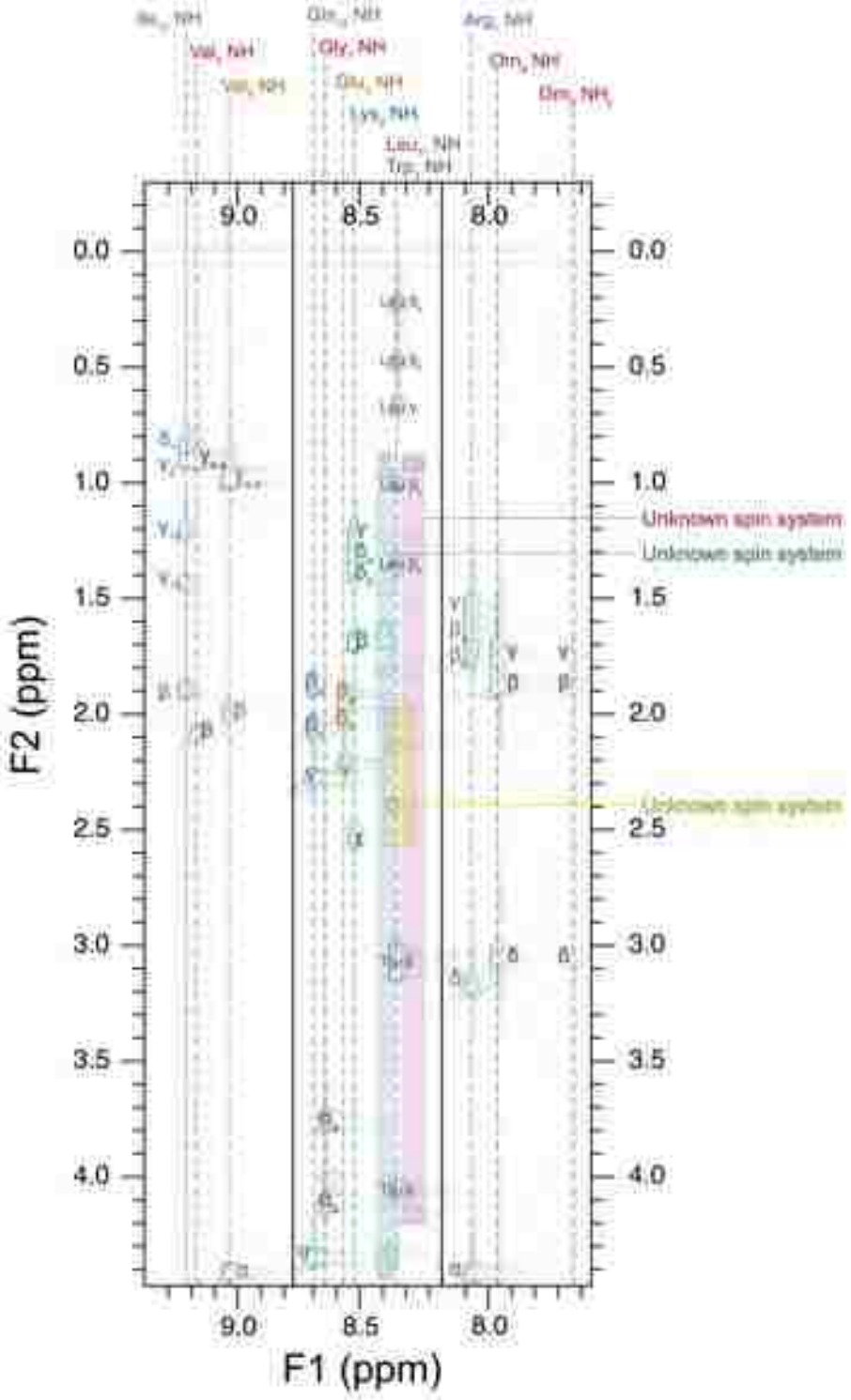


**Figure 3.19.** Multiple spin systems in the TOCSY spectra of **152ab**.

The tables listing major NOE peaks of peptides **152**,**153** & **167b** are given below (**Tables 3.1–3.9**).

**Table 3.1.** Ac-R-W-V-E-V-**N-G**-O-K-I-L-Q-$NH_2$ (**153a**).

| Res I | Res II | Peak |
|---|---|---|
| **2**Trp H2,4 | **11**Leu δ | S |
| **2**Trp H7 | **11**Leu δ | M |
| **2**Trp α | **11**Leu δ | M |
| **2**Trp β | **11**Leu δ | W |
| **2**Trp H6 | **11**Leu γ | M |
| **2**Trp H2,7 | **11**Leu α | M |
| **2**Trp H2 | **11**Leu β | M |
| **2**Trp H6 | **11**Leu β | W |
| **2**Trp β, H7 | **11**Leu β | S |
| **2**Trp α | **11**Leu α | S |
| **1**Arg α | **11**Leu δ | M |
| **1**Arg β | **12**Gln H | W |
| **4**Glu H | **10**Ile γ | S |
| **2**Trp H6,7 | **10**Ile α | S |
| **2**Trp H2 | **10**Ile α, γ | M |
| **5**Val γ | **8**Orn H | M |
| **5**Val H | **8**Orn H | S |
| **2**Trp H2,6,7 | **9**Lys γ | S |
| **2**Trp H7 | **9**Lys α | W |
| **5**Val γ | **6**Asn δ | S |

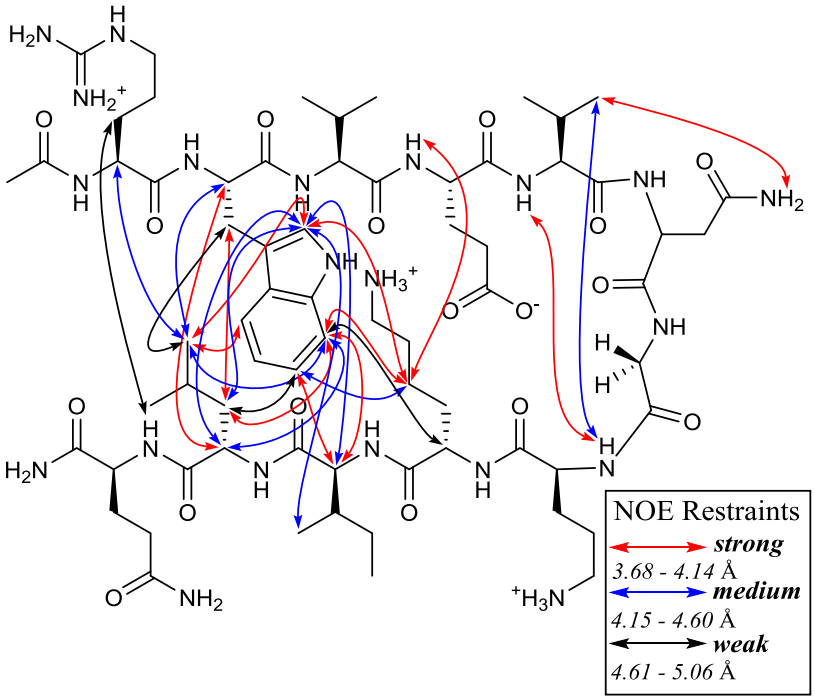


**Table 3.2.** Ac-R-W-V-E-V-**p-G**-O-K-I-L-Q-$NH_2$ (**153b**).

| Res I | Res II | Peak |
|---|---|---|
| **2**Trp H4 | **11**Leu α | M |
| **2**Trp α, H2 | **11**Leu α | S |
| **2**Trp H1,7 | **11**Leu δ | S |
| **2**Trp α | **11**Leu δ | W |
| **2**Trp H1,4 | **11**Leu δ | W |
| **2**Trp H1,5 | **11**Leu γ | M |
| **2**Arg α | **11**Leu δ | M |
| **2**Trp H2 | **9**Lys γ | W |
| **2**Trp H4 | **9**Lys γ, δ | M |
| **2**Trp H1,4 | **9**Lys β | S |
| **2**Trp α | **10**Ile H | S |
| **2**Trp H5 | **10**Ile α | S |
| **2**Trp H1 | **10**Ile α | M |
| **2**Trp H4 | **10**Ile α | W |
| **4**Glu γ | **8**Orn H | M |
| **6**D-Pro α | **8**Orn H | M |
| **5**Val H | **8**Orn H | M |
| **1**Arg δ | **12**Gln α | M |
| **2**Trp H2 | **12**Gln γ | M |
| **5**Val γ | **6**D-Pro δ | S |

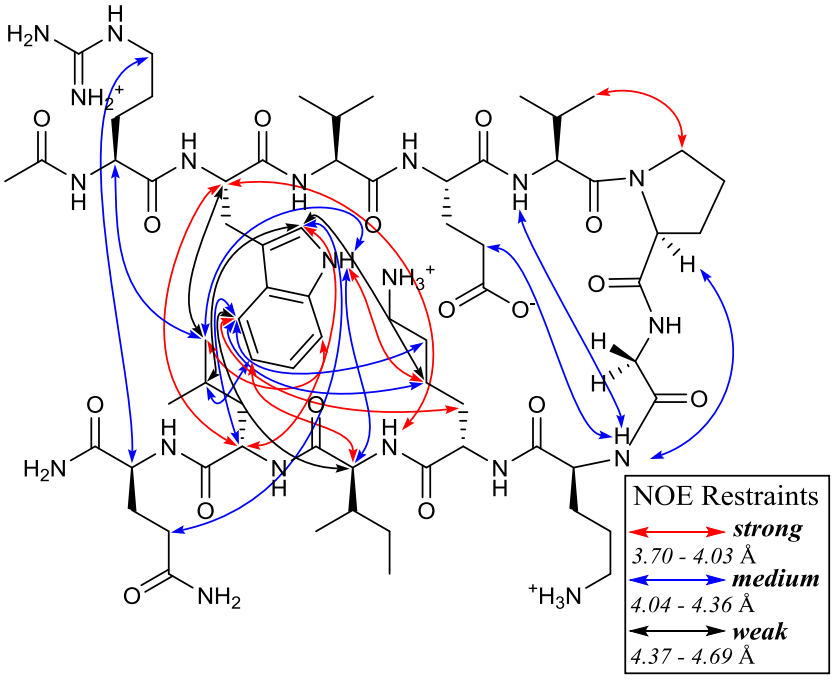

**Table 3.3.** Ac-R-W-V-E-V-ΔVal-G-O-K-I-L-Q-$NH_2$ (**152aa**).

| Res I | Res II | Peak |
|---|---|---|
| **2**Trp H1,4 | **11**Leu δ | W |
| **2**Trp H7 | **11**Leu δ | M |
| **2**Trp H2 | **11**Leu δ | S |
| **2**Trp α, β | **11**Leu δ | M |
| **2**Trp H2,5 | **11**Leu γ | M |
| **2**Trp H2,4 | **11**Leu α | M |
| **2**Trp α | **11**Leu α | S |
| **2**Trp H2 | **11**Leu β | W |
| **1**Arg α | **11**Leu δ | M |
| **4**Glu β | **11**Leu δ | M |
| **2**Trp H2,5 | **9**Lys β | M |
| **2**Trp H4d | **9**Lys δ | M |
| **2**Trp H4 | **9**Lys γ | W |
| **2**Trp H4 | **9**Lys β | S |
| **2**Trp H4 | **10**Ile α | M |
| **2**Trp H2 | **10**Ile α | W |
| **2**Trp H5 | **10**Ile α | S |
| **2**Trp H4 | **10**Ile γ | S |
| **5**Val H | **8**Orn H | S |
| **2**Trp H2 | **12**Gln γ | W |
| **1**Arg H | **12**Gln β | W |
| **6**ΔVal γ | **5**Val γ | S |

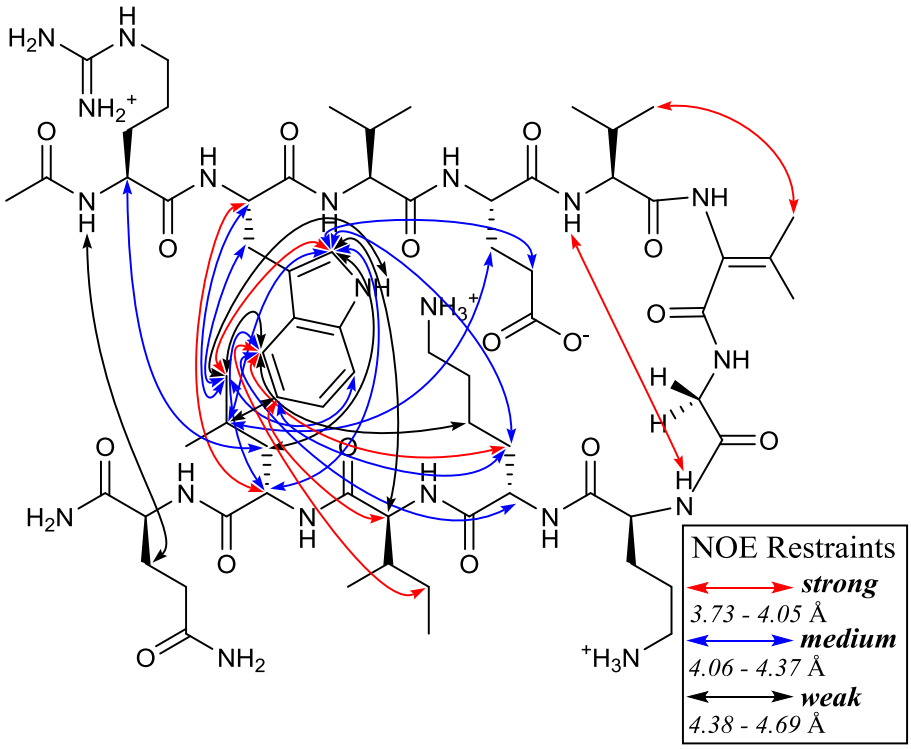


**Table 3.4.** Ac-R-W-V-E-V-ΔEnv-G-O-K-I-L-Q-$NH_2$ (**152ab**).

| Res I | Res II | Peak |
|---|---|---|
| **2**Trp H2 | **11**Leu δ | S |
| **2**Trp α, H4,5 | **11**Leu δ | W |
| **2**Trp H7 | **11**Leu δ | M |
| **2**Trp H2,5 | **11**Leu γ | M |
| **2**Trp H4,7 | **11**Leu γ | W |
| **2**Trp α | **11**Leu α | S |
| **2**Trp H2 | **10**Leu α | W |
| **2**Trp H4 | **11**Leu α | M |
| **2**Trp H5 | **10**Ile α | M |
| **2**Trp H2 | **10**Ile α | W |
| **2**Trp H2 | **9**Lys β | M |
| **9**Lys β, γ, δ | **2**Trp H4 | S |
| **9**Lys γ, ε | **2**Trp H2 | W |
| **2**Trp H5 | **9**Lys β | M |
| **2**Trp H4 | **12**Gln γ | S |
| **8**Orn β | **5**Val H | S |
| **6**ΔEnv δ | **5**Val α | W |
| **1**Arg δ | **12**Gln ε | S |
| **1**Arg α | **11**Leu δ | S |

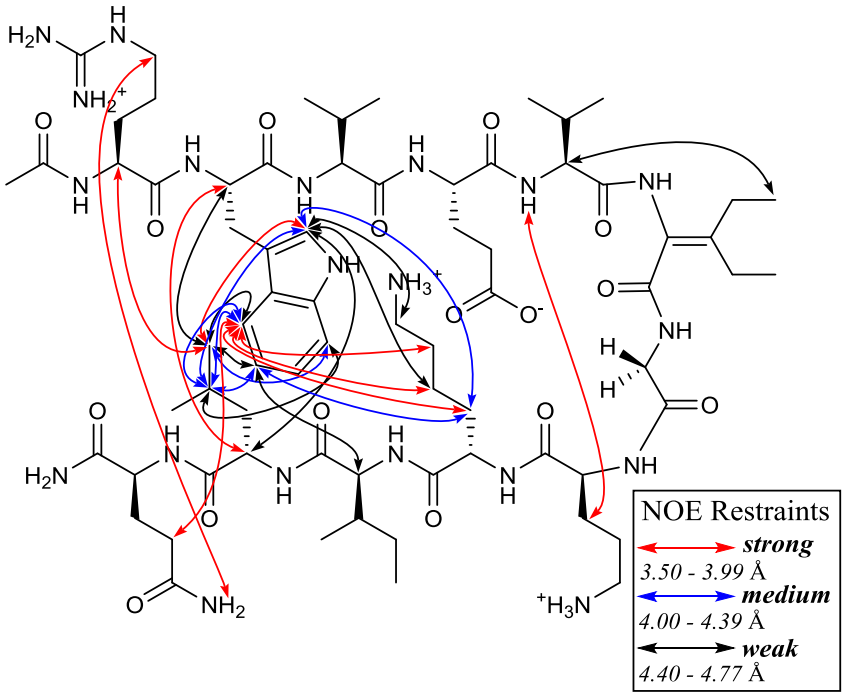

**Table 3.5.** Ac-R-W-V-E-V-**N-ΔVal**-O-K-I-L-Q-$NH_2$ (**152ba**).

| Res I | Res II | Peak |
|---|---|---|
| **1**Arg ε | **12**Gln γ | W |
| **1**Arg ε | **10**Ile γ | M |
| **2**Trp H2 | **10**Ile γ | M |
| **2**Trp H1,7 | **11**Leu δ | W |
| **2**Trp H2,4 | **11**Leu δ | M |
| **2**Trp β | **11**Leu δ | W |
| **2**Trp α | **11**Leu δ | M |
| **2**Trp α | **11**Leu α | S |
| **2**Trp H7 | **9**Lys γ | S |
| **2**Trp H2 | **9**Lys γ | W |
| **2**Trp H7 | **11**Leu α | S |
| **2**Trp H2 | **11**Leu α | M |
| **2**Trp H7 | **10**Ile α | M |
| **2**Trp H2 | **10**Ile α | W |
| **2**Trp H6 | **10**Ile α | S |
| **2**Trp H2,7 | **11**Leu β | S |
| **2**Trp H7 | **11**Leu δ | S |
| **5**Val H | **9**Orn H | M |
| **4**Glu γ | **7**ΔVal H | S |
| **4**Glu γ | **8**Orn H | S |

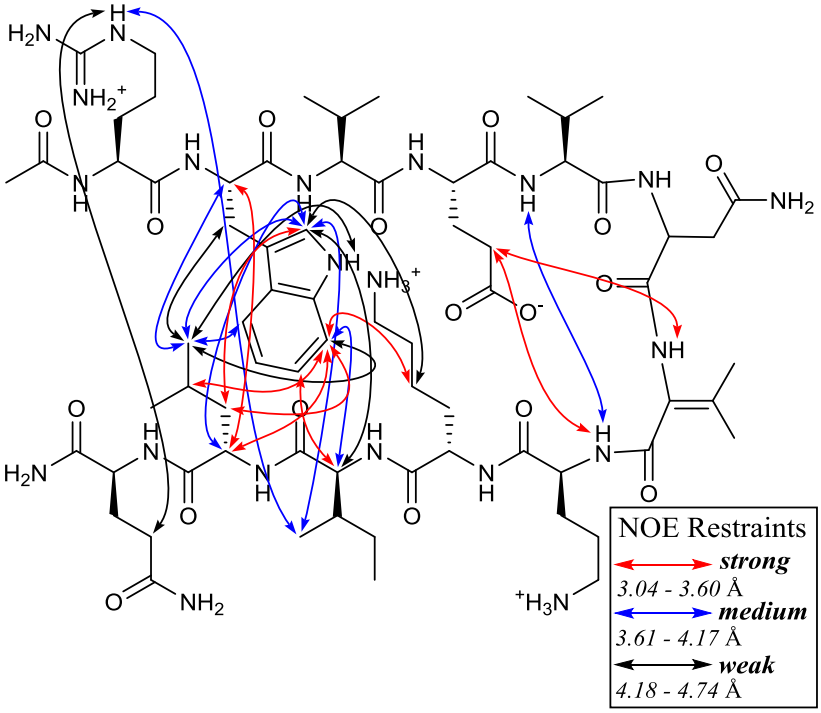


**Table 3.6.** Ac-R-W-V-E-V-**N-ΔEnv**-O-K-I-L-Q-$NH_2$ (**152bb**).

| -Res I | Res II | Peak |
|---|---|---|
| **2**Trp H2,7 | **11**Leu δ | M |
| **2**Trp H1,4 | **11**Leu δ | W |
| **2**Trp α | **11**Leu δ | S |
| **2**Trp H7 | **11**Leu β | S |
| **2**Trp H5 | **11**Leu γ | W |
| **2**Trp α | **11**Leu α | S |
| **2**Trp H7 | **11**Leu α | M |
| **1**Arg H | **11**Leu δ | M |
| **2**Trp H2 | **9**Lys β | M |
| **2**Trp H7 | **9**Lys β | S |
| **2**Trp H2 | **9**Lys δ | W |
| **2**Trp H7 | **9**Lys γ | S |
| **1**Arg ε | **9**Lys β | M |
| **2**Trp H2 | **4**Glu γ | S |
| **1**Arg ε | **10**Ile γ | W |
| **5**Val H | **8**Orn H | M |
| **11**Leu α | **2**Trp H2 | W |
| **6**Asn δ | **5**Val γ | S |

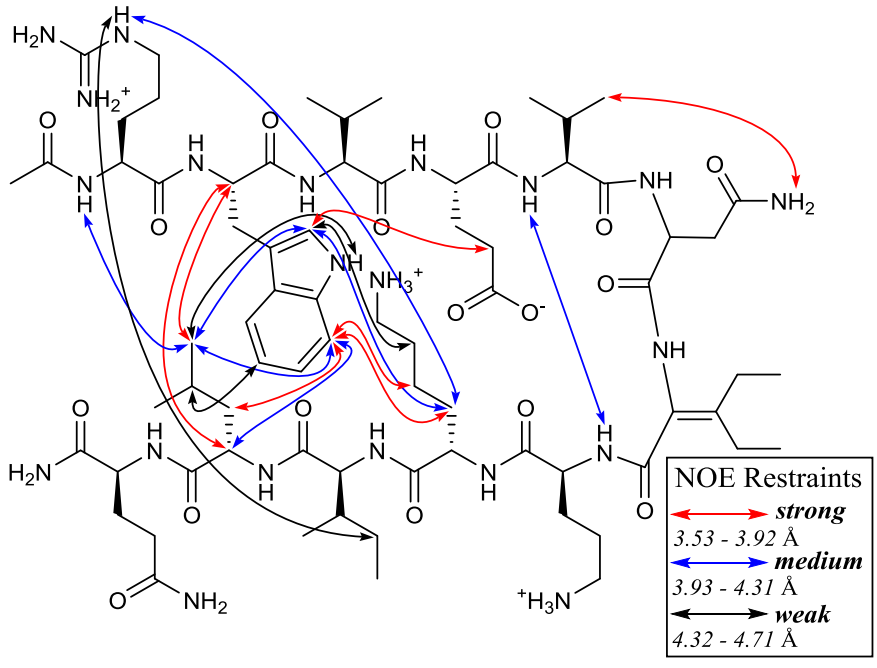

**Table 3.7.** Ac-R-W-V-E-V-**p-ΔVal**-O-K-I-L-Q-$NH_2$ (**152ca**).

| Res I | Res II | Peak |
|---|---|---|
| **2**Trp H1,4,7 | **11**Leu δ | M |
| **2**Trp H6,α | **11**Leu δ | W |
| **2**Trp H2 | **11**Leu δ | S |
| **2**Trp H2,6 | **11**Leu γ | W |
| **2**Trp H2,7 | **11**Leu α | W |
| **2**Trp α | **11**Leu α | S |
| **2**Trp H7,β | **11**Leu β | S |
| **1**Arg H,α | **11**Leu δ | M |
| **2**Trp H6 | **10**Ile α | S |
| **2**Trp H7 | **10**Ile H | M |
| **2**Trp H2 | **10**Ile γ | W |
| **2**Trp H7 | **9**Lys β | S |
| **2**Trp H7,β | **9**Lys γ | M |
| **2**Trp H6 | **9**Lys δ | W |
| **4**Glu H | **9**Lys α | S |
| **4**GluH | **10**Ile γ | S |
| **1**Arg H | **12**Gln H | S |
| **2**Trp α | **12**Gln H | W |
| **5**Val H | **8**Orn H | S |
| **5**Val γ | **6**D-Pro δ | S |

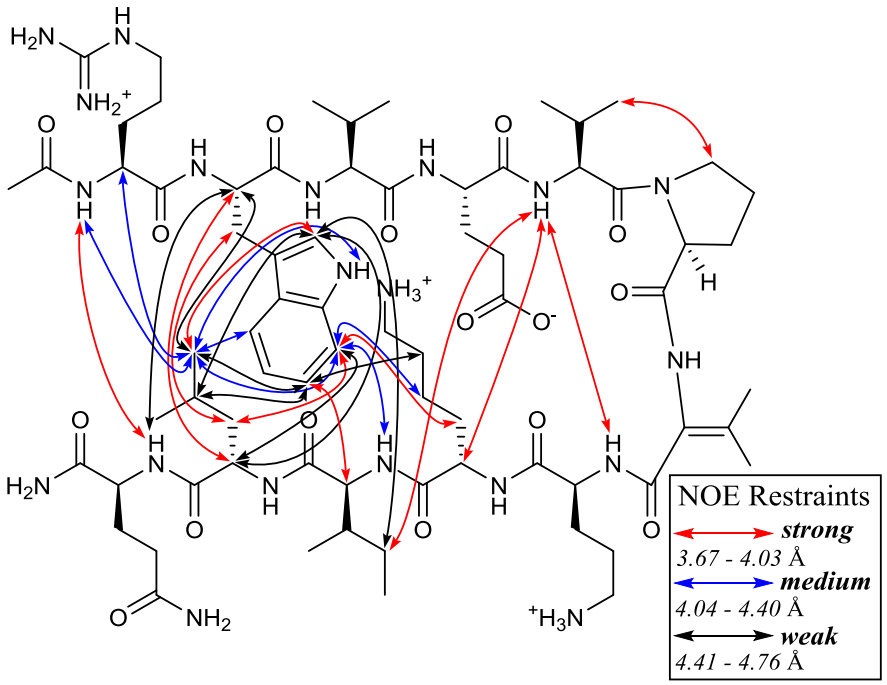


**Table 3.8.** Ac-R-W-V-E-V-**p-ΔEnv**-O-K-I-L-Q-$NH_2$ (**152cb**).

| Res I | Res II | Peak |
|---|---|---|
| **2**Trp H1,4 | **11**Leu δ | W |
| **2**Trp H2,7, α | **11**Leu δ | M |
| **2**Trp α | **11**Leu δ | M |
| **2**Trp H4, α | **11**Leu α | S |
| **2**Trp H2 | **11**Leu α | M |
| **2**Trp H4 | **11**Leu β | M |
| **1**Arg α | **11**Leu δ | W |
| **1**Arg H | **12**Gln β | W |
| **2**Trp H4 | **12**Gln α | W |
| **2**Trp H4 | **9**Lys β | S |
| **2**Trp H2 | **9**Lys β | M |
| **2**Trp H2,5 | **9**Lys γ | W |
| **4**Trp H2 | **9**Lys δ | W |
| **1**Trp H4 | **9**Lys δ | M |
| **4**Glu H | **9**Lys α | S |
| **5**Val H | **8**Orn H | S |
| **2**Trp H5 | **10**Ile α | S |
| **2**Trp H2 | **10**Ile α | W |
| **2**Trp H4 | **10**Ile γ | M |
| **4**Glu H | **10**Ile γ | S |
| **6**D-Pro δ | **7**ΔEnv | S |
| **5**Val γ | **6**D-Pro δ | S |

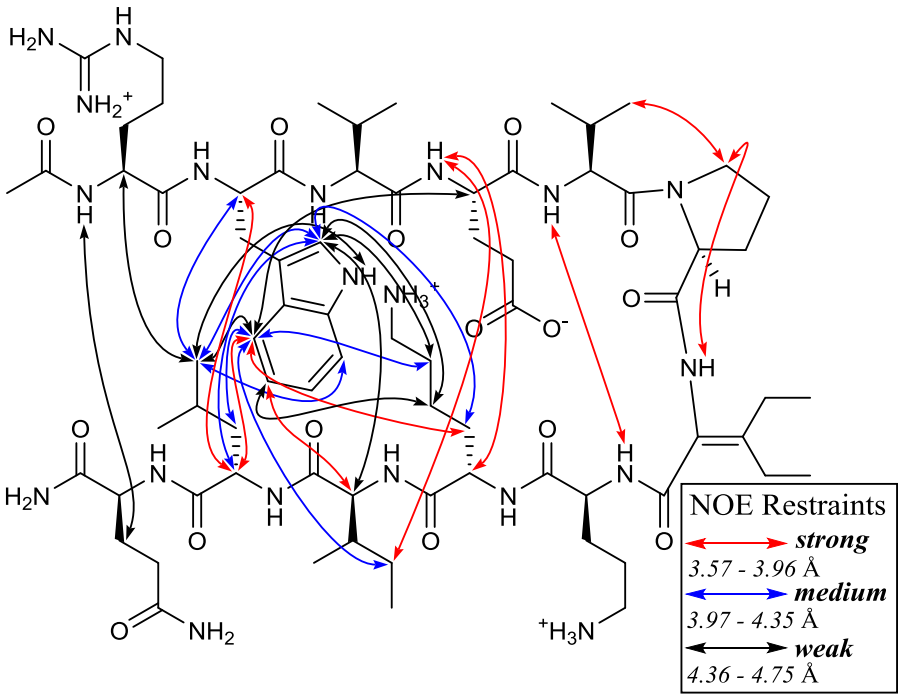

**Table 3.9**. c[Ac-Cys-R-W-V-E-V-ΔVal-G-O-K-I-L-Q-Cys-$NH_2$] (**167b**).

| Res I | Res II | Peak |
|---|---|---|
| **2**Trp α | **11**Leu δ | M |
| **2**Trp H1,2,4 | **11**Leu δ | M |
| **2**Trp H5,7 | **11**Leu δ | W |
| **2**Trp H4,2 | **11**Leu γ | W |
| **2**Trp H4 | **11**Leu α | W |
| **2**Trp H2 | **11**Leu α | S |
| **2**Trp α | **11**Leu α | S |
| **2**Trp H5 | **11**Leu H | W |
| **2**Trp H2 | **11**Leu H | M |
| **1**Arg α | **11**Leu δ | M |
| **2**Trp H2 | **9**Lys β | S |
| **2**Trp H4 | **9**Lys β | W |
| **2**Trp H5 | **9**Lys β | M |
| **2**Trp H2 | **9**Lys ε | W |
| **2**Trp H2 | **9**Lys δ | M |
| **2**Trp H2 | **10**Ile α | M |
| **2**Trp H5 | **10**Ile α | S |
| **5**Val H | **8**Orn H | S |
| **6**ΔVal γ | **6Val** γ | S |

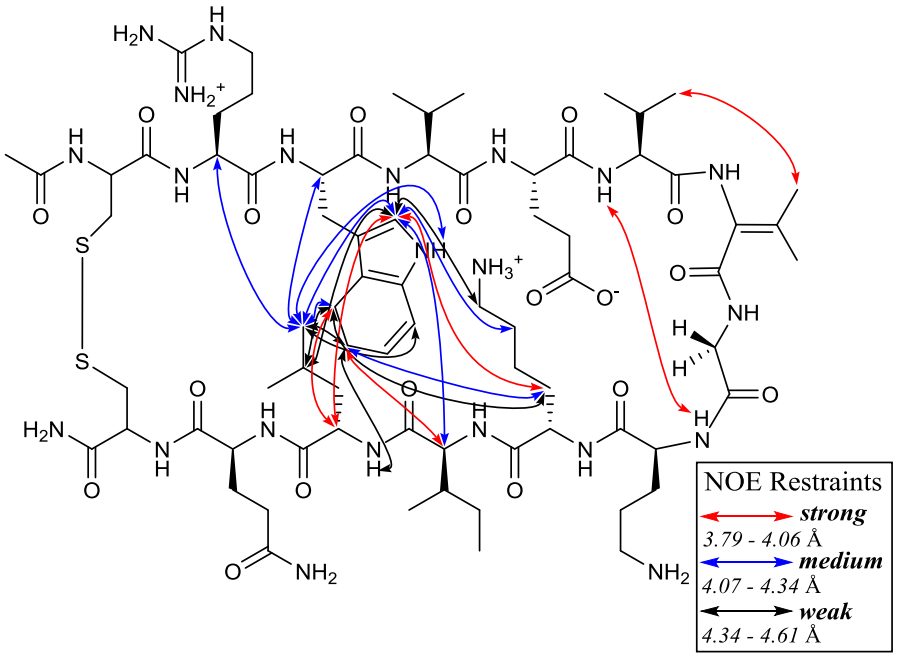


### 3.5.1 Determination of the *β*-hairpin population in solution (percent folded)

Along with the qualitative estimation of folding, $^1$H NMR chemical shifts have also been used reliably to compute the percent folded in solution.[29, 36] The percent folded state was determined using two methods.

First, the Hα chemical shifts of residues that form cross-strand hydrogen bonds in peptides **152aa** and **153a** were compared to the corresponding Hα chemical shifts in random coil 7-mers **168** representing the unfolded structures ($\delta_0$) and Hα chemical shifts in cyclic controls **167** (Section 2.7) representing the fully folded structures ($\delta_{100}$). The Hα chemical shifts of residues in peptides **153a** and **152aa** were designated as $\delta_{obs}$. The percent folded at each residue was determined by Equation (i):

$$\textbf{Percent Folded} = [(\delta_{obs} - \delta_o)/\delta_{100} - \delta_o)] \text{ X } 100\ \% \quad \text{(i)}$$

The overall percent folded was calculated by averaging the percent folded values for residues Val3, Val5, Orn8, and Ile10, each of which are involved in cross-strand hydrogen bonds (**Table 3.10** and **Table 3.11**).

**Table 3.10.** Percent folded state of Ac-R-W-V-E-V-**ΔVal-G**-O-K-I-L-Q-$NH_2$ (**152aa**).

| Amino Acids | 152aa | 167b | Random Coil | % Folded | Average % Folded | Standard Error |
|---|---|---|---|---|---|---|
| Val 3 | 4.534 | 4.608 | 4.009 | 87.64 | 89.99 | 2.0 |
| Val 5 | 4.385 | 4.397 | 4.151 | 95.12 | | |
| Orn 8 | 4.666 | 4.697 | 4.354 | 90.96 | **K** | **Std. error** |
| Ile 10 | 4.635 | 4.715 | 4.134 | 86.23 | 9.0 | 2.0 |
| | | | | | **ΔG(kcal/mol)** | **Std. error (kcal/mol)** |
| | | | | | –1.30 | 0.13 |

**Table 3.11.** Percent folded state of Ac-R-W-V-E-V-**N-G**-O-K-I-L-Q-$NH_2$ (**153a**).

| Amino Acids | 153a | 167a | Random Coil | % Folded | Average % Folded | Standard Error |
|---|---|---|---|---|---|---|
| Val 3 | 4.447 | 4.586 | 4.003 | 76.16 | 77.30 | 2.0 |
| Val 5 | 4.222 | 4.249 | 4.090 | 83.02 | | |
| Orn 8 | 4.620 | 4.696 | 4.364 | 77.11 | **K** | **Std error** |
| Ile 10 | 4.564 | 4.717 | 4.152 | 72.92 | 3.4 | 0.4 |
| | | | | | **ΔG (kcal/mol)** | **Std. error (kcal/mol)** |
| | | | | | –0.73 | 0.07 |

This method showed that peptide **152aa** and **153a** existed in ca. 90% and 77% folded states respectively.

The overall percent folded was also determined by measuring the differences in chemical shift of the two diastereotopic H⟨ signals from the glycine residues in **153a** and **152aa**. This was done using equation (ii):

$$\textbf{Percent Folded} = (\Delta\delta_{\textbf{Observed}}/\otimes\delta_{100})\ \textbf{X 100 \%} \qquad \text{(ii)}$$

where $\Delta\delta_{\text{Observed}}$ is the difference between the two diastereotopic glycine Hα chemical shifts observed for **153a** or **152aa** and $\otimes\delta_{100}$ is the difference between the two diastereotopic glycine Hα chemical shifts of the corresponding cyclic peptide **167a** or **167b** (**Table 3.12 and 3.13**).

**Table 3.12.** Percent folded state of Ac-R-W-V-E-V-**ΔVal-G**-O-K-I-L-Q-$NH_2$ (**152aa**).

| Peptide | Gly $H\alpha_a$ | Gly $H\alpha_b$ | Glycine Splitting | % Folded |
|---|---|---|---|---|
| **Cyclic peptide (167b)** | 4.1322 | 3.7217 | 0.4105 ($\Delta\delta_{100}$) | 93.7 |
| **152aa** | 4.1141 | 3.7296 | 0.3845 ($\Delta\delta_{\text{Observed}}$) | K = **14.79** |
| | | | **ΔG (kcal/mol)** | **–1.60** |

**Table 3.13.** Percent folded state of Ac-R-W-V-E-V-**N-G**-O-K-I-L-Q-$NH_2$ (**153a**).

| Peptide | Gly $H\alpha_a$ | Gly $H\alpha_b$ | Glycine Splitting | % Folded |
|---|---|---|---|---|
| **Cyclic peptide (167a)** | 4.1354 | 3.6865 | 0.4489 ($\Delta\delta_{100}$) | 72.8 |
| **153a** | 4.0941 | 3.7674 | 0.3267 ($\Delta\delta_{\text{Observed}}$) | K = **2.67** |
| | | | **ΔG (kcal/mol)** | **–0.58** |

This method also supports our previous results that the *α,β*-dehydroamino acid containing peptide **152aa** is forming a *β*-hairpin in solution. Peptide **152aa** showed improved folding (ca. 94%) than the parent peptide **153a** (ca. 73%) corroborating our hypothesis that ΔAAs could induce

$\beta$-turns. In terms of Gibbs free energy for folding, ΔVal incorporation at the *i+1* position in a $\beta$-turn favors $\beta$-hairpin formation or folding by ca. 0.6–1.0 kcal/mol.

### 3.6 Circular dichroism spectroscopy of $\alpha,\beta$-dehydroamino acid containing $\beta$-hairpins

The NMR observations are further supported by the CD spectra of **153a**, **153b**, **152aa** and **152ca**. They all exhibited the characteristic $\beta$-sheet or $\beta$-hairpin minima at 215 nm as shown below (**Figure 3.20–3.21**).

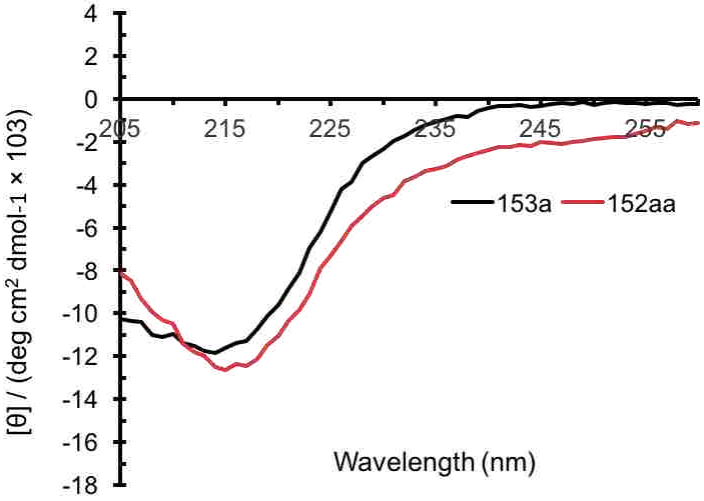


**Figure 3.20.** CD wavelength scan for peptides **153a** and **152aa** at 25 °C.

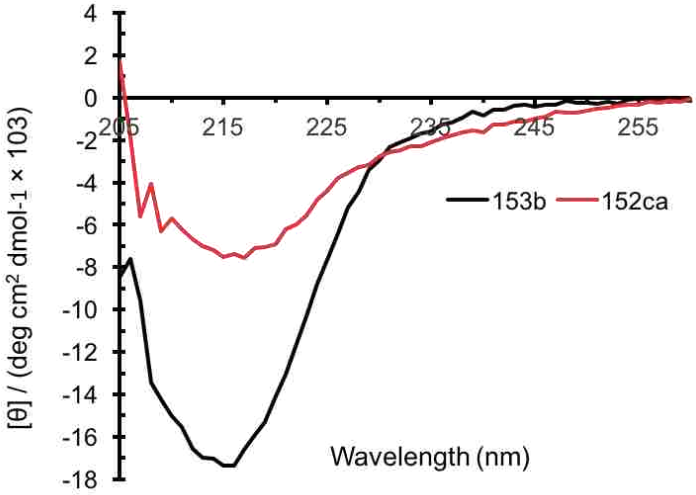


**Figure 3.21.** CD wavelength scan for peptides **153b** and **152ca** at 25 °C.

## 3.7 NOE-restrained structural calculations and peptide ensembles

In order to support our experimental observations, we performed NOE-restrained structural calculations using the simulated annealing algorithm CYANA. This could provide further insights pertaining to the peptide structures in solution. We generated conformational ensembles of all the peptides by using unambiguous cross-strand ROESY peaks, which are presented in **Tables 3.1–3.8** for each peptide. We used four hydrogen bonding restraints for the residues that are engaged in H-bonding across the opposite strands, but were unable to use any dihedral angle restraints because of insufficient secondary chemical shift data available for several nonstandard residues in our peptides.

We selected and superimposed the 10 lowest-energy conformations determined by the CYANA objective function, from 100 preliminary conformations obtained. All the ensembles of the 10 best conformations showed the expected hydrogen bonding pattern along the strands, dihedral angles and the overall secondary structure that is in good agreement with the $\beta$-hairpin motif. Conformational similarities between parent peptide **153a** and the $\beta$-hairpin containing ΔVal at *i+1* (**152aa)** could be seen clearly from their ensembles (**Figure 3.22**).

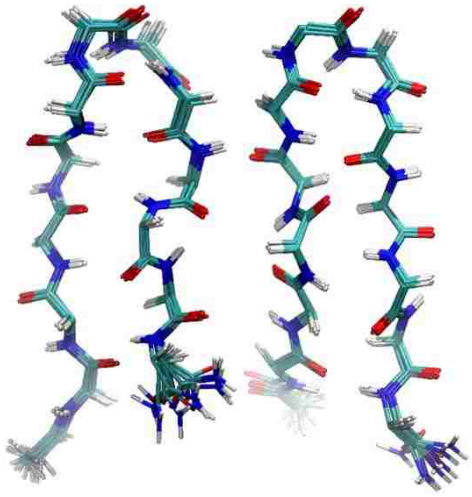

**Figure 3.22.** Solution-phase structures of **153a** (left) and **152aa** (right) as calculated by NOE-restrained molecular dynamics. Side chains have been removed for clarity.

A qualitative examination of the simulated structures indicated that *β*-hairpins containing ΔVal were more stable or rigid than the ones containing ΔEnv. It is rational to see less rigid conformations for **152bb** and **152cb** as multiple spin systems were observed in their 2D NMR spectra. This is also evident from their relatively larger backbone RMSD values obtained from the structural calculations.

Structural ensembles of all the *β*-hairpin peptides are shown below in **Figures 3.23–3.29**. RMSD values were calculated based on the backbone atoms and only include residues 3–10 to avoid the impact of fraying of the ends of the strands where less NOEs were found. Graphic representations were generated using VMD. [37]

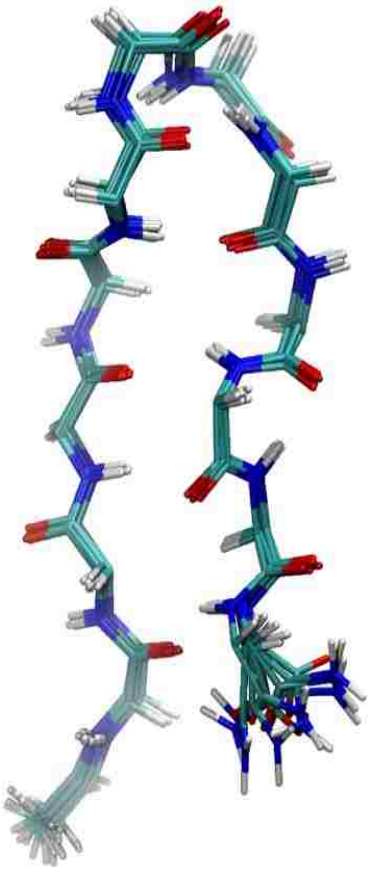

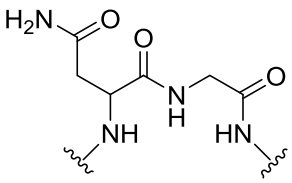


| Position | Res. |
|---|---|
| ***i*** | Val |
| ***i* + *1*** | Asn |
| ***i* + *2*** | Gly |
| ***i* + *3*** | Orn |

**Backbone RMSD (Å):**

**0.180** ± 0.008

**Figure 3.23.** Solution structure of the peptide **153a**.

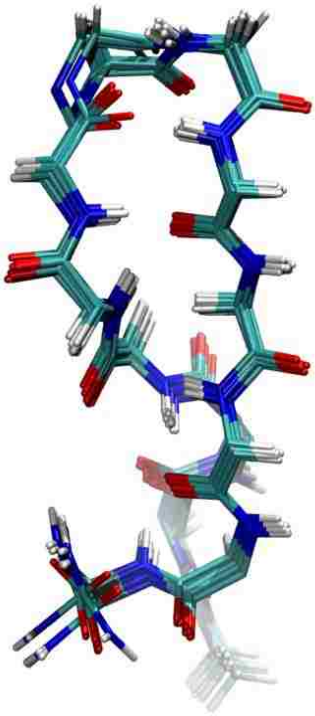

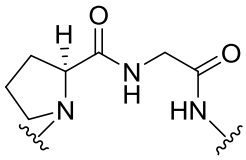


| Position | Res. |
|---|---|
| ***i*** | Val |
| ***i* + *1*** | D-Pro |
| ***i* + *2*** | Gly |
| ***i* + *3*** | Orn |

**Backbone RMSD (Å):**
**0.396** ± 0.143

**Figure 3.24.** Solution structure of the peptide **153b**.

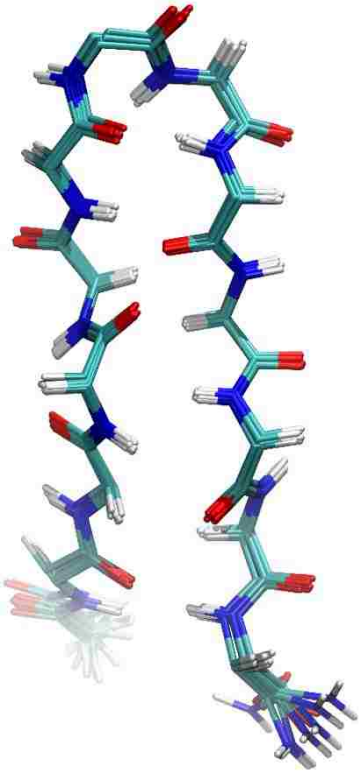

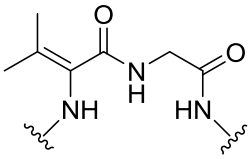


| Position | AA |
|---|---|
| ***i*** | Val |
| ***i* + *1*** | ΔVal |
| ***i* + *2*** | Gly |
| ***i* + *3*** | Orn |

**Backbone RMSD (Å):**
**0.128** ± 0.037

**Figure 3.25**. Solution structure of the peptide **152aa**.

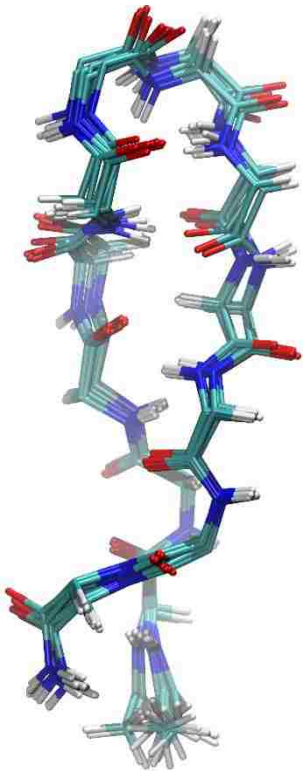

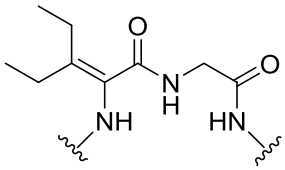


| Position | AA |
|---|---|
| ***i*** | Val |
| ***i + 1*** | ΔEnv |
| ***i + 2*** | Gly |
| ***i + 3*** | Orn |

**Backbone RMSD (Å):**

**0.335** ± 0.075

**Figure 3.26.** Solution structure of the peptide **152ab**.

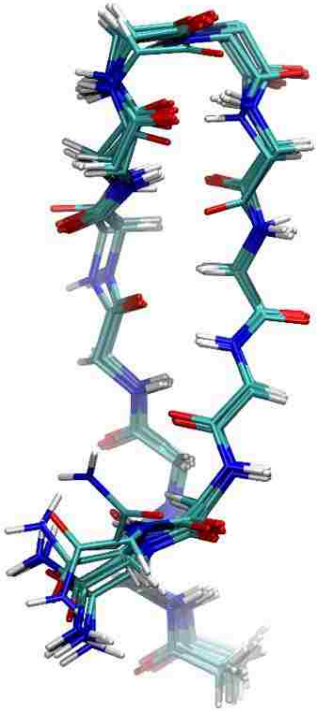

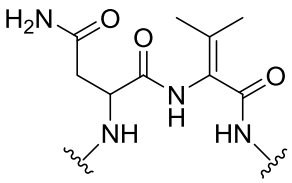


| Position | Res. |
|---|---|
| ***i*** | Val |
| ***i + 1*** | Asn |
| ***i + 2*** | ΔVal |
| ***i + 3*** | Orn |

**Backbone RMSD (Å)**

**0.256** ± 0.120

**Figure 3.27.** Solution structure of the peptide **152ba**.

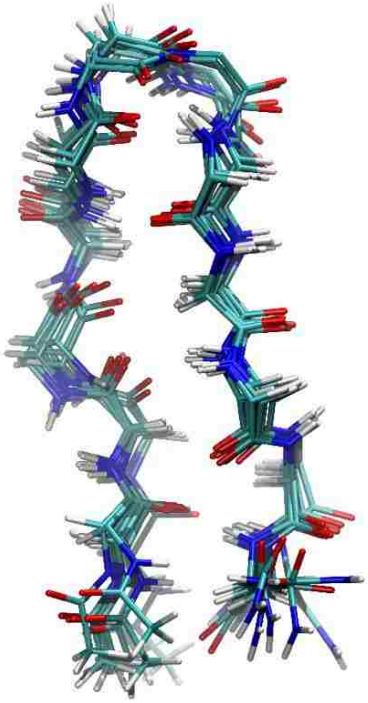

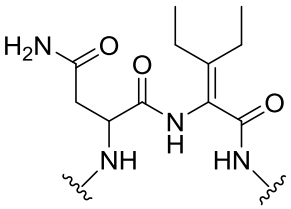

| Position | Res. |
|---|---|
| ***i*** | Val |
| ***i* + *1*** | Asn |
| ***i* + *2*** | ΔEnv |
| ***i* + *3*** | Orn |

**Backbone RMSD (Å)**

**0.601** ± 0.113

**Figure 3.28.** Solution structure of the peptide **152bb**.

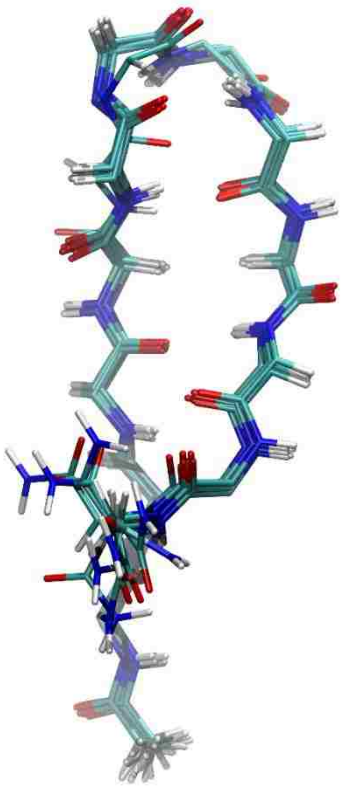

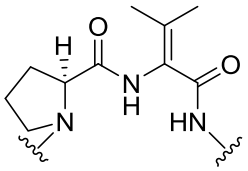

| Position | AA |
|---|---|
| ***i*** | Val |
| ***i* + *1*** | D-Pro |
| ***i* + *2*** | ΔVal |
| ***i* + *3*** | Orn |

**Backbone RMSD (Å):**
**0.262** ± 0.184

**Figure 3.29.** Solution structure of the peptide **152ca**.

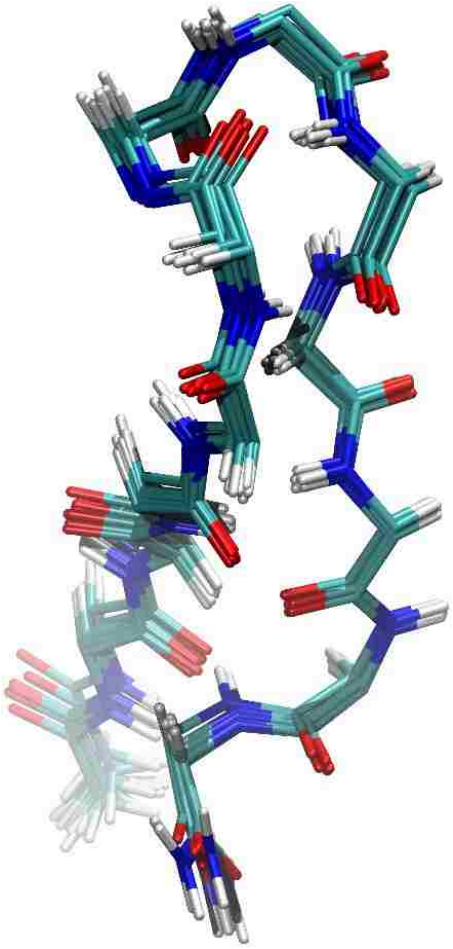

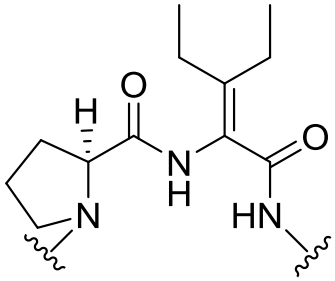


| Position | AA |
|---|---|
| ***i*** | Val |
| ***i + 1*** | D-Pro |
| ***i + 2*** | ΔEnv |
| ***i + 3*** | Orn |

**Backbone RMSD (Å):**

**0.312** ± 0.108

**Figure 3.30.** Solution structure of the peptide **152cb**.

We relied on cross-strand peaks for structural calculations because of their high quality signals caused by the proximity of the strands, and they are listed in **Tables 3.1–3.9** along with their relative intensities. The details of the restraints used in the structural constraints are tabulated below (**Table 3.14**).

**Table 3.14.** Restraints and calculation parameters.

| Structure | 1 | 2 | 152aa | 152ab | 152ba | 152bb | 152ca | 152cb |
|---|---|---|---|---|---|---|---|---|
| **Conformational restraints** | | | | | | | | |
| Total Distance Restraints | 32 | 28 | 28 | 31 | 29 | 24 | 29 | 31 |
| Cross-strand | 31 | 26 | 28 | 30 | 29 | 22 | 27 | 29 |
| Sequential | 1 | 2 | 0 | 1 | 0 | 2 | 2 | 2 |
| Intra-residue | 0 | 0 | 0 | 0 | 0 | 0 | 0 | 0 |
| Strong Intensity | 14 | 8 | 6 | 11 | 9 | 8 | 10 | 12 |
| Medium Intensity | 11 | 14 | 14 | 9 | 9 | 9 | 10 | 9 |
| Weak Intensity | 7 | 6 | 8 | 11 | 11 | 7 | 9 | 10 |
| Hydrogen Bonds | 4 | 4 | 4 | 4 | 4 | 4 | 4 | 4 |
| Dihedral Restraints | 0 | 0 | 0 | 0 | 0 | 0 | 0 | 0 |
| **RMSD from Ideality:** | | | | | | | | |
| Backbone (Å) | 0.18 ± 0.01 | 0.40 ± 0.14 | 0.13 ± 0.04 | 0.34 ± 0.08 | 0.26 ± 0.12 | 0.60 ± 0.11 | 0.26 ± 0.18 | 0.31 ± 0.11 |
| All atoms (Å) | 0.57 ± 0.08 | 0.74 ± 0.11 | 0.54 ± 0.08 | 0.67 ± 0.09 | 0.72 ± 0.17 | 1.32 ± 0.34 | 0.86 ± 0.25 | 0.77 ± 0.26 |

## 3.8 Conclusions

We have established with strong evidence that incorporation of a bulky $\alpha,\beta$-dehydroamino acid at either the *i+1* or the *i+2* positon in the turn region of a known $\beta$-hairpin can impart considerable proteolytic stability and enhance folding. Proteolysis experiments, NMR studies and structural calculation results suggest that backbone rigidification and increased folding may be partly responsible for proteolytic stability. ΔVal-containing $\beta$-hairpins are either more stable or equally stable to proteolysis than their ΔEnv-containing analogues, and this can be in part

attributed to their more rigid conformations in solution. The *β*-hairpin **152aa** with ΔVal at the *i+1* position in the turn was found to be more folded than the parent peptide **153a**, with its folding favored by ca. 0.6–1.0 kcal/mol. Since folded peptides and proteins are less susceptible to enzymatic decomposition, we can confidently propose that a part of the significantly enhanced proteolytic stability of peptide **152aa** (ca. 7 times more stable than **153a**) is due to its high folded population. Substitution of the *i+1* residue with ΔEnv led to multiple conformations with a slightly smaller enhancement in proteolytic resistance, whereas as the *i+2* substitution with either ΔVal or ΔEnv was less favorable for both proteolytic resistance and folding. Nevertheless, all the bulky ΔAA-containing peptides were more stable to proteolysis than the parent peptide **153a** and showed *β*-hairpin formation. We have also demonstrated that the synergistic pairing of D-Pro (*i+1*) and a bulky ΔAA (*i+2*) can improve the proteolytic resistance to enzymatic degradation.

Though it is still unclear if the incorporation of a ΔAA stabilizes the folded states or destabilizes the unfolded states, we propose that a bulky ΔAA can destabilize several unfolded or random coil conformations of peptides **152** due to their inherently high $A_{1,3}$ strain, thereby shifting the equilibrium towards folded conformations. Since the insertion of a bulky *α*,*β*-dehydroamino acid into the turn regions of *β*-hairpins can promote proteolytic stability without perturbing the secondary structures, we believe that this novel approach is very promising in stabilizing bioactive turn-containing peptides for therapeutic use.

### 3.9 References

1. a) James, R. C.; Pierce, J. G.; Okano, A.; Xie, J.; Boger, D. L. *ACS Chem. Biol.* **2012**, *7*, 797; b) Blum, R. H.; Carter, S. K.; Agre, K. *Cancer.* **1973**, *31*, 903; c) Chatterjee, C.; Paul, M.; Xie, L.; van der Donk, W. A. *Chem. Rev.* **2005**, *105*, 633; d) Bolla, M.; Gonzalez, D.; Warde, P.; Dubois, J. B.; Mirimanoff, R. O.; Storme, G.; Bernier. C.; Kuten, A.; Sternberg, C.; Gil, T.; Collette, L.; Pierart, M. *N. Engl. J. Med.* **1997**, *337*, 295; e) Adams, J.; Kauffman, M. *Cancer Invest.* **2009**, *22*,

304; f) Schreiber, S. L.; Crabtree, G. R. *Immunol. Today* **1992**, *13*, 136; g) Cai, L.; Jiang, S. *ChemMedChem* **2010**, *5*, 1813; h) Gentilella, R.; Bianchi, C.; Rossi, A.; Rotella, C. M. *Diabetes, Obes. Metab.* **2009**, *11*, 544.

2. Henninot, A.; Collins, J. C.; Nuss, J. M. "The Current State of Peptide Drug Discovery: Back to the future?" *J. Med. Chem.* **2017** https://doi.org/10.1021/acs.jmedchem.7b00318

3. Fowler, S. A.; Blackwell, H. E. *Org. Biomol. Chem.* **2009**, *7*, 1508.

4. Cheng, R. P.; Gellman, S. H.; DeGrado, W. F. *Chem. Rev.* **2001**, *101*, 3219.

5. Weinstock, M. T.; Francis, J. N.; Redman, J. S.; Kay, M. S. *Biopolymers (Pept. Sci.)* **2012**, *98*, 431.

6. Toniolo, C.; Formaggio, F.; Kaptein, B.; Broxterman, Q. B. *Synlett* **2006**, *9*, 1295.

7. Blackwell, H. E.; Grubbs, R. H. *Angew. Chem., Int. Ed.* **1998**, *37*, 3281.

8. Patgiri, A.; Jochim, A. L.; Arora, P. S. *Acc. Chem. Res.* **2008**, *41*, 1289.

9. Kang, J. S.; DeLuca, P. P.; Lee, K. C. *Expert Opin. Emerg. Drugs* **2009**, *14*, 363.

10. a) Jaeger, S.; Aloy, P. IUBMB Life, **2012**, 64, 529 b) Taylor, I. W.; Wrana, J., L. Proteomics, 2012, 12, 1706 c) J.M. Reichert Peptide Therapeutic Foundation (2012).

11. Nero, T. L.; Morton, C. J.; Holien, J. K.; Wielens, J.; Parker, M. W. *Nat. Rev. Cancer* **2014**, *14*, 248; b) Tse, C.; Shoemaker, A. R.; Adickes, J.; Anderson, M. G., Chen, J.; Jin, S.; Johnson, E. F., Marsh, K. C.; Mitten, M. J.; Nimmer, P.; Roberts, L.; Tahir, S. K.; Xiao, Y.;Yang, X.; Zhang, H.; Fesik, S.; Rosenberg, S. H.; Elmore, S. W. *Cancer Res.* **2008**, *68*, 3421; c) Vassilev, L. T.; Vu, B. T.; Graves, B.; Carvajal, D.; Podlaski F.; Filipovic, Z.; Kong, N.; Kammlott, U.; Lukacs, C.; Klein, C.; Fotouhi, N.; Liu, E. A. *Science* **2004**, *303*, 844; d) Zhao, Y.; Yu, S.; Liu, L.; Lu, J.; McEachern, D.; Shargary, S.; Bernard, D.; Li, X.; Zhao, T.; Zou, P.; Sun, D.; Wang, J. *J. Med. Chem.* **2013**, *56*, 5553; e) Udumula, V.; Nazari, S. H., Burt, S. R.; Alfindee, M. N.; Michaelis, D. J. *ACS Catal.* **2016**, *6*, 4423; f) Leão, M.; Pereira, C.; Bisio, A.; Ciribilli, Y.; Paiva, A. M.; Machado, N.; Palmeira, A.; Fernandes, M. X.; Sousa, E.; Pinto, M.; Inga, A.; Saraiva, L. *Biochem. Pharmacol.* **2013**, *85*, 1234; g) Thanos, C. D.; DeLano, W. L.; Wells, J. A. *Proc. Natl. Acad. Sci. U. S. A.* **2006**, *103*, 15422.

12. Buchwald P. *IUBMB Life* **2010**, *62*, 724.

13. a) Fuller, J. C.; Burgoyne, N. J.; Jackson, R. M. *Drug Discov. Today* **2009**, *14*, 155; b) Clackson, T.; Wells, J. A. *Science* **1995**, *267*, 383.

14. London, N.; Raveh, B.; Schueler-Furman, O. *Curr. Opin. Chem. Biol.* **2013**, *17*, 952.

15. a) Craik, D. J.; Fairlie, D. P.; Liras, S.; Price, D. *Chem. Biol. Drug Des.* **2013**, 81, 136; b) Vlieghe, P.; Lisowski, V.; Martinez, J.; Khrestchatisky, M. *Drug Discov. Today* **2010**, *15*, 40.

16. Wójcik, P.; Berlicki Ł. *Bioorg. Med. Chem. Lett.* **2016**, *26*, 707.

17. Schafmeister, C. E.; Po, J.; Verdine, G. L. *J. Am. Chem. Soc.* **2000**, *122*, 5891.

18. Walensky, L. D.; Kung, A. L.; Escher, I.; Malia, T. J.; Barbuto, S.; Wright, R. D.; Wagner, G.; Verdine, G. L.; Korsmeyer, S. J. *Science* **2004**, *305*, 1466.

19. Bernal, F.; Tyler, A. F.; Korsmeyer, S. J.; Walensky, L. D.; Verdine, G. L. *J. Am. Chem. Soc.*, **2007**, *129*, 2456.

20. Chang, Y. S.; Graves, B.; Guerlavais, V.; Tovar, C.; Packman, K.; To, K. –H.; Olson, K. A.; Kesavan, K.; Gangurde, P.; Mukherjee, A.; Baker, T.; Darlak, K.; Elkin, C.; Filipovic, Z.; Qureshi, F. Z.; Cai, H.; Berry, P.; Feyfant, E.; Shi, X. E.; Horstick, J.; Annis, D. A.; Manning, A. M.; Fotouhi, N.; Nash, H.; Vassilev, L. T.; Sawyer, T. K. *Proc. Natl. Acad. Sci. U. S. A.* **2013**, *110*, E3445.

21. a) Stewart, M. L.; Fire, E.; Keating, A. E.; Walensky, L. D. *Nat. Chem. Biol.* **2010**, *6*, 595; b) Kim, W.; Bird, G. H.; Neff, T.; Guo, G.; Kerenyi, M. A.; Walensky, L. D.; Orkin, S. H. *Nat. Chem. Biol.*, **2013**, *9*, 643.

22. Zhang, H.; Zhao, Q.; Bhattacharya, S.; Waheed, A. A.; Tong, X.; Hong, A.; Heck, S.; Curreli, F.; Goger, M.; Cowburn, D.; Freed, E. O.; Debnath, A. K. *J. Mol. Biol.* **2008**, *378*, 565.

23. Chapman, R. N.; Dimartino, G.; Arora, P. S. *J. Am. Chem. Soc.* **2004**, *126*, 12252.

24. Wang, D.; Lu, M.; Arora, P. S. *Angew. Chem. Int. Ed.* **2008**, *47*, 1879.

25. Seebach, D.; Ciceri, P. E.; Overhand, M.; Jaun, B.; Rigo, D.; Oberer, L.; Hommel, U.; Amstutz, R.; Widmer, H. *Helv. Chim. Acta* **1996**, *79*, 2043.

26. English, M. L.; Stammer, C. H. *Biochem. Biophys. Res. Commun.* **1978**, 83, 1464.

27. English, M. L.; Stammer, C. H. *Biochem. Biophys. Res. Commun.* **1978**, 85, 780.

28. Fisher, G. H.; Berryer, P.; Ryan, J. W.; Chauhan, V.; Stammer, C. H. *Arch. Biochem. Biophys.* **1981**, *211*, 269.

29. Cline, L. L.; Waters, M. L. *Biopolymers* **2009**, *92*, 502.

30. a) Hook, D. F.; Bindschädler, P.; Mahajan, Y. R.; Šebesta, R.; Kast, P. Seebach, D. *Chem. Biodiversity* **2005**, *2*, 591; b) Awad, W. M.; Soto, A. R.; Siegel, S.; Skiba, W. E.; Bernstrom, G. G.; Ochoa, M. S. *J. Biol. Chem.* **1972**, *247*, 4144; c) Spungin, A.; Blumberg, S. *Eur. J. Biochem.* **1989**, *183*, 471.

31. Frackenpohl, J.; Arvidsson, P. I.; Schreiber, J. V.; Seebach, D. *ChemBioChem* **2001**, *2*, 445.

32. a) Wishart, D. S.; Sykes, B. D.; Richards, F. M. *Biochemistry* **1992**, *31*, 1647; b) Merutka, G.; Dyson, H. J.; Wright, P. E. *J. Biomol. NMR* **1995**, *5*, 14; c) Wishart, D. S.; Bigam, C. G.; Holm, A.; Hodges, R. S.; Sykes, B. D. *J. Biomol. NMR* **1995**, *5*, 67; d) Blanco, F. J.; Rivas, G.; Serrano, L. *Nat. Strut. Biol.* **1994**, *1*, 584.

33. Fesinmeyer, R. M.; Hudson, F. M.; Olsen, K. A.; White, G. W. N.; Euser, A. Andersen, N. H. *J. Biomol. NMR* **2005**, *33*, 213.

34. Sharman, G. J.; Griffiths-Jones, S. R.; Jourdan, M.; Searle, M. S. *J. Am. Chem. Soc.* **2001**, *123*, 12318.

35. Wüthrich, K. NMR of Proteins and Nucleic Acids, Wiley: New York (1986).

36. Syud, F. A.; Espinosa, J. F.; Gellman, S. H. *J. Am. Chem. Soc.* **1999**, *121*, 11577.

37. Humphrey, W.; Dalke, A.; Schulten, K. *J. Mol. Graphics* **1996**, *14*, 33.
http://www.ks.uiuc.edu/Research/vmd/

# 4 PROGRESS TOWARDS THE TOTAL SYNTHESIS OF YAKU'AMIDE A

## 4.1 Isolation, structure, and biological activity

Several biologically active natural peptides with unprecedented chemical structures have been isolated from marine organisms. Marine sponges are one of the richest sources of secondary metabolites that are pharmacologically active. In order to survive in the harsh ocean environment and evade predators, these marine invertebrates produce highly potent toxins. Researchers have isolated several types of polyketides and nonribosomal peptides from marine sponges.[1] In 2010, Matsunaga and co-workers isolated the acyclic peptides yaku'amide A and B from the deep sea sponge *Ceratopsion* sp. obtained at a depth of 150 m at Yakushinsone in the East China Sea, which exhibited potent cytotoxicity (**Figure 4.1**).[2]

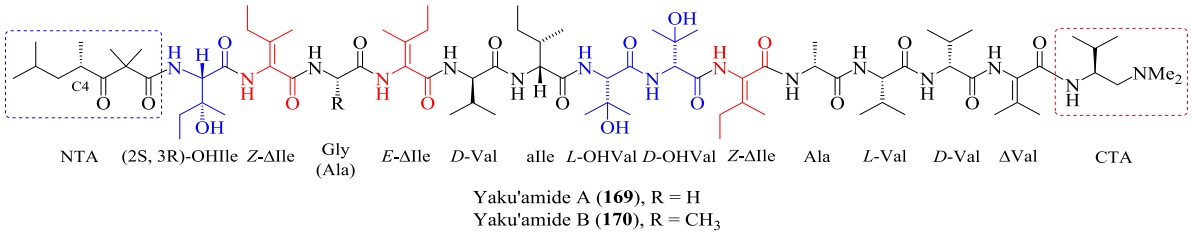


**Figure 4.1.** Initially proposed structure of Yaku'amide A and B.

These acyclic peptides (**169** and **170**) contain a variety of *β*-hydroxyamino acid (*β*-OHAA) and *α*,*β*-dehydroamino acid (ΔAA) residues. They exhibited three *β*-OHAA residues including (2*S*, 3*R*)-hydroxyisoleucine (OHIle) and D- and L-hydroxyvaline (OHVal) along with four ΔAA residues including *Z*-ΔIle, *E*-ΔIle, and ΔVal. *Z*-ΔIle is unique, as it has never been seen in natural

products before.[3] Moreover, they have unique C-terminal and N-terminal groups, which were also unprecedented.

Yaku'amide A and B were tested against P388 murine leukemia cells (JCRB17), and found to be highly cytotoxic with low $IC_{50}$ values of 14 and 4 ng/mL, respectively. Notably, the cytotoxicity profile of yaku'amide A towards a panel of 39 human cancer cell lines (JFCR39) including various types of human cancers was found to be unique when compared to 38 anticancer drugs that have been examined in this panel of cell lines.[4] Hence, it is very significant to investigate and discover the biological target of yaku'amide A for the development of novel anticancer agents.

### 4.2 Total synthesis of Yaku'amide A by Inoue and co-workers

Since yaku'amide A has a complex chemical structure with several *β*-OHAA and asymmetric ΔAA, its total synthesis is very challenging. However, Inoue et al. reported the first total synthesis of yaku'amide A (**169**) in 2013. They synthesized *β*-OHAA residues (2*S*, 3*R*)-hydroxyisoleucine (OHIle) and D- and L-hydroxyvaline (OHVal) via previously known protocols.[5] Both the isomers of *β*-OHVal were constructed based upon the method developed by Lubell and co-workers, whereas (2*S*, 3*R*)-OHIle was prepared according to the protocol developed by Guanti et al.[6]

The synthesis of *Z*-ΔIle and *E*-ΔIle was more challenging. The previously reported methods for the construction of *E*-ΔIle were reliable, but tedious.[7] Inoue and co-workers developed a Cu-catalyzed cross-coupling reaction for the synthesis of the *Z*-ΔIle and *E*-ΔIle as reported in Chapter 1.[8]

In 2015, they revised the structures of yaku'amide A and B after extensive investigations and corrected the configurations of the two Val residues near the C-terminal and both the *β*-OHVal

residues (**Figure 4.2**). Their total synthesis consists of 86 total steps and a 25-step longest linear sequence.

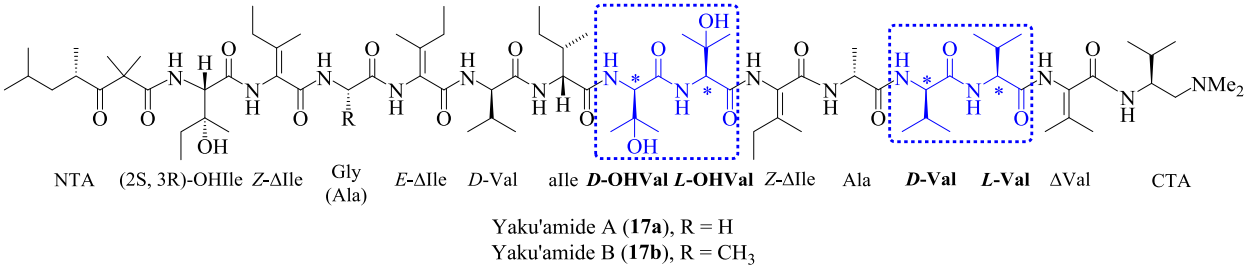


**Figure 4.2.** Revised structure of Yaku'amide A and B.

## 4.3 Retrosynthetic analysis of yaku'amide A

Castle and Ma developed more efficient methods for the syntheses of the three *β*-hydroxyamino acids (*β*-OHAAs) and asymmetric Δ AAs seen in yaku'amide A. *β*-OHAAs were synthesized via a base-free $OsO_4$-catalyzed aminohydroxylation protocol and stereoselective *anti*-dehydration of *β*-OHIle afforded the *E*- and *Z*-Δ Ile residues.[9] Our retrosynthetic analysis of yaku'amide A (**17a**) is shown in **Scheme 4.1**. Yaku'amide A (**17a**) can be disconnected at the two amides as indicated into three important intermediates. Left-hand pentapeptide **173** and right-hand nonapeptide **174** can be further deconstructed to give simpler building blocks. The synthesis of *E*- and *Z*-Δ Ile residues is challenging as the activation of the carboxyl functional group of an asymmetric Δ AA can cause isomerization via azlactone formation, thereby scrambling the stereochemistry. Previous works on *E*- and *Z*-Δ Ile construction report compulsory backbone amide protection to prevent isomerization. Hence, a one-pot sequence including stereoselective *anti*-dehydration mediated by Martin Sulfurane, azide reduction, and O→N acyl transfer was devised to access the components containing *E*- and *Z*-Δ Ile residues.

(2*S*, 3*R*)-OHIle (**181**) was synthesized via base-free $OsO_4$-catalyzed aminohydroxylation with a chiral nitrogen source[10] because of the lack of a catalytic enantioselective aminohydroxylation method for its synthesis. This protocol is considerably useful as the other diastereomer (*2R, 3S*)-OHIle can be used to synthesize *Z*- Δ Ile.

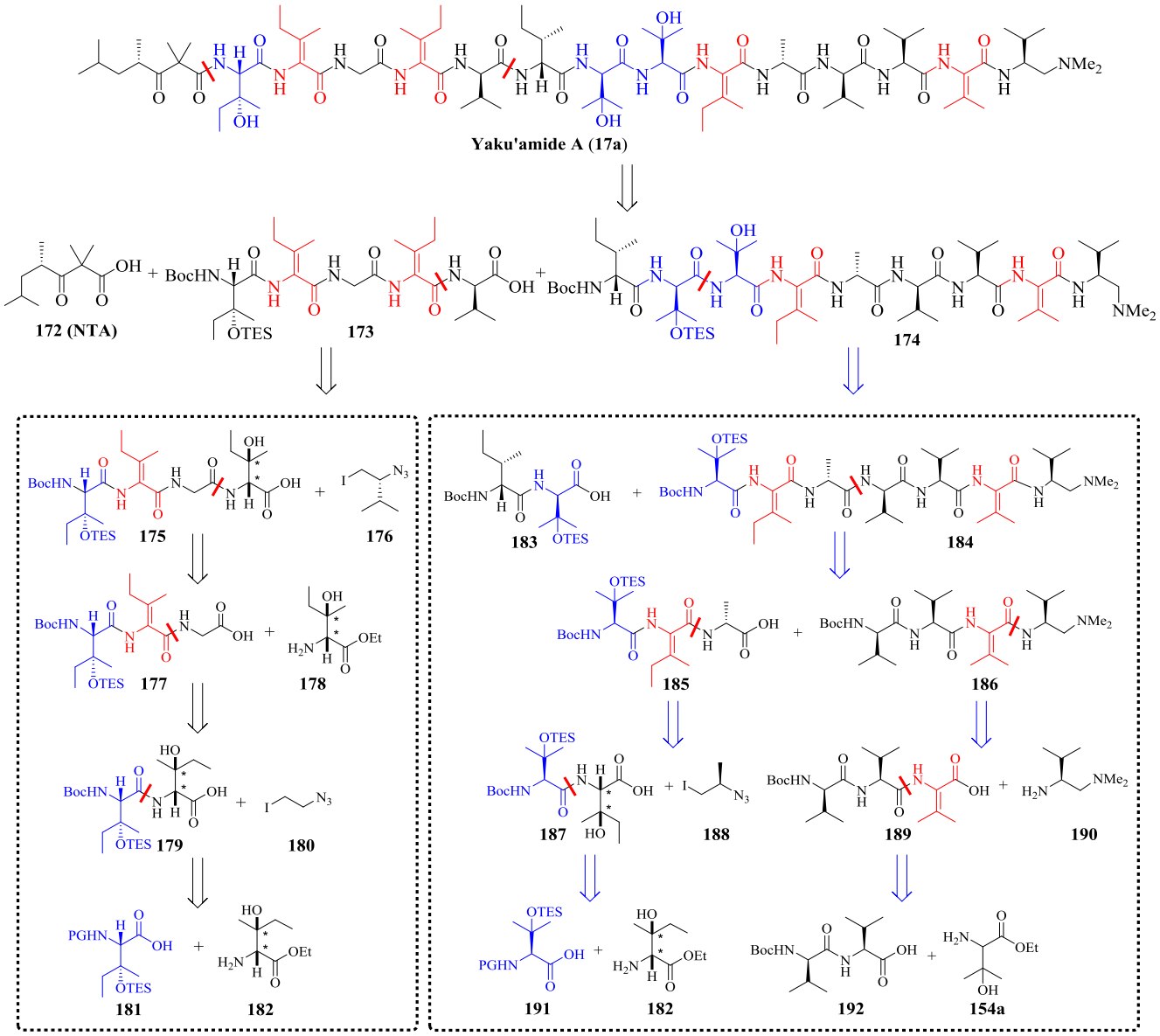


Note: Stereocenters marked by asterisks (*) possess the indicated relative stereochemistry. PG in **181** and **191** means protecting group

**Scheme 4.1.** Retrosynthetic route of Yaku'amide A (**17a**).

The N-terminal acyl group **172** would be prepared via Myers' asymmetric alkylation followed by a Mukaiyama-type Claisen reaction. This is a more efficient synthetic route to **172** when compared to Inoue's synthesis of **172**.[8]

## 4.4 Synthesis of β-OHIle (178 and 182) for the preparation of fragments containing *Z*- and *E*-ΔIle residues

While working on the solid-phase synthesis of (SPPS) of β-hairpins containing bulky α,β-dehydroamino acids, I was also engaged in the synthesis of β-OHAAs for yaku'amide A. I synthesized racemic mixture of β-OHVal **154a** via aminohydroxylation protocol developed in our lab (**Scheme 2.2**).[11] This amine is the precursor to ΔVal, which was required in the synthesis of both bulky α,β- dehydroamino-acid-containing β-hairpins and yaku'amide A.

Apart from the precursor for ΔVal, I provided both *cis*- and *trans*-amines **182** and **178**, which were then later transformed to *Z*- and *E*-ΔIle residues respectively. Amines **178** and **182** were synthesized by base-free regioselective aminohydroxylation developed by Ma and Castle (**Scheme 4.2**).

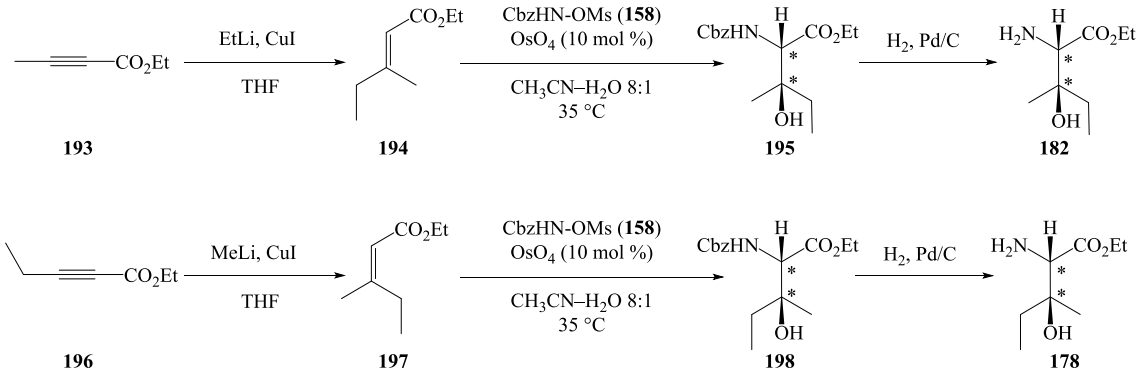


193 194 195 182

196 197 198 178

Note: Stereocenters marked by asterisks (*) indicate relative stereochemistry

**Scheme 4.2.** Synthesis of racemic amines **182** and **178** by base-free regioselective aminohydroxylation.

$OsO_4$-Catalyzed regioselective aminohydroxylation of *trans*-trisubstituted enoate **194** with mesyloxycarbamate **158** provided racemic **195** which upon Cbz deprotection provided amine **182**. Similarly, amine **178** was synthesized from *cis*-trisubstituted enoate **197**. These amines **182** and **178** were then utilized by the fellow graduate student Yu Cai to prepare fragments containing *Z*- and *E*- Δ Ile residues (**Scheme 4.3**).[9]

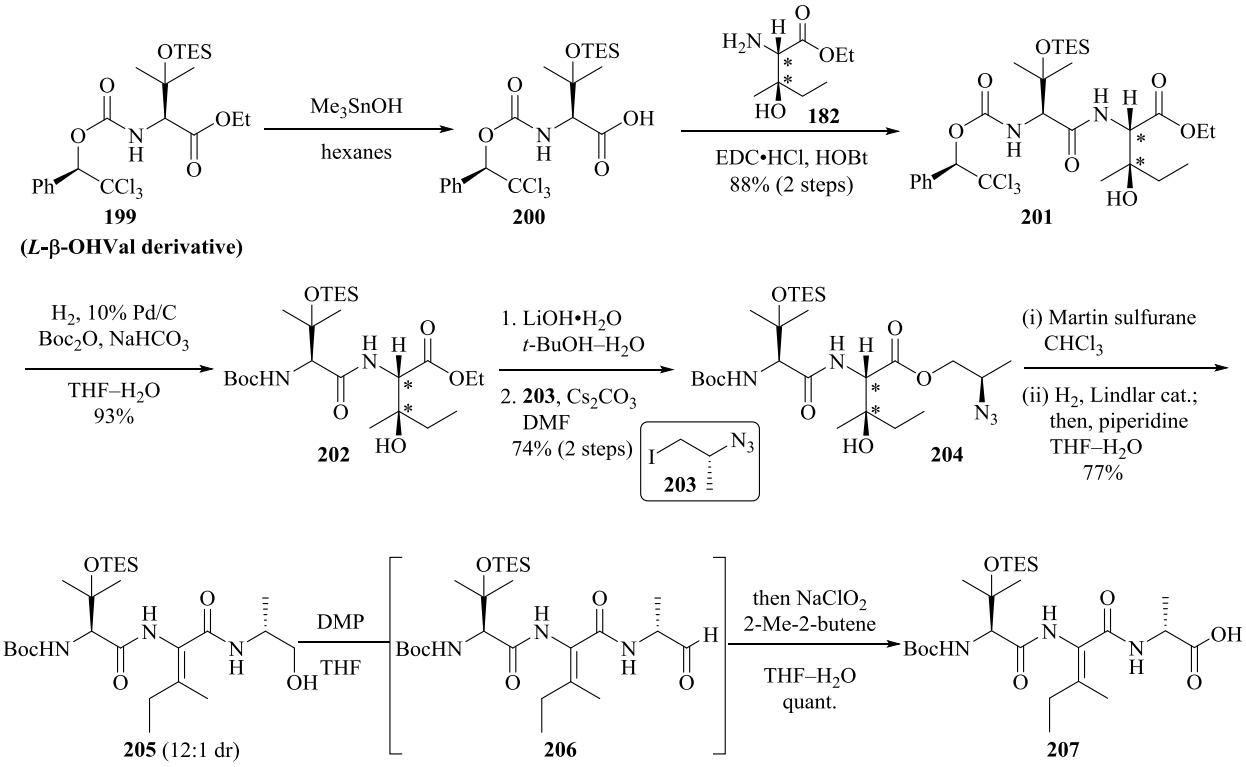


**Scheme 4.3.** Synthesis of tripeptide **207**, a subunit of nonapeptide **174**.

It is noteworthy that the one-pot stereospecific *anti*-dehydration mediated by Martin Sulfurane, azide reduction, and O→N acyl transfer proceeded with excellent diastereoselectivity. This is a more efficient and convenient method of preparing *Z*- Δ Ile as it does not require amide backbone protection and is not prone to isomerization.

Similarly, Yu Cai utilized amines **182** and **178** to incorporate *Z*- and *E*- Δ Ile residues respectively in the left-hand pentapeptide **173**.

## 4.5 Synthesis of (2*S*,3*R*)-OHIle for left-hand pentapeptide 173

Chiral mesyloxycarbamate **211** was synthesized from benzaldehyde by the 5-step procedure developed by Lebel et al.[10] This chiral nitrogen source was used in the synthesis of a 1:1 diastereomeric mixture of $\beta$-OHIle **181** as shown in **Scheme 4.4**.

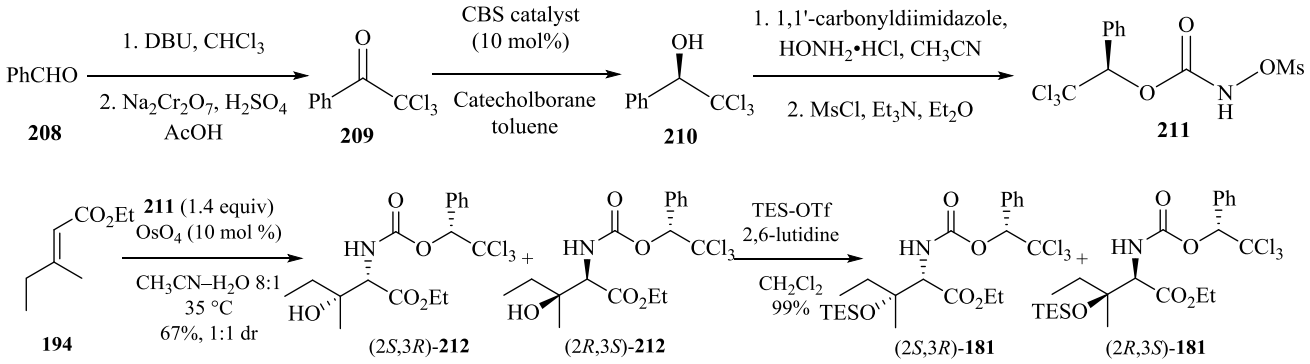


**Scheme 4.4.** Regioselective aminohydroxylation to prepare (2*S*, 3*R*)- $\beta$-OHIle.

Regioselective aminohydroxylation of *trans*-enoate **194** with the chiral mesyloxycarbamate **211** yielded a 1:1 mixture of (*2S*, *3R*)-**212** and (*2R*, *3S*)-**212** (**Scheme 4.4**). It was not possible to separate the two diastereomers at this stage, hence they were separated after TES protection of the tertiary alcohol. Separation was performed by Dr. Castle and undergraduate labmate Blake Christensen. The diastereomer (2*S*, 3*R*)-**181** is more polar and eluted later. This was utilized by Yu Cai in the construction of the left-hand pentapeptide **173**, whereas the less polar isomer (2*R*, 3*S*)-**181** was used in the formation of *Z*- Δ Ile.

## 4.6 Synthesis of 172, the N-terminal acyl group (NTA)

Inoue and co-workers elegantly synthesized the NTA (**172**), but it required 10-steps for them to accomplish it. We proposed a shorter and more efficient route to access **172.** Our synthetic route to prepare **172** is shown in **Scheme 4.5** and was developed by Dr. Castle and graduate student Zhiwei Ma along with Yu Cai.

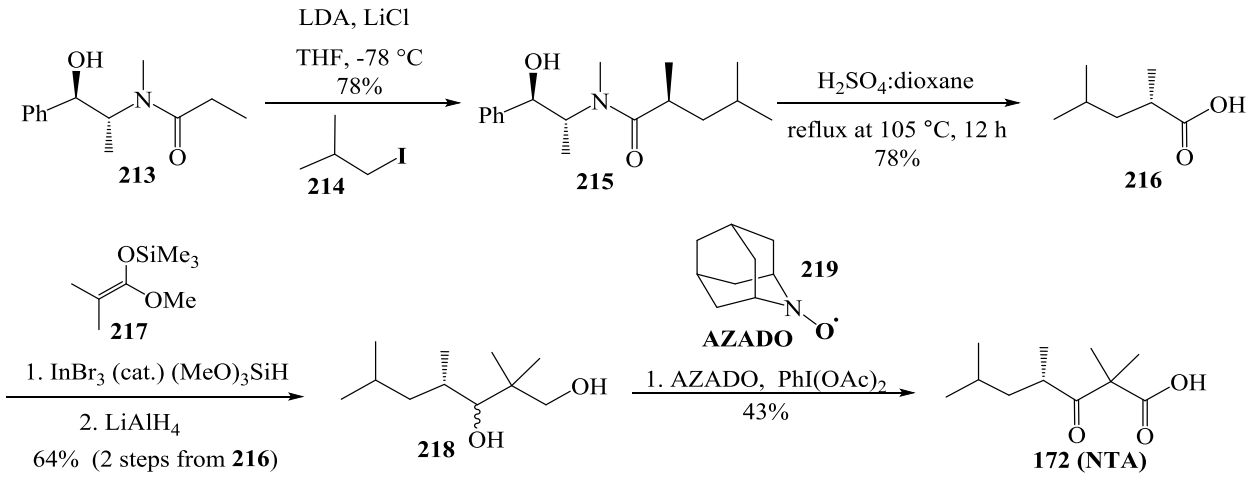


**Scheme 4.5.** Synthesis of the NTA (**172**).

The chiral amide (*1R,2R*)-**213** was prepared from (*1R,2R*)-(–)-pseudoephedrine and propionyl chloride. It was then subjected to Myers' asymmetric alkylation with 1-iodo-2-methylpropane (**214**) to afford the amide **215** in 78% yield.[12] (*S*)-2,4-dimethylpentanoic acid (**216**) was obtained by acid-catalyzed hydrolysis of the chiral auxiliary in good yield. The chiral acid **216** was subjected to cross-Claisen condensation with the ketene silyl acetal **217** in the presence of catalytic amounts of $InBr_3$ to yield a $\beta$-ketoester.[13] This $\beta$-ketoester was reduced in one-pot to give diol **218** in 64% yield from **216**. Previous attempts to hydrolyze the methyl $\beta$-ketoester to **172** were unsuccessful; hence, it was directly reduced to the diol **218**. I prepared about 1.5 g of the diol **218.** Even though Inoue et al. reported the oxidation of the diol with AZADO (**219**), it was very challenging and not reproducible in our hands. Yu Cai accomplished the oxidation only once in

good yield, but, he was unable to reproduce it. We tried several different batches of AZADO (Sigma Aldrich Inc., USA), but we were unsuccessful in obtaining even a few milligrams of the *β*-ketoacid **172** again. We contacted Assistant Professor Dr. Hiroaki Itoh from the laboratory of Professor Dr. Masayuki Inoue for insights on the oxidation of diol **218** and information about their vendor for AZADO. They also purchased AZADO from Sigma Aldrich. We contacted Sigma Aldrich and were told that the batch of AZADO was made about 2 years ago. I only obtained **NTA** in 43% yield once from the AZADO (purchased in 2015) that was stored under Ar at cold temperatures, but none of the new batches of AZADO worked successfully. We believe that the quality of AZADO was bad and hence, the reaction was not reproducible. Going forward, our lab will synthesize AZADO and use it fresh.

## 4.7 Synthesis of yaku'amide A (17a)

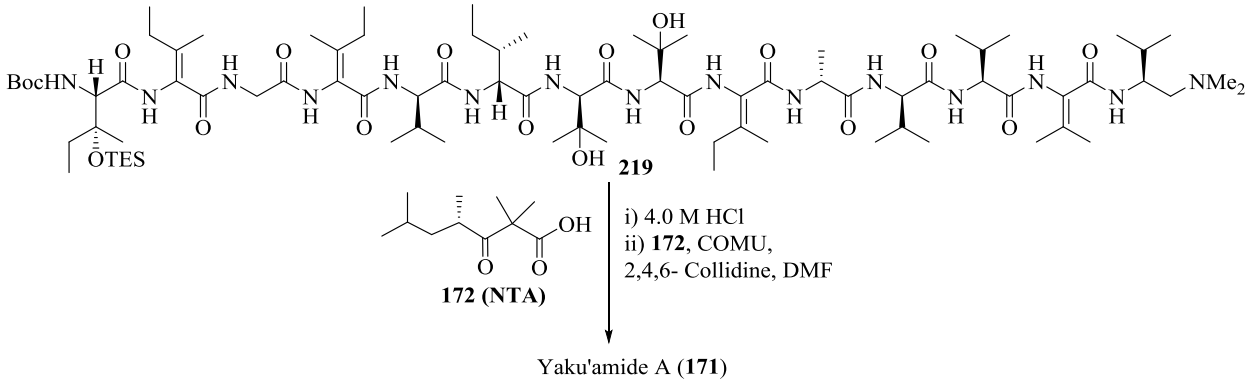


**Scheme 4.6.** Synthesis of yaku'amide A (**17a**).

The tetradecapeptide **219** was treated with HCl solution to remove the Boc and TES protecting groups, and then coupled with NTA (**172**) using COMU. Mass spectrometry of the reaction mixture showed that the coupling was complete. Rough purification by flash chromatography was performed, followed by RP-HPLC isocratic elution on COSMOSIL-π-NAP

columns with 50% v/v n-propanol and water (1% acetic acid). Multiple peaks with the correct *m/z* were found. The major peak matched an authentic sample of yaku'amide A obtained from Prof. Inoue, but the quantity of the compound obtained was insufficient for a good $^{1}$H NMR.

## 4.8 Conclusion

Unfortunately, I was unable to obtain a sufficient amount of yaku'amide A (**17a**) for the $^{1}$H NMR and $^{13}$C NMR. The quality of the tetradecapeptide **219** and the challenges in preparing NTA **(172**) along with the purification of yaku'amide A hampered my goal to make enough amount of it to perform NMR studies. It was found that oxidation of the diol **218** requires high-quality AZADO. Nevertheless, we have successfully performed the final coupling of the unprotected tetradecapeptide with the NTA (**172**) and investigated the purification of yaku'amide A, which will help my colleagues in the lab to successfully synthesize and purify yaku'amide A.

## 4.9 References


1. Matsunaga, S.; Fusetani, N. *Curr. Org. Chem.* **2003**, *7*, 945.

2. Ueoka, R.; Ise, Y.; Ohtsuka, S.; Okada, S.; Yamori, T.; Matsunaga, S. *J. Am. Chem. Soc.* **2010**, *132*, 17692.

3. Jiang, J.; Ma, Z.; Castle, S. L. *Tetrahedron* **2015**, *71*, 5431.

4. a) Yamori, T.; Matsunaga, A.; Sato, S.; Yamazaki, K.; Komi, A.; Ishizu, K.; Mita, I.; Edatsugi, H.; Matsuba, Y.; Takezawa, K.; Nakanishi, O.; Kohno, H.; Nakajima, Y.; Komatsu, H.; Andoh, T.; Tsuruo, T. *Cancer Res.* **1999**, *59*, 4042; b) Yaguchi, S.; Fukui, Y.; Koshimizu, I.; Yoshimi, H.; Matsuno, T.; Gouda, H.; Hirono, S.; Yamazaki, K.; Yamori, T. *J. Natl. Cancer Inst.* **2006**, *98*, 545; c) Yamori, T. *Cancer Chemother. Pharmacol.* **2003**, *52*, S74.

5. Dettwilter, J. E.; Lubell, W. D. *J. Org. Chem*. **2003**, *68*, 177.

6. Ageno, G.; Banfi, L.; Cascio, G.; Guanti, G.; Manghisi, E.; Riva, R.; Rocca, V. *Tetrahedron* **1995**, *51*, 8121.

7. Stohlmeyer, M. M.; Tanaka, H.; Wandless, T. J. *J. Am. Chem. Soc.* **1999**, *121*, 6100
8. Kuranaga, T.; Sesoko, Y.; Sakata, K.; Maeda, N.; Hayata, A.; Inoue, M. *J. Am. Chem. Soc.* **2013**, *135*, 5467.

9. Ma, Z.; Jiang, J.; Luo, S.; Cai, Y.; Cardon, J. M.; Kay, B. M.; Ess, D. H.; Castle, S. L. *Org. Lett.* **2014**, *16*, 4044.

10. Lebel, H.; Trudel, C.; Spitz, C. *Chem. Commun.* **2012**, *48*, 7799.

11. Ma, Z.; Naylor, B. C.; Loertscher, B. M.; Hafen, D. D.; Li, J. M.; Castle, S. L. *J. Org. Chem.* **2012**, *77*, 1208.

12. a) Ghosh, A. K.; Anderson, D. D. *Org. Lett.* **2012**, *14*, 4730; b) Turk, J. A.; Visbal, G. S.; Lipton, M. A. *J. Org. Chem.* **2003**, *68*, 7841; c) Myers, A. G.; Yang, B. H.; Chen, H.; McKinstry, L.; Kopecky, D. J.; Gleason, J. L. *J. Am. Chem. Soc.* **1997**, *119*, 6496.

13. Nishimoto, Y.; Okita A.; Yasuda, M.; Baba, A. *Angew. Chem. Int. Ed.* **2011**, *50*, 8623.

# 5 EXPERIMENTAL SECTION

## 5.1 General Experimental Details

*N*,*N*-Dimethylformamide and tetrahydrofuran were dried by passage through a solvent drying system containing cylinders of activated alumina.[1] Other solvents and reagents were purchased from commercial vendors and used without purification. Flash chromatography was carried out using 60–230 mesh silica gel. $^{1}$H NMR spectra were acquired on a 500 MHz spectrometer with chloroform (7.27 ppm) as internal reference. Signals are reported as follows: s (singlet), d (doublet), t (triplet), q (quartet), p (pentet), h (hextet), dd (doublet of doublets), dt (doublet of triplets), tt (triplet of triplets), qd (quartet of doublets), br s (broad singlet), m (multiplet). Coupling constants are reported in hertz (Hz). $^{13}$C NMR spectra were acquired on a spectrometer operating at 125 MHz with chloroform (77.23 ppm) as internal reference. Infrared spectra were obtained on an FT-IR spectrometer. Mass spectral data were obtained using ESI techniques. Circular dichroism measurements were made with an Aviv 420 Circular Dichroism Spectropolarimeter, using quartz cuvettes with a path length of 0.1 cm.

[1] Pangborn, A. B.; Giardello, M. A.; Grubbs, R. H.; Rosen, R. K.; Timmers, F. J. *Organometallics* **1996**, *15*, 1518.

## 5.2 Experimental procedures and spectral data

### 5.2.1 Synthesis of Dipeptides 148

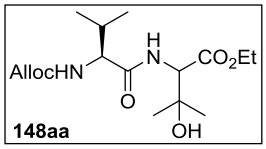

148aa

**Ethyl 2-((*S*)-2-(((allyloxy)carbonyl)amino)-3-methylbutanamido)-3-hydroxy-3-methylbutanoate (148aa).** A solution of Alloc-Val-OH (**155a**, 658.3 mg, 3.27 mmol, 1.5 equiv) in DMF (30 mL) at 0 °C was treated with EDC·HCl (627.7 mg, 3.27 mmol, 1.5 equiv) and HOBt·$H_2O$ (552.9 mg, 3.27 mmol, 1.5 equiv). The resulting mixture was stirred at 0 °C for 15 min, then treated with a solution of ®-hydroxyamino ester **154a**[2] (351.6 mg, 2.18 mmol) in DMF (7.5 mL) and stirred at 0 °C to rt for 12 h. The reaction was then quenched with sat aq $NaHCO_3$ (15 mL) and extracted with EtOAc (3 × 50 mL). The combined organic layers were washed with $H_2O$ (3 × 25 mL) and brine (25 mL), dried ($Na_2SO_4$), and concentrated in vacuo. Flash chromatography (100 mL of $SiO_2$, 0–2.5% MeOH in $CH_2Cl_2$ gradient elution) afforded **148aa** (632.7 mg, 1.84 mmol, 84%) as a colorless oil that was a 1:1 mixture of diastereomers: $^1$H NMR ($CDCl_3$, 500 MHz) δ 6.90 (d, *J* = 8.7 Hz, 1H), 5.96–5.86 (m, 1H), 5.50–5.43 (m, 1H), 5.34–5.27 (m, 1H), 5.24–5.19 (m, 1H), 4.61–4.55 (m, 2H), 4.51 (t, *J* = 8.5 Hz, 1H), 4.29–4.19 (m, 2H), 4.17–4.12 and 4.11–4.06 (2m, 1H), 3.12 and 2.92 (2 br s, 1H), 2.25–2.17 and 2.16–2.07 (2m, 1H), 1.32–1.28 (m, 3H), 1.30 (s, 3H), 1.26 (s, 3H), 1.00 and 0.97 (2d, *J* = 6.9 and 6.7 Hz, 3H), 0.95 and 0.92 (2d, *J* = 6.8 and 6.7 Hz, 3H); $^{13}$C NMR ($CDCl_3$, 125 MHz) δ 171.6, 171.3 and 171.1, 156.3, 132.5, 117.9, 71.9 and 71.8, 65.9, 61.7 and 61.6, 60.3 and 60.2, 59.9 and 59.8, 31.1, 26.8, 26.7, 19.3 and

[2] Ma, Z.; Naylor, B. C.; Loertscher, B. M.; Hafen, D. D.; Li, J. M.; Castle, S. L. *J. Org. Chem.* **2012**, *77*, 1208.

19.1, 17.9 and 17.3, 14.1; IR (film) $\nu_{max}$ 3324, 2973, 1729, 1660, 1536, 1214 $cm^{-1}$; HRMS (ESI) *m/z* 345.1976 ($MH^+$, $C_{16}H_{28}N_2O_6H^+$ requires 345.1981).

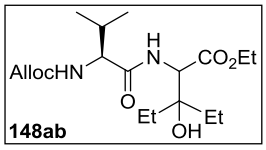


**Ethyl 2-((*S*)-2-(((Allyloxy)carbonyl)amino)-3-methylbutanamido)-3-ethyl-3-hydroxypentanoate (148ab).** Subjection of ®-hydroxyamino ester **154b**[3] (323.2 mg, 1.71 mmol) to the procedure described above for the synthesis of **148aa** with Alloc-Val-OH (**155a**, 514.8 mg, 2.56 mmol, 1.5 equiv) as coupling partner, stirring for 16 h, and purification by flash chromatography (75 mL of $SiO_2$, 0–4% MeOH in $CH_2Cl_2$ gradient elution) afforded **148ab** (498.7 mg, 1.34 mmol, 78%) as a colorless liquid that was a 1:1 mixture of diastereomers: $^1H$ NMR ($CDCl_3$, 500 MHz) δ 6.69 and 6.63 (2d, *J* = 8.7 and 8.2 Hz, 1H), 5.97–5.88 (m, 1H), 5.37–5.28 (m, 2H), 5.23 (d, *J* = 10.4 Hz, 1H), 4.62–4.55 (m, 3H), 4.29–4.17 (m, 2H), 4.14–4.09 and 4.08–4.03 (2m, 1H), 2.47 (br s, 1H), 2.25–2.17 and 2.16–2.09 (2m, 1H), 1.59–1.44 (m, 4H), 1.31 (t, *J* = 7.2 Hz, 3H), 1.00 and 0.97 (2d, *J* = 6.8 and 6.8 Hz, 3H), 0.96–0.91 (m, 6H), 0.87 (t, *J* = 7.4 Hz, 3H); $^{13}C$ NMR ($CDCl_3$, 125 MHz) δ 171.8 and 171.7, 171.2, 156.2, 132.6, 117.9 and 117.8, 76.2, 65.9, 61.6 and 61.5, 60.2, 56.8 and 56.7, 31.2, 28.4, 26.7, 19.3 and 19.1, 17.7 and 17.2, 14.1, 7.6, 7.5; IR (film) $\nu_{max}$ 3336, 2969, 1727, 1659, 1530 $cm^{-1}$; HRMS (ESI) *m/z* 373.2276 ($MH^+$, $C_{18}H_{32}N_2O_6H^+$ requires 373.2294).

[3] Jiang, J.; Luo, S.; Castle, S. L. *Tetrahedron Lett.* **2015**, *56*, 3311.

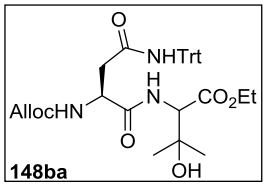


**Ethyl 2-((*S*)-2-(((Allyloxy)carbonyl)amino)-4-oxo-4-(tritylamino) butanamido)-3-hydroxy-3-methylbutanoate (148ba).** Subjection of ®-hydroxyamino ester **154a** (163.6 mg, 1.01 mmol) to the procedure described above for the synthesis of **148aa** with Alloc-Asn(Trt)-OH (**155b**, 695.2 mg, 1.52 mmol, 1.5 equiv) as coupling partner, stirring for 12 h, and purification by flash chromatography (75 mL of $SiO_2$, 0–6% MeOH in $CH_2Cl_2$ gradient elution), afforded **148ba** (472.7 mg, 0.786 mmol, 77%) as a white film that was a 1:1 mixture of diastereomers: $^1$H NMR ($CDCl_3$, 500 MHz) δ 7.38 (d, $J$ = 8.4 Hz, 1H), 7.33–7.23 (m, 9H), 7.18 (d, $J$ = 7.8 Hz, 6H), 6.86 (br s; 1H), 6.43 (d, $J$ = 8.1 Hz, 1H), 5.97–5.85 (m, 1H), 5.31 (dd, $J$ = 17.2, 1.3 Hz, 1H), 5.23 (dd, $J$ = 10.4, 1.2 Hz, 1H), 4.63–4.56 (m, 2H), 4.56–4.51 (m, 1H), 4.47 (d, $J$ = 8.8 Hz, 1H), 4.29–4.16 (m, 2H), 3.11 (dd, $J$ = 15.6, 3.7 Hz, 1H), 2.72–2.63 (m, 1H), 2.69 (br s, 1H), 1.30 (t, $J$ = 7.0 Hz, 3H), 1.21 (s, 3H), 1.14 (s, 3H); $^{13}$C NMR ($CDCl_3$, 125 MHz) δ 171.1, 170.8, 170.2, 156.4, 144.2 (3C), 132.3, 128.7 (6C), 128.0 (6C), 127.1 (3C), 118.0, 71.9, 70.9, 66.1, 61.6, 60.3, 51.7, 37.6, 26.7, 26.4, 14.1; IR (film) $\nu_{max}$ 3330, 2923, 1659, 1524 cm$^{-1}$; HRMS (ESI) *m/z* 602.2831 ($MH^+$, $C_{34}H_{39}N_3O_7H^+$ requires 602.2822).

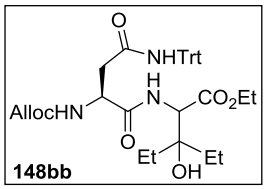


**Ethyl 2-((*S*)-2-(((Allyloxy)carbonyl)amino)-4-oxo-4-(tritylamino) butanamido)-3-ethyl-3-hydroxypentanoate (148bb).** Subjection of ®-hydroxyamino ester **154b** (135.2 mg, 0.714 mmol) to the procedure described above for the synthesis of **148aa** with stirring for 16 h with Alloc-Asn(Trt)-OH (**155b**, 497.6 mg, 1.09 mmol, 1.5 equiv) as coupling partner and purification by flash chromatography (60 mL of $SiO_2$, 0–5% MeOH in $CH_2Cl_2$ gradient elution),

afforded **148bb** (320.4 mg, 0.509 mmol, 71%) as a white film that was a 1:1 mixture of diastereomers: $^1$H NMR ($CD_3OD$, 500 MHz) δ 7.30–7.19 (m, 15H), 6.00–5.91 (m, 1H), 5.34 (d, *J* = 17.2 Hz, 1H), 5.21 (d, *J* = 10.3 Hz, 1H), 4.60–4.56 (m, 2H), 4.55–4.51 (m, 1H), 4.50 (s, 1H), 4.23–4.17 and 4.16–4.09 (2m, 2H), 2.86–2.66 (m, 2H), 1.65–1.45 (m, 4H), 1.27 and 1.26 (2t, *J* = 7.3 and 7.3 Hz, 3H), 0.93 (t, *J* = 7.4 Hz, 3H), 0.84 and 0.83 (2t, *J* = 7.5 and 7.4 Hz, 3H); $^{13}$C NMR ($CD_3OD$, 125 MHz) δ 172.1, 170.4 and 170.3, 170.1, 156.7 and 156.6, 144.4 (3C), 132.7, 128.6 (6C), 127.3 (6C), 126.4 (3C), 116.5, 75.6 and 75.5, 70.4, 65.6 and 65.5, 60.9, 57.8 and 57.7, 52.1, 38.2, 27.4, 27.0 and 26.9, 13.0, 6.7, 6.6; IR (film) $\nu_{max}$ 3328, 2970, 1735, 1663, 1522, 1275, 1268 cm$^{-1}$; HRMS (ESI) *m/z* 630.3110 ($MH^+$, $C_{36}H_{43}N_3O_7H^+$ requires 630.3135).

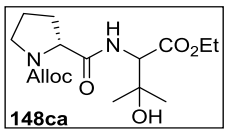

148ca

**Allyl (2*R*)-2-((1-Ethoxy-3-hydroxy-3-methyl-1-oxobutan-2-yl)carbamoyl) pyrrolidine-1-carboxylate (148ca).** Subjection of Ⓡ-hydroxyamino ester **154a** (220.7 mg, 1.37 mmol) to the procedure described above for the synthesis of **148aa** with Alloc-D-Pro-OH (**155c**, 406.3 mg, 2.04 mmol, 1.5 equiv) as coupling partner and purification by flash chromatography (60 mL of $SiO_2$, 0–6.5% MeOH in $CH_2Cl_2$ gradient elution) afforded **148ca** (378.8 mg, 1.11 mmol, 81%) as a colorless oil that was a 1:1 mixture of diastereomers: $^1$H NMR ($CD_3OD$, 500 MHz, mixture of rotamers and diastereomers) δ 6.03–5.83 (m, 1H), 5.40–5.09 (m, 2H), 4.64–4.52 (m, 2H), 4.46–4.35 (m, 2H), 4.27–4.14 (m, 2H), 3.64–3.56 (m, 1H), 3.55–3.46 (m, 1H), 2.34–2.16 (m, 1H), 2.07–1.85 (m, 3H), 1.33–1.27 (m, 6H); 1.24 (s, 3H); $^{13}$C NMR ($CD_3OD$, 125 MHz, mixture of rotamers and diastereomers) δ 175.2/175.0, 171.7/171.6, 156.7/156.3, 134.2/134.1/134.0, 117.9/117.7/117.6, 72.5/72.4, 67.2, 62.3/62.2, 61.9, 61.6/61.5/61.2, 48.1, 32.6/32.5/31.3/31.2, 27.7/27.4/27.3, 27.2/27.1, 25.4/25.3/24.6/24.5, 14.5; IR (film) $\nu_{max}$ 3417, 2917, 1678, 1540, 1408 cm$^{-1}$; HRMS (ESI) *m/z* 343.1824 ($MH^+$, $C_{16}H_{26}N_2O_6H^+$ requires 343.1824).

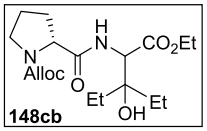


**Allyl (2*R*)-2-((1-Ethoxy-3-ethyl-3-hydroxy-1-oxopentan-2-yl)carbamoyl) pyrrolidine-1-carboxylate (148cb).** Subjection of ®-hydroxyamino ester **154b** (278.1 mg, 1.47 mmol) to the procedure described above for the synthesis of **148aa** with Alloc-D-Pro-OH (**155c**, 437.9 mg, 2.20 mmol, 1.5 equiv) as coupling partner, stirring for 16 h, and purification by flash chromatography (75 mL of $SiO_2$, 0–6% MeOH in $CH_2Cl_2$ gradient elution) afforded **148cb** (431.7 mg, 1.17 mmol, 79%) as a colorless oil that was a 1:1 mixture of diastereomers: $^1$H NMR ($CD_3OD$, 500 MHz, mixture of rotamers and diastereomers) δ 6.03–5.85 (m, 1H), 5.39–5.11 (m, 2H), 4.64–4.49 (m, 3H), 4.44–4.33 (m, 1H), 4.28–4.13 (m, 2H), 3.65–3.56 (m, 1H), 3.55–3.47 (m, 1H), 2.36–2.15 (m, 1H), 2.08–1.84 (m, 3H), 1.72–1.49 (m, 4H), 1.33–1.25 (m, 3H), 0.93 (t, $J$ = 7.6 Hz, 3H), 0.90–0.82 (m, 3H); $^{13}$C NMR ($CD_3OD$, 125 MHz, mixture of rotamers and diastereomers) δ 173.6/173.5, 170.5/170.4, 155.0/154.9, 132.7/132.6, 116.4/116.3/116.2/116.1, 75.6/75.5, 65.9/65.8, 60.8/60.7, 60.3/59.9, 57.7/57.6/57.4, 46.7, 31.1/31.0/29.9/29.8, 27.4, 27.0/26.9, 24.0/23.9/23.0, 13.0, 6.7, 6.6; IR (film) $\nu_{max}$ 3414, 2969, 1679, 1444, 1408 cm$^{-1}$; HRMS (ESI) *m/z* 371.2127 ($MH^+$, $C_{18}H_{30}N_2O_6H^+$ requires 371.2137).

### 5.2.2 Synthesis of Azlactone Dipeptides 149

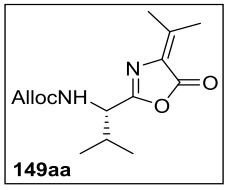


**Allyl (*S*)-(2-methyl-1-(5-oxo-4-(propan-2-ylidene)-4,5-dihydrooxazol-2-yl)propyl)carbamate (149aa).** A solution of dipeptide **148aa** (394.2 mg, 1.14 mmol) in 3:1 *t*-BuOH–$H_2O$ (20 mL) at 0 °C was treated with LiOH·$H_2O$ (239.7 mg, 5.71 mmol, 5.0 equiv) and stirred at 0 °C for 4 h. The reaction was quenched with 1.0 M HCl solution to adjust the pH to 2,

and the resulting mixture was extracted with EtOAc (4 × 30 mL). The combined organic layers were washed with brine (20 mL), dried ($Na_2SO_4$), and concentrated *in vacuo*. The crude acid (357.9 mg, 1.13 mmol) was then dissolved in anhydrous THF (20 mL), treated with NaOAc (139.4 mg, 1.70 mmol, 1.5 equiv) and $Ac_2O$ (540 μL, 583 mg, 5.71 mmol, 5.0 equiv), then stirred at rt under Ar for 12 h. The reaction was quenched with MeOH (10 mL), stirred at rt for 30 min, diluted with $H_2O$ (10 mL), and extracted with EtOAc (4 × 25 mL). The combined organic layers were washed with brine (25 mL), dried ($Na_2SO_4$), and concentrated *in vacuo*. Flash chromatography (50 mL of $SiO_2$, 1% $Et_3N$ in 1–10% EtOAc in hexanes gradient elution) afforded **149aa** (257.7 mg, 0.919 mmol, 80%) as a colorless oil: $[\alpha]^{25}_D$ –18 (*c* 0.44, $CHCl_3$); $^1$H NMR ($CDCl_3$, 500 MHz) δ $^1$H NMR ($CDCl_3$, 500 MHz) δ 6.01–5.89 (m, 1H), 5.34 (d, *J* = 17.1 Hz, 1H), 5.31–5.27 (m, 1H), 5.25 (d, *J* = 10.9 Hz, 1H), 4.64–4.56 (m, 3H), 2.36 (s, 3H), 2.26 (s, 3H), 2.24–2.17 (m, 1H), 1.02 (d, *J* = 6.8 Hz, 3H), 0.96 (d, *J* = 6.8 Hz, 3H); $^{13}$C NMR ($CDCl_3$, 125 MHz) δ 164.9, 162.1, 155.9, 154.7, 132.6, 130.1, 118.0, 66.0, 55.0, 31.3, 22.8, 19.7, 18.9, 17.5; IR (film) $\nu_{max}$ 3293, 2917, 1693, 1650, 1536 $cm^{-1}$; HRMS (ESI) *m/z* 281.1484 ($MH^+$, $C_{14}H_{20}N_2O_4H^+$ requires 281.1457).

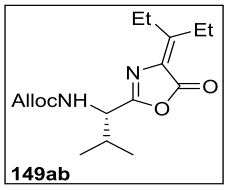

149ab

**Allyl (*S*)-(2-methyl-1-(5-oxo-4-(pentan-3-ylidene)-4,5-dihydrooxazol-2-yl)propyl)carbamate (149ab).** Subjection of dipeptide **148ab** (338.6 mg, 0.909 mmol) to the saponification procedure described above for the synthesis of **149aa** with 6 h of stirring afforded 307.3 mg (0.892 mmol) of the crude acid. Subjection of this crude mixture to the conditions described previously with NaOAc (109.9 mg, 1.34 mmol, 1.5 equiv), $Ac_2O$ (430 μL, 464 mg, 4.55 mmol, 5.1 equiv), and purification by flash chromatography 65 mL of $SiO_2$, 1% $Et_3N$ in 1–10% EtOAc in hexanes gradient elution) afforded **149ab** (208.6 mg, 0.676 mmol, 74%) as a colorless

oil: $[\alpha]^{25}_D$ –14 (*c* 0.36, $CHCl_3$); $^1H$ NMR ($CD_3OD$, 500 MHz) δ 6.01–5.90 (m, 1H), 5.33 (dd, *J* = 17.3, 1.6 Hz, 1H), 5.19 (d, *J* = 10.6 Hz, 1H), 4.56 (d, *J* = 5.4 Hz, 2H), 4.02 (d, *J* = 6.8 Hz, 1H), 2.58 (q, *J* = 7.6 Hz, 2H), 2.28–2.18 (m, 2H), 2.17–2.09 (m, 1H), 1.11 (t, *J* = 7.4 Hz, 3H), 1.04 (t, *J* = 7.5 Hz, 3H), 1.03 (d, *J* = 7.3 Hz, 3H), 0.99 (d, *J* = 6.8 Hz, 3H); $^{13}C$ NMR ($CD_3OD$, 125 MHz) δ 172.6, 166.5, 157.0, 155.7, 132.9, 121.3, 116.2, 65.2, 60.4, 30.6, 25.4, 24.3, 18.4, 17.0, 12.0, 11.0; IR (film) $\nu_{max}$ 3293, 2966, 1693, 1650, 1561 $cm^{-1}$; HRMS (ESI) *m/z* 309.1746 ($MH^+$, $C_{16}H_{24}N_2O_4H^+$ requires 309.1770).

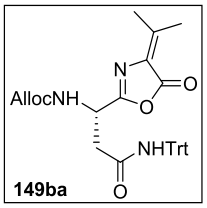


**Allyl (*S*)-(3-oxo-1-(5-oxo-4-(propan-2-ylidene)-4,5-dihydrooxazol-2-yl)-3-(tritylamino)propyl)carbamate (149ba).** A solution of dipeptide **148ba** (402.9 mg, 0.670 mmol) in 3:1 *t*-BuOH–$H_2O$ (16 mL) at 0 °C was treated with $LiOH·H_2O$ (141.4 mg, 3.37 mmol, 5.0 equiv) and stirred at 0 °C for 4 h. The reaction was quenched with sat aq $KHSO_4$ to adjust the pH to 2, and the resulting mixture was extracted with EtOAc (4 × 25 mL). The combined organic layers were washed with brine (15 mL), dried ($Na_2SO_4$), and concentrated *in vacuo*. The crude acid (363.6 mg, 0.634 mmol) was then dissolved in anhydrous THF (20 mL), treated with NaOAc (78.1 mg, 0.952 mmol, 1.5 equiv) and $Ac_2O$ (300 μL, 324 mg, 3.17 mmol, 5.0 equiv), then stirred at rt under Ar for 12 h. The reaction was quenched with MeOH (10 mL), stirred at rt for 30 min, diluted with $H_2O$ (10 mL), and extracted with EtOAc (4 × 25 mL). The combined organic layers were washed with brine (15 mL), dried ($Na_2SO_4$), and concentrated *in vacuo*. Flash chromatography (50 mL of $SiO_2$, 1% $Et_3N$ in 2–10% EtOAc in hexanes gradient elution) afforded **149ba** (252.4 mg, 0.469 mmol, 70%) as a white solid: $[\alpha]^{25}_D$ –2.1 (*c* 0.86, $CHCl_3$); $^1H$ NMR ($CDCl_3$, 500 MHz) δ 7.31–

7.23 (m, 9H), 7.17–7.12 (m, 6H), 6.78 (s, 1H), 6.17 (d, $J$ = 8.5 Hz, 1H), 5.97–5.82 (m, 1H), 5.32 (d, $J$ = 17.1 Hz, 1H), 5.21 (d, $J$ = 10.4 Hz, 1H), 5.01–4.91 (m, 1H), 4.64–4.52 (m, 2H), 3.08 (dd, $J$ = 15.6, 4.3 Hz, 1H), 2.92 (dd, $J$ = 15.5, 4.5 Hz, 1H), 2.35 (s, 3H), 2.19 (s, 3H); $^{13}$C NMR ($CDCl_3$, 125 MHz) δ 168.7, 164.8, 161.7, 155.9, 154.5, 144.2 (3C), 132.5, 130.5, 128.6 (6C), 128.0 (6C), 127.2 (3C), 117.7, 70.9, 65.9, 46.9, 37.9, 22.9, 19.7; IR (film) $\nu_{max}$ 3286, 2917, 1794, 1673, 1530, 1447, 1158 cm$^{-1}$; HRMS (ESI) *m/z* 538.2273 ($MH^+$, $C_{32}H_{31}N_3O_5H^+$ requires 538.2297).

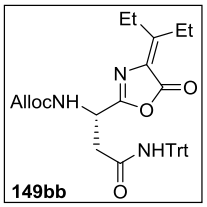


**Allyl (*S*)-(3-oxo-1-(5-oxo-4-(pentan-3-ylidene)-4,5-dihydrooxazol-2-yl)-3-(tritylamino)propyl)carbamate (149bb).** Subjection of dipeptide **148bb** (342.7 mg, 0.544 mmol) to the saponification procedure described above for the synthesis of **149ba** afforded 316.4 mg (0.526 mmol) of the crude acid. Subjection of this crude mixture to the conditions described previously with NaOAc (65.7 mg, 0.801 mmol, 1.5 equiv), $Ac_2O$ (250 μL, 270 mg, 2.64 mmol, 5.0 equiv), and purification by flash chromatography (60 mL of $SiO_2$, 1% $Et_3N$ in 1–10% EtOAc in hexanes gradient elution) afforded **149bb** (197.7 mg, 0.349 mmol, 64%) as a white solid: $[\alpha]^{25}_D$ –5.4 (*c* 1.0, $CHCl_3$); $^1$H NMR ($CDCl_3$, 500 MHz) δ 7.31–7.22 (m, 9H), 7.14–7.11 (m, 6H), 6.78 (s, 1H), 6.15 (d, $J$ = 8.6 Hz, 1H), 5.98–5.84 (m, 1H), 5.32 (d, $J$ = 17.3 Hz, 1H), 5.21 (d, $J$ = 10.5 Hz, 1H), 5.00–4.92 (m, 1H), 4.64–4.52 (m, 2H), 3.10 (dd, $J$ = 15.6, 4.4 Hz, 1H), 2.92 (dd, $J$ = 15.5, 4.7 Hz, 1H), 2.85–2.71 (m, 2H), 2.69–2.54 (m, 2H), 1.14 (t, $J$ = 7.5 Hz, 3H), 1.09 (t, $J$= 7.7 Hz, 3H); $^{13}$C NMR ($CDCl_3$, 125 MHz) δ 168.7, 165.4, 164.7, 161.9, 155.9, 144.2 (3C), 132.5, 129.6, 128.6 (6C), 128.0 (6C), 127.2 (3C), 117.6, 71.0, 65.9, 47.0, 37.9, 26.6, 23.4, 12.5, 12.3; IR (film)

$\nu_{max}$ 3277, 2918, 1789, 1648, 1526, 1447, 1268 $cm^{-1}$; HRMS (ESI) *m/z* 566.2639 ($MH^+$, $C_{34}H_{35}N_3O_5H^+$ requires 566.2610).

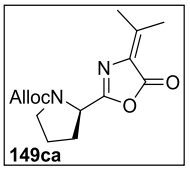


**Allyl (*R*)-2-(5-oxo-4-(propan-2-ylidene)-4,5-dihydrooxazol-2-yl)pyrrolidine-1-carboxylate (149ca).** Subjection of dipeptide **148ca** (268.6 mg, 0.784 mmol) to the saponification procedure described above for the synthesis of **149aa** afforded 236.1 mg (0.751 mmol) of the crude acid. Subjection of this crude mixture to the conditions described previously with NaOAc (92.8 mg, 1.13 mmol, 1.5 equiv), $Ac_2O$ (360 μL, 389 mg, 3.81 mmol, 5.1 equiv), and purification by flash chromatography (50 mL of $SiO_2$, 1% $Et_3N$ in 2–10% EtOAc in hexanes gradient elution) afforded **149caa** (157.9 mg, 0.567 mmol, 72%) as a colorless oil: $[\alpha]^{25}_D$ +93 (*c* 0.64, $CHCl_3$); $^1H$ NMR ($CDCl_3$, 500 MHz, ca. 1.2:1 mixture of rotamers) δ 5.99–5.90 and 5.88–5.78 (2m, 1H), 5.33 and 5.25 (2d, *J* = 17.2 and 18.8 Hz, 1H), 5.22 and 5.13 (2d, *J* = 10.9 and 10.5 Hz, 1H), 4.75–4.68 (m, 1H), 4.65–4.59 and 4.52 (m and dd, *J* = 13.7, 5.1 Hz, 1H), 4.61 (d, *J* = 5.4 Hz, 1H), 3.68–3.59 (m, 1H), 3.59–3.50 (m, 1H), 2.35 and 2.33 (2s, 3H), 2.32–2.26 (m, 1H), 2.24 (s, 3H), 2.18–2.03 (m, 2H), 2.02–1.92 (m, 1H); $^{13}C$ NMR ($CDCl_3$, 125 MHz, ca. 1.2:1 mixture of rotamers) δ 165.3, 165.1, 163.1 and 162.9, 154.5 and 154.1, 132.8 and 132.6, 130.7 and 130.5, 117.4 and 117.0, 66.0 and 65.9, 55.7 and 55.1, 46.9 and 46.5, 31.2 and 30.4, 24.3 and 23.4, 22.8 and 22.7, 19.7; IR (film) $\nu_{max}$ 2917, 1794, 1707, 1675, 1406, 1158 $cm^{-1}$; HRMS (ESI) *m/z* 279.1325 ($MH^+$, $C_{14}H_{18}N_2O_4H^+$ requires 279.1300).

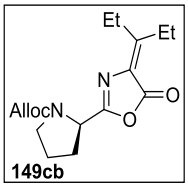


**Allyl (*R*)-2-(5-oxo-4-(pentan-3-ylidene)-4,5-dihydrooxazol-2-yl)pyrrolidine-1-carboxylate (6bb).** Subjection of dipeptide **148cb** (337.4 mg, 0.911 mmol) to the saponification procedure described above for the synthesis of **149aa** afforded 308.2 mg (0.900 mmol) of the crude acid. Subjection of this crude mixture to the conditions described previously with NaOAc (110.9 mg, 1.35 mmol, 1.5 equiv), $Ac_2O$ (430 μL, 464 mg, 4.55 mmol, 5.1 equiv), and purification by flash chromatography (75 mL of $SiO_2$, 1% $Et_3N$ in 1–10% EtOAc in hexanes gradient elution) afforded **149cb** (204.8 mg, 0.668 mmol, 73%) as a colorless oil: $[\alpha]^{25}_D$ +83 (*c* 1.0, $CHCl_3$); $^1H$ NMR ($CDCl_3$, 500 MHz, ca. 1.1:1 mixture of rotamers) δ 6.00–5.89 and 5.87–5.76 (2m, 1H), 5.32 and 5.23 (2d, *J* = 17.8 and 18.5 Hz, 1H), 5.22 and 5.12 (2d, *J* = 9.4 and 10.4 Hz, 1H), 4.74 and 4.69 (2dd, *J* = 8.2, 3.0 Hz and 8.1, 3.4 Hz, 1H), 4.65–4.58 and 4.50 (m and dd, *J* = 13.6, 5.2 Hz, 1H), 4.61 (d, *J* = 4.6 Hz, 1H), 3.68–3.60 (m, 1H), 3.59–3.51 (m, 1H), 2.83–2.74 (m, 2H), 2.69–2.59 (m, 2H), 2.34–2.24 (m, 1H), 2.18–2.03 (m, 2H), 2.01–1.91 (m, 1H), 1.17–1.07 (m, 6H); $^{13}C$ NMR ($CDCl_3$, 125 MHz, ca. 1.1:1 mixture of rotamers) δ 165.2, 165.0 and 164.9, 163.2 and 163.1, 154.5 and 154.2, 132.8 and 132.6, 129.8 and 129.6, 117.4 and 117.1, 66.0 and 65.9, 55.7 and 55.1, 46.9 and 46.5, 31.2 and 30.4, 26.6, 24.3 and 23.6, 23.4, 12.5 and 12.4, 12.3; IR (film) $\nu_{max}$ 2975, 1791, 1709, 1668, 1406, 1156 $cm^{-1}$; HRMS (ESI) *m/z* 307.1625 ($MH^+$, $C_{16}H_{22}N_2O_4H^+$ requires 307.1613).

### 5.2.3 General Procedures for Solid-Phase Peptide Synthesis

**Attachment of *C*-terminal amino acid to resin.** Rink amide MBHA resin (100–200 mesh, 100 μmol) was added to a fritted polypropylene syringe. The resin was swelled in $CH_2Cl_2$ (10 min),

and then in DMF (5 min). The swelling solvents were drained from the resin using a vacuum manifold. After Fmoc deprotection (see below for procedure, repeated twice), the amino acid was coupled to the resin (see below for procedure, repeated twice).

**Fmoc Deprotection.** The resin (100 μmol) was treated with piperidine (20% solution in DMF, 5.0 mL) and allowed to stand for 5 min. The solution was drained from the resin using a vacuum manifold, and additional piperidine (20% solution in DMF, 5.0 mL) was added. The resulting mixture was stirred twice at 80 °C in a microwave oven for 4 min. The solution was drained from the resin using a vacuum manifold, and the resin was rinsed with DMF (5 × 10 mL).

**Peptide coupling.** The Fmoc-protected amino acid (500 μmol, 5 equiv) and HBTU (190 mg, 500 μmol, 5 equiv) were dissolved by vortexing in a 0.1 M HOBt solution in NMP (5.0 mL, 500 μmol, 5 equiv). *i*Pr$_2$NEt (176 μL, 1000 μmol, 10 equiv) was added to this solution, and it was allowed to stand for ca. 1 min. The solution was added to the resin (100 μmol), and the resulting mixture was stirred at 70 °C in a microwave oven for 10 min. The solution was drained from the resin using a vacuum manifold, and the resin was rinsed with DMF (5 × 10 mL). The *N*-terminal amino acid of each peptide (i.e., Arg) was coupled by gently stirring the solution at rt under Ar for ca. 10–12 h after the microwave heating was completed.

**Coupling of azlactones 149 with resin-bound peptides.** A solution of **149** (500 μmol, 5 equiv) and Et$_3$N (150 μL, 1.08 mmol, 10 equiv) in NMP (10 mL) was added to the resin-bound peptide (100 μmol). The resulting mixture was gently stirred at 80 °C for 24–36 h. The solution was drained from the resin using a fritted polypropylene syringe into a 20 mL glass vial (**note:** the unreacted azlactone present in the solution can be reused), and the resin was rinsed with DMF (5 × 10 mL). Any unreacted amines were then capped by addition of a solution of Ac$_2$O (1.0 mL,

1.08 g, 10.6 mmol, 106 equiv) and $Et_3N$ (200 μL, 145.2 mg, 1.44 mmol, 14.4 equiv.) in $CH_2Cl_2$ (5 mL), followed by stirring at rt under Ar for 90 min and washing with $CH_2Cl_2$ (5 × 10 mL).

**Alloc deprotection.** The resin-bound peptide (100 μmol) was placed under an Ar atmosphere and treated with a solution of $PhSiH_3$ (700 μL, 613.9 mg, 5.67 mmol, 56.7 equiv) in $CH_2Cl_2$ (3 mL) with stirring, followed by addition of a solution of $Pd(PPh_3)_4$ (56.8 mg, 49.2 μmol, 0.49 equiv) in $CH_2Cl_2$ (3 mL). The resulting mixture was stirred at rt under Ar for 20 min. The resin was rinsed with $CH_2Cl_2$ (5 × 10 mL), and the deprotection protocol was repeated once.

**Acetylation of the *N*-terminus of resin-bound peptides.** The *N*-terminus of each peptide was capped by addition of a solution of $Ac_2O$ (1.0 mL, 1.08 g, 10.6 mmol, 106 equiv) and $Et_3N$ (200 μL, 145.2 mg, 1.44 mmol, 14.4 equiv.) in $CH_2Cl_2$ (5 mL), followed by stirring at rt under Ar for 2 h. The resin was then rinsed with $CH_2Cl_2$ (5 × 10 mL).

**Cleavage of peptide from resin and purification.** The resin-bound peptide (100 μmol) was treated carefully with a solution of phenol (500 mg, 5.31 mmol), $H_2O$ (500 μL), thioanisole (500 μL, 528.5 mg, 4.26 mmol), ethanedithiol (250 μL, 280.8 mg, 2.98 mmol), and triisopropylsilane (100 μL, 77.3 mg, 488 μmol) in TFA (8.0 mL) in order to avoid the buildup of excess $CO_2$ pressure in the reaction vessel. The resulting mixture was stirred at rt for ca. 4 h, and the peptide was precipitated by filtering the mixture and pouring the filtrate into cold $Et_2O$ (40 mL). The resin was rinsed with TFA (3 mL), and the precipitate was collected by centrifugation. The crude peptide was lyophilized and purified by HPLC (see entries for individual peptides for elution conditions).

**Synthesis of cyclic and random coil control peptides (167–168).** Ac-Cys-Trp-Val-Glu-Val-Asn-Gly-Orn-Lys-Ile-Leu-Gln-Cys-$NH_2$ (**167a**) and Ac-Cys-Trp-Val-Glu-Val-ΔVal-Gly-

Orn-Lys-Ile-Leu-Gln-Cys-$NH_2$ (**167b**) were synthesized according to the previously described general procedures and purified by HPLC. They were then cyclized by stirring in open air for ca. 24 h in a 10 mM phosphate buffer solution (pH 7.5) containing 5% DMSO, affording cyclic controls **167a** and **167b** respectively. Random coil peptides **168a**, **168b**, **168c,** and **168d** were synthesized according to the previously described general procedures. Azlactones **149aa** and **Ac-ΔVal**[4] were used to synthesize **168c** and **168d** respectively.

**Peptide Concentration Determination and NMR Sample Preparation.** Peptide solutions were prepared in 20 mM sodium phosphate buffer (pH 7), and peptide concentrations were determined spectroscopically based on tryptophan absorbance at 280 nm in 6 M guanidine hydrochloride (Trp $\varepsilon_{280} = 5690\ M^{-1}cm^{-1}$). NMR samples were prepared with 1–3.5 mM peptide in 10% v/v $D_2O/H_2O$ buffered to pD 3.9 with 5000 μM NaOAc-$d_3$.

[4] El-Baba, S., Nuzillard, J.M., Poulin, J.C., Kagan, H.B. *Tetrahedron* **1986**, *42*, 3851.

### 5.2.4 Tabulated $^1$H NMR Data for Peptides

**Table 5.1.** Ac-R-W-V-E-V-**N-G-**O-K-I-L-Q-$NH_2$ (**153a**).

| | Amide | α | β | Others (γ, δ, ε) |
|---|---|---|---|---|
| **Arg** | 8.11 | 4.38 | 1.65, 1.71 | γ $CH_2$ 1.52; δ $CH_2$ 3.15; ε H 7.14 |
| **Trp** | 8.34 | 5.09 | 3.09 | H1 10.2; H2 7.25; H4 7.50; H6 7.08; H7 7.34 |
| **Val** | 9.00 | 4.45 | 2.04 | γ $CH_3$ 0.871, 0.889 |
| **Glu** | 8.55 | 4.92 | 1.93, 2.02 | γ $CH_2$ 2.28 |
| **Val** | 8.90 | 4.22 | 1.96 | γ $CH_3$ 0.928 |
| **Asn** | 9.41 | 4.48 | 2.77, 3.07 | δ $NH_2$ 6.96, 7.64 |
| **Gly** | 8.64 | 3.75, 4.09 | | |
| **Orn** | 7.87 | 4.62 | 1.83, 1.87 | γ $CH_2$ 1.73; δ $CH_2$ 3.05; ε NH 7.66 |
| **Lys** | 8.51 | 4.74 | 1.70 | γ $CH_2$ 1.23; δ $CH_2$ 1.36; ε $CH_2$ 2.58; ζ $NH_3$ 7.28 |
| **Ile** | 9.11 | 4.57 | 1.89 | γ $CH_2$ 1.21, 1.43; δ $CH_3$ 0.836; γ $CH_3$ 0.902 |
| **Leu** | 8.35 | 4.10 | 1.09, 1.37 | γ CH 0.792; δ $CH_3$ 0.319, 0.529 |
| **Gln** | 8.67 | 4.33 | 1.89, 2.05 | γ $CH_2$ 2.28; ε $NH_2$ 6.89, 7.36 |

**Table 5.2.** Ac-R-W-V-E-V-**p-G**-O-K-I-L-Q-$NH_2$ (**153b**).

| | H | α | β | Others (γ, δ, ε) |
|---|---|---|---|---|
| **Arg** | 8.07 | 4.41 | 1.64, 1.72 | γ $CH_2$ 1.53; δ $CH_2$ 3.16; ε NH 6.88 |
| **Trp** | 8.36 | 5.13 | 3.08 | H1 10.20; H2 7.23; H4 7.27; H5 7.05; H7 7.49 |
| **Val** | 9.25 | 4.51 | 2.05 | γ $CH_3$ 0.889, 0.873 |
| **Glu** | 8.59 | 5.06 | 2.03, 1.95 | γ $CH_2$ 2.33 |
| **Val** | 8.98 | 4.63 | 1.99 | γ $CH_3$ 0.941 |
| **D-Pro** | | 4.38 | 2.20, 2.40 | γ $CH_2$ 2.01, 2.08; δ $CH_2$ 3.88 |
| **Gly** | 8.62 | 3.80, 4.04 | | |
| **Orn** | 7.93 | 4.66 | 1.85 | γ $CH_2$ 1.71; δ $CH_2$ 3.03, ε $NH_3$ 7.65 |
| **Lys** | 8.48 | 4.86 | 1.67 | γ $CH_2$ 1.20; δ $CH_2$ 1.28; ε $CH_2$ 2.48 |
| **Ile** | 9.24 | 4.62 | 1.88 | γ $CH_2$ 1.19, 1.40; δ $CH_3$ 0.816; γ $CH_3$ 0.889 |
| **Leu** | 8.36 | 4.02 | 0.966, 1.32 | γ CH 0.595; δ $CH_3$ 0.166, 0.445 |
| **Gln** | 8.73 | 4.33 | 1.86, 2.03 | γ $CH_2$ 2.25; ε $NH_2$ 7.71, 7.12 |

**Table 5.3.** Ac-R-W-V-E-V-Δ**Val-G**-O-K-I-L-Q-$NH_2$ (**152aa**).

| | H | α | β | Others (γ, δ, ε) |
|---|---|---|---|---|
| **Arg** | 8.08 | 4.41 | 1.73, 1.65 | γ $CH_2$ 1.54; δ $CH_2$ 3.16; ε NH 7.14 |
| **Trp** | 8.34 | 5.15 | 3.04, 3.09 | H1 10.2; H2 7.24; H4 7.29; H6 7.06; H7 7.50 |
| **Val** | 9.24 | 4.54 | 2.08 | γ $CH_3$ 0.880 |
| **Glu** | 8.57 | 5.14 | 2.01, 1.93 | γ $CH_2$ 2.27, 2.30 |
| **Val** | 9.08 | 4.38 | 1.96 | γ $CH_3$ 0.994, 0.955 |
| **ΔVal** | 10.3 | | | γ $CH_3$ 1.99, 1.89 |
| **Gly** | 8.63 | 4.11, 3.73 | | |
| **Orn** | 7.98 | 4.66 | 1.72 | γ $CH_2$ 1.85; δ $CH_2$ 3.03; ε $NH_3$ 7.65 |
| **Lys** | 8.50 | 4.82 | 1.67, 1.35 | γ $CH_2$ 1.20; δ $CH_2$ 1.28, 1.35; ε $CH_2$ 2.50, 2.45; ζ $NH_3$7.20 |
| **Ile** | 9.26 | 4.63 | 1.90 | γ $CH_2$ 1.21, 1.41; δ $CH_3$ 0.813; γ $CH_3$ 0.888 |
| **Leu** | 8.35 | 4.04 | 0.990, 1.33 | γ CH 0.641; δ $CH_3$ 0.194, 0.454 |
| **Gln** | 8.72 | 4.33 | 1.87, 2.03 | γ $CH_2$ 2.26; ε $NH_2$ 7.12, 7.71 |

**Table 5.4.** Ac-R-W-V-E-V-**ΔEnv-G**-O-K-I-L-Q-$NH_2$ (**152ab**).

| | H | α | β | Others (γ, δ, ε) |
|---|---|---|---|---|
| **Arg** | 8.08 | 4.42 | 1.66, 1.73 | γ $CH_2$ 1.54; δ $CH_2$ 3.17; ε NH 7.15 |
| **Trp** | 8.35 | 5.14 | 3.04, 3.10 | H1 10.2; H2 7.24; H4 7.31; H5 7.07; H7 7.51 |
| **Val** | 9.18 | 4.52 | 2.07 | γ $CH_3$ 0.885, 0.907 |
| **Glu** | 8.57 | 5.09 | 2.22 | γ $CH_2$ 1.92, 2.00 |
| **Val** | 9.04 | 4.41 | 1.99 | γ $CH_3$ 0.965, 0.982 |
| **ΔEnv** | 10.1 | | | γ $CH_2$ 2.36, 2.20; δ $CH_3$ 1.05, 0.992 |
| **Gly** | 8.65 | 3.76, 4.11 | | |
| **Orn** | 7.97 | 4.67 | 1.87 | γ $CH_2$ 1.74; δ $CH_2$ 3.05; ε $NH_3$ 7.63 |
| **Lys** | 8.53 | 4.83 | 1.68 | γ $CH_2$ 1.21; δ $CH_2$ 1.30, 1.38; ε $CH_2$ 2.52 |
| **Ile** | 9.23 | 4.62 | 1.89 | γ $CH_2$ 1.21, 1.42; δ $CH_3$ 0.829; γ $CH_3$ 0.898 |
| **Leu** | 8.34 | 4.05 | 1.01, 1.34 | γ CH 0.663; δ $CH_3$ 0.224, 0.476 |
| **Gln** | 8.71 | 4.34 | 1.88, 2.05 | γ $CH_2$ 2.27; ε $NH_2$ 7.71, 7.12 |

**Table 5.5.** Ac-R-W-V-E-V-**N-ΔVal**-O-K-I-L-Q-$NH_2$ (**152ba**).

| | H | α | β | Others (γ, δ, ε) |
|---|---|---|---|---|
| **Arg** | 8.12 | 4.30 | 1.64 | γ $CH_2$ 1.47; δ $CH_2$ 3.11; ε NH 7.11 |
| **Trp** | 8.27 | 4.97 | 3.14 | H1 10.18; H2 7.23; H4 7.42; H5 7.08; H7 7.49 |
| **Val** | 8.62 | 4.30 | 2.01 | γ $CH_3$ 0.851 |
| **Glu** | 8.45 | 4.75 | 1.90, 1.98 | γ $CH_2$ 2.23 |
| **Val** | 8.70 | 4.18 | 1.99 | γ $CH_3$ 0.915 |
| **Asn** | 9.15 | 4.61 | 2.80, 3.01 | δ $NH_2$ 6.95, 7.62 |
| **ΔVal** | 9.34 | | | γ $CH_3$ 1.81, 0.917 |
| **Orn** | 7.78 | 4.49 | 1.72, 1.76 | γ $CH_2$ 1.86; δ $CH_2$ 3.04; ε $NH_3$ 7.64 |
| **Lys** | 8.36 | 4.57 | 1.73 | γ $CH_2$ 1.26; δ $CH_2$ 1.42; ε $CH_2$ 2.68 |
| **Ile** | 8.76 | 4.39 | 1.87 | γ $CH_2$ 1.17, 1.42; δ $CH_3$ 0.805; γ $CH_3$ 0.805 |
| **Leu** | 8.33 | 4.16 | 1.42, 1.25 | γ CH 1.05; δ $CH_3$ 0.484, 0.619 |
| **Gln** | 8.49 | 4.30 | 1.91, 2.05 | γ $CH_2$ 2.30; ε $NH_2$ 7.12, 7.62 |

**Table 5.6.** Ac-R-W-V-E-V-**N-ΔEnv**-O-K-I-L-Q-$NH_2$ (**152bb**).

| | H | α | β | Others (γ, δ, ε) |
|---|---|---|---|---|
| **Arg** | 8.14 | 4.27 | 1.64 | γ $CH_2$ 1.47; δ $CH_2$ 3.11; ε NH 7.11 |
| **Trp** | 8.25 | 4.92 | 3.18 | 1H 10.2; H2 7.24; H5 7.10; H7 7.48 |
| **Val** | 8.44 | 4.25 | 2.01 | γ $CH_3$ 0.856 |
| **Glu** | 8.40 | 4.66 | 1.97, 2.09 | γ $CH_2$ 2.32 |
| **Val** | 8.58 | 4.16 | 2.02 | γ $CH_3$ 0.935 |
| **Asn** | 8.98 | 4.70 | 2.80, 3.01 | δ $NH_2$ 7.00, 7.64 |
| **ΔEnv** | 9.21 | | | γ $CH_2$ 2.139, 2.215; δ $CH_3$ 0.971 |
| **Orn** | 7.85 | 4.41 | 1.87 | γ $CH_2$ 1.74; δ $CH_2$ 3.04; ε $NH_3$ 7.65 |
| **Lys** | 8.24 | 4.50 | 1.77 | γ $CH_2$ 1.30; δ $CH_2$ 1.49 ε $CH_2$ 2.75; ζ $NH_3$ 7.41 |
| **Ile** | 8.61 | 4.30 | 1.90 | γ $CH_2$ 1.18, 1.45; δ $CH_3$ 0.804; γ $CH_3$ 0.879 |
| **Leu** | 8.33 | 4.19 | 1.39, 1.48 | γ CH 1.23; δ $CH_3$ 0.585, 0.685 |
| **Gln** | 8.62 | 4.30 | 2.09 | γ $CH_2$ 2.43; ε $NH_2$ 7.15, 7.57 |

**Table 5.7.** Ac-R-W-V-E-V-**p-ΔVal**-O-K-I-L-Q-$NH_2$ (**152ca**).

| | H | α | β | Others (γ, δ, ε) |
|---|---|---|---|---|
| **Arg** | 8.08 | 4.40 | 1.71, 1.63 | γ $CH_2$ 1.513, δ $CH_2$ 3.15, ε CH 7.13 |
| **Trp** | 8.35 | 5.11 | 3.06 | H1 10.2; H2 7.23; H4 7.50; H6 7.05; H7 7.30 |
| **Val** | 9.15 | 4.48 | 2.05 | γ $CH_2$ 0.876 |
| **Glu** | 8.55 | 5.07 | 1.89, 1.97 | γ $CH_2$ 2.16, 2.22 |
| **Val** | 8.95 | 4.62 | 2.00 | γ $CH_3$ 0.947 |
| **D-Pro** | | 4.42 | 2.19, 2.47 | γ $CH_2$ 2.10; δ $CH_2$ 3.88, 3.94 |
| **ΔVal** | 9.25 | | | γ $CH_3$ 1.80, 2.18 |
| **Orn** | 7.77 | 4.63 | 1.80, 1.86 | γ $CH_2$ 1.73; δ $CH_2$ 3.03; ε $NH_3$ 7.64 |
| **Lys** | 8.48 | 4.82 | 1.67 | γ $CH_2$ 1.20; δ $CH_2$ 1.30; ε $CH_2$ 2.53 |
| **Ile** | 9.17 | 4.58 | 1.87 | γ $CH_2$ 1.19, 1.40; δ $CH_3$ 0.814; γ $CH_3$ 0.885 |
| **Leu** | 8.36 | 4.04 | 1.01, 1.34 | γ CH 0.671; δ $CH_3$ 0.217, 0.470 |
| **Gln** | 8.69 | 4.32 | 1.86, 2.03 | γ $CH_2$ 2.26; ε $NH_2$ 6.89, 7.33 |

**Table 5.8.** Ac-R-W-V-E-V-**p-ΔEnv**-O-K-I-L-Q-$NH_2$ (**152cb**).

| | H | α | β | Others (γ, δ, ε) |
|---|---|---|---|---|
| **Arg** | 8.08 | 4.39 | 1.64, 1.71 | γ $CH_2$ 1.52; δ $CH_2$ 3.15; ε NH 7.14 |
| **Trp** | 8.32 | 5.10 | 3.07 | H1 10.2; H2 7.23; H4 7.31; H5 7.05; H7 7.50 |
| **Val** | 9.10 | 4.48 | 2.07 | γ $CH_3$ 0.884 |
| **Glu** | 8.53 | 5.09 | 1.90, 1.97 | γ $CH_2$ 2.14, 2.29 |
| **Val** | 8.89 | 4.61 | 2.01 | γ $CH_3$ 0.955 |
| **D-Pro** | | 4.44 | 2.17, 2.47 | γ $CH_2$ 2.09; δ $CH_2$ 3.87, 3.97 |
| **ΔEnv** | 9.33 | | | γ $CH_2$ 2.23, 2.061; δ $CH_3$ 0.969 |
| **Orn** | 7.78 | 4.62 | 1.88 | γ $CH_2$ 1.74; δ $CH_2$ 3.05; ε $NH_3$ 7.63 |
| **Lys** | 8.44 | 4.82 | 1.67 | γ $CH_2$ 1.21; δ $CH_2$ 1.34; ε $CH_2$ 2.55 |
| **Ile** | 9.12 | 4.56 | 1.88 | γ $CH_2$ 1.20, 1.42; δ $CH_3$ 0.823; γ $CH_3$ 0.891 |
| **Leu** | 8.36 | 4.06 | 1.36, 1.06 | γ $CH_2$ 0.730; δ $CH_3$ 0.258, 0.499 |
| **Gln** | 8.66 | 4.33 | 1.89, 2.05 | γ $CH_2$ 2.27; ε $NH_2$ 7.12, 7.69 |

**Table 5.9.** c[Ac-C-R-W-V-E-V-Δ**Val-G**-O-K-I-L-Q-C-$NH_2$] (**167b**).

| | H | α | β | Others (γ, δ, ε) |
|---|---|---|---|---|
| **Cys** | 8.38 | 5.23 | 3.00, 2.41 | |
| **Arg** | 8.73 | 4.62 | 1.67, 1.81 | γ $CH_2$ 1.51; δ $CH_2$ 3.18; ε NH 7.12 |
| **Trp** | 8.66 | 5.15 | 3.10, 2.96 | H1 10.2; H2 7.25; H4 7.29; H5 7.01; H7 7.50 |
| **Val** | 9.55 | 4.61 | 2.09 | γ $CH_3$ 0.888 |
| **Glu** | 8.54 | 5.16 | 1.99, 1.90 | γ $CH_2$ 2.18, 2.19 |
| **Val** | 9.12 | 4.40 | 1.95 | γ $CH_3$ 0.968 |
| **ΔVal** | 10.3 | | | δ $CH_2$ 0.985, 1.89 |
| **Gly** | 8.66 | 3.72, 4.13 | | |
| **Orn** | 7.98 | 4.70 | 1.86 | γ $CH_2$ 1.72; δ $CH_2$ 3.04; ε $NH_3$ 7.64 |
| **Lys** | 8.53 | 4.99 | 1.75 | γ $CH_2$ 1.38; δ $CH_2$ 1.38; ε $CH_2$ 2.56 |
| **Ile** | 9.40 | 4.71 | 1.86 | γ $CH_2$ 1.17, 1.41; γ $CH_3$ 0.826; δ $CH_3$ 0.888 |
| **Leu** | 8.35 | 3.91 | 0.772, 1.31 | γ $CH_2$ 0.379; δ $CH_3$ -0.338, 0.078 |
| **Gln** | 9.05 | 4.58 | 1.83, 2.08 | γ $CH_2$ 2.24 |
| **Cys** | 8.94 | 5.05 | 2.94, 3.04 | |

**167a**

| Amino Acid | Hα |
|---|---|
| **Cys** | 5.22 |
| **Arg** | 4.62 |
| **Trp** | 5.14 |
| **Val** | 4.59 |
| **Glu** | 5.04 |
| **Val** | 4.25 |
| **Asn** | 4.41 |
| **Gly** | 3.69, 4.14 |
| **Orn** | 4.70 |
| **Lys** | 4.97 |
| **Ile** | 4.72 |
| **Leu** | 3.90 |
| **Gln** | 4.57 |
| **Cys** | 5.05 |

**168a**

| Amino Acid | Hα |
|---|---|
| **Arg** | 4.18 |
| **Trp** | 4.72 |
| **Val** | 4.00 |
| **Glu** | 4.25 |
| **Val** | 4.09 |
| **Asn** | 4.69 |
| **Gly** | 3.91 |

**168b**

| Amino Acid | Hα |
|---|---|
| **Asn** | 4.70 |
| **Gly** | 3.96 |
| **Orn** | 4.36 |
| **Lys** | 4.32 |
| **Ile** | 4.15 |
| **Leu** | 4.40 |
| **Gln** | 4.32 |

**168c**

| Amino Acid | Hα |
|---|---|
| **Arg** | 4.18 |
| **Trp** | 4.73 |
| **Val** | 4.01 |
| **Glu** | 4.27 |
| **Val** | 4.15 |
| **ΔVal** | - |
| **Gly** | 3.94 |

**168d**

| Amino Acid | Hα |
|---|---|
| **ΔVal** | - |
| **Gly** | 3.94 |
| **Orn** | 4.35 |
| **Lys** | 4.30 |
| **Ile** | 4.13 |
| **Leu** | 4.38 |
| **Gln** | 4.31 |

### 5.2.5 Procedures for proteolysis assays

**Proteolysis assays for 153a and its analogues**

Pronase E from *Streptomyces griseus* (EC 3.4.24.31) was purchased from EMD Millipore. This mixture of enzymes was dissolved in 1X PBS buffer (10 mM sodium phosphate, 137 mM NaCl, 2.7 mM KCl buffer, pH 7.4) at a concentration of 0.128 mg/mL. Then, solutions of each peptide (**153a, 152aa, 152ab, 152ba, and 152bb**) in 1X PBS buffer (0.10 mM, 1.5 mL) at 37 °C were treated with an aliquot (5 μL) of the pronase E solution. Aliquots (50 μL) were removed after 0, 30, 60, 90, 150, 210, 270, 360 180, 300, and 360 min. The aliquots were quenched with 25% v/v glacial acetic acid (10 μL), diluted to 75 μL with 1X PBS buffer, and analyzed by HPLC (Phenomenex Jupiter C18, 5 μm particle size, 300 Å pore size, 4.6 × 250 mm, 40 μL injection volume, 10%–60% $CH_3CN$ in $H_2O$ gradient over 50 min, then 95% $CH_3CN$ in $H_2O$ for 10 min, flow rate: 1 mL/min).

**Proteolysis assays for 153b and its analogues**

Pronase E from *Streptomyces griseus* (EC 3.4.24.31) was purchased from EMD Millipore. This mixture of enzymes was dissolved in 1X PBS buffer (10 mM sodium phosphate, 137 mM NaCl, 2.7 mM KCl buffer, pH 7.4) at a concentration of 0.462 mg/mL. Then, solutions of each peptide (**153b, 152ca, and 152cb**) in 1X PBS buffer (0.40 mM, 1.5 mL) at 37 °C were treated with an aliquot (10 μL) of the pronase E solution. Aliquots (50 μL) were removed after 0, 30, 60, 90, 150, 210, 270, 360 180, 300, and 360 min. The aliquots were quenched with glacial acetic acid (10 μL), diluted to 75 μL with 1X PBS buffer, and analyzed by HPLC (Phenomenex Jupiter C18, 5 μm particle size, 300 Å pore size, 4.6 × 250 mm, 40 μL injection volume, 10%–60% $CH_3CN$ in $H_2O$ gradient over 50 min, then 95% $CH_3CN$ in $H_2O$ for 10 min, flow rate: 1 mL/min).

### 5.2.6 Procedure for circular dichroism (CD) experiments

Peptide solutions were prepared in 20 mM sodium phosphate buffer (pH 7.4), and concentrations were determined spectroscopically based on tryptophan absorbance at 280 nm in 6 M guanidine hydrochloride (Trp $\varepsilon_{280}$ = 5690 $M^{-1}cm^{-1}$). 0.10 mM solutions of **153a** and **152aaa** in 10 mM sodium phosphate buffer (pH 7.4) and 6 M guanidine hydrochloride were used to perform wavelength scans in duplicate at 25 °C. 0.10 mM solutions of **153b** and **152ca** in 10 mM sodium phosphate buffer (pH 7.4) and 2.5 M urea were used to run wavelength scans in duplicate at 25 °C.

## 5.3 Procedure for the synthesis of NTA (172)

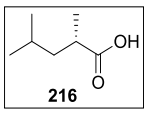

216

**(*S*)-2,4-Dimethylpentanoic acid (216)**. A solution of amide **215**[5] (4.24 g, 15.3 mmol) in 9N $H_2SO_4$–dioxane (1:1, 100 mL) was stirred at 105 °C for 12 h. The resulting mixture was cooled to 0 °C, stirred for 15 min, and then quenched by addition of 50% w/w aq NaOH until pH ≥10. The mixture was extracted with $CH_2Cl_2$ (3 × 75 mL) to remove the pseudoephedrine auxiliary. The aqueous layer was then acidified with 6N $H_2SO_4$ to pH ≤2 and extracted with $CH_2Cl_2$ (3 × 100 mL). The combined organic layers were washed with 1N HCl (2 × 25 mL), dried ($Na_2SO_4$), and concentrated in vacuo to afford **216** (1.558 g, 12.0 mmol, 78%) as a yellow oil: $[\alpha]^{25}_D$ +19 (*c* 5.2, $Et_2O$), lit.[6] $[\alpha]^{25}_D$ +18.8 (*c* 5.2, $Et_2O$), $^1H$ NMR ($CDCl_3$, 500 MHz) δ COOH (1H), 2.58–2.52 (m, 1H), 1.67–1.60 (m, 1H), 1.28–1.23 (m, 2H), 1.18 (d, J = 7.0 Hz, 3H), 0.93 (d, J = 6.0 Hz, 3H), 0.90 (d, J = 6.0 Hz, 3H); $^{13}C$ NMR ($CDCl_3$, 125 MHz) δ 182.8, 42.7, 37.3, 25.8, 22.5, 22.4, 17.3; IR

[5] J. A. Turk, G. S. Visbal, M. A. Lipton, *J. Org. Chem.* **2003**, *68*, 7841.
[6] Levene P. A.; Bass, L. W. *J. Biol. Chem.* **1926**, *70*, 211.

(film) $\nu_{max}$ 2959, 1709, 1469 $cm^{-1}$ HRMS (ESI) m/z 131.1076 (MH+, $C_7H_{14}O_2H$+ requires 131.1072).

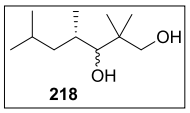

218

**(4*S*)-2,2,4,6-tetramethylheptane-1,3-diol (218).** A solution of acid **216** (1.51 g, 11.6 mmol) in anhydrous $CH_2Cl_2$ (50 mL) at rt under Ar was treated with $InBr_3$ (411.3 mg, 1.16 mmol, 0.1 equiv) and $(MeO)_3SiH$ (1.63 mL, 1.56 g, 12.8 mmol, 1.1 equiv), then stirred for 5 min. Evolution of $H_2$ was observed. Silyl ketene acetal **217** (5.00 mL, 4.29 g, 24.6 mmol, 2.1 equiv) was added to the resulting suspension, which turned light yellow. The mixture was stirred at 50 °C under Ar for 3.5 h, then at 0 °C for 30 min. It was then diluted with anhydrous THF (10 mL) and treated slowly with $LiAlH_4$ (1.53 g, 40.3 mmol, 3.5 equiv), at which point the yellow suspension turned bright orange. The resulting mixture was stirred at rt under Ar for 12 h, then cooled to 0 °C and quenched by the slow addition of $H_2O$ (2.0 mL), 10% aq NaOH (2.5 mL), and $H_2O$ (6.0 mL). The resulting mixture was stirred at rt for 30 min, then filtered through a sintered glass filter. The precipitate was washed with $CH_2Cl_2$ (5 × 50 mL). The combined organic layers were washed with sat aq $NH_4Cl$ (25 mL), dried ($Na_2SO_4$), and concentrated in vacuo. Flash chromatography (65 mL of $SiO_2$, 5–35% EtOAc in hexanes gradient elution), afforded **218** (1.40 g, 7.43 mmol, 64%) as a light yellow oil that was a mixture of diastereomers. $^1H$ NMR ($CDCl_3$, 500 MHz) δ; $^{13}C$ NMR ($CDCl_3$, 125 MHz) δ; IR (film) $\nu_{max}$ $cm^{-1}$; HRMS (ESI) *m/z* 189.1827 ($MH^+$, $C_{11}H_{24}O_2H^+$ requires 189.1810).

## 5.4 Spectra and chromatograms

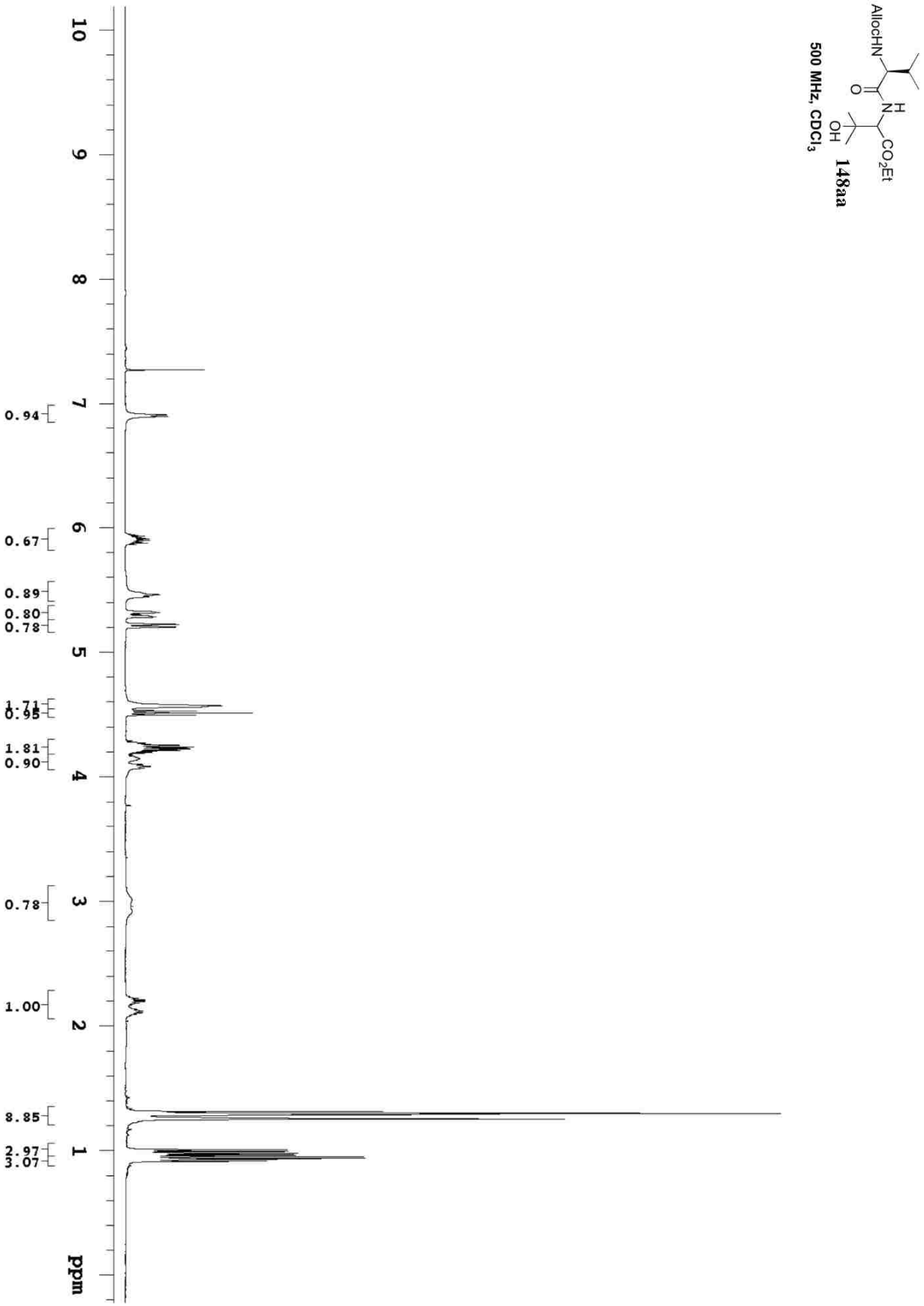
AllocHN
O
H
N
OH
CO2Et
148aa
500 MHz, CDCl3
10
9
8
7
6
5
4
3
2
1
ppm
0.94
0.67
0.89
0.80
0.78
1.71
0.95
1.81
0.90
0.78
1.00
8.85
2.97
3.07

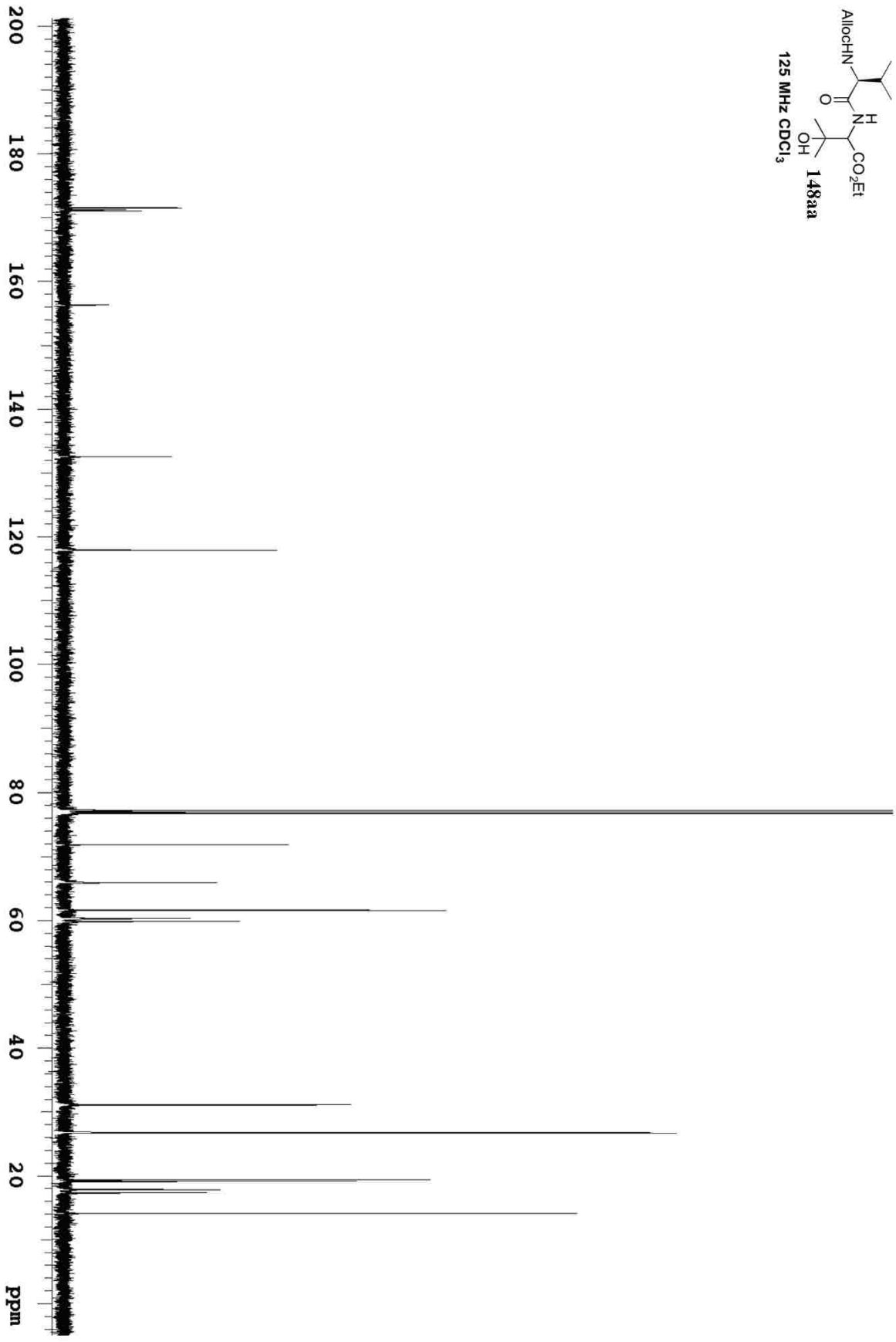
AllocHN
O
H
N
OH
CO2Et
148aa
125 MHz CDCl3
200
180
160
140
120
100
80
60
40
20
ppm

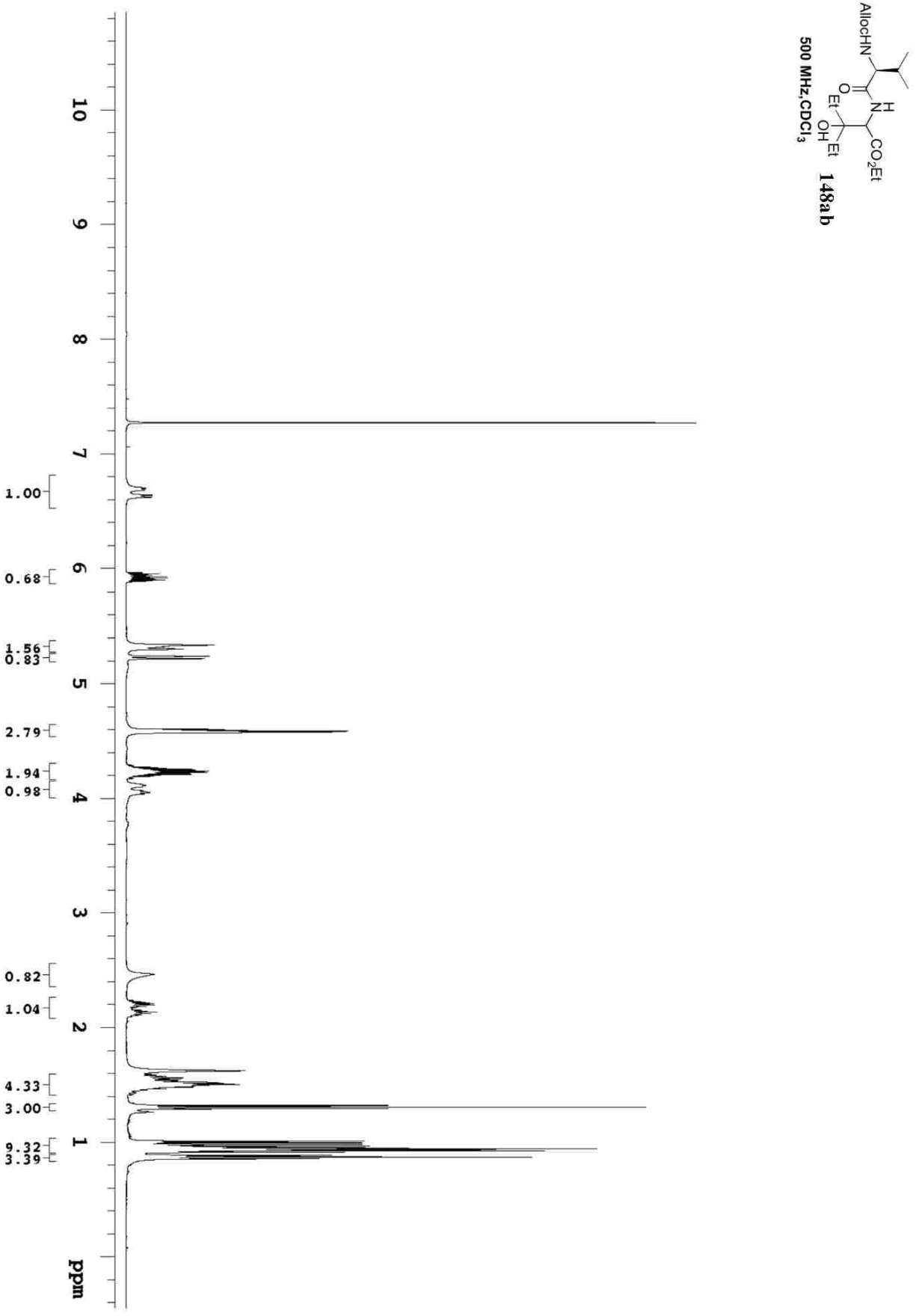
AllocHN
O
H
N
Et
OH
Et
CO2Et
148a b
500 MHz,CDCl3
10
9
8
7
6
5
4
3
2
1
ppm
1.00
0.68
1.56
0.83
2.79
1.94
0.98
0.82
1.04
4.33
3.00
9.32
3.39

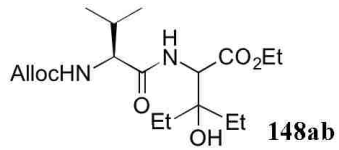


**148ab**

**125 MHz,$CDCl_3$**

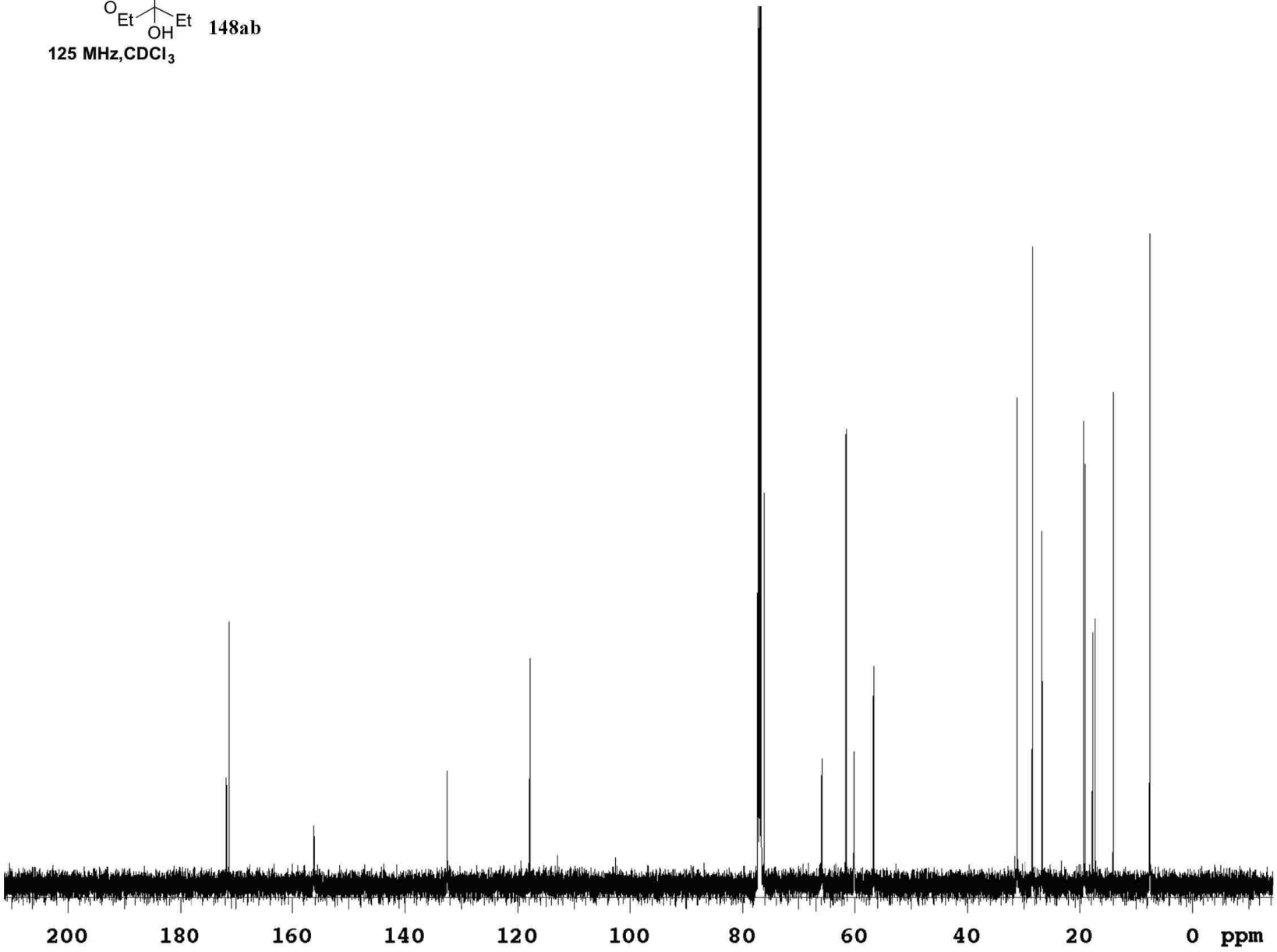

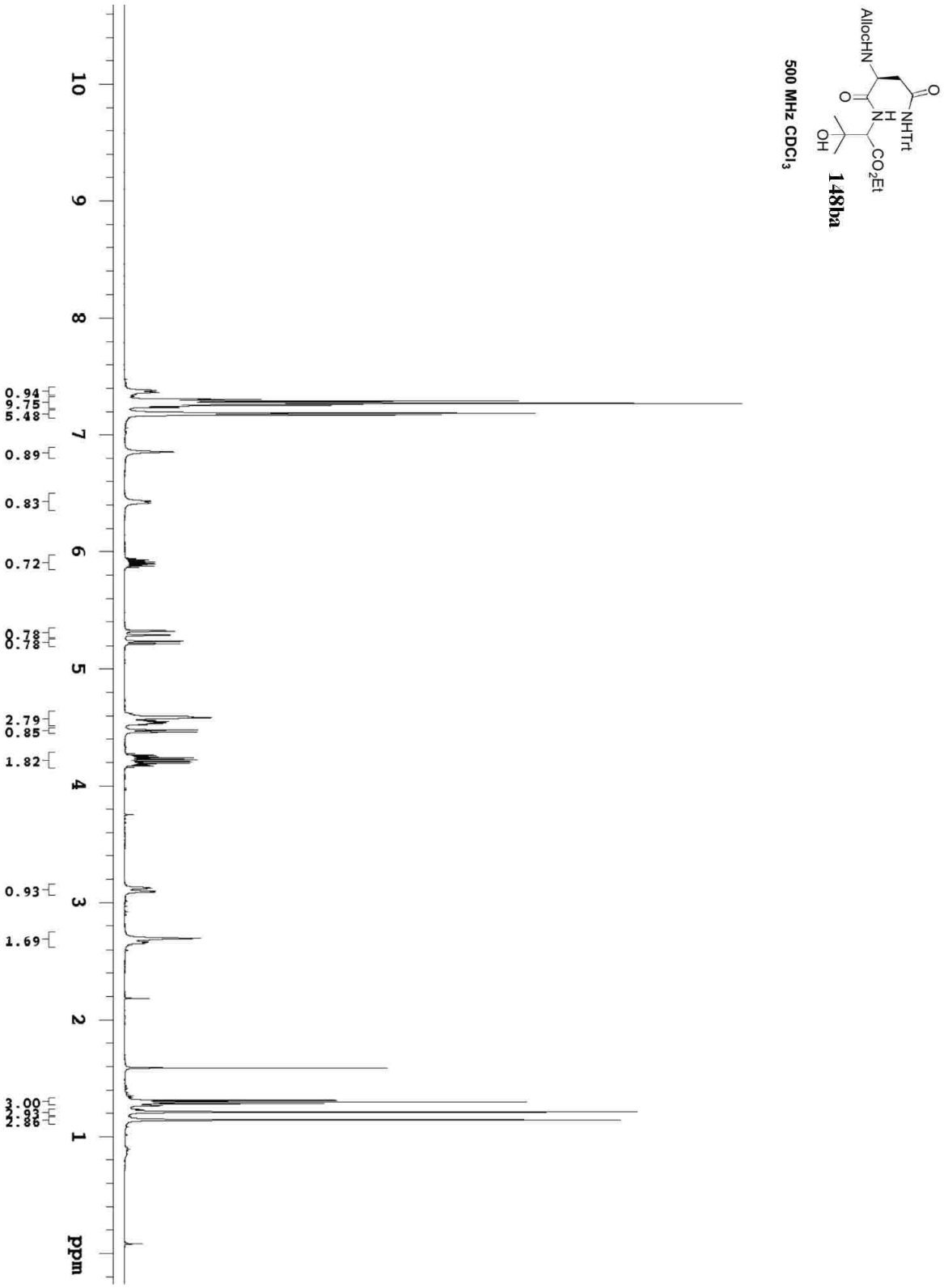
AllocHN
O
NHTrt
O
H
N
OH
CO2Et
148ba
500 MHz CDCl3
0.94
9.75
5.48
0.89
0.83
0.72
0.78
0.78
2.79
0.85
1.82
0.93
1.69
3.00
2.93
2.86
ppm

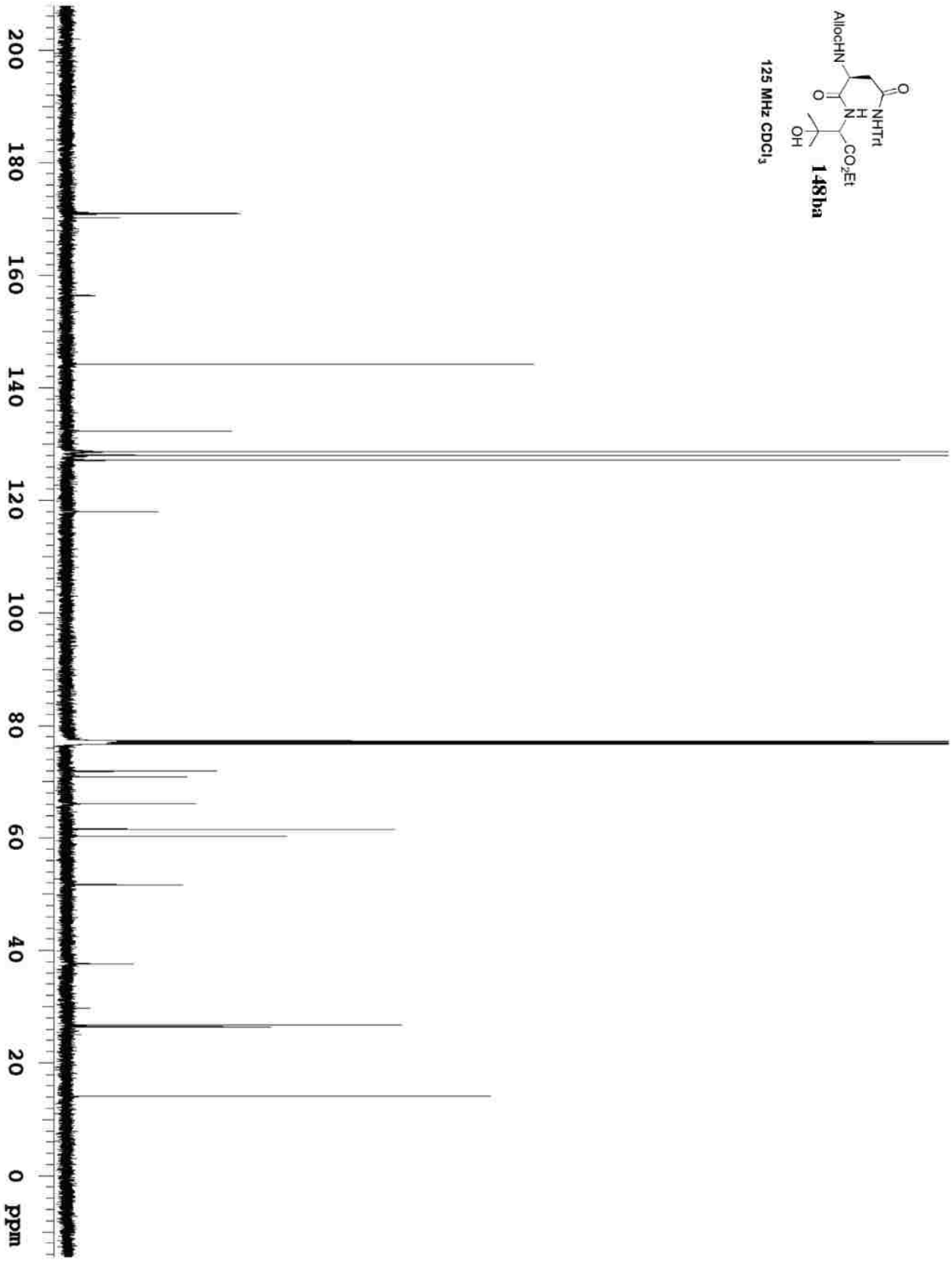
AllocHN
NHTrt
CO2Et
OH
148ba
125 MHz CDCl3
200
180
160
140
120
100
80
60
40
20
0
ppm

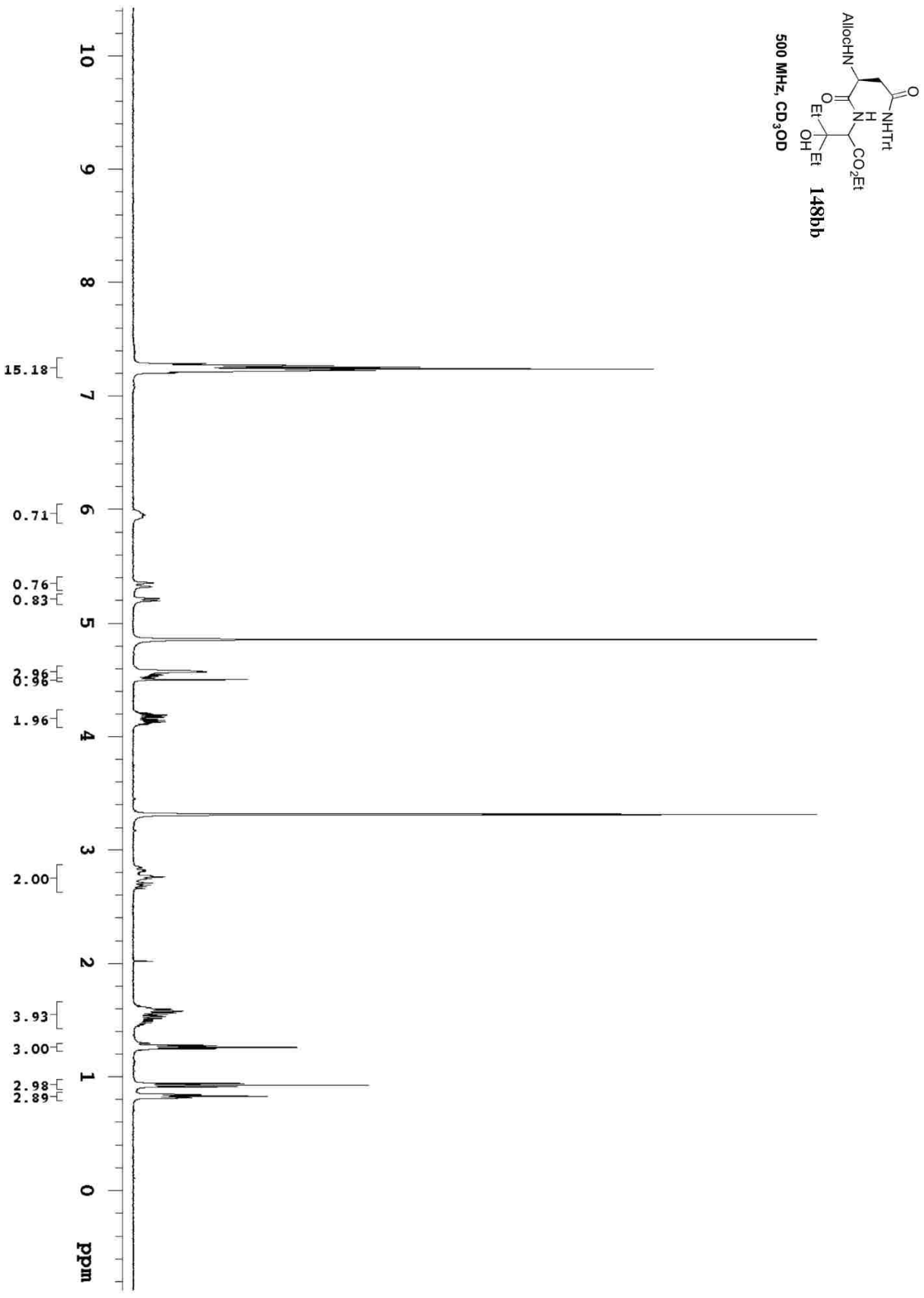
AllocHN
NHTrt
O
O
N
H
Et
OH
Et
CO2Et
148bb
500 MHz, CD3OD
15.18
0.71
0.76
0.83
2.86
0.98
1.96
2.00
3.93
3.00
2.98
2.89
10
9
8
7
6
5
4
3
2
1
0
ppm

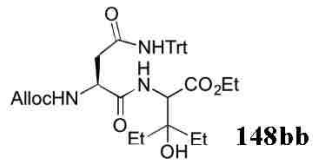


**148bb**

**125 MHz, $CD_3OD$**

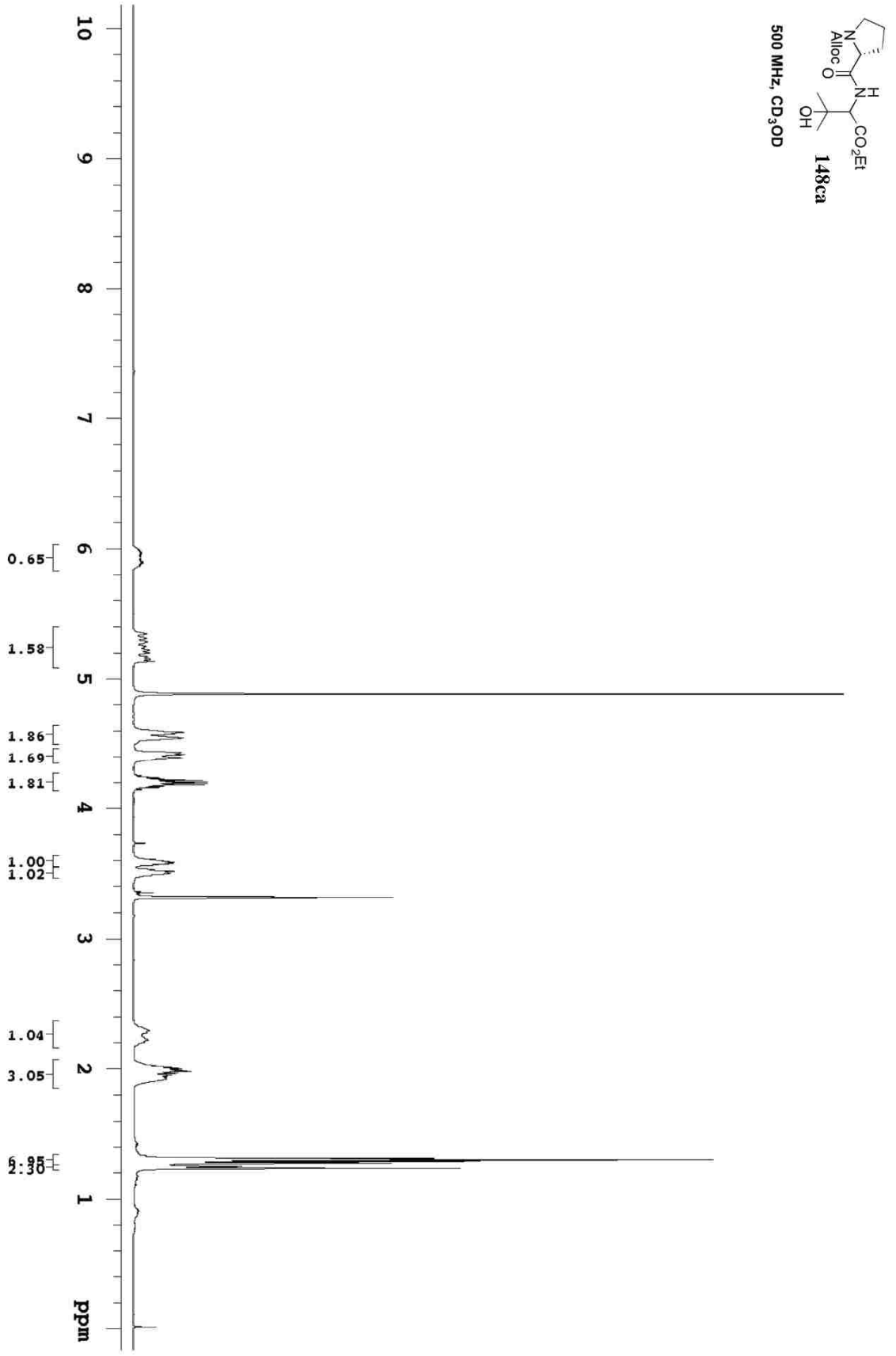
500 MHz, CD3OD
148ca
Alloc
N
H
N
CO2Et
OH
0.65
1.58
1.86
1.69
1.81
1.00
1.02
1.04
3.05
6.95
2.30
10
9
8
7
6
5
4
3
2
1
ppm

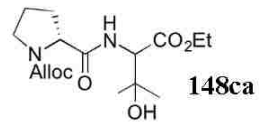


**148ca**

**125 MHz, $CD_3OD$**

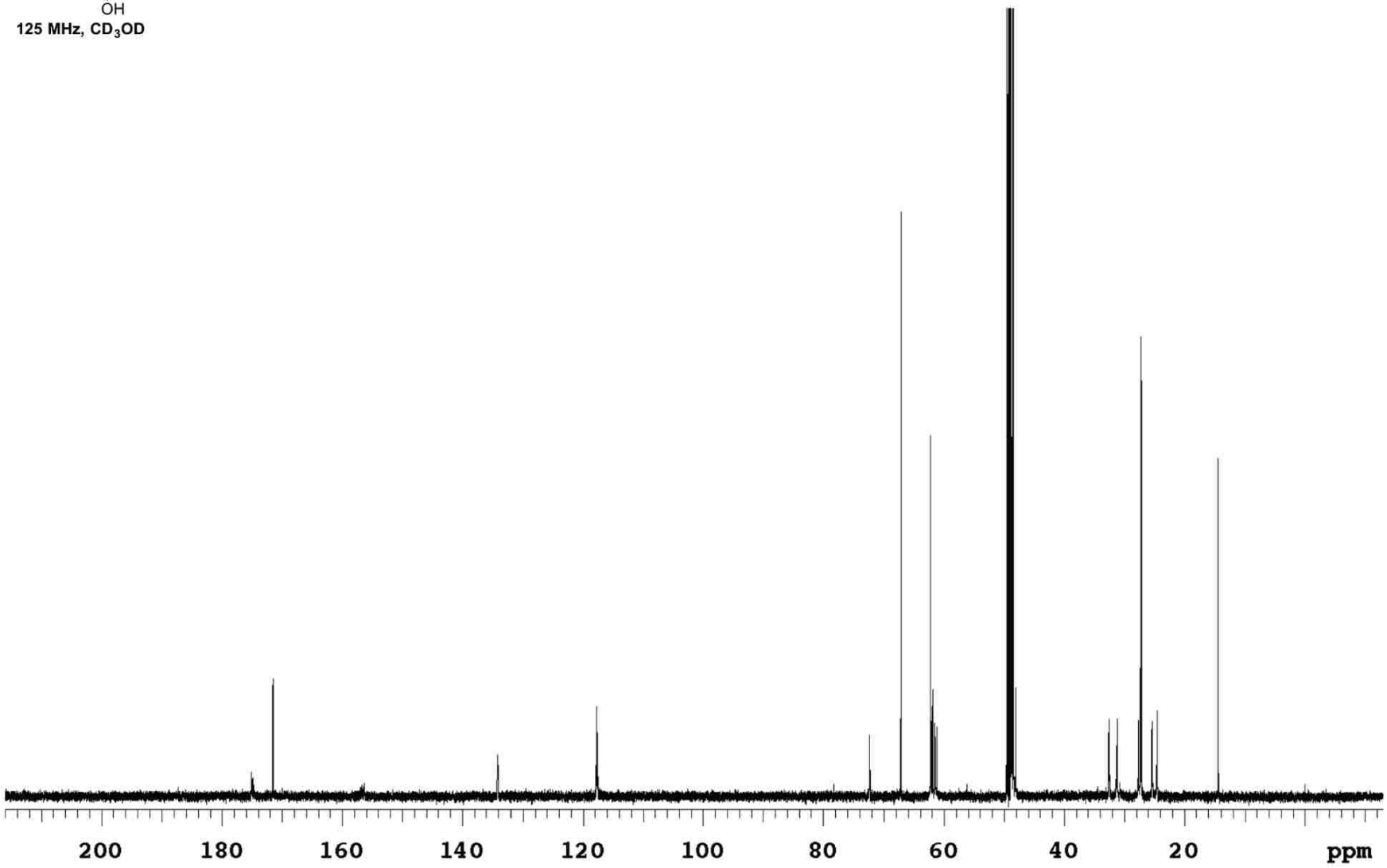

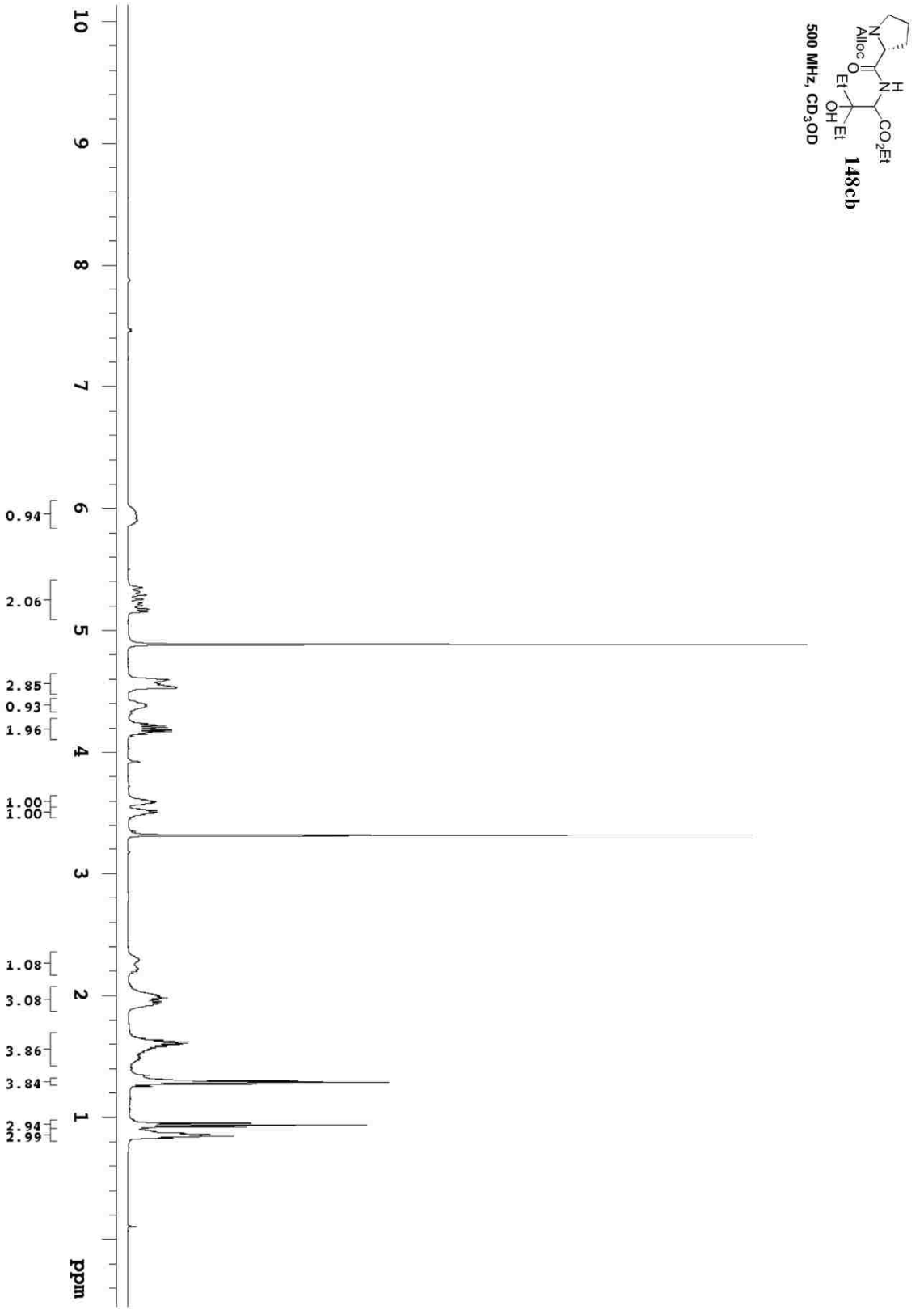
500 MHz, CD3OD
148cb
0.94
2.06
2.85
0.93
1.96
1.00
1.00
1.08
3.08
3.86
3.84
2.94
2.99
ppm

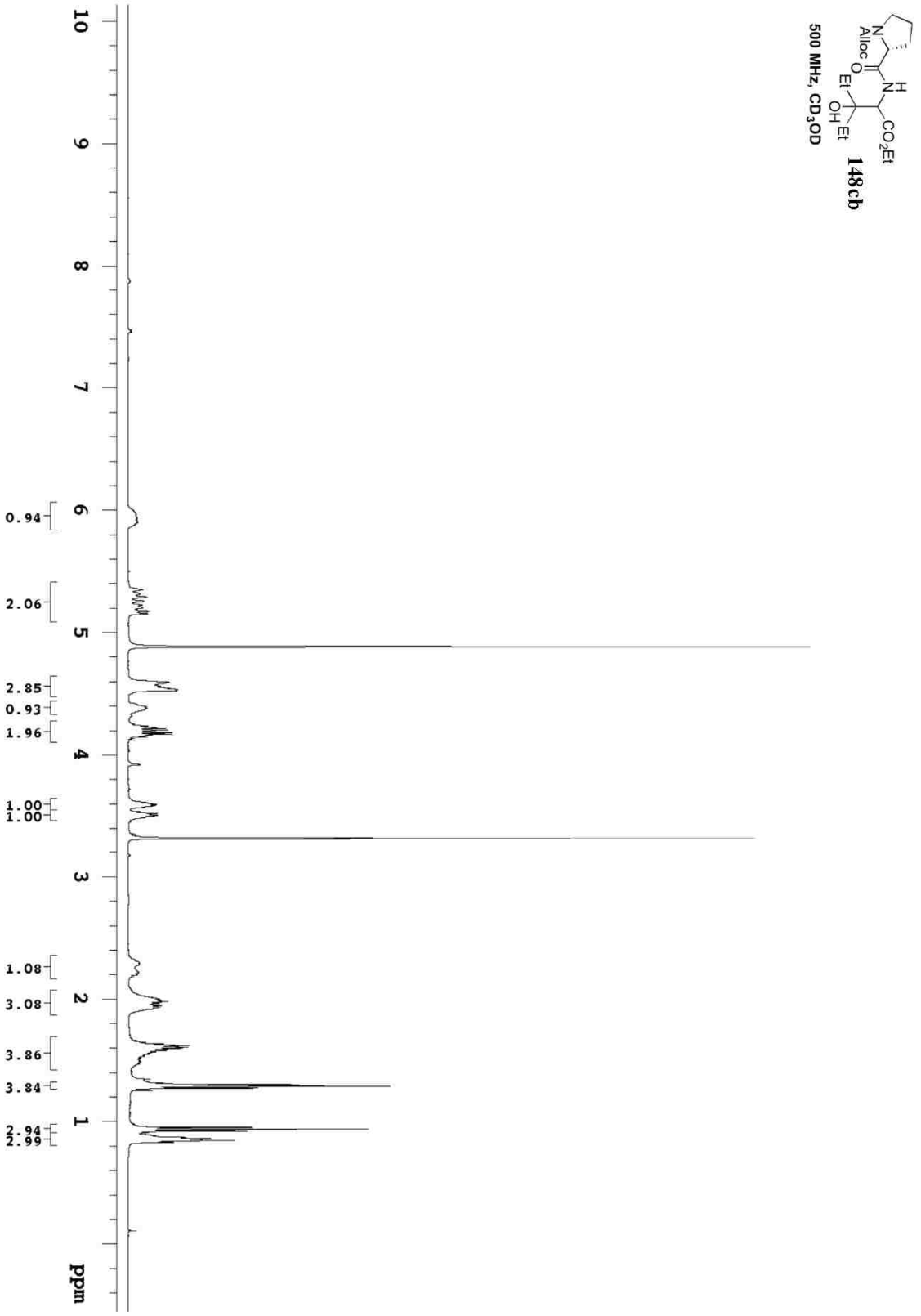
148cb
500 MHz, CD3OD
ppm
0.94
2.06
2.85
0.93
1.96
1.00
1.00
1.08
3.08
3.86
3.84
2.94
2.99

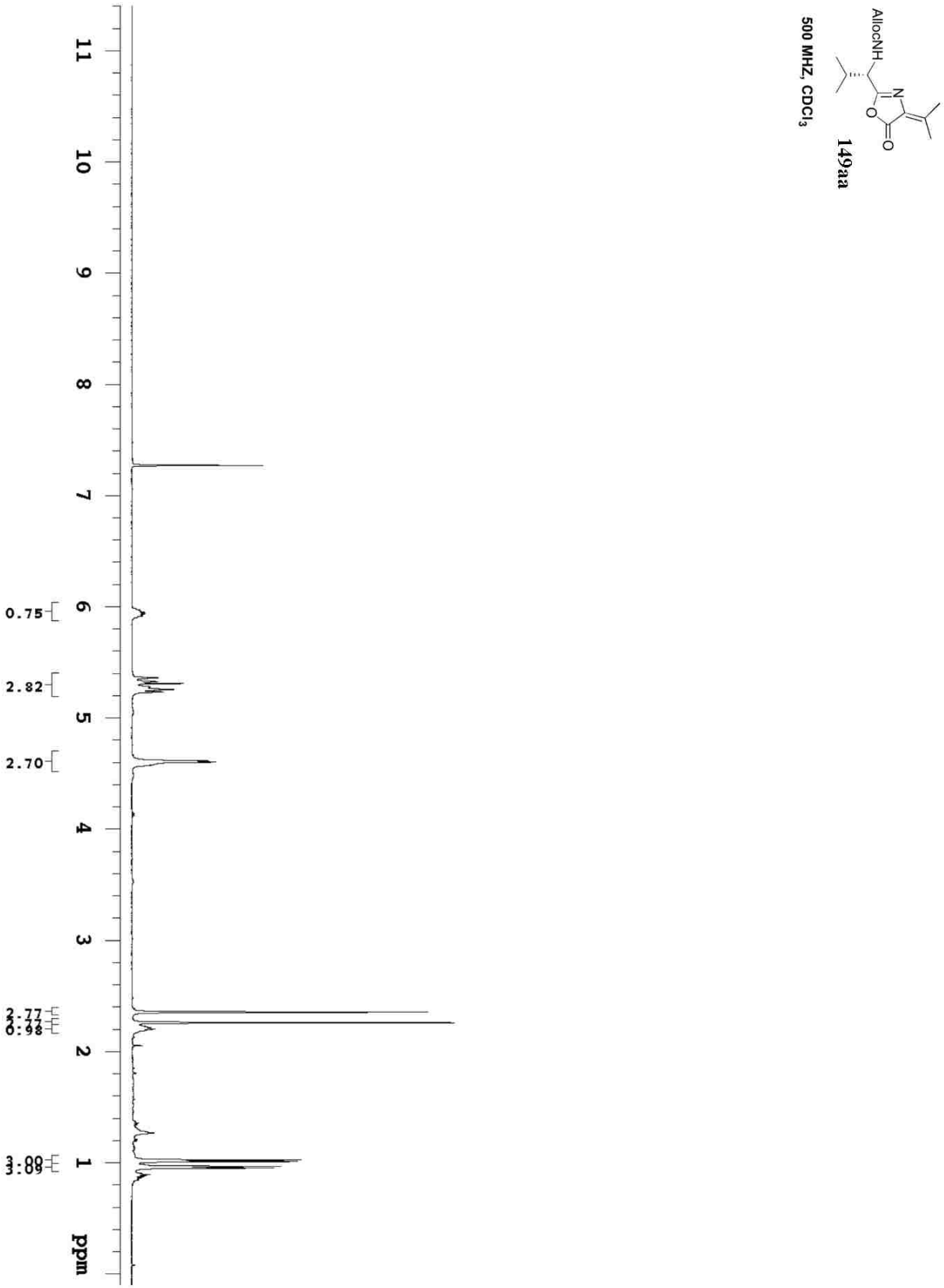
AllocNH
N
O
O
149aa
500 MHZ, CDCl3
11
10
9
8
7
6
5
4
3
2
1
ppm
0.75
2.82
2.70
2.77
0.98
3.00
3.09

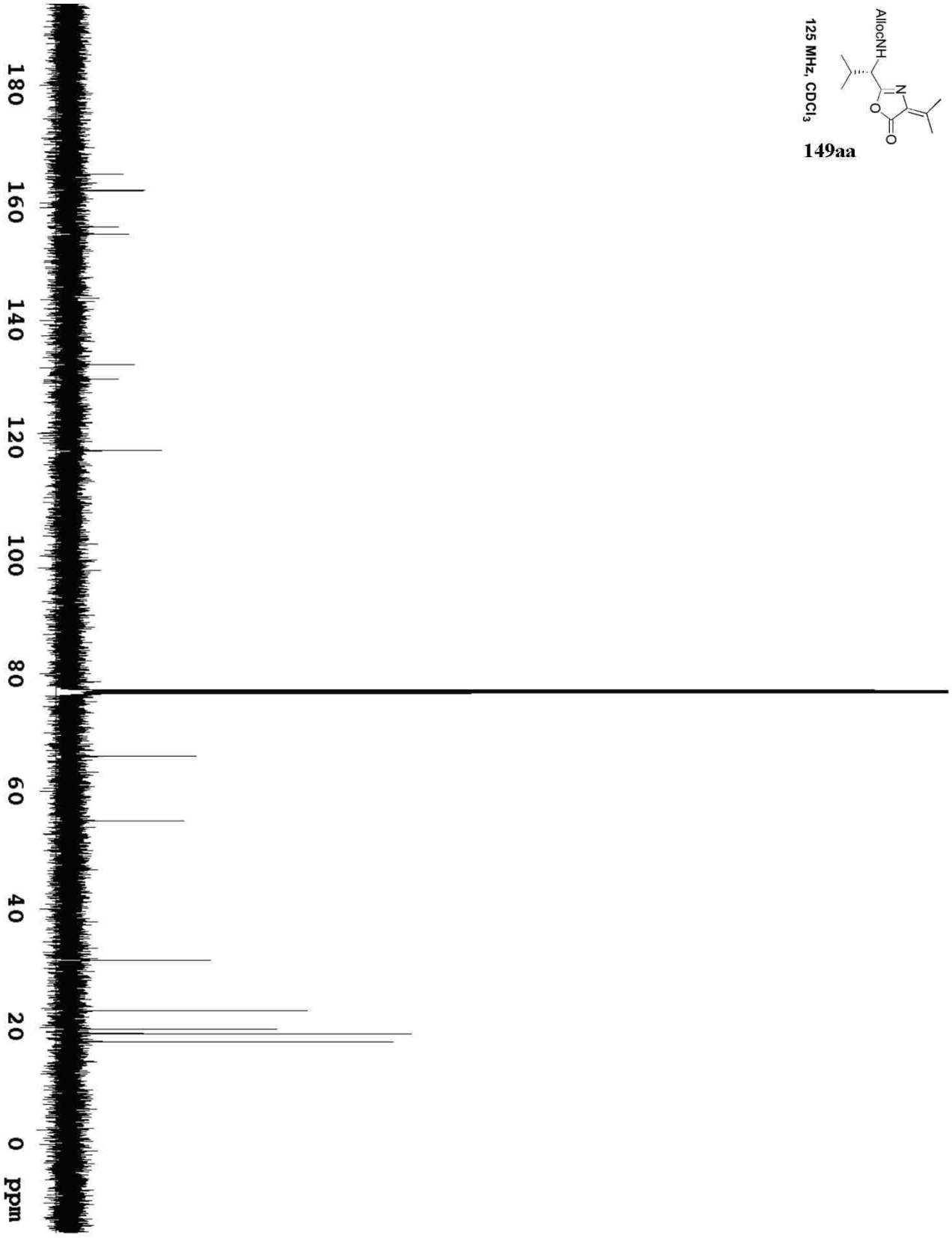
AllocNH
N
O
O
125 MHz, CDCl3
149aa
180
160
140
120
100
80
60
40
20
0
ppm

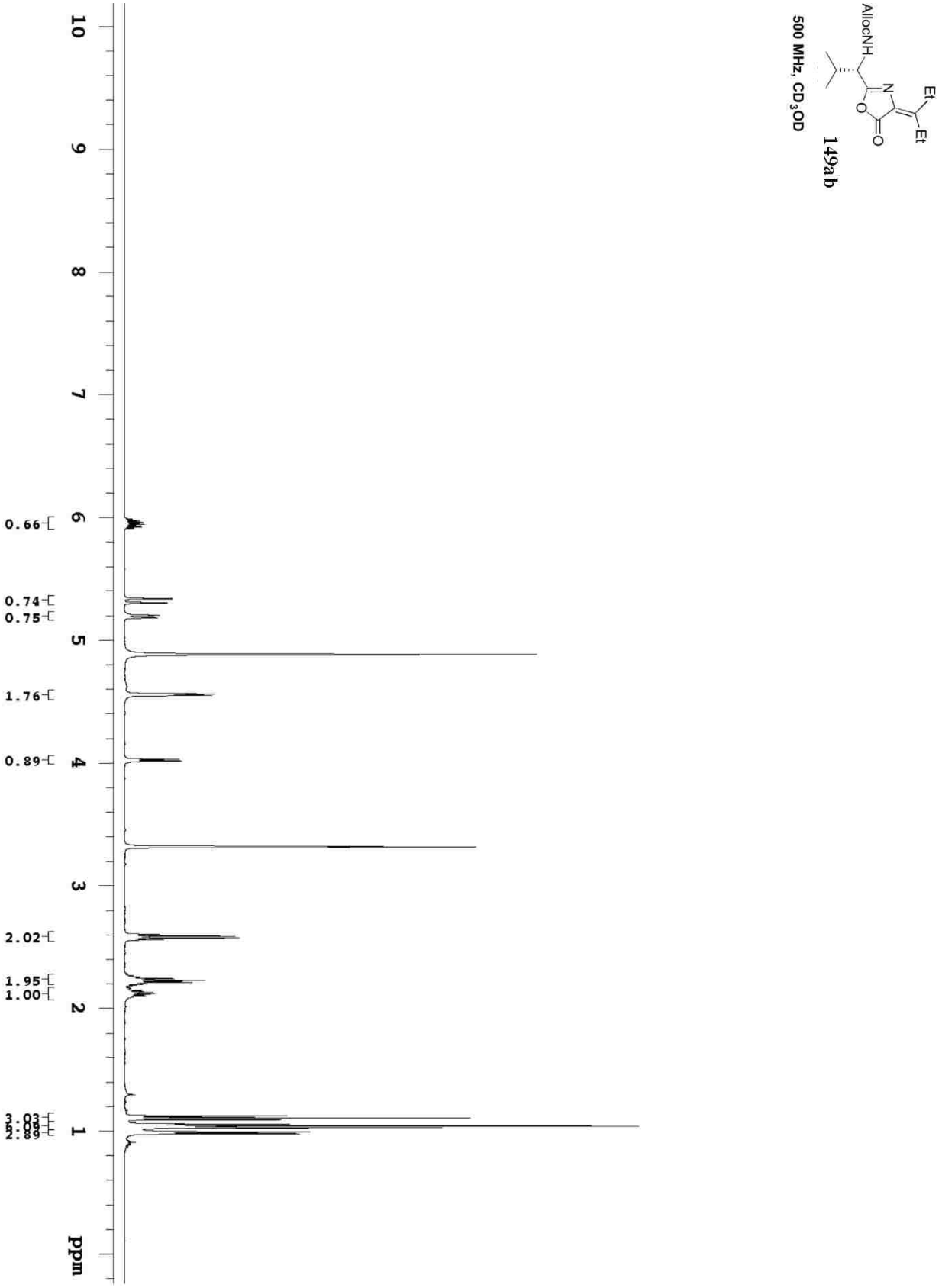
AllocNH
N
O
O
Et
Et
149a b
500 MHz, CD3OD
10
9
8
7
6
5
4
3
2
1
ppm
0.66
0.74
0.75
1.76
0.89
2.02
1.95
1.00
3.03
5.09
2.89

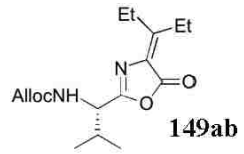


**149ab**

**125 MHz, $CD_3OD$**

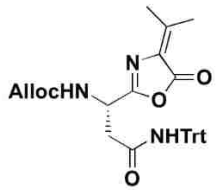


**149ba**

**500 MHz, $CDCl_3$**

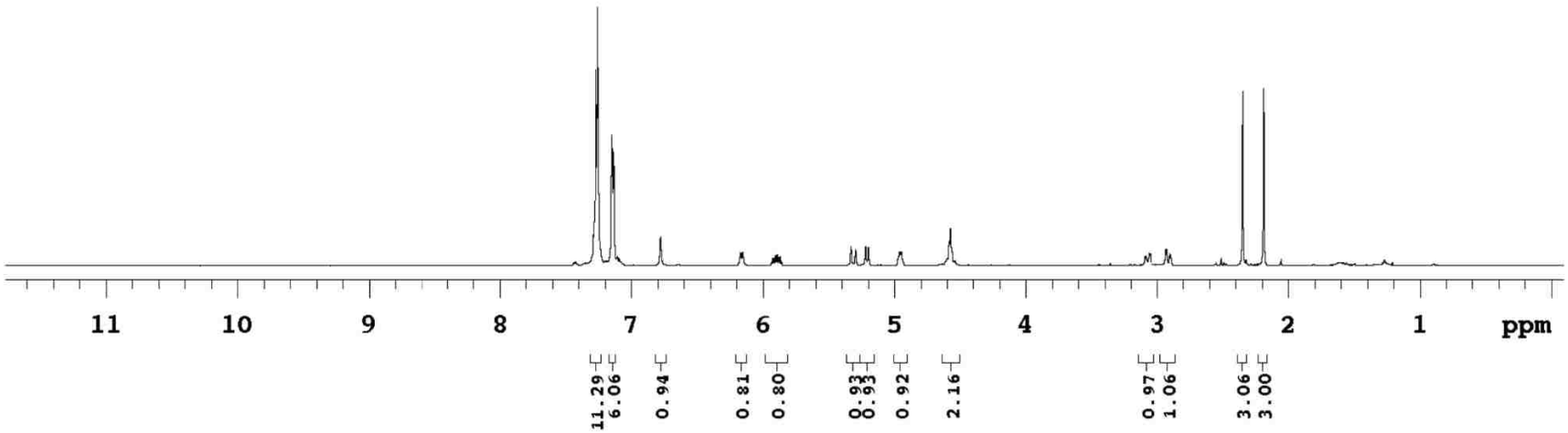

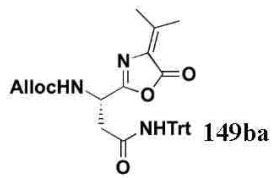


149ba

125 MHz, $CDCl_3$

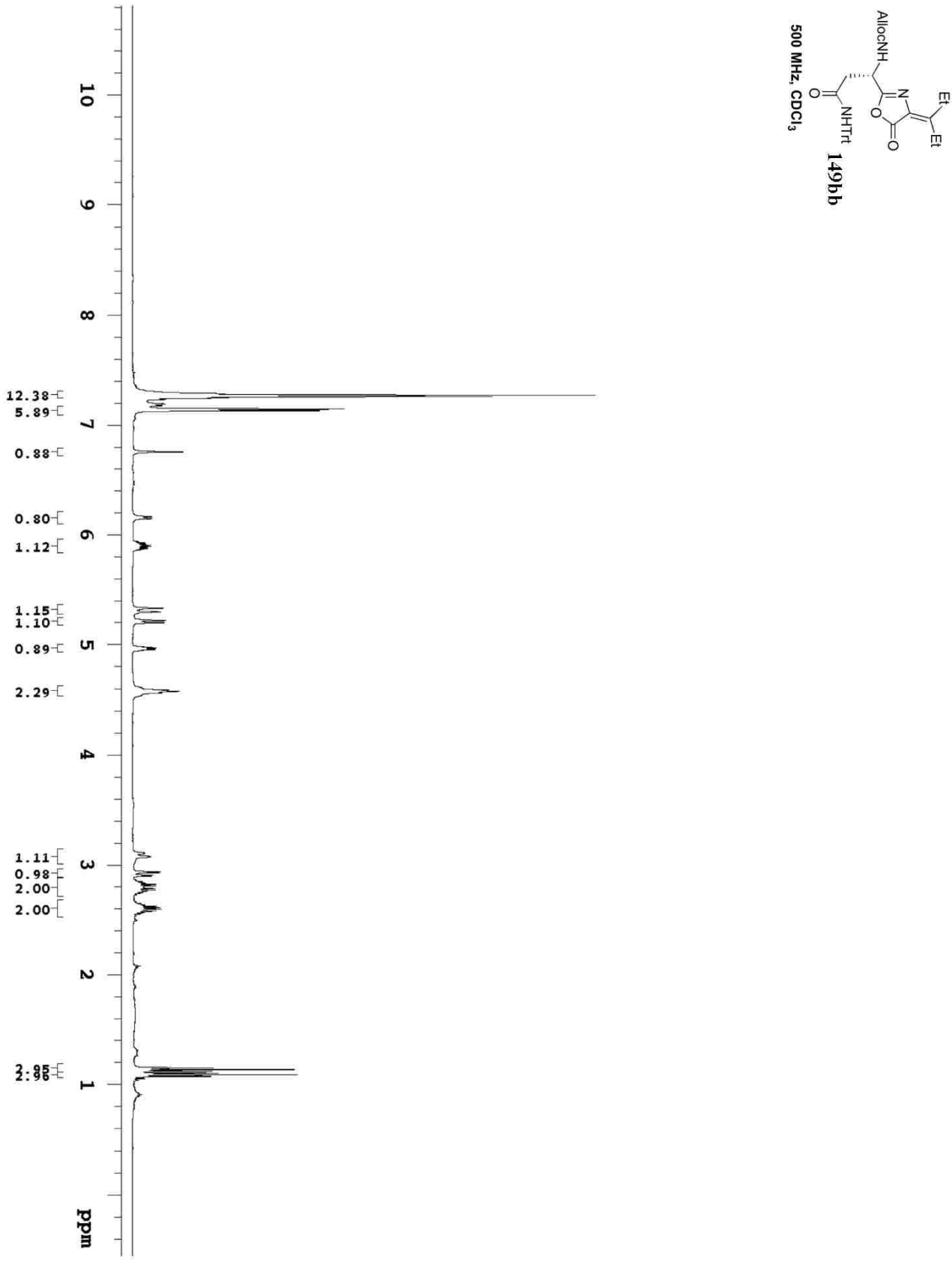
AllocNH
Et
Et
NHTrt
149bb
500 MHz, CDCl3
12.38
5.89
0.88
0.80
1.12
1.15
1.10
0.89
2.29
1.11
0.98
2.00
2.00
2.95
2.96
ppm

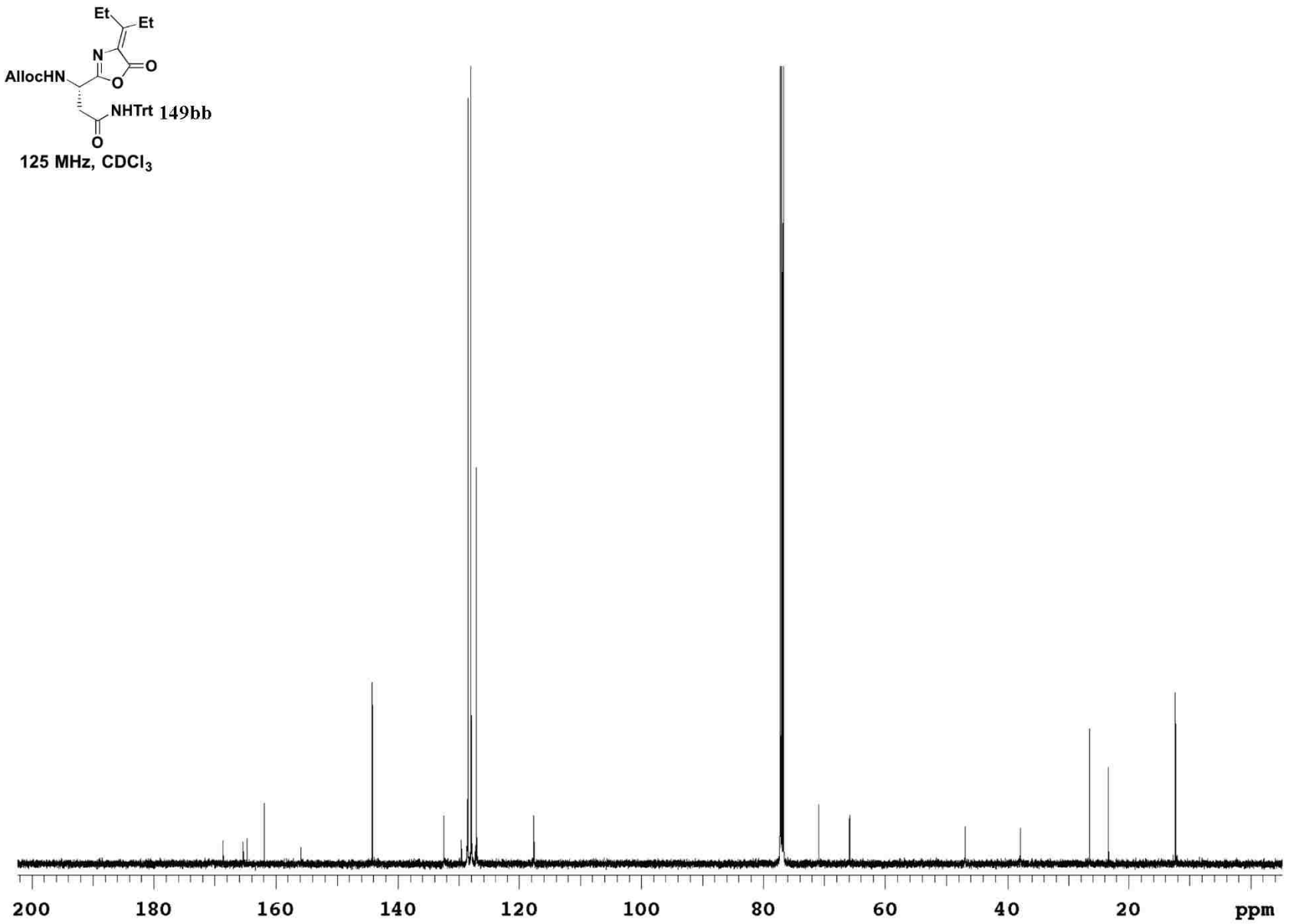
Et
Et
N
O
AllocHN
O
NHTrt
O
149bb
125 MHz, CDCl3
200
180
160
140
120
100
80
60
40
20
ppm

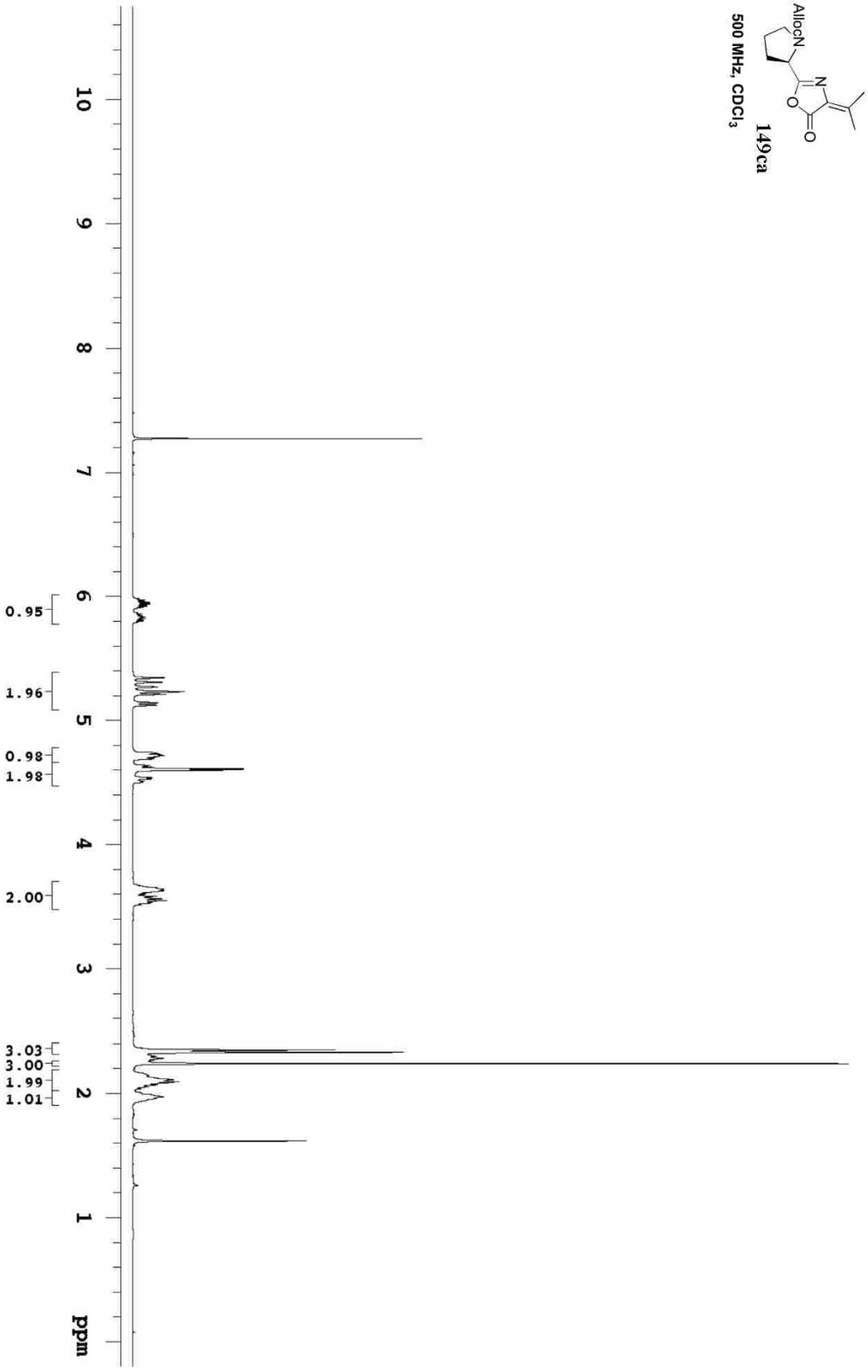
AllocN
N
O
O
149ca
500 MHz, CDCl3
10
9
8
7
6
5
4
3
2
1
ppm
0.95
1.96
0.98
1.98
2.00
3.03
3.00
1.99
1.01

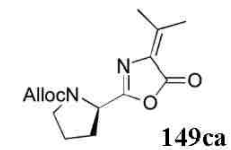


**149ca**

**125 MHz, $CDCl_3$**

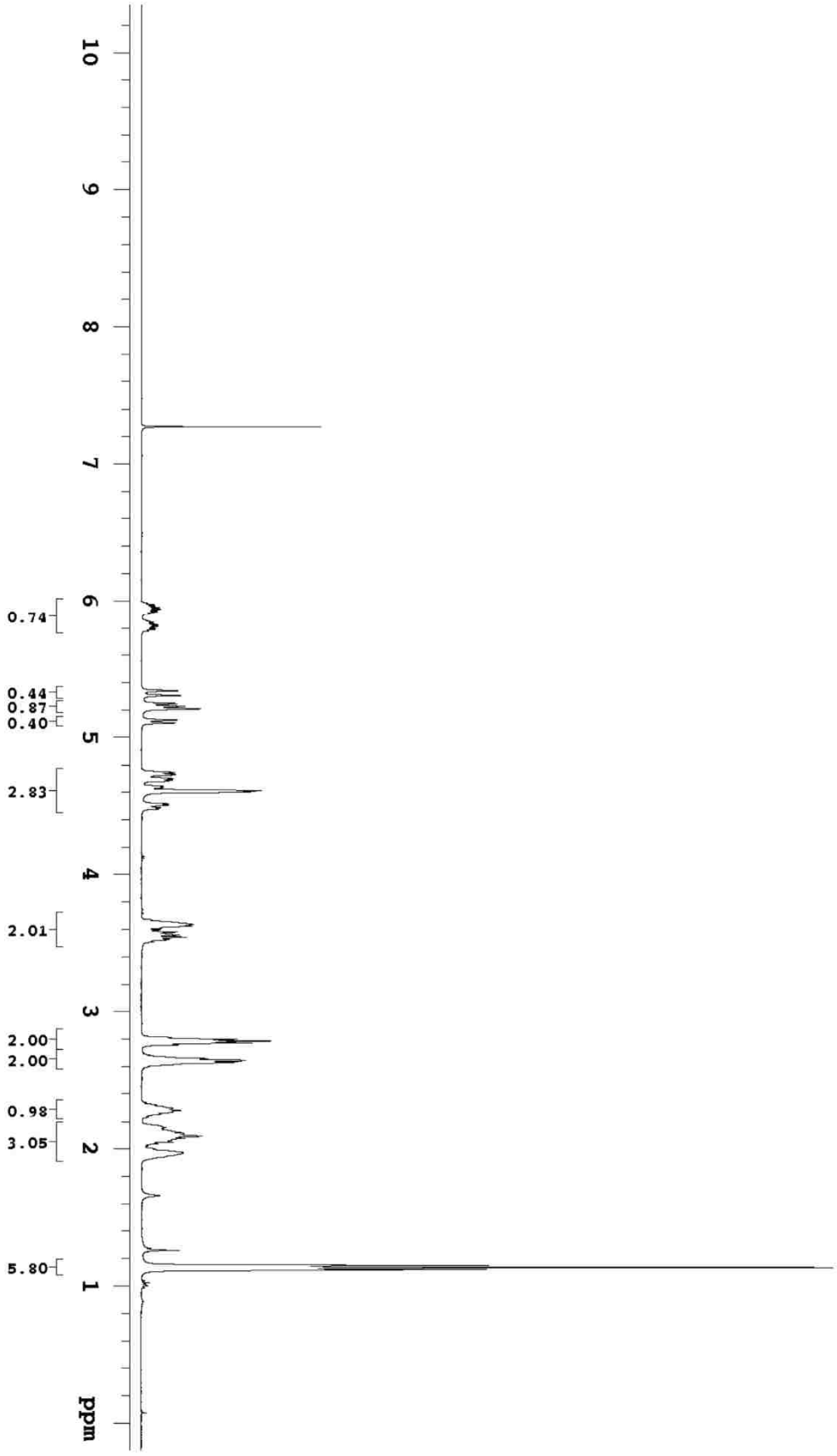
AllocN
N
O
O
Et
Et
149cb
500 MHz, CDCl3
10
9
8
7
6
5
4
3
2
1
ppm
0.74
0.44
0.87
0.40
2.83
2.01
2.00
2.00
0.98
3.05
5.80

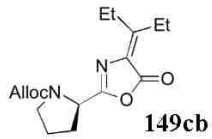


**149cb**

**125 MHz, $CDCl_3$**

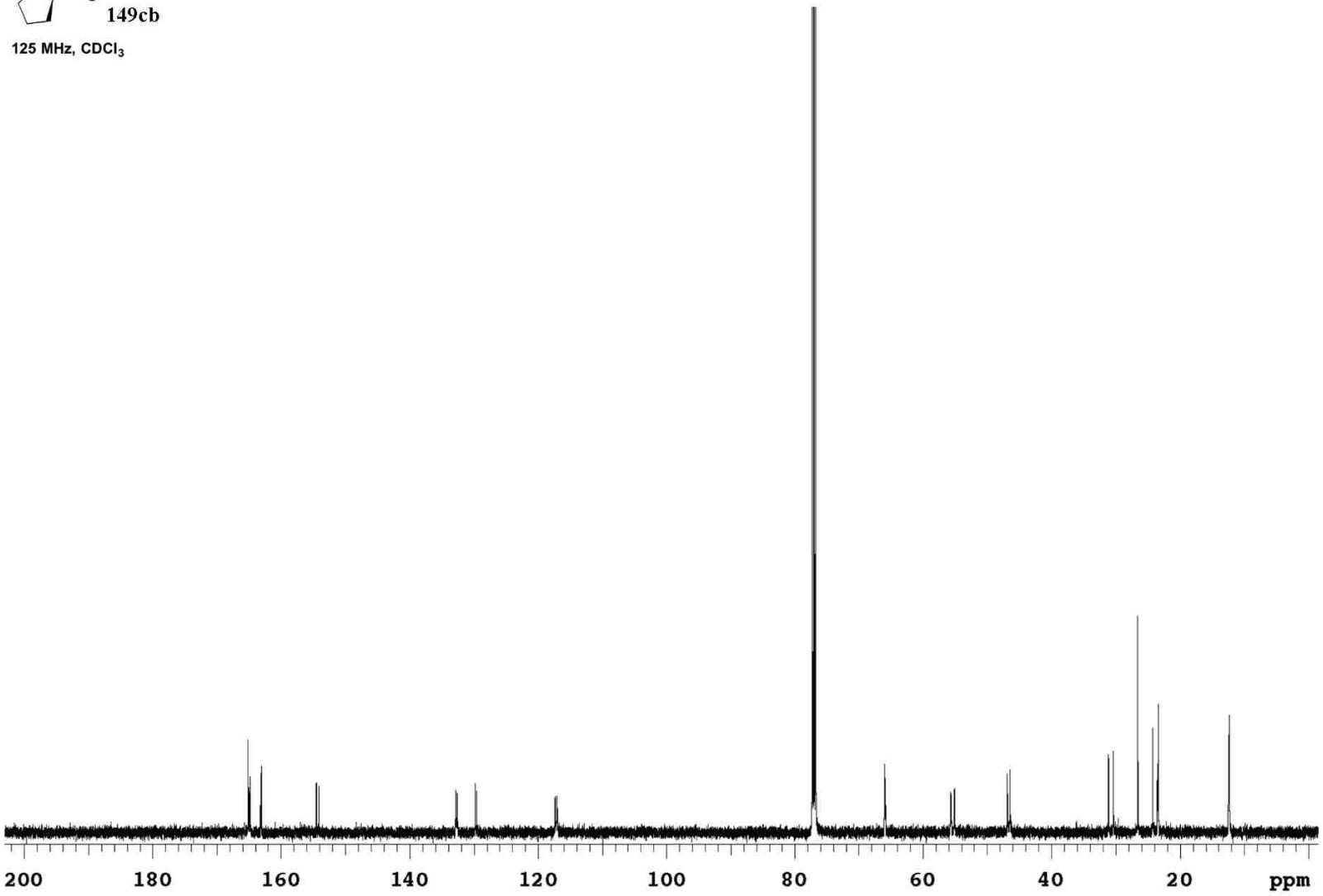

**153a**

500 MHz
10% $D_2O$ in $H_2O$

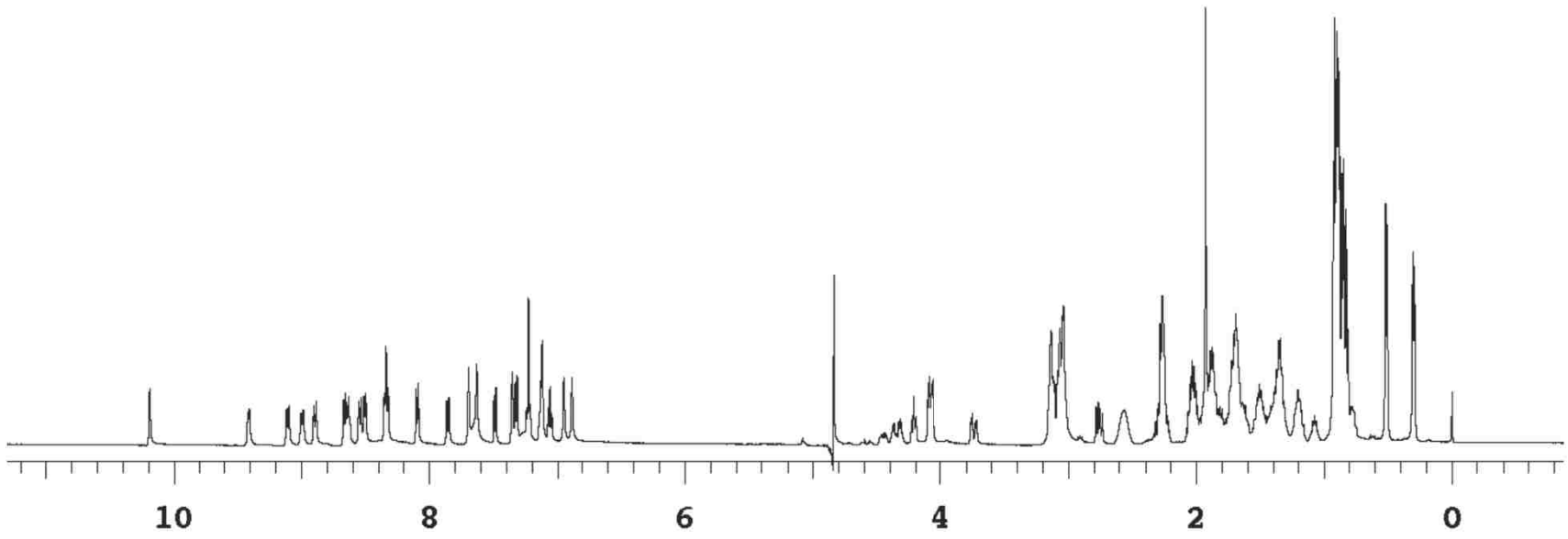

**153b**

500 MHz
10% $D_2O$ in $H_2O$

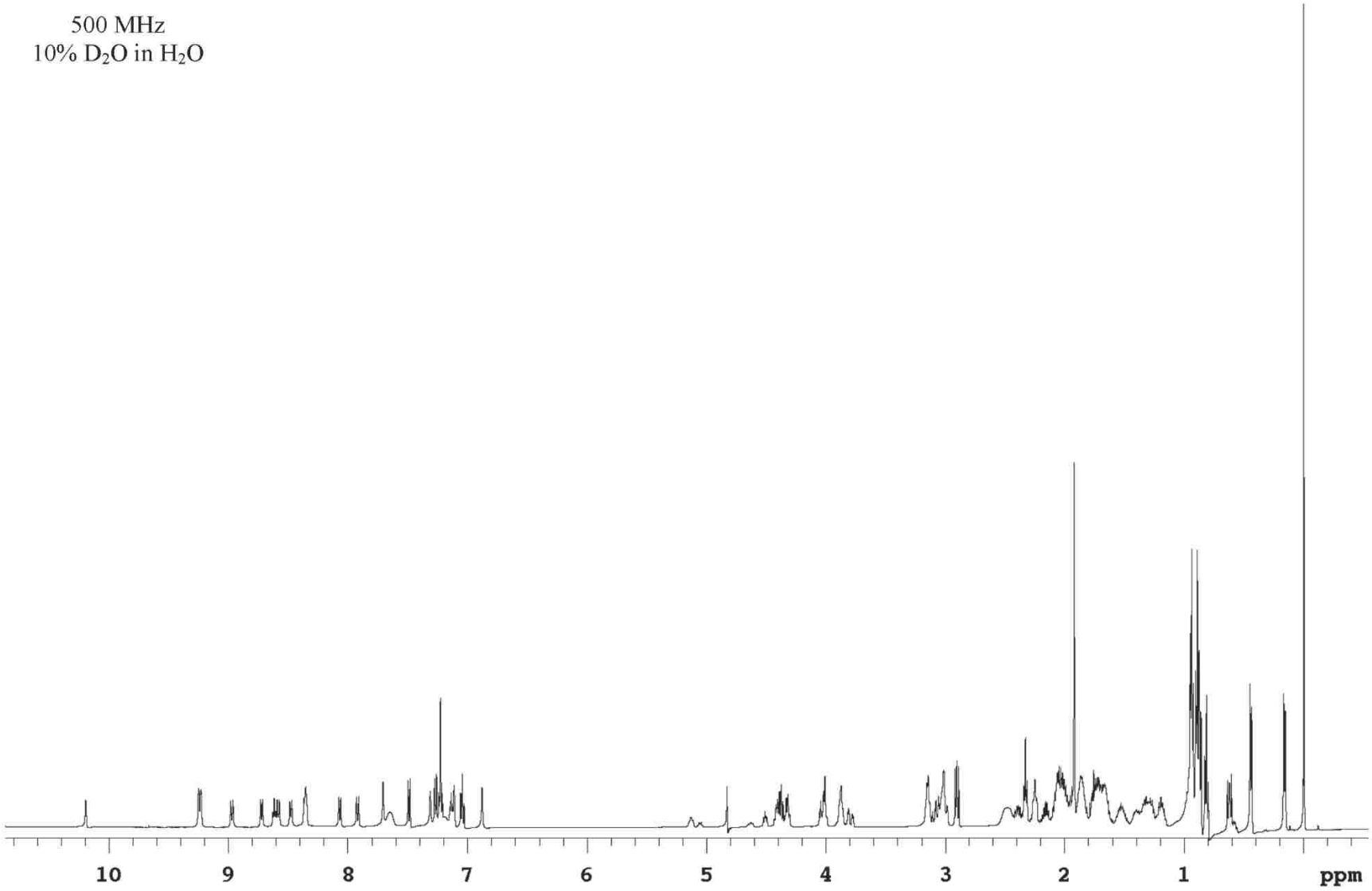

**152aa**

500 MHz
10% $D_2O$ in $H_2O$

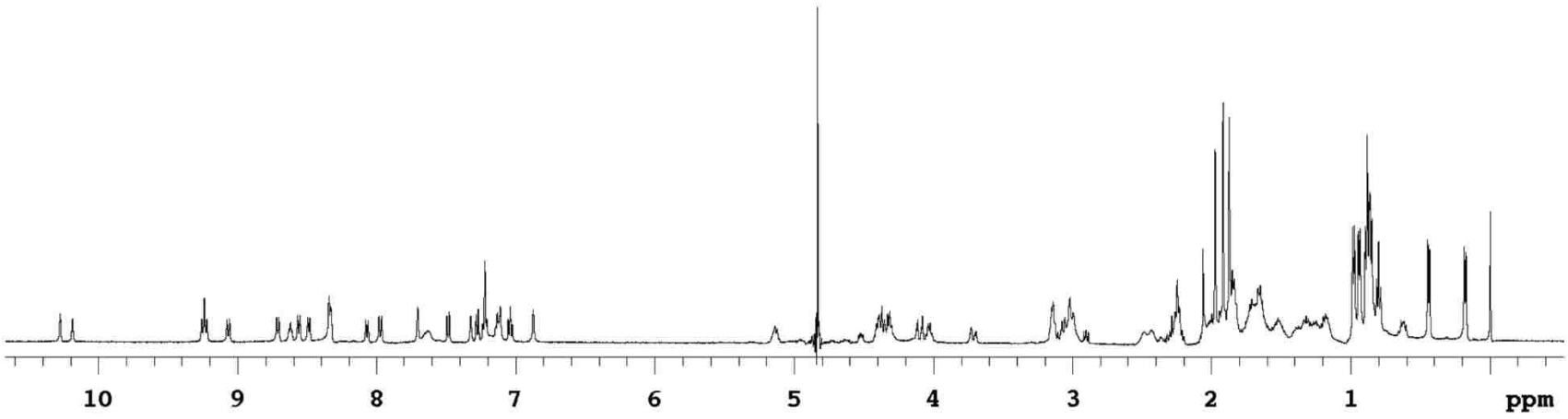

**153ab**

500 MHz

10% $D_2O$ in $H_2O$

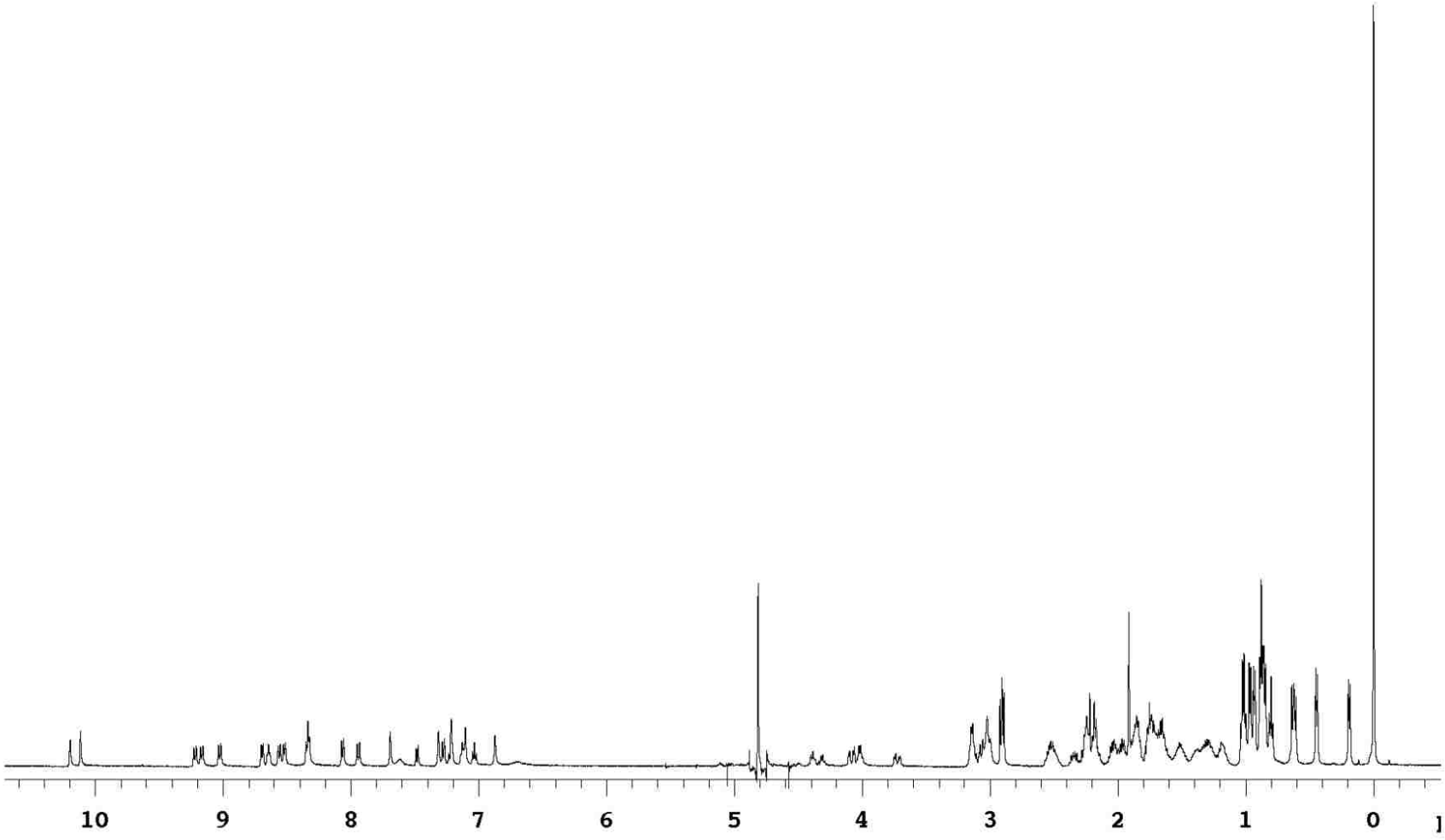

**153ba**

500 MHz
10% $D_2O$ in $H_2O$

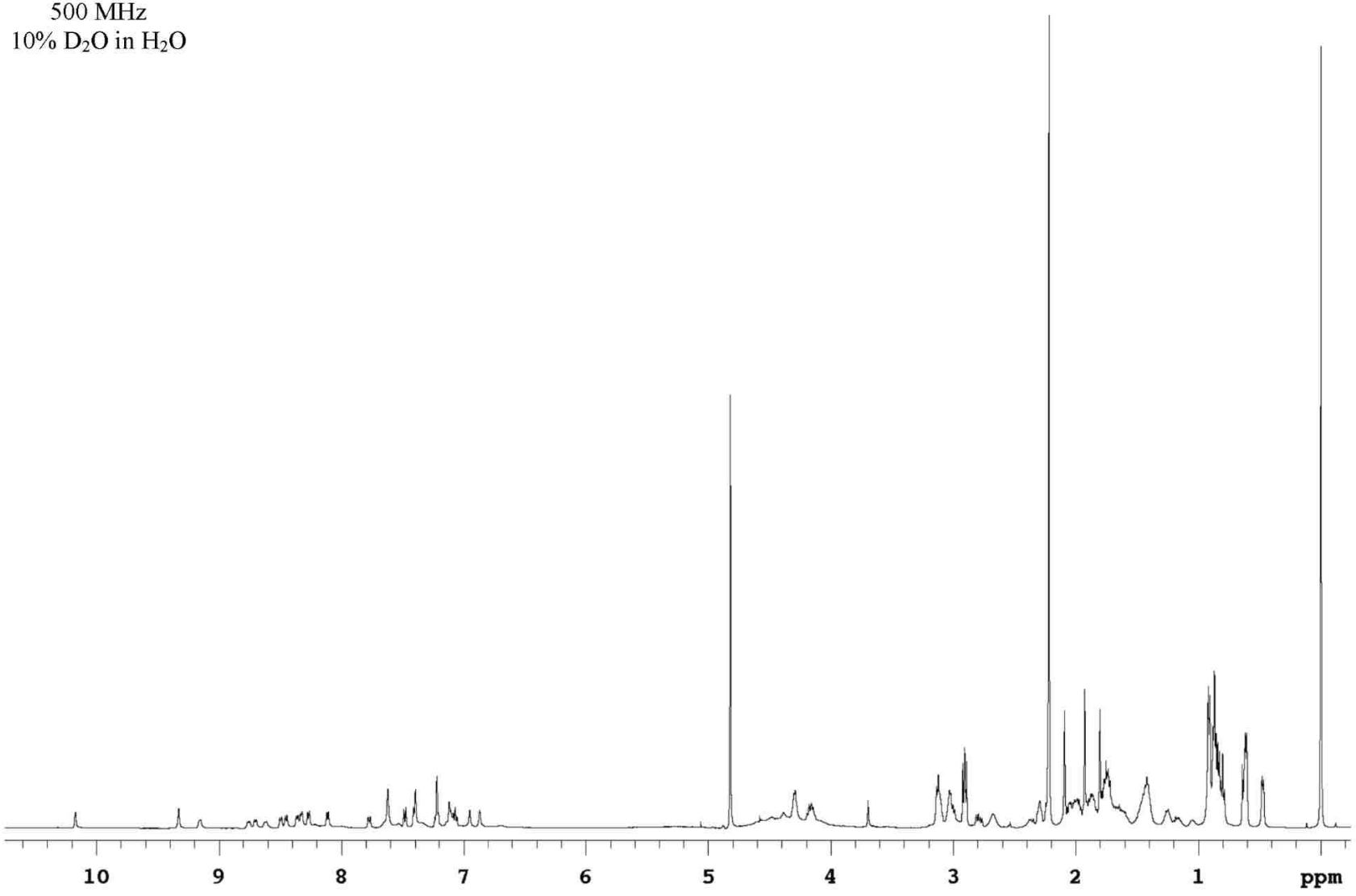

**153bb**

500 MHz
10% $D_2O$ in $H_2O$

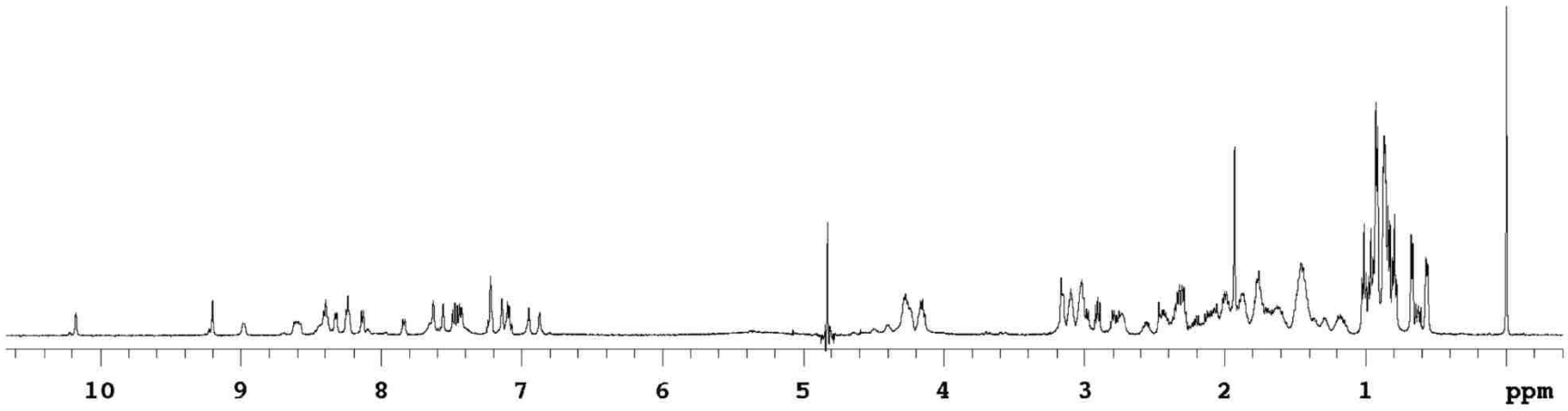

**153ca**

500 MHz
10% $D_2O$ in $H_2O$

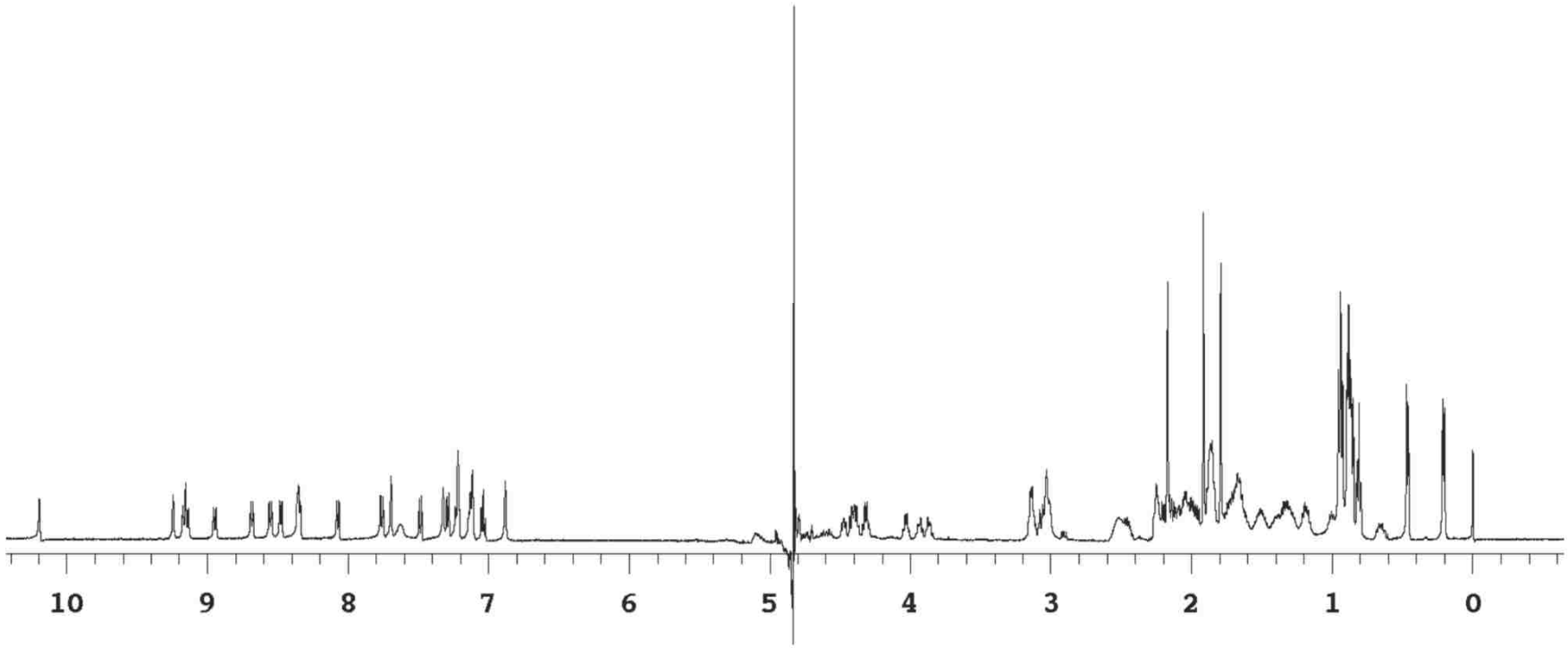

**153cb**

500 MHz
10% $D_2O$ in $H_2O$

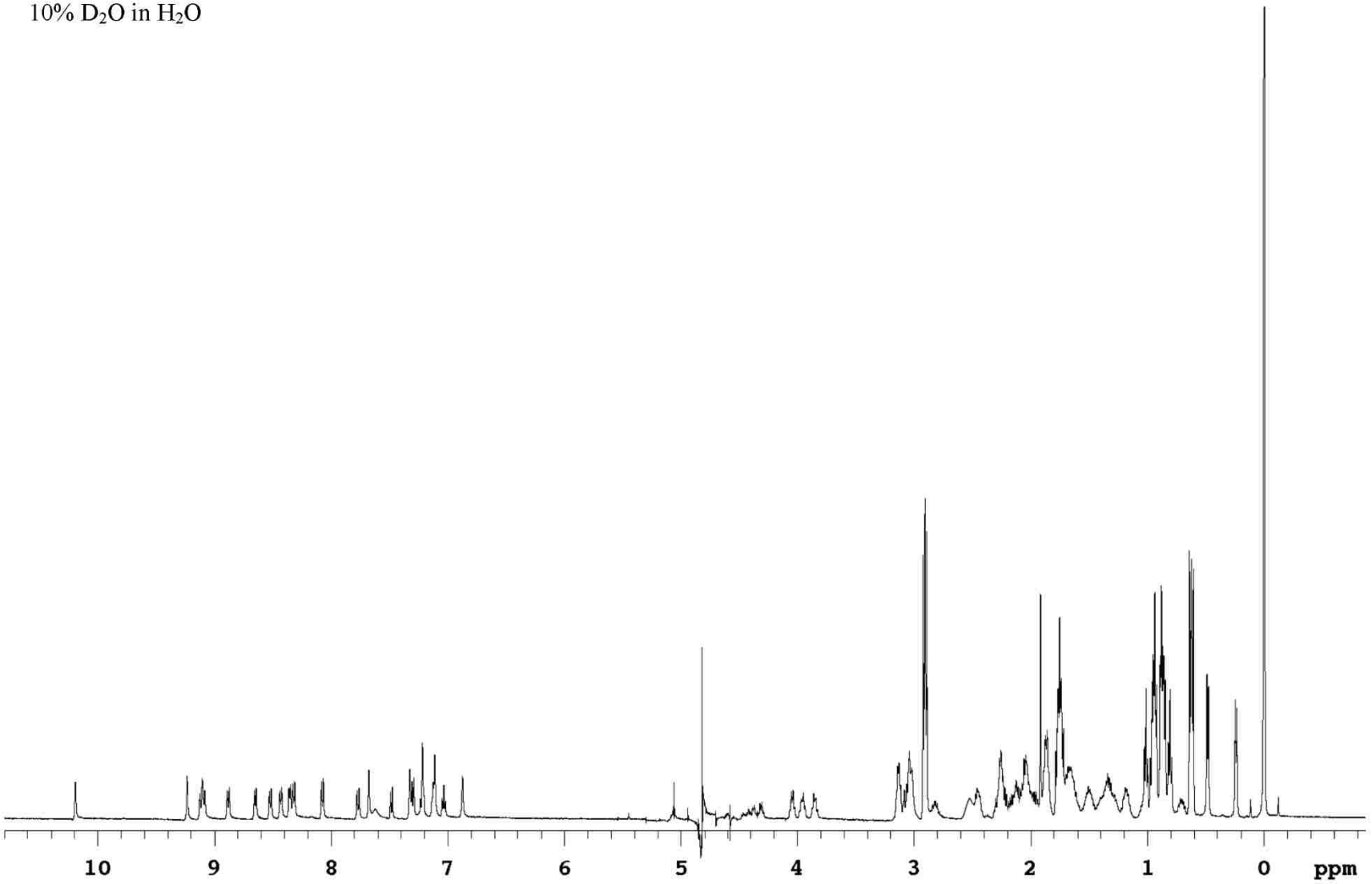

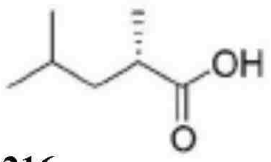


**216**

($CDCl_3$, 500 MHz)

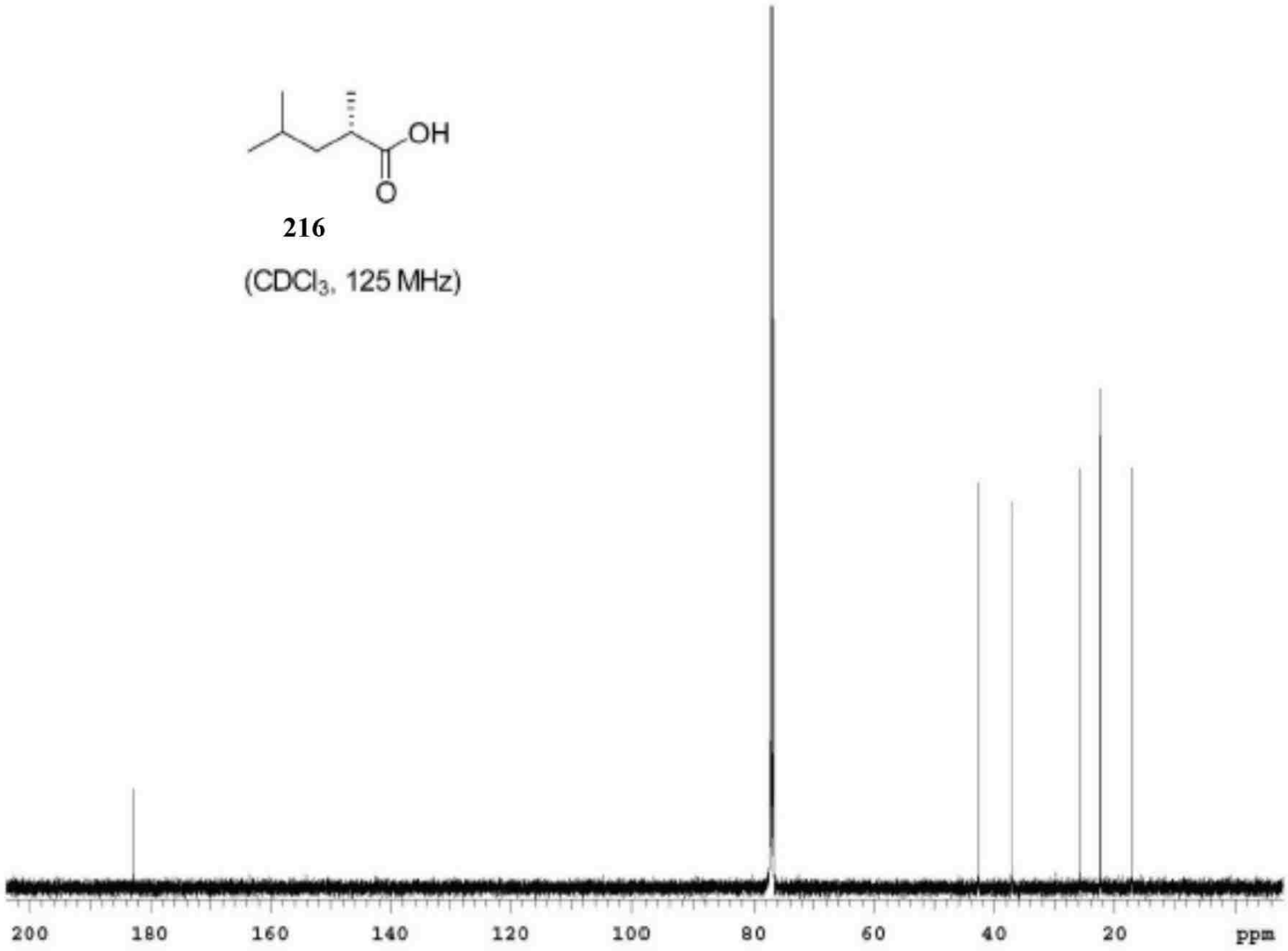


**216**

($CDCl_3$, 125 MHz)

**ROESY Spectra**. The spectra are presented with ROESY peaks in orange and TOCSY peaks superimposed in black for comparison. Peak labels use the standard CCPNMR nomenclature and their corresponding cross-peaks are marked with a crosshair.

ROESY Spectrum of **153a**.

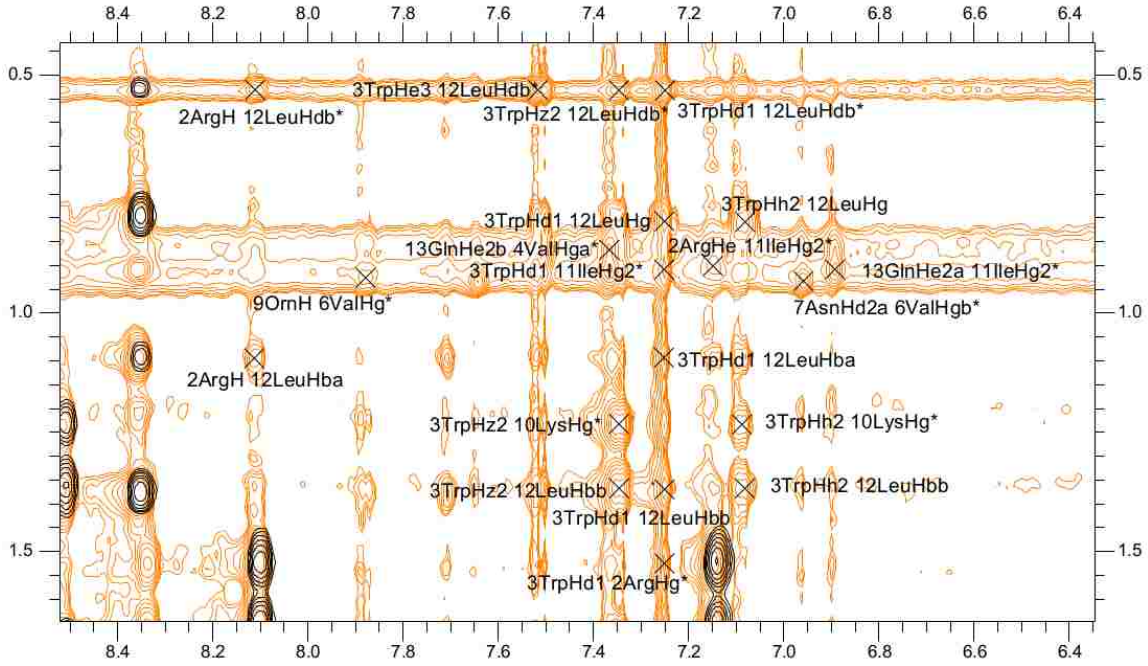


ROESY Spectrum of **153b**.

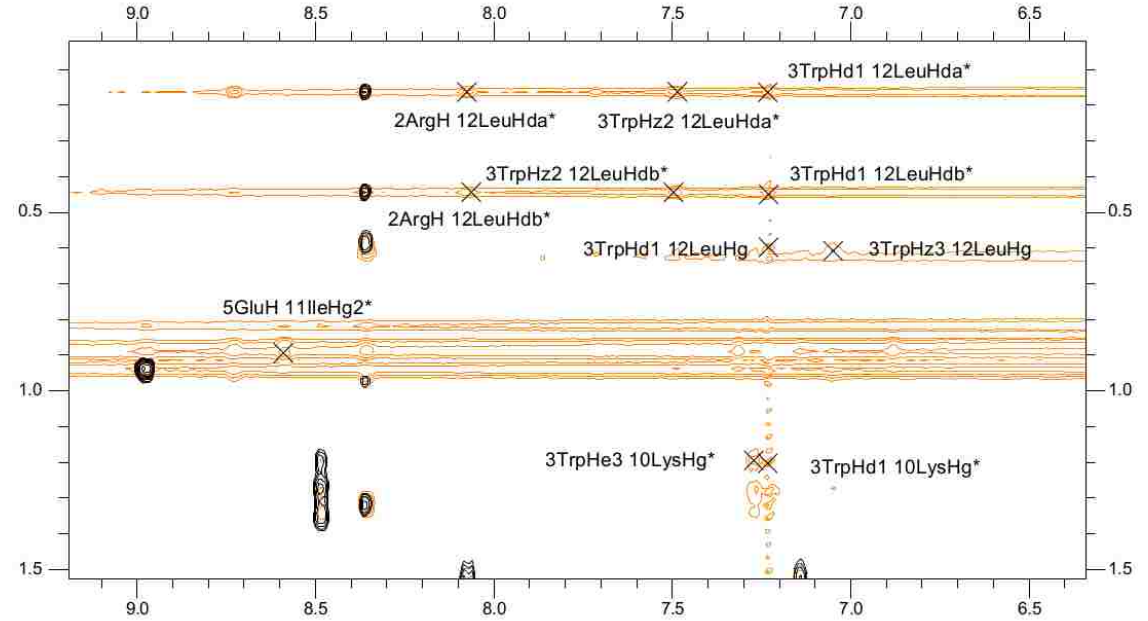

ROESY Spectrum of **152aa**.

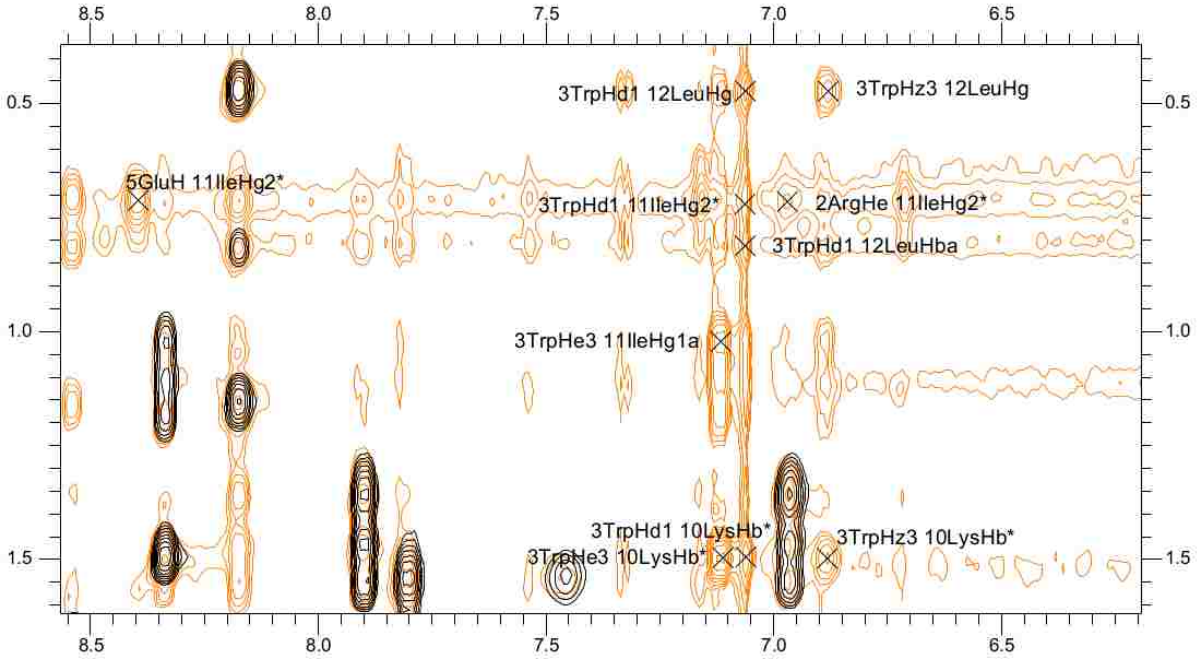


ROESY Spectrum of **152ab**.

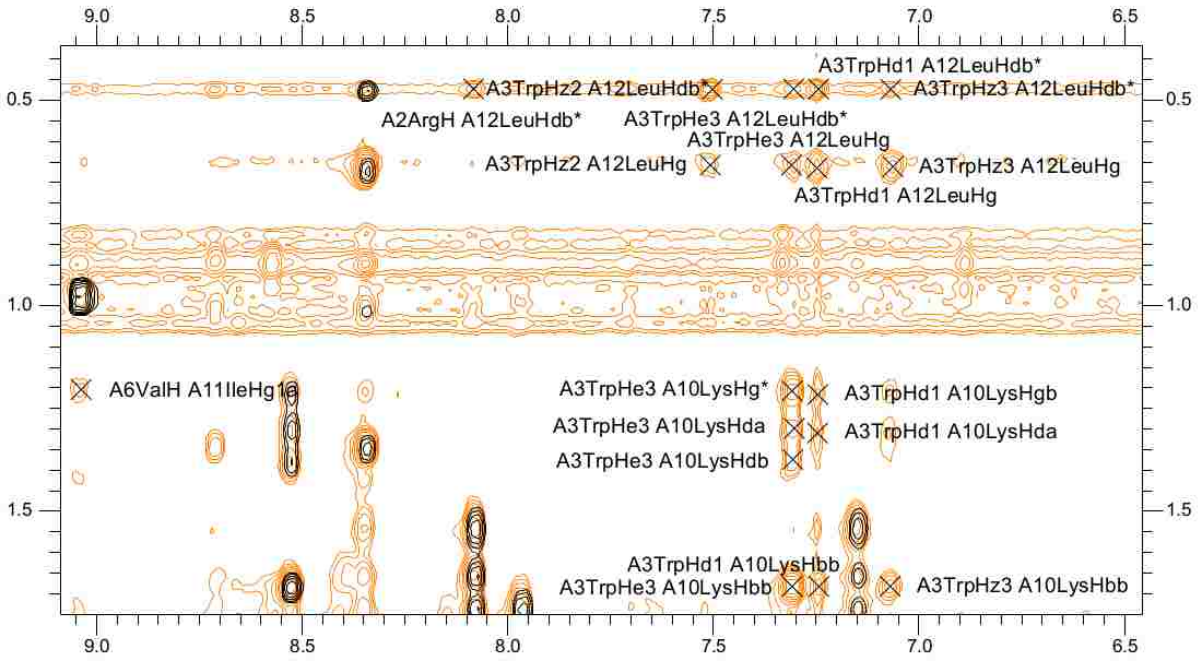

ROESY Spectrum of **152ba**.

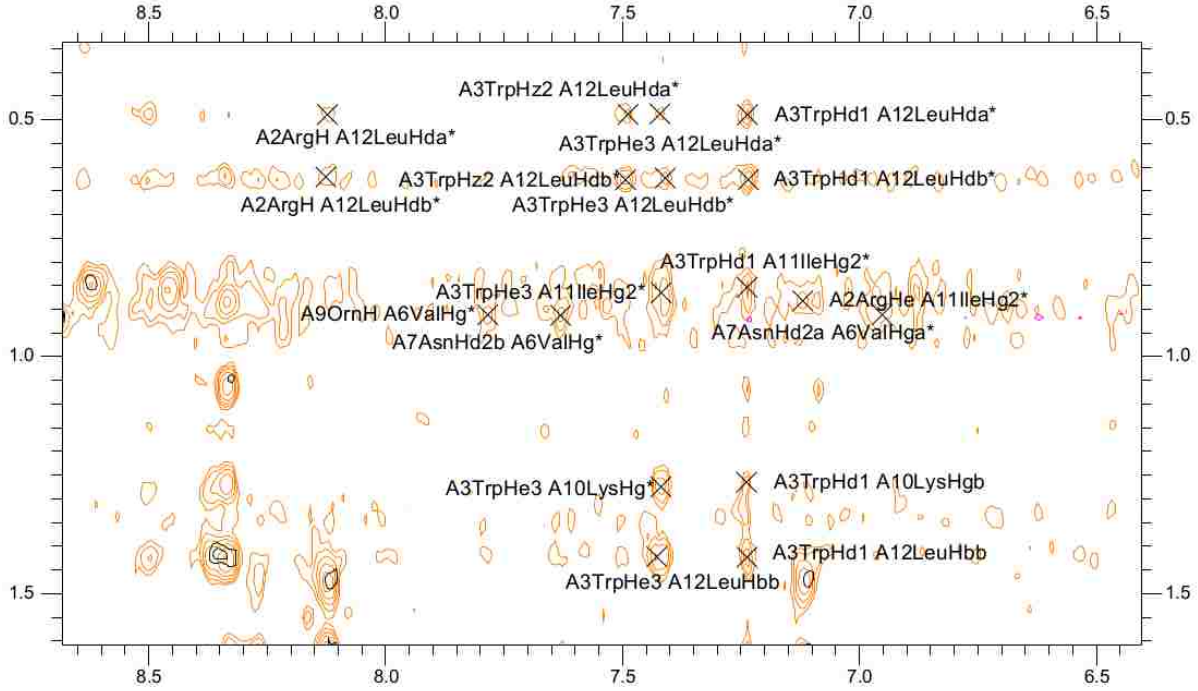


ROESY Spectrum of **152bb**.

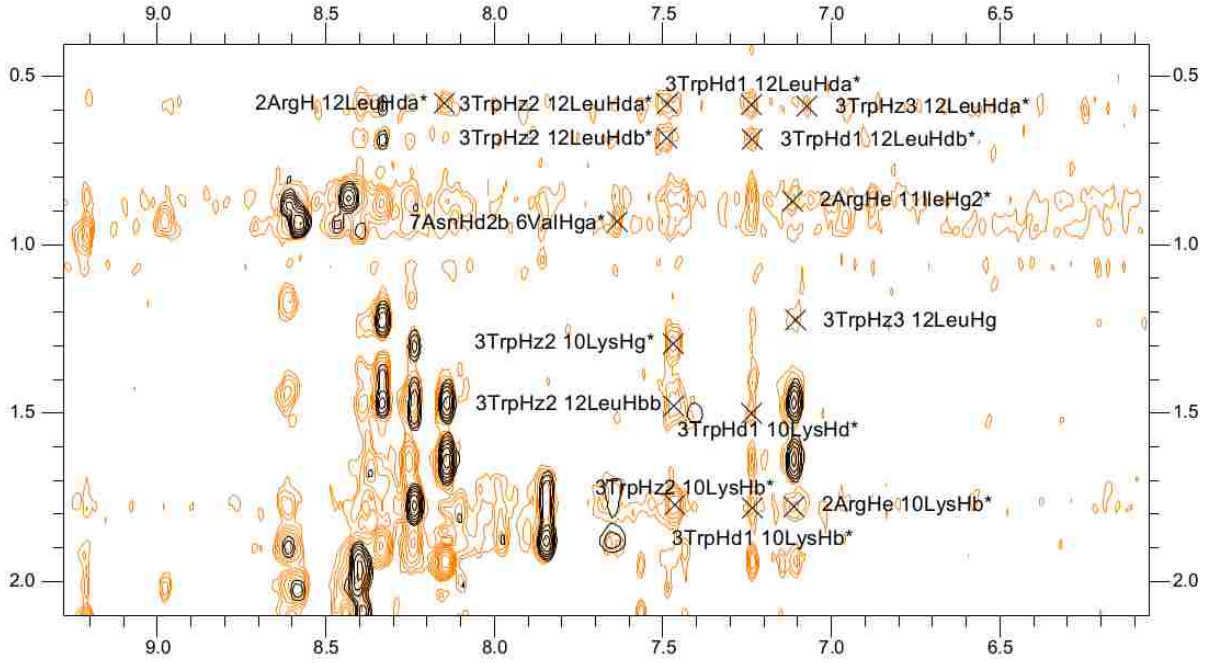

ROESY Spectrum of **152ca**.

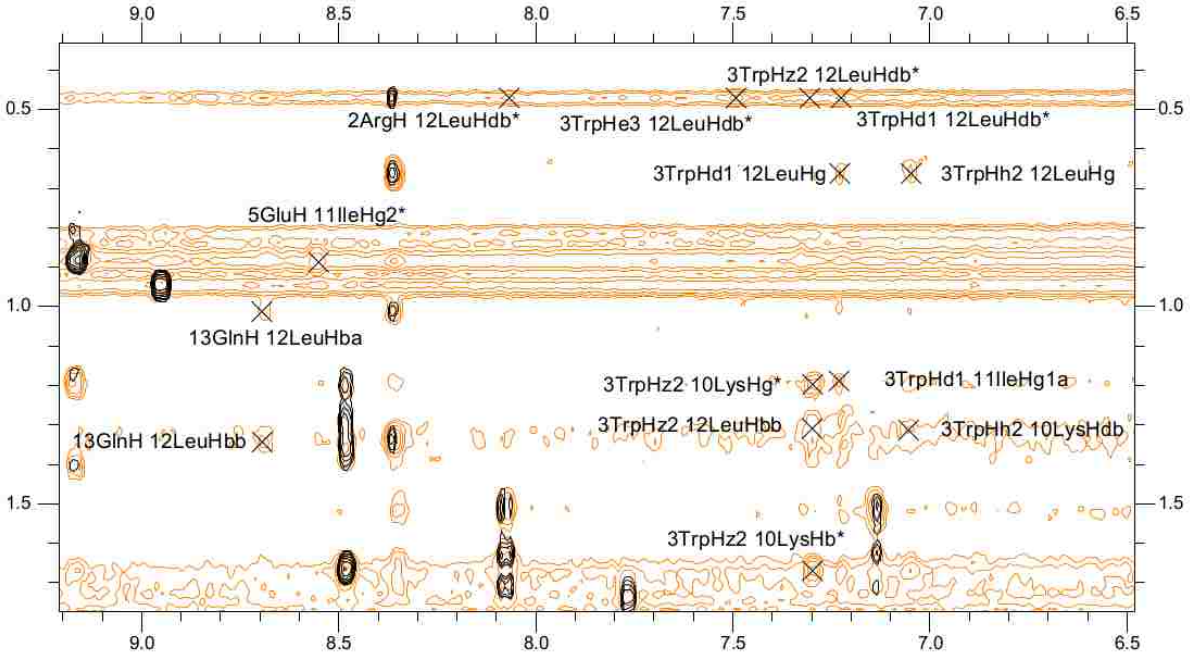


ROESY Spectrum of **152cb**.

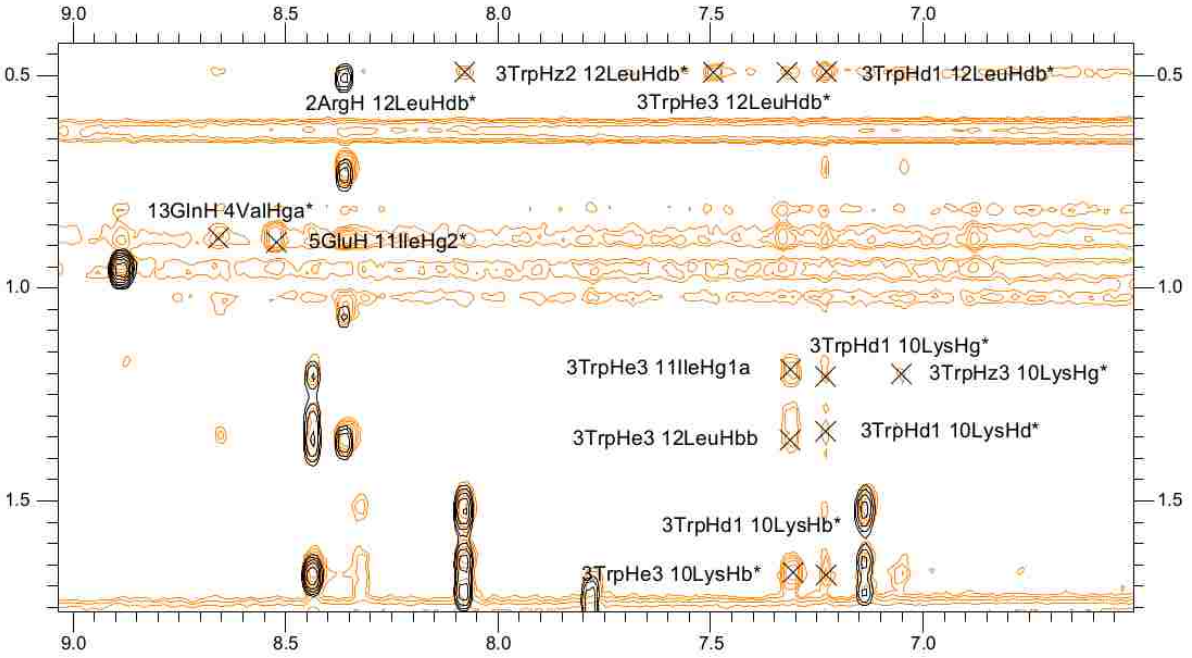

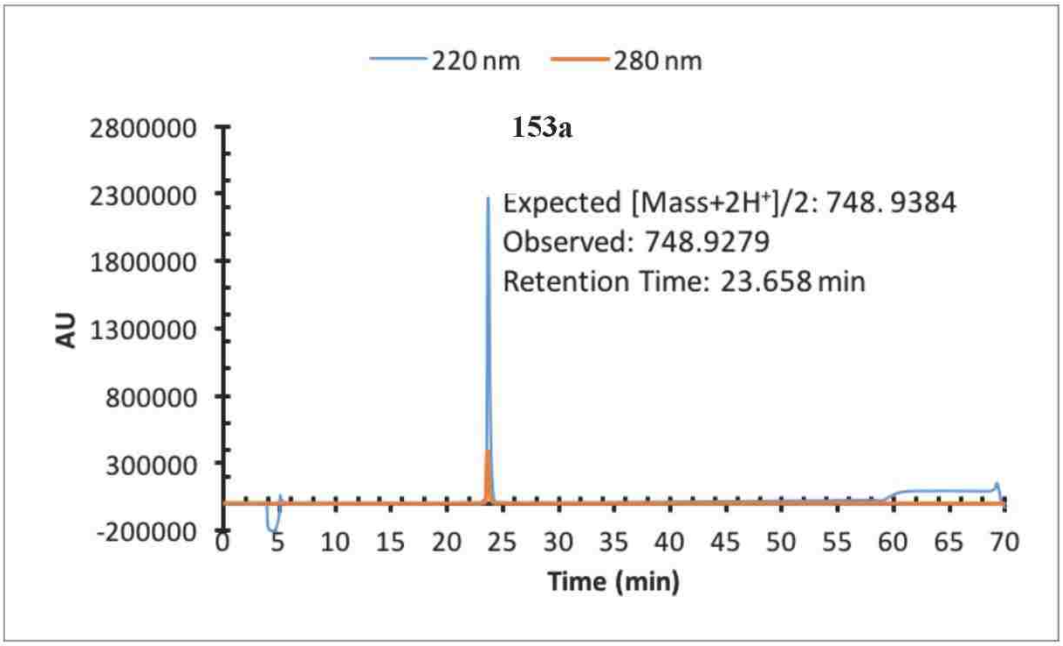


**Figure 5.1.** Analytical HPLC data for peptide **153a** after preparative purification. Sample was injected onto a C18 analytical column (4.6 mm × 25 cm) and eluted using a linear gradient of 10–60% $CH_3CN$ in $H_2O$ (constant 0.1% TFA) over 50 min.

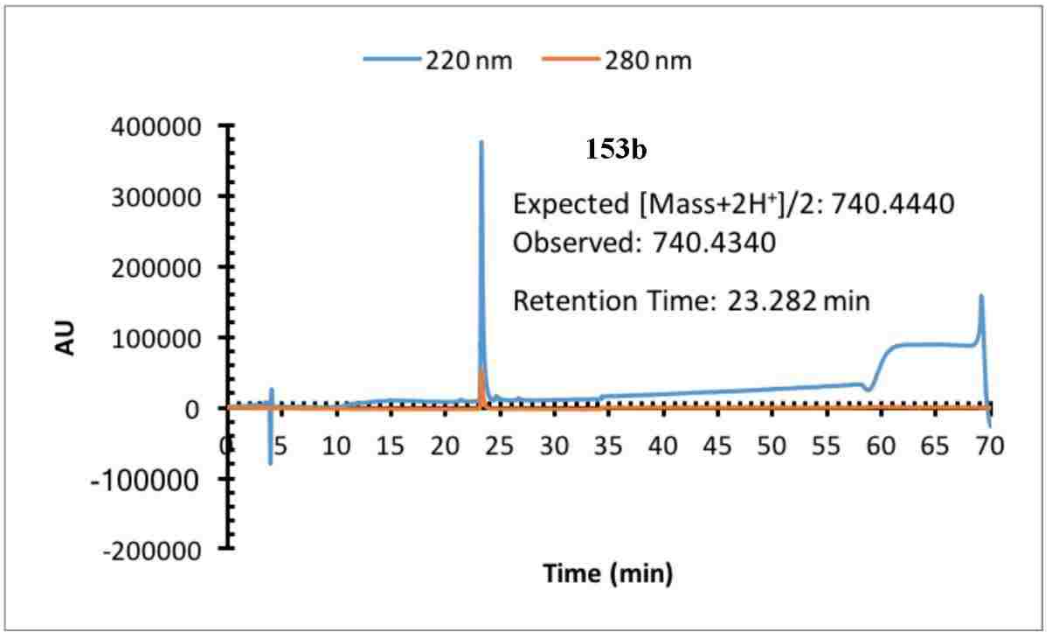


**Figure 5.2.** Analytical HPLC data for peptide **153b** after preparative purification. Sample was injected onto a C18 analytical column (4.6 mm × 25 cm) and eluted using a linear gradient of 10–60% $CH_3CN$ in $H_2O$ (constant 0.1% TFA) over 50 min.

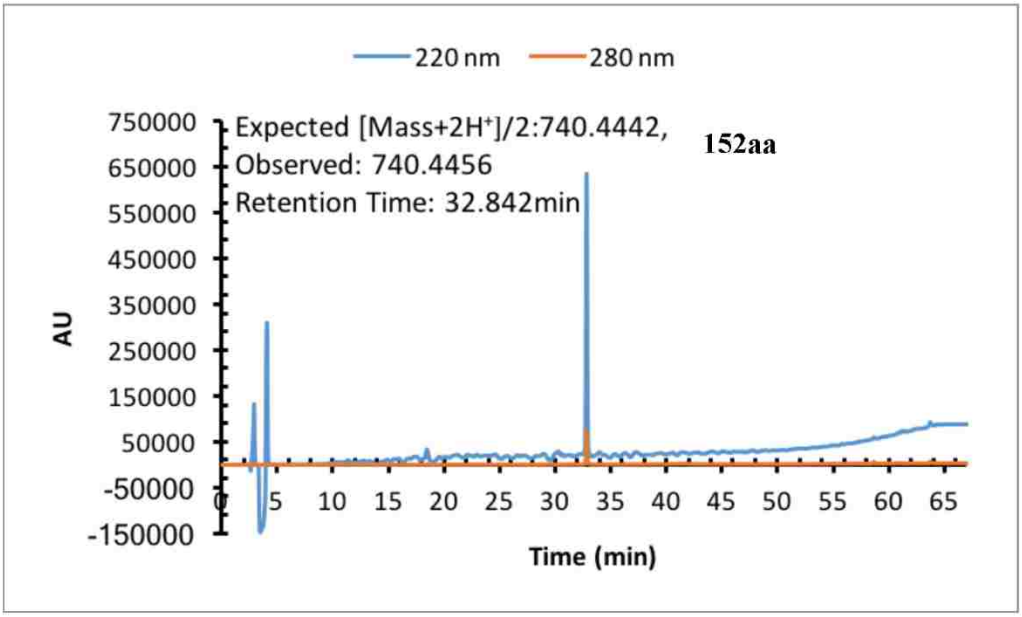


**Figure 5.3.** Analytical HPLC data for peptide **152aa** after preparative purification. Sample was injected onto a C18 analytical column (4.6 mm × 25 cm) and eluted using a linear gradient of 10–60% $CH_3CN$ in $H_2O$ (constant 0.1% TFA) over 50 min.

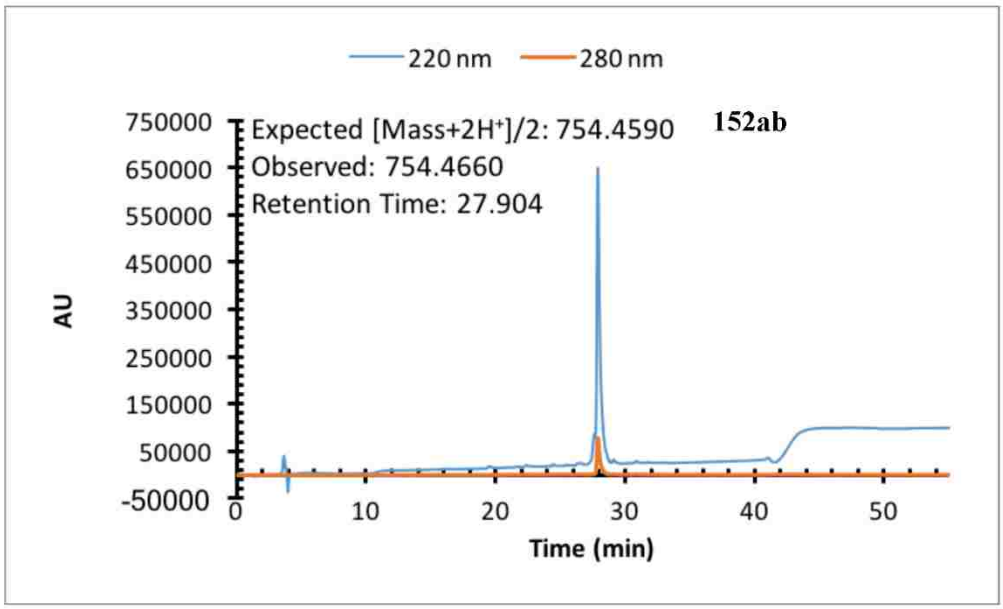


**Figure 5.4.** Analytical HPLC data for peptide **152ab** after preparative purification. Sample was injected onto a C18 analytical column (4.6 mm × 25 cm) and eluted using a linear gradient of 10–60% $CH_3CN$ in $H_2O$ (constant 0.1% TFA) over 50 min (run was terminated ~25 min after the product eluted).

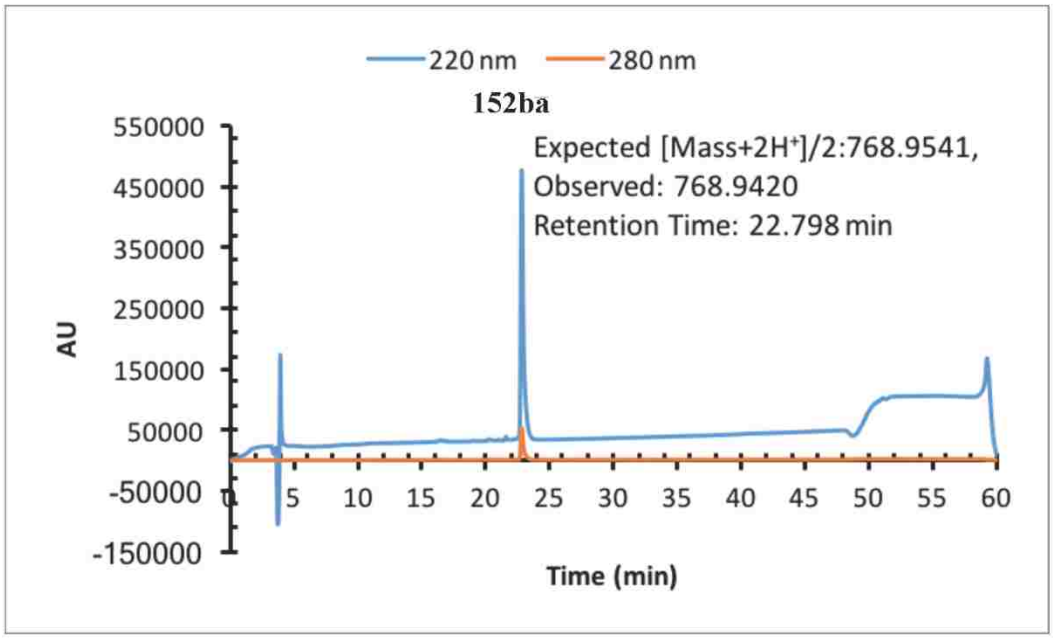


**Figure 5.5.** Analytical HPLC data for peptide **152ba** after preparative purification. Sample was injected onto a C18 analytical column (4.6 mm × 25 cm) and eluted using a linear gradient of 20–60% $CH_3CN$ in $H_2O$ (constant 0.1% TFA) over 40 min.

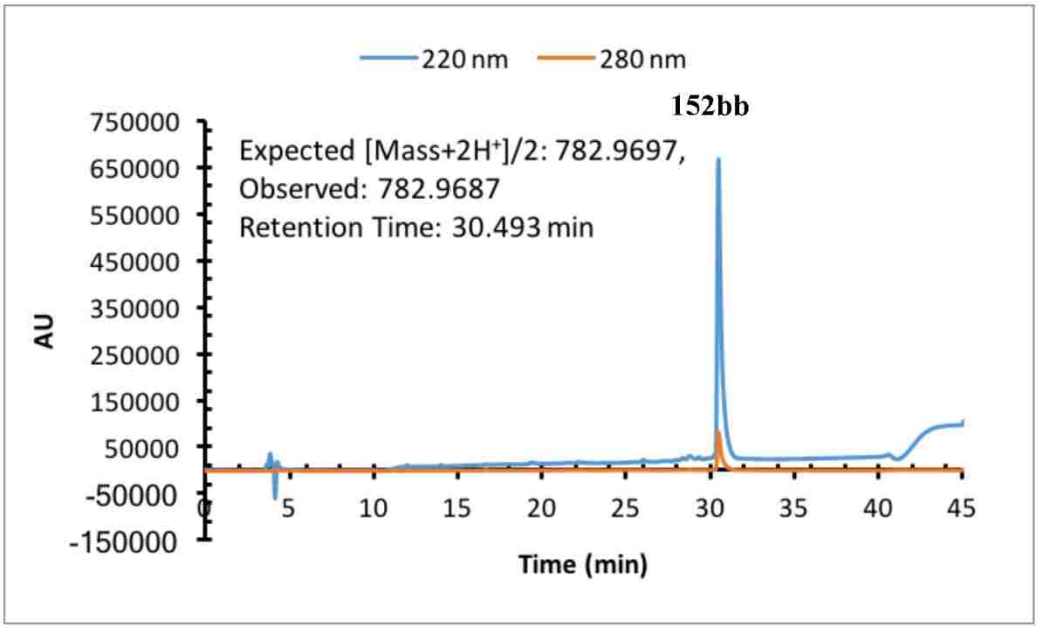


**Figure 5.6.** Analytical HPLC data for peptide **152bb** after preparative purification. Sample was injected onto a C18 analytical column (4.6 mm × 25 cm) and eluted using a linear gradient of 10–60% $CH_3CN$ in $H_2O$ (constant 0.1% TFA) over 38 min (run was terminated ~15 min after the product eluted).

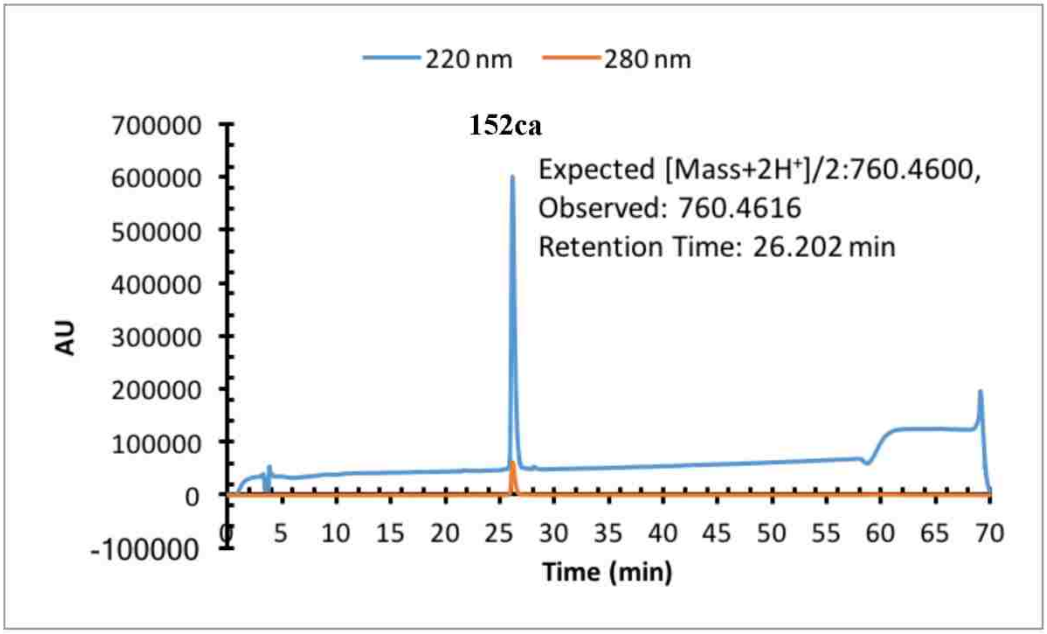


**Figure 5.7.** Analytical HPLC data for peptide **152ca** after preparative purification. Sample was injected onto a C18 analytical column (4.6 mm × 25 cm) and eluted using a linear gradient of 10–60% $CH_3CN$ in $H_2O$ (constant 0.1% TFA) over 50 min.

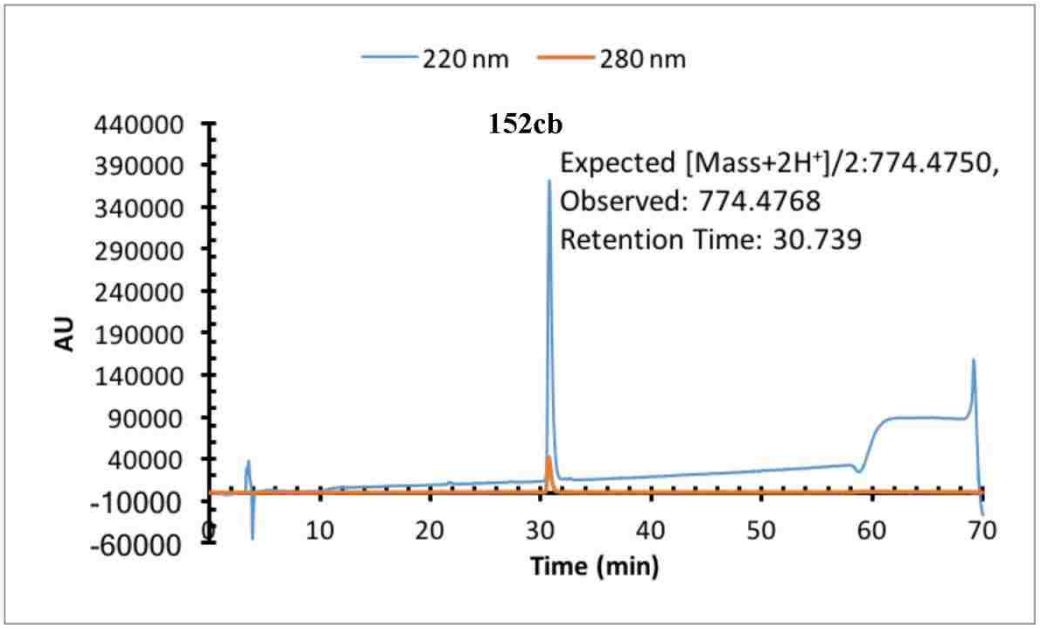


**Figure 5.8.** Analytical HPLC data for peptide **152cb** after preparative purification. Sample was injected onto a C18 analytical column (4.6 mm × 25 cm) and eluted using a linear gradient of 10–60% $CH_3CN$ in $H_2O$ (constant 0.1% TFA) over 50 min.

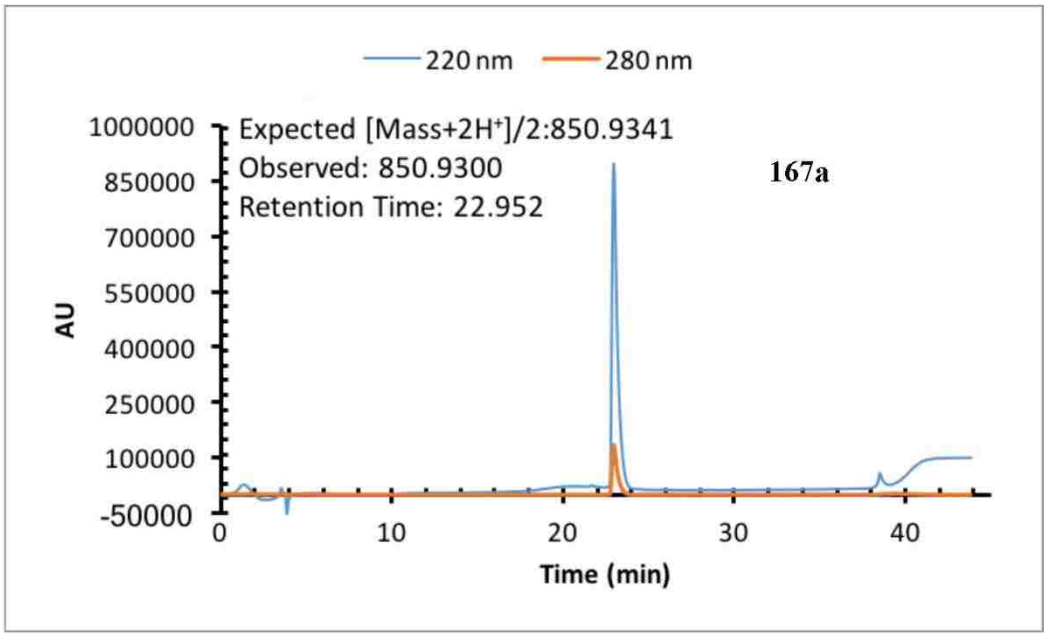


**Figure 5.9.** Analytical HPLC data for peptide **167a** after preparative purification. Sample was injected onto a C18 analytical column (4.6 mm × 25 cm) and eluted using a linear gradient of 10–40% $CH_3CN$ in $H_2O$ (constant 0.1% TFA) over 25 min.

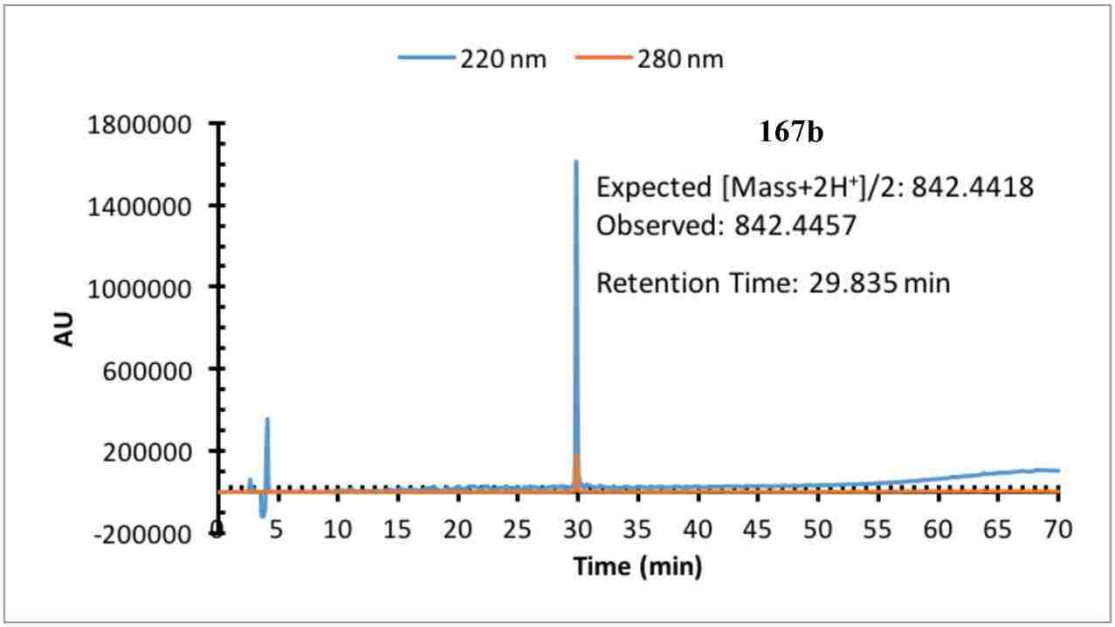


**Figure 5.10.** Analytical HPLC data for peptide **167b** after preparative purification. Sample was injected onto a C18 analytical column (4.6 mm × 25 cm) and eluted using a linear gradient of 10–60% $CH_3CN$ in $H_2O$ (constant 0.1% TFA) over 50 min.

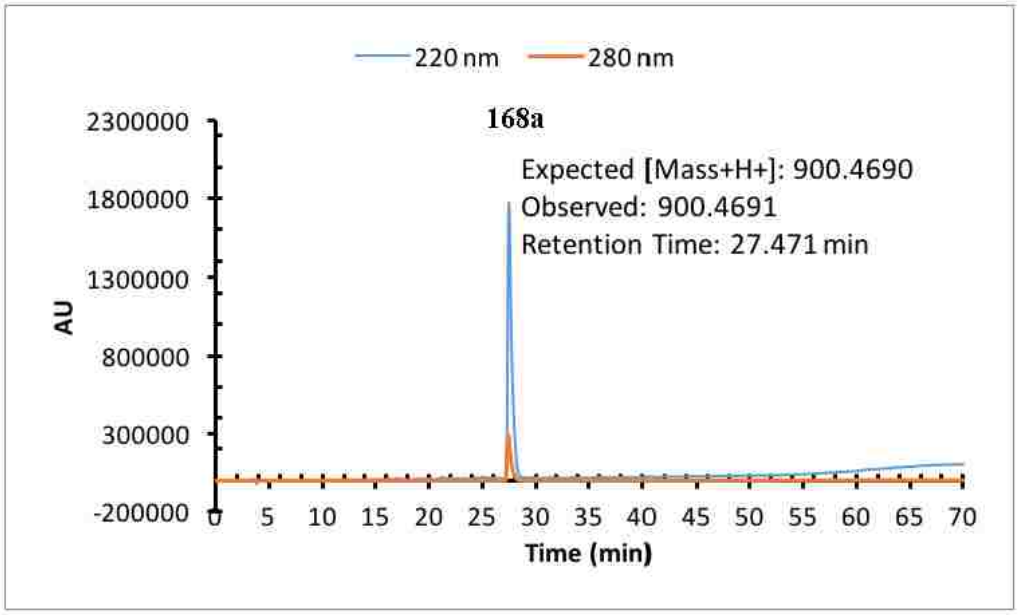


**Figure 5.11.** Analytical HPLC data for peptide **168a** after preparative purification. Sample was injected onto a C18 analytical column (4.6 mm × 25 cm) and eluted using a linear gradient of 10–60% $CH_3CN$ in $H_2O$ (constant 0.1% TFA) over 50 min.

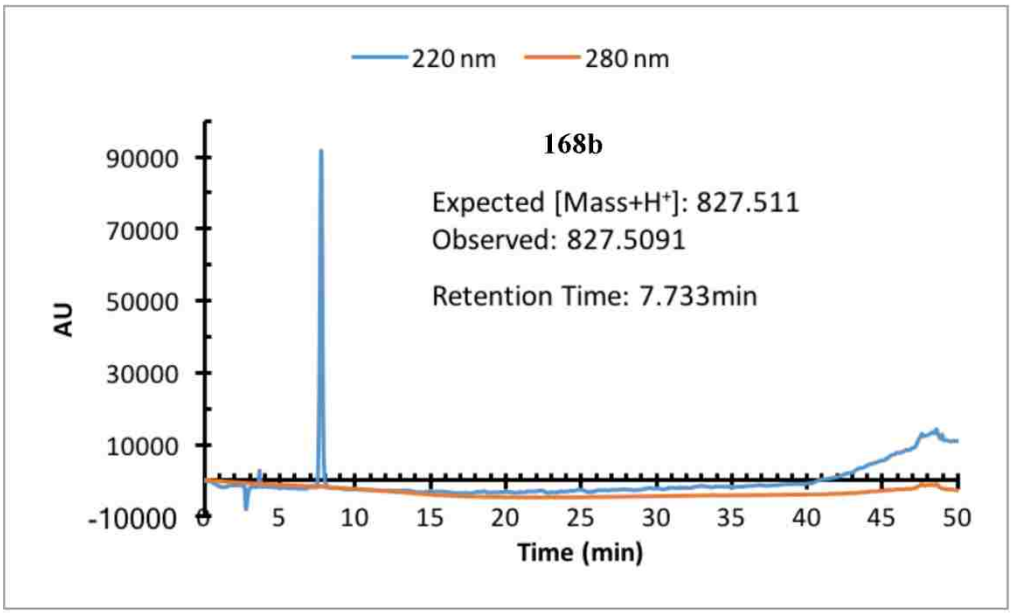


**Figure 5.12.** Analytical HPLC data for peptide **168b** after preparative purification. Sample was injected onto a C18 analytical column (4.6 mm × 25 cm) and eluted using a linear gradient of 10–28% $CH_3CN$ in $H_2O$ (constant 0.1% TFA) over 35 min.

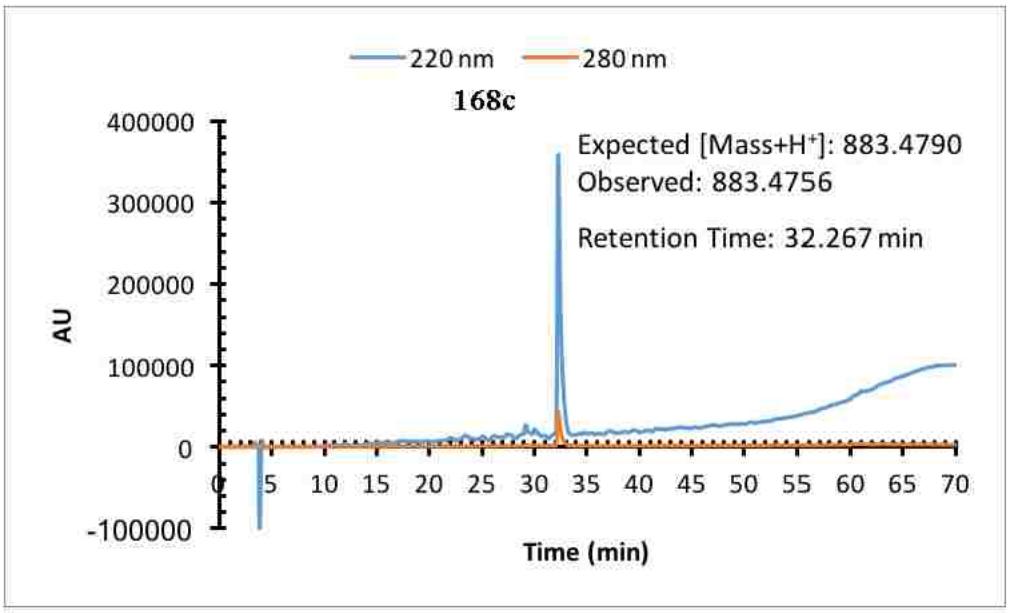


**Figure 5.13.** Analytical HPLC data for peptide **168c** after preparative purification. Sample was injected onto a C18 analytical column (4.6 mm × 25 cm) and eluted using a linear gradient of 10–60% $CH_3CN$ in $H_2O$ (constant 0.1% TFA) over 50 min.

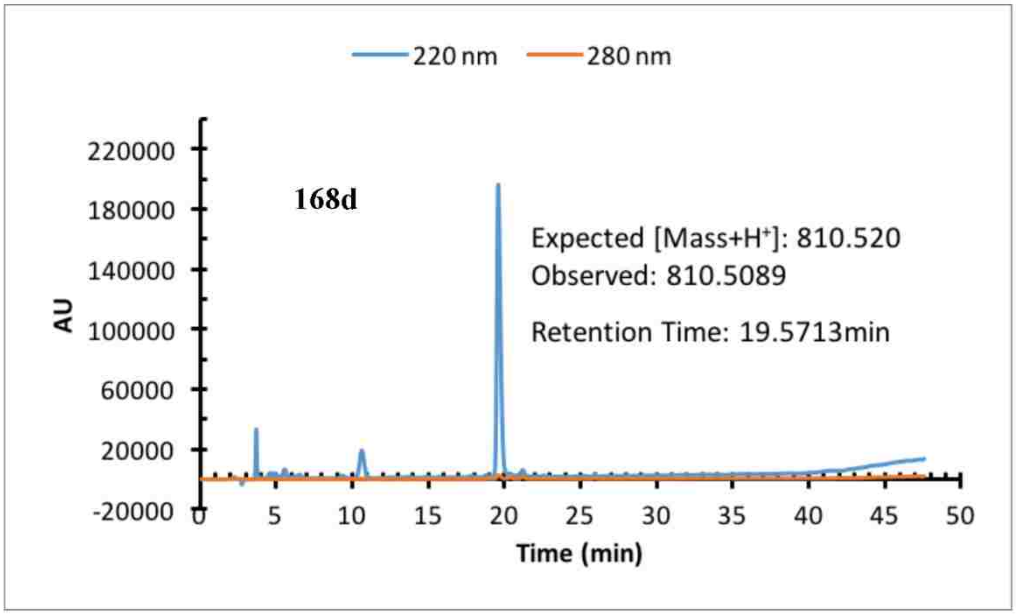


**Figure 5.14.** Analytical HPLC data for peptide **168d** after preparative purification. Sample was injected onto a C18 analytical column (4.6 mm × 25 cm) and eluted using a linear gradient of 10–28% $CH_3CN$ in $H_2O$ (constant 0.1% TFA) over 35 min (run was terminated ~25 min after the product eluted).